ENZYMATIC SYNTHESIS OF PHENOLIC LIPIDS FROM KRILLOIL IN SOLVENT-FREE MEDIA AND THEIR MICROENCAPSULATION

by

Sarya Aziz

A thesis submitted to the Faculty of Graduate Studies and Research in partial fulfillment of the requirements of the degree of Doctor of Philosophy

Department of Food Science & Agricultural Chemistry
McGill University
Montreal, Canada

October 2013

SHORT TITLE

ENZYMATIC SYNTHESIS OF PHENOLIC LIPIDS FROM KRILL OIL

This thesis is dedicated to my supportive family and husband,
with love

ABSTRACT

Ph.D. Sarya Aziz

The optimization of the synthesis of phenolic lipids (PLs), obtained by the enzymatic transesterification of krill oil (KO) with selected phenolic acids (PAs) in solvent-free media (SFM), as well as their separation, characterization and encapsulation were investigated. Using high-performance liquid chromatography (HPLC), the evaporative light-scattering detector (ELSD) was shown to be a more appropriate tool, in terms of detection and repeatability, for the qualitative and quantitative analyses of the components of KO and its esterified PLs. In addition, the structural analyses of the synthesized PLs by HPLC/mass spectrometry (MS) suggested the formation of two phenolic monoacylglycerols. Using two immobilized commercial enzymes, Novozym 435 and Lipozyme TL IM, the enzymatic synthesis of PLs from KO with two phenolic acid (PA) models, including 3,4-dihydroxyphenylacetic acid (DHPA) and dihydrocaffeic acid (DHCA), was investigated. The use of Novozym 435 and DHPA resulted in the highest bioconversion yield (BY). The central composite rotatable design (CCRD) was used to evaluate the effects of PA concentration (PAC) and lipase concentration (LC) as well as the agitation speed (AS) on the BY of PLs. For the models with PAC, fixed at 10 and 20 mM, the results revealed that LC had a significant quadratic effect (P <0.05) on the BY, whereas a significant linear effect was only obtained with PAC, fixed at 20 mM. The AS had a significant quadratic effect (P <0.05) on the BY, only for the model, with a PAC fixed at 10 mM. At fixed PAC of 20 mM, the response surface model predicted a BY of 75%, using a LC of 62 mg/mL and an AS of 154 rpm. The antioxidant capacity (AOC) and the oxidative stability of PLs, obtained by the enzymatic transesterification of PAs with the selected edible oils (EOs), including flaxseed (FSO), fish liver (FO) and krill (KO) oils, were determined. The statistical analyses of Tukey's test at P <0.05 revealed that the difference in AOC between that of the esterified oils of flaxseed (EFSO) and krill (EKO) and their control trials of EOs was significant (P <0.05). In addition, the experimental findings showed that all esterified oils containing PLs had higher oxidative stability when they were subjected to light, oxygen and agitation at 50ºC as compared to that of the EOs; nevertheless, only the esterified fish oil (EFO) showed a significant difference in its peroxide value (PV), when it was placed in the dark at 25ºC. The

development of a process to yield gelatin (GE)-gum arabic (GA) multinuclear microcapsules of KO, via complex coacervation, was investigated. A three-level-by-three factor Box-Behnken design (BBD) was used to evaluate the effects of the ratio of the core material to the wall (RCW), with x_1 of 1.25:1 to 1.75:1, the stirring speed (SP) with x_2 of 2 to 4, over a scale of 10 and the pH with x_3 of 3.8 to 4.2, on the encapsulation efficiency (EE). The experimental findings indicated that x_3 had the most significant linear and quadratic effects on the EE of KO and a bilinear one with x_1; however, x_2 did not have any effect. The optimal predicted conditions for a 92% of EE were 1.75:1 for RCW, 3.8 for pH and 3 for SP. The microcapsules, formed by complex coacervation and without any cross-linking agent, were multinucleated, circular in shape and had sufficient stability to maintain their structure. The microencapsulation of the esterified krill oil (EKO), obtained by complex coacervation, was carried out. The experimental findings showed that the presence of DHPA and PLs, in the EKO, affected the stability of GE-EKO emulsion. The ultrasonic liquid processor was found to be a more appropriate device for the emulsification of the EKO into GE, as compared to the high-shear homogenizer. In addition, the capsules prepared with a GE at pH 8.0 showed higher storage stability, with significantly (P <0.05) lower primary oxidative products, as compared to those prepared with a GE at pH 6.5. The microencapsulation of the EKO was effective in delaying the development of primary and secondary oxidation products during a period of 25 days of storage at room temperature.

RÉSUMÉ

Ph.D. Sarya Aziz

L'optimisation de la synthèse de lipides phénoliques (PLs), obtenus par la transésterification enzymatique de l'huile de krill (KO) avec des acides phénoliques sélectionnés en milieu réactionnel sans solvant (SFM) ainsi que de leur séparation, caractérisation et encapsulation ont été étudiées. En utilisant la chromatographie en phase liquide (HPLC), le détecteur évaporatif à diffusion de lumière (ELSD) a été sélectionné pour son pouvoir de détection et pour la repeatibilité des analyses qualitatives et quantitatives des composants de KO et ses PLs estérifiés. De plus, les analyses structurales des PLs synthétisés par HPLC/spectrométrie de masse (HPLC/MS) ont suggéré la formation de deux lipides phénoliques monoacylglycéroles. En utilisant deux enzymes commerciales immobilisées, Novozym 435 et Lipozyme TL IM et deux acides phénoliques (PA) modèles y compris l'acide 3,4-dihydroxyphénylacétique (DHPA) et l'acide dihydrocaffeique, la synthèse enzymatique des PLs à partir de KO, a été investiguée. Le meilleur rendement de bioconversion (BY) a été obtenu avec la Novozym 435 et le DHPA. Le plan composite central à caractère rotatif (CCRD) a été utilisé pour évaluer les effets de la concentration de l'acide phénolique (PAC) et de celle de la lipase (LC) ainsi que de la vitesse d'agitation (AS) sur le BY des PLs. Pour les modèles avec PAC, fixée à 10 et 20 mM, les résultats ont montré que la LC a un effet quadratique significatif ($P < 0,05$) sur le BY, alors qu'un effet linéaire a été seulement obtenu avec PAC fixée à 20 mM. L'AS avait un effet quadratique significatif ($P < 0,05$) sur le BY, seulement pour le modèle, avec une PAC fixée à 10 mM. à PAC fixée à 20 mM, la surface de réponse du modèle a prédit un BY de 75%, en utilisant la LC de 62 mg/mL et la AS de 154 rpm. La capacité antioxydante (AOC) et la stabilité oxydative des PLs, obtenus par la transésterification enzymatique des PAs avec des huiles comestibles (EOs) sélectionnées y compris les huiles de lin (FSO), de poisson (FO) et de krill, ont été déterminées. Les analyses statistiques du test Tukey à $P < 0,05$ ont révélé que la différence en AOC entre celle des huiles estérifiées de lin (EFSO) et de krill (EKO) et celle des blancs a été significative ($P < 0,05$). De plus, les résultats expérimentaux tendent à montrer que tous les huiles estérifiées avec PLs avaient une stabilité oxydative plus élevée quant ils étaient exposés à la lumière et en présence de l'oxygène mais aussi

soumis à l'agitation et à 50ºC comparée à celle des EOs; néanmoins, seul l'huile de poisson estérifiée (EFO) a montré une différence significative en sa valeur de peroxyde (PV) quand les huiles estérifiées ont été placées en obscurité et à 25ºC. Le développement d'un processus pour produire des microcapsules multinucléaires, en utilisant l'association de gélatine (GE)-gomme arabique (GA) par la coacervation complexe a été investigué. Le plan Box-Behnken (BBD) à trois-niveaux-par-trois facteurs a été utilisé pour évaluer les effets du ratio huile/polymères (RCW) avec x1 de 1,25:1 à 1,75:1, la vitesse de la turbine (SP) avec x_2 de 2 à 4, sur une échelle de 10 et un pH avec x_3 de 3,8 à 4,2, sur l'efficience d'encapsulation (EE). Les résultats expérimentaux ont indiqué que x_3 avait les effets linéaires et quadriques les plus significatifs sur la EE de KO et un effet bilinéaire avec x1; Par contre, x_2 n'avait aucun effet. Les conditions optimales prédites pour une EE de 92% étaient 1,75:1 pour RCW, 3,8 pour pH et 3 pour SP. Les microcapsules, formées par la coacervation complexe et sans aucun agent d'articulation, étaient multinucléées, circulaires et assez stables pour maintenir leurs structures. La microencapsulation de l'huile de krill estérifiée par la coacervation complexe a été effectuée. Les résultats expérimentaux tendent à montrer que la présence du DHPA et des PLs, dans l'EKO, avait un effet sur la stabilité de l'émulsion de GE-EKO. L'ultrason utilisé pour traitement liquide a été plus approprié pour l'émulsification de l'EKO dans GE, par rapport à l'homogénéisateur à haut débit. De plus, les capsules préparées avec un GE à pH 8,0 ont montré une stabilité d'entreposage plus élevée avec une PV significativement ($P < 0,05$) moins élevée que celles pour les capsules préparées avec un GE à pH 6,5. La microencapsulation de EKO a été effective pour retarder le développement de produits d'oxydation primaires et secondaires durant une période de d'entreposage de 25 jours à température ambiante.

ACKNOWLEDGMENT

My deepest and sincere thanks go to my supervisor, Dr. Selim Kermasha, for his valuable advices, constant encouragement, continuous enthusiasm and support throughout my study. You were a great mentor and I credit you for making me a better researcher.

I would like to extend my appreciation to Dr. Richard St-Louis for his contribution to the LC/MS structural analyses of phenolic lipid products. My appreciation and thanks also go to Dr. Pierre R.L. Dutilleul for his collaboration and advices in the statistical analyses. I am thankful to Dr. Varoujan Yaylayan for his collaboration and input in the FTIR analysis. I would like also to acknowledge Dr. Ronald J. Neufeld for his valuable advice in the encapsulation of krill oil and its esterified phenolic lipids. I am thankful to Dr. Jaqueline C. Bede for providing me the access to the use of the stereomicroscope in the laboratory. I would like also to thank Jagpreet Gill for her technical assistance, in particular in the microencapsulation studies.

My appreciation goes to the Food Science Department secretaries Ms. Leslie Ann La Duke and Ms. Diane Chan-Hum, for their assistance and help. I am thankful to all my colleagues, especially Marwa, Watcha, Noha, Shan, Christelle, Maryam, Haydar, Marya and Sabrina for their constant support and friendship.

I would like to acknowledge the Fonds Québécois de la Recherche sur la Nature et les Technologies (FQRNT) for the attribution of my fellowships to pursue my graduate studies.

Last but definitively not least, my deep and sincere thanks go to my parents, my sister, my grandmother and my friends for their unconditional love, constant encouragement and support. My gratitude is beyond word. I couldn't have done this without them. A very special thanks goes to my loving and supportive husband for believing in me and for being the source of my motivation.

CONTRIBUTION OF AUTHORS

The present author, Sarya Aziz, was responsible for the concepts, the design of the experimental work and the manuscript preparation of the published papers and the thesis document.

Dr. Selim Kermasha, the thesis supervisor, supervised the research work, provided valuable input and advices, monitored the progress of the work and critically reviewed and edited the manuscripts and the thesis document, prior to their submission.

Dr. Richard St-Louis carried out the LC/MS structural analyses of phenolic lipid products and contributed to the analysis of data.

Dr. Varoujan Yaylayan contributed to the FTIR analysis and reviewed this part in the published manuscript.

Dr. Pierre R.L. Dutilleul contributed to the statistical analyses using response-surface methodology and reviewed this part in the published manuscript.

Dr. Ronald J. Neufeld provided valuable advices for the research work aimed at the encapsulation of krill oil and its esterified phenolic lipids.

Jagpreet Gill participated technically in the research work, in particular in the microencapsulation studies.

CLAIMS OF ORIGINAL RESEARCH

1. It is the first time where the development of a method for the separation and the characterization of the components of krill oil and its esterified phenolic lipids, obtained by its enzymatic transesterification with 3,4-dihydroxyphenylacetic acid in solvent-free media, was carried out.

2. A developed process for the transesterification of krill oil with selected phenolic acids, using two immobilized lipases was optimized by central composite rotatable design.

3. The determination of the antioxidant capacity using oxygen radical absorbance capacity and the oxidative stability of esterified edible oils containing phenolic lipids which were obtained by lipase-catalyzed transesterification of phenolic acids with selected edible oils, including flaxseed, fish liver and krill oils, were investigated for the first time.

4. Using Box-Behnken design, this is the first time where a process to yield gelatin/gum arabic multinuclear microcapsules of krill oil via complex coacervation, was optimized.

5. This is the first study where the effects of the presence of the phenolic acid and phenolic lipids in the esterified krill oil on the complex coacervation process were investigated.

TABLE OF CONTENTS

LIST OF FIGURES

Figure Number **Page**

LIST OF TABLES

Table Number **Page**

LIST OF ABBREVIATIONS

AAPH: 2,2'-azobis(2-amidinopropane) dihydrochloride

AAPI: Atmospheric pressure photoionization

ACN: Acetonitrile

ALA: α-linolenic acid

ANOVA: Analysis of variance

p-AnV: *p*-Anisidine value

AOC: Antioxidant capacity

APCI: Atmospheric pressure chemical ionization

API-MS: Atmospheric pressure ionization-mass spectrometry

AS: Agitation speed

ATR: Attenuated total reflectance

AUC: Area under curve

a_w: Water activity

BBD: Box-Behnken design

BET: Brunauer–emmett–teller

BHA: Butylated hydroxyanisole

BHT: Butylated hydroxytoluene

B.P.: Boiling point

BY: Bioconversion yield

CAA: Cellular antioxidant activity

CCRD: Central composite rotatable design

CTB: Clear titration beaker

CV: Coefficient of variation

CWM: Concentration of wall materials

DAGs: Diacylglycerols

DCF: Dichlorofluorescein

DCFH: 2',7'-dichlorofluorescin

DCFH-DA: 2',7'-dichlorofluorescin diacetate

DHA: Docosahexaenoic acid

DHCA: Dihydrocaffeic acid

DHPA: 3,4-dihydroxyphenylacetic acid

DPPH: 2,2-diphenyl-1-picrylhydrazyl

DTGS: Deuterated triglycine sulfate

EE: Encapsulation efficiency

EFAs: Essential fatty acids

EFO: Esterified fish oil

EFSO: Esterified flaxseed oil

EKO: Esterified krill oil

ELSD: Evaporative light-scattering detector

EO: Edible oil

EPA: Eicosapentaenoic acid

ESI: Electrospray ionization

ET: Electron transfer

FA: Fatty acid

FDA: Food and Drug Administration

FFA: Free fatty acid

FID: Flame ionization detector

FO: Fish oil

FOX: Ferrous oxidation-xylenol oxygen

FRAP: Ferric reducing antioxidant power

FSO: Flaxseed oil

FTIR: Fourier transform infrared spectroscopy

GA: Gum arabic

GC: Gas chromatography

GE: Gelatin

GLC: Gas-liquid chromatography

GRAS: Generally regarded as safe

HAT: Hydrogen atom transfer

HP: Hydroperoxide

HPLC: High-performance liquid chromatography

HSH: High-shear homogenizer

IDF: International dairy federation

IP: Isoelectric point

IPA: Isopropanol

KO: Krill oil

LC: Lipase concentration

LLSD: Laser light-scattering detector

Lyso-PtdCho: Lyso-phosphatidylcholine

MA: Malonaldehyde

MAG: Monoacylglycerol

MeOH: Methanol

MS: Mass spectrometry

MUFA: Monounsaturated fatty acid

n: Theoretical plate number

N: Plates per meter

n-6: Omega-6

n-3 FAs: Omega-3 fatty acids

n-3-PUFAs: Omega-3-polyunsaturated fatty acids

-OH: Hydroxyl

ORAC: Oxygen radical absorbance capacity

OSM: Organic solvent media

PA: Phenolic acid

PAC: Phenolic acid concentration

PL: Phenolic lipid

PLU: Propryl laurate units

PtdCho: Phosphatidylcholine

PUFA: Polyunsaturated fatty acid

PV: Peroxide value

R: Resolution

RCW: Ratio of the core material to the wall

RMCD: Randomly methylated β-cyclodextrin

RNS: Reactive nitrogen species

ROS: Reactive oxygen species

RP-HPLC: Reversed-phase high-performance liquid chromatography

RR: Retention rate

RSD: Relative standard deviation

RSM: Response surface methodology

RT: Retention time

SAR: Structure-activity relationship

SB: StableBond

SDG: Secoisolariciresinol diglucoside

SECO: Secoisolariciresinol

SFA: Saturated fatty acid

SFM: Solvent-free medium/Solvent-free media

SP: Stirring speed

STD: Standard deviation

TAG: Triacylgycerol

TBA: Thiobarbituric acid

TBRAS: Thiobarbituric acid-reactive substances

TE: Trolox equivalent

TEAC: Trolox equivalent antioxidant capacity

TLC: Thin–layer chromatography

Trolox: 6-hydroxy-2,5,7,8-tetramethylchroman-2-carboxylic acid

ULP: Ultrasonic liquid processor

UV: Ultraviolet

UV-DAD: Ultraviolet diode array detector

CHAPTER I

INTRODUCTION

There has been growing evidence supporting the nutritional benefits of long-chain *n*-3-polyunsaturated fatty acids (LC *n*-3-PUFAs), in particular eicosapentaenoic acid (EPA, $C_{20:5}$ *n*-3) and docosahexaenoic acid (DHA, $C_{22:6}$ *n*-3), for human health (Kidd, 2007). The human body cannot synthesize these *n*-3-PUFAs *de novo* and they can be obtained by a direct intake from food (Schmitz and Ecker, 2008). Although fish and fish oils are currently the major sources of these PUFAs in the human diet, the declining in such resources of fish has led to the emergence of a new supply on the market, krill oil (Tou *et al*., 2007). The interest in krill oil (KO) was initially due to its important biomass, estimated between 500 to 2,500 million tons (Martin, 2007), and to its being distinct from other marine oils in that most of the EPA and DHA are esterified onto phospholipids. In addition, KO is also rich in naturally-occurring antioxidants, including astaxanthin, which confers to the oil its chromogenic red-orange color (Massrieh, 2008).

Due to their high content in PUFAs, oils of marine origins are among the highly unstable oils (Shahidi and Zhong, 2010). In the presence of air, heat, light and oxidizing agents, PUFAs are prone to oxidation, where the absorbed oxidized lipids in mammals are considered as the main inducers of atherosclerosis (Choe and Min, 2009). For decades, antioxidants have been added to food and food products to control the oxidative processes (de Pinedo *et al*., 2007). In addition to their biological activities, phenolic acids (PAs) are commonly known as natural antioxidants (Balasundram *et al*., 2006); their antioxidant capacity is due to their ability of scavenging the free radicals, by donating hydrogen/electrons and breaking hence the free radical chain reaction (Morton *et al*., 2000). However, the use of PAs in fat and oil systems is limited by their hydrophilic nature (Stamatis *et al*., 2001). One way to improve the solubility and miscibility characteristics of PAs is by their incorporation into triacylglycerols (TAGs) or phospholipids (Akoh and Yee, 1998). This approach could result in the synthesis of novel molecules, phenolic lipids (PLs), that possess nutritional, health and functional benefits (Karam *et al*., 2009). The synthesis of PL esters may be accomplished through lipase-

catalyzed transesterification as an alternative to the conventional chemical processes, which do not meet the necessary requirement for food applications (Lue *et al*., 2005; Sabally *et al*., 2005b). The wide use of lipases in such processes is due to their availability, low cost and selectivity (Gandhi *et al*., 2000).

Research work, carried out in our laboratory, has succeeded in the enzymatic synthesis of structured PLs in organic solvent media (OSM), including lipase-catalyzed esterification of fatty alcohols and PAs (Lue *et al*., 2005), and the transesterification of PAs with acylglycerol models (Sabally *et al*., 2005b; Safari *et al*., 2006) as well as edible oils (EOs), including flaxseed oil (FSO) and fish oil (FO) (Sabally *et al*., 2006a; Sabally *et al*., 2007; Karboune *et al*., 2008; Karam *et al*., 2009). However, a major drawback limiting the enzymatic synthesis at a large scale of PLs in OSM is the low volumetric productivity. One of the most promising approaches consists of using solvent-free media (Dossat *et al*., 2002). With the increasing interest in developing processes in friendly environment, the synthesis of such biomolecules in solvent-free media (SFM) could be beneficial for the food industry. The absence of solvents does not facilitate only the downstream processing and prevent the solvent-induced inactivation of the biocatalyst, it also offers great increase in reactant concentrations and consequently in the volumetric productivity (Yamane, 2005). Recently, work in our laboratory on the enzymatic synthesis of PLs using edible oils, including FSO (Sorour *et al*., 2012a,b) and FO (Sorour, 2010), was successfully carried out in SFM.

The incorporation of PLs in foods and food products, however, could be limited because of their low solubility in the hydrophilic medium (Liu *et al*., 2010) and their oxidative instability (Bustos *et al*., 2003). The entrapment of the PLs within the micron-sized particles could be an effective approach for their protection and delivery into food system, where the complex coacervation involves the electrostatic attraction between two biopolymers of opposing charges (Liu *et al*., 2010). As compared to other technologies, the complex coacervation has been successfully commercialized, since it offers several advantages including higher payload (normally at least 60%), traces of surface oil ($\leq$ 0.02%) and a relatively thick outer shell (Barrow *et al*., 2007). The microencapsulation of the PLs via complex coacervation could be an effective method for their protection,

increasing their shelf life and facilitating their delivery in food products (Champagne and Fustier, 2007).

In order to investigate the individual, combined and cumulative effects of different factors, the response surface methodology (RSM) is considered as an effective statistical technique (Myers *et al*., 2009). Central composite rotatable design (CCRD) is the most appropriate design for response surface optimization (Jeong and Park, 2006); its main advantage is the reduced number of experimental runs, needed to obtain sufficient information for statistically acceptable results. The use of CCRD for optimizing the lipase-catalyzed synthesis of esters has been recently reported (Aybastler and Demir, 2010; Rodrigues and Ayub, 2011). On the other hand, the use of Box-Behnken designs (BBDs), which are a class of rotatable or nearly rotatable second-order designs, is an alternative to the CCRD (Ferreira *et al*., 2007). One distinguishing feature for the BBD is that there are only three levels per factor, whereas in CCRD there are five levels. Another important difference between the two designs is that the BBD has no points on the vertices of the cube and this could be sometimes useful, in particular, when these points are to be avoided for engineering considerations. The use of BBD for optimizing the microencapsulation of lutein has been recently reported (Qv *et al*., 2011).

The present work was aimed at the optimization of synthesis of PLs, obtained by the lipase-catalyzed transesterification of KO with 3,4-dihydroxyphenylacetic acid (DHPA), in SFM as well as their separation, characterization and encapsulation. The specific objectives were as follows:

(1) To develop a chromatographic separation method for the characterization of the components of KO and its esterified PLs, obtained by its enzymatic transesterification with DHPA in SFM.

(2) To develop a process for the enzymatic synthesis in SFM of PLs from KO with DHPA, using the central composite rotatable design (CCRD).

(3) To determine the antioxidant capacity and the oxidative stability of selected esterified edible oils containing PLs which were obtained by the lipase-catalyzed transesterification of PAs with selected EOs, including FSO, FO and KO.

(4) To develop a process for yielding gelatin-gum arabic multinuclear microcapsules of KO, via complex coacervation, using the Box-Behnken design (BBD).

(5) To investigate the effects of the presence of PA and PLs in the esterfied krill oil on the complex coacervation process.

The thesis consists of seven chapters. Chapter one provides a general introduction, whereas Chapter two covers the literature review, related to topics and concepts used to undertake the research work. Chapter three describes the development of chromatographic separation for the characterization of the components of KO and its esterified PLs, obtained by its enzymatic transesterification in SFM with DHPA. Chapter four reports on the optimization of the process of synthesis of these PLs, using CCRD. Chapter five details the determination of the antioxidant capacity and the oxidative stability of the esterified EOs containing PLs, obtained by the lipase-catalyzed transesterification of PAs with selected EOs, including FSO, FO and KO. Chapter six describes the optimization of a process to yield the gelatin/gum arabic multinuclear microcapsules of KO via complex coacervation, using BBD. Finally, the effects of the presence of PA and PLs, in the esterified krill oil, on the complex coacervation process were investigated in Chapter seven.

CHAPTER II

LITERATURE REVIEW

2.1. Introduction

Krill oil (KO) offers a new abundant source of omega-3-polyunsaturated fatty acids (*n*-3-PUFAs) on the market (Massrieh, 2008), in particular eicosapentaenoic acid (EPA, $C_{20:5}$ *n*-3) and docosahexaenoic acid (DHA, $C_{22:6}$ *n*-3), which are widely recognized for their nutritional and health benefits (Kidd, 2007). However, its incorporation in foods is limited because of its low solubility in the hydrophilic medium (Liu *et al*., 2010) and to its instability against oxidation (Bustos *et al*., 2003). The transesterification of phenolic antioxidants into unsaturated lipids could result in the biosynthesis of novel biomolecules, phenolic lipids (PLs) with the combined functional, nutritional and health benefits of both molecules (Karam *et al*., 2009). In addition, the microencapsulation of these PLs could be an effective approach for their protection and their delivery into food systems. The entrapment of the PLs from krill oil within micron-sized particles could increase their use as nutraceuticals and antioxidant additive in food products.

2.2. Krill Oil

2.2.1. Sources

Krill is a Norwegian word that translates into "young fry of fish" and describes a class of marine crustaceans belonging to the order of Euphausiacea (Tou *et al*., 2007). There are 85 species of *Euphausia*; of the different species of krill, only Antarctic krill (*Euphausia superba*) and Pacific krill (*Euphausia pacifica*) have been harvested to any significant degree for human consumption (Martin, 2007). *E*. *superba* is the most studied specie in the literature and lives in the Antarctic Ocean at a depth surface of 500 meter (Tou *et al*., 2007).

2.2.2. Characteristics of Krill Oil

KO is distinct from other marine oils in that the omega-3 polyunsaturated fatty acids (*n*-3-PUFAs) are mainly attached to phospholipids, which make up to 40% of the oil content. Due to their amphiphilic nature, they highly facilitate the passage of fatty acid

(FA) molecules through the intestinal wall (Sampalis *et al*., 2003; Bunea *et al*., 2004; Massrieh, 2008), increasing its bioavailability and ultimately improving the *n*-3: omega-6 (*n*-6) FAs ratio (Cansell *et al*., 2003; Werner *et al*., 2004).

Interest in krill is initially due to its important biomass, estimated to be between 500 to 2,500 million tons (Martin, 2007). Krill are found in oceans worldwide, making them among the most populous animal species (Tou *et al*., 2007). Despite this abundance, the commercial harvest of krill has mainly focused on its use as feed in aquariums, aquaculture and sport fishing. When coupled with a conscientious ecosystem approach for managing krill stocks, their abundance and underutilization make it a long-term sustained food source for humans.

Being at the bottom of the food chain and living in the Antarctic Ocean makes the krill and thus the krill oil (KO) low in heavy metals, dioxins and pesticides (Deutsch, 2007). The contamination of krill with persistent organic pollutant is one of the least among the Antarctic marine organisms, including fish, birds and mammals, which could explain its low position in the trophic chain of these regions (Martin, 2007).

In addition of being a source of EPA and DHA, KO contains natural antioxidants including astaxanthin, vitamins E and A as well as a bioflavonoid similar to 6,8-di-C-glucosyl luteolin but with two or more glucose molecules and one aglycone (Bunea *et al*., 2004; Deutsch, 2007; Massrieh, 2008). The presence of these antioxidants creates a natural protection against oxidation of the oil - a property that does not exist normally in ordinary fish oil (FO) (Massrieh, 2008). The association between these natural inherent antioxidants and phospholipids confers the stability and the antioxidant potency to the oil (Deutsch, 2007; Massrieh, 2008).

2.2.3. Composition of Krill Oil

The method of oil extraction used can have an impact on the yield and on the content of the KO in phospholipids. For instance, the high-pressure extraction of the oil from krill has a limited yield, whereas the supercritical carbon dioxide extraction has a better yield but produces oil deprived of phospholipids. On the other hand, the solvent extraction

presents a better yield and result in oil particularly rich in phospholipids as compared to FOs (Martin, 2007). Consequently, pending on the methodology of extraction used, the content in phospholipids can vary between 40 and 66%, with the remaining being essentially composed of triacylglycerols (TAGs) and a variable quantity of free fatty acids (FFAs) (Martin, 2007). The KO has a dense orange reddish color due to the presence of astaxanthin, with more than 10 mg/100g (Martin, 2007).

The content and profile of KO may vary considerably depending on many factors, including season, species, age, the lag time between capture and freezing, the fishing areas, the richness as well as the nature of the feed of the krill (Tou *et al*., 2007). The content in long-chain polyunsaturated fatty acids (PUFAs) can vary between 28 to 54% by raising the krill with a particular specie of zooplankton (Martin, 2007). Nevertheless, common characteristics can be found, especially the important proportion of long-chain PUFAs with EPA being more abundant than DHA (Martin, 2007). KO is low in both saturated fatty acids (SFAs) (26.1%) and monounsaturated fatty acids (MUFAs) (24.2%), but high in PUFAs (48.5%) (Tou *et al*., 2007). Antarctic KO contains more than 30% of EPA and DHA (Zhu *et al*., 2008). This is not surprising given that krill feed on marine phytoplankton such as single-cell microalgae, which synthesize large amounts of EPA and DHA (Tou *et al*., 2007). The relative abundance of palmitoleic acid ($C_{16:1}$ *n*-7) is also noted (Martin, 2007). Palmitic acid ($C_{16:0}$) is the predominant SFA whereas oleic acid ($C_{18:1}$ *n*-9) is the predominant MUFA (Tou *et al*., 2007).

KO content in phospholipids is predominantly composed of choline-containing phospholipids, mainly phosphatidylcholines (PtdCho) and lyso-phosphatidylcholine (Lyso-PtdCho) (Le Grandois *et al*., 2009; Winther *et al*., 2011). Winther *et al*. (2011) reported the presence of 69 choline-containing phospholipids and confirmed the complexity of the phospholipids composition of KO. The variability in the phospholipids composition of KO reported in literature (Le Grandois *et al*., 2009; Winther *et al*., 2011) may be due to the different composition of the analyzed KO. However, the literature (Le Grandois *et al*., 2009; Winther *et al*., 2011) reported the presence of three PtdChos among the five most prevalent ones, including (16:0–20:5) (16:0–22:6) and (16:0–18:1).

2.2.4. Bioavailability of n-3 FAs from KO

The bioavailability of long-chain *n*-3 FAs is dependent on many factors, including the influence of the type of chemical bond, the matrix effects and the galenic form (Schuchardt and Hahn, 2013). Because of the EPA and DHA are bound to phospholipids in KO, their intestinal digestion and absorption might me more efficient than long-chain *n*-3 FAs linked to TAGs or ethyl esters; The different type of chemical bonds in KO and FO could explain the possible differences reported in literature (Schuchardt and Hahn, 2013) regarding the availability of these long-chain *n*-3 FAs in these oils (Schuchardt *et al*., 2011). Studies (Kling *et al*., 2011; Davidson *et al*., 2012) have shown that ingesting a sufficient amount of fat in a meal improves the efficiency of the digestion and absorption of long-chain *n*-3 FAs. On the other hand, the galenic formulation of the supplement has an influence on the bioavailability of the long-chain *n*-3 FAs (Schuchardt and Hahn, 2013). For instance, Raatz *et al*. (2009) reported that the consumption of long-chain *n*-3 FA oils was significantly more effective in emulsified form as compared to its consumption in the unmodified form.

2.2.5. Potential Health Benefits

Several studies (Bunea *et al*., 2004; Massrieh, 2008; Zhu *et al*., 2008; Tandy *et al*., 2009) have indicated that the consumption of KO may provide benefits in reducing the risk of cardiovascular diseases. The exact mechanisms of action for KO's lipid lowering effects is not yet entirely clear (Bunea *et al*., 2004). The lipid-lowering effect of KO exhibited on the level of the small intestine and on blood lipid could be due to its unique biomolecular profile of EPA and DHA already incorporated into phospholipids as well its abundance in antioxidants (Zhu *et al*., 2008). In addition, KO has been found to be promising in controlling inflammation (Deutsch, 2007; Ierna *et al*., 2010), premenstrual syndrome and dysmenorrhea (Sampalis *et al*., 2003), depression and cognitive disease (Sampalis *et al*., 2003; Massrieh, 2008).

2.3. Oxidation of Fats and Oils

2.3.1. Generality

Lipid oxidation is a complex process, where the rate and the course are influenced by many factors, including the degree of unsaturation and positional distribution of FAs, the

lipid class, the presence of minor components as well as the environmental factors; oils originating from marine origins are among the highly unstable oils due to their high content in PUFAs. PUFAs, including EPA and DHA are highly susceptible to oxidation because of having a high methylene bridge index, which refers to the mean number of bis-allylic methylene position (Shahidi and Zhong, 2010).

2.3.2. Lipid Autoxidation Pathways

Lipid autoxidation occurs through a free radical chain mechanism that includes initiation, propagation and termination steps (Figure 2-1). In autooxidation, fats and oils should be in radical form to react with atmospheric triplet oxygen (Choe and Min, 2006). Normally, lipids are in nonradical singlet state and heat, light, enzymes as well as metal ions/metalloproteins can accelerate their radical formation (Shahidi and Zhong, 2010). The energy required to remove hydrogen from FAs or acylglycerols is dependent on the hydrogen position in the molecules (Choe and Min, 2006). Allylic hydrogen, especially hydrogen attached to the carbon between 2 double bonds, is easily removed due to low bond dissociation and the lowest carbon and hydrogen dissociation energies are at the bis-allylic methylene position (Choe and Min, 2009).

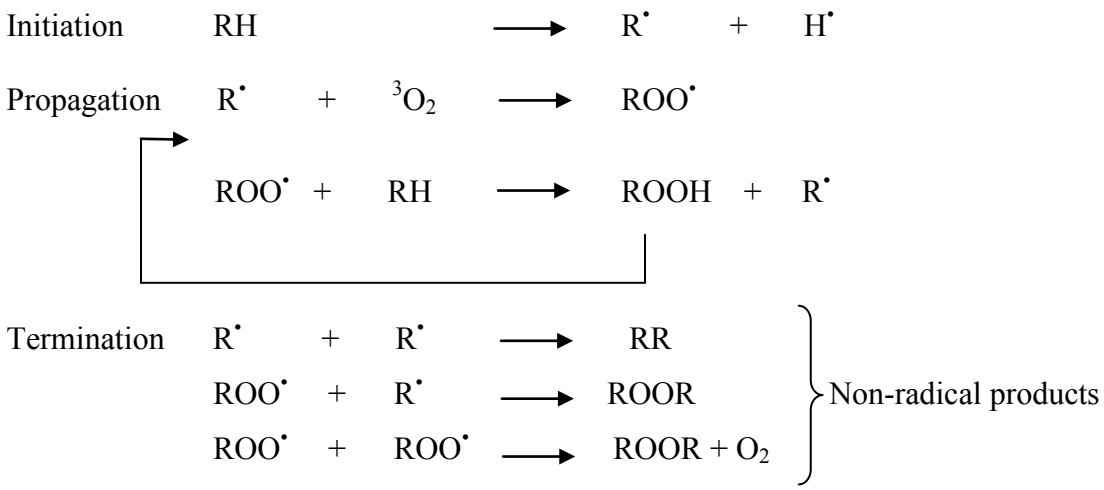

Figure 2-1. Autoxidation reaction, species identification is as follows: lipid, atmospheric triplet oxygen ($^3O_2$), free radicals, ($R^•$ and $H^•$), peroxy radical ($ROO^•$) and non-radical products, including RR, ROOR and hydroperoxides (ROOH).

2.4. Phenolic Compounds

2.4.1. Structure and Sources

Phenolic compounds refer to substances that possess an aromatic ring bearing one or more hydroxyl (-OH) substituent (Lule and Xia, 2005). They are ubiquitous in the plant kingdom with more than 8,000 phenolic structures currently known. Natural polyphenols can range from simple molecules (phenolic acids (PAs), phenylpropanoids, flavonoids) to highly polymerized compounds (lignins, melanins, tannins) (Balasundram *et al*., 2006). Most naturally occurring phenolic compounds are present as conjugates with mono- and polysaccharides, linked to one or more of the phenolic groups, and may also occur as functional derivatives such as esters and methyl esters. Phenolic compounds can basically be categorized in several classes (Lule and Xia, 2005). Of these, PAs, flavonoids and tannins are regarded as the main dietary phenolic compounds. PAs consist of two subgroups, i.e., the hydroxybenzoic with a common structure of C_6–C_1 and hydroxycinnamic acids with a common structure of C_6–C_3 and the predominant PAs in food from plant sources are substituted derivatives of hydroxybenzoic and hydroxycinnamic acids (Figure 2-2) (Balasundram *et al*., 2006). Fruits, vegetables and beverages are the major sources of phenolic compounds in the human diet (Lule and Xia, 2005).

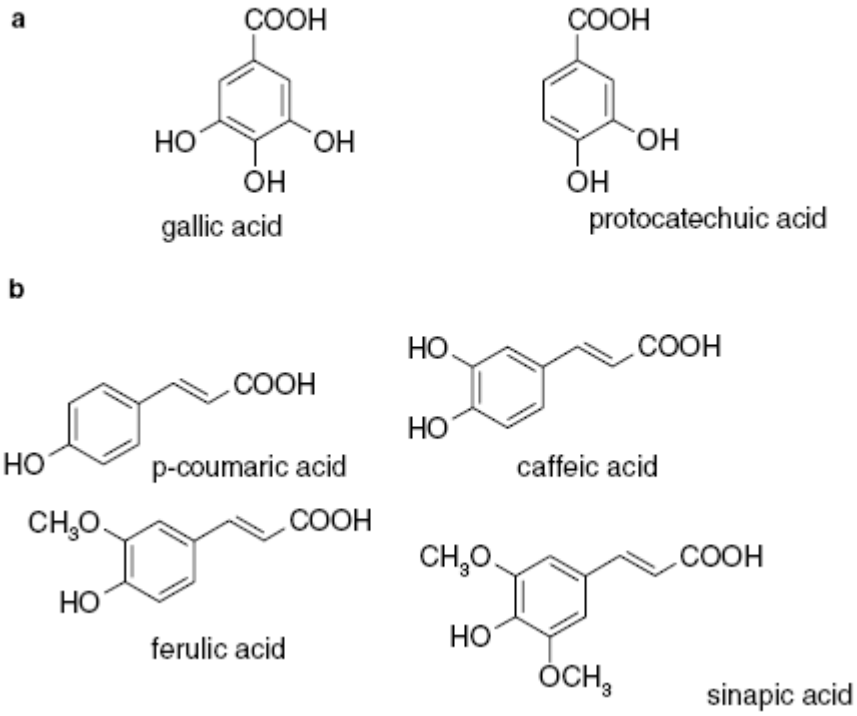

Figure 2-2. Examples of hydroxybenzoic (a) and hydroxycinnamic (b) acids (Balasundram *et al*., 2006)

2.4.2. Bioavailability of Phenolic Compounds

Before the evaluation of the biological activity and the potential nutritional value of phenolic compounds, an understanding of their absorption and bioavailability is critical. In human nutrition, the term "bioavailability" generally defines the efficiency with which nutrients are digested, absorbed and metabolically utilized (Cermak *et al*., 2009). The absorption and metabolism of dietary phenolic compounds is dependent on their structure including their conjugation with other phenolics, degree of glycosylation/acylation, molecular size and solubility (Balasundram *et al*., 2006). It is estimated that relative to the total intake of phenolic compounds, about 5-10% is absorbed in the small intestines. A recent review of the literature (Crozier *et al*., 2010) revealed that the colon may play an important role in the bioavailability of dietary phenolic and polyphenolic compounds. Even when the absorption occurs in the small intestine, substantial quantities pass to the large intestine where the parent compounds and their catabolites will be subjected to the action of colonic microflora. A diversity of colonic-derived catabolites is absorbed into

the bloodstream and passes through the body prior to excretion in urine (Crozier *et al*., 2010).

2.4.3. Functional and Antioxidant Properties

In food, phenolics may contribute to the bitterness, astringency, color, flavor, odor, and oxidative stability of products (Lule and Xia, 2005). However, phenolic compounds exhibit several antinutritional activities by interacting with proteins, carbohydrates, vitamins and minerals. They have the ability to reduce the digestibility of proteins, either by direct precipitation or inhibition of enzyme activity (Balasundram *et al*., 2006). Due to starch-phenol association and phenol-enzyme interaction, polyphenols found in beans and peas has been found to inhibit the activity of amylases *in vitro* and may be responsible for diminishing the overall digestibility of carbohydrates in the intestinal tract of rats (Lule and Xia, 2005). Tannins may precipitate a wide range of essential minerals, thus, lowering their bioavailability, including iron and copper (Balasundram *et al*., 2006). In addition, phenolic compounds can be responsible for off-flavor and enzymatic discoloration of food. The presence of polyphenoloxidase in plant tissues is mainly responsible for spoilage of foods. The phenols undergo oxidation by polyphenoloxidase. The enzyme browning reaction is considered harmful as it causes deterioration of food quality due to browning discoloration and/or development of off-flavor and off-odor (Lule and Xia, 2005).

On the other hand, phenolic compounds exhibit a wide range of physiological properties, such as anti-allergenic, anti-atherogenic, anti-inflammatory, anti-microbial, antioxidant, anti-cancer, anti-viral, anti-thrombotic, cardioprotective and vasodilatory effects (Balasundram *et al*., 2006).

Phenolic compounds, such as flavonoids and PAs can act as antioxidants through many pathways, mainly due to their ability to scavenge free radicals, by donating hydrogen/electrons, thus breaking the free radical chain reaction (Morton *et al*., 2000). The resulting phenoxy radical is relatively stable and this is usually achieved via delocalization of unpaired electrons around the aromatic ring and the lack of appropriate sites for attack by molecular oxygen (Figure 2-3) (Morton *et al*., 2000).

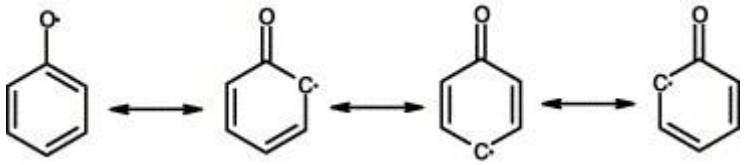

Figure 2-3. Stabilization of phenoxy radical by delocalization.

Phenolic compounds can also chelate metal ions, such as iron and copper and inhibit enzymes involved in the initiation of free radical production process (Balasundram *et al*., 2006). In addition, they have been shown to have effects on cell signaling pathways and on gene expression (Soobrattee *et al*., 2005). They can act as physical barriers to prevent reactive oxygen species (ROS) generation or ROS access to important biological cells (Karadag *et al*., 2009). The structure of phenolic compounds is a key determinant of their radical scavenging and metal chelating activity, and this is referred to as structure-activity relationships (SAR) (Balasundram *et al*., 2006). The number and the position of H-donating -OH groups in relation to the carboxyl functional group, the degree of hydroxylation and the nature of substitutions on the aromatic rings are the main structural features influencing their antioxidant capacity of PAs (Soobrattee *et al*., 2005; Balasundram *et al*., 2006). Phenolic compounds can also quench ROS and reactive nitrogen species (RNS), potentially modifying pathogenic mechanisms relevant to cardiovascular disease. However, the specific mechanisms of how these compounds may affect cardiovascular health and disease still need to be uncovered (Morton *et al*., 2000; Elizabeth *et al*., 2007). The effectiveness of a dietary antioxidant will depend on a number of factors, such as which ROS or RNS is being scavenged, how and where they are being generated and the accessibility of the antioxidant to possible sites of damage (Morton *et al*., 2000).

2.5. Lipases

2.5.1. Generality

Lipases are enzymes that play an important role in fat digestion and metabolism. They are defined as acylhydrolases that cleaves long-chain TAGs into polar lipids. Due to an opposite polarity between the hydrophilic enzyme and their lipophilic substrates, lipase

reaction occurs at the lipid-water interface (Reis *et al*., 2009). Lipases are ubiquitous enzymes that play many biological functions in bacteria, fungi, plants and higher animals. In addition to that, the high versatility of lipases makes them as powerful biocatalysts in numerous industrial processes such as cheese making, oils and fats. They are widely used because of their availability, low cost of production and enormous utility in organic synthesis (Gandhi *et al*., 2000).

2.5.2. Structure and Mechanism of Action

A triad composed of serine, histidine and aspartate characterizes the active site of lipases. This catalytic triad is also found in serine proteases (Reis *et al*., 2009). The lid is the helical oligopeptide unit of lipases that shields the active site. Upon interaction with a hydrophobic interface such as a lipid droplet, the so-called lid undergoes movement in such a way that exposes the active site providing free access for the substrate. This is known as interfacial activation (Gandhi *et al*., 2000). The reaction follows a ping-pong mechanism in which the serine of the lipase is activated by deprotonation, for which histidine and aspartate are required. The nucleophilicity of the -OH residue of serine attacks the carbonyl group of the substrate forming an acyl–enzyme intermediate. The presence of an oxyanion hole contributes to the stabilization of charge distribution and reduction of the ground state energy of the tetrahedral intermediate (Reis *et al*., 2009). The intermediate then reacts with the chiral alcohol which releases the ester and the catalytic site is regenerated (Reis *et al*., 2009).

2.5.3. Lipase-Catalyzed Reactions

Lipases catalyze several types of reactions involving water insoluble esters. These reactions are hydrolysis, esterification and transesterification reactions. The two main categories can be classified as hydrolysis (i) and synthesis (ii). The last three reactions (b, c, d) are often grouped together into the single term transesterification.

(i) Hydrolysis

$$RCOOR' + H_2O \rightleftharpoons RCOOH + R'OH$$

(ii) Synthesis

(a) Esterification

$$RCOOH + R'OH \rightleftharpoons RCOOR' + H_2O$$

(b) Interesterification

$$RCOOR' + R''COOR \rightleftharpoons RCOOR + R''COOR'$$

(c) Alcoholysis

$$RCOOR' + R''OH \rightleftharpoons RCOOR'' + R'OH$$

(d) Acidolysis

$$RCOOR' + R''COOH \rightleftharpoons R''COOR + RCOOH$$

Figure 2-4. Lipase-catalyzed reactions.

2.5.4. Lipase Specificity

The main advantage of lipases that differentiates enzymatic esterification from chemical esterification is their specificity (Willis and Marangoni, 2008). Lipase specificity refers to an enzyme's ability to distinguish between several substrates competing for its active site. Specificity of lipases is controlled by the molecular properties of the enzyme, structure of the substrate and factors affecting binding of the enzyme to the substrate. Lipases display varying degrees of selectivity toward their substrates (Diks and Bosley, 2000). Nearly all lipases have some degree of carboxyl acid selectivity. Based on their specificity or selectivity, lipases can be divided into four classes, (i) regio- or positional specific, (ii) FA type specific and (iii) specific for a certain class of acylglycerols, i.e. mono-, di- or triglycerides and (iv) non-specific (Diks and Bosley, 2000). Positional or regiospecific lipases, such as those from *Rhizomucor miehei* and pancreatic lipase, attack *sn-1,3* position on the triacylglycerol (TAG) molecule (Reis *et al*., 2009). Substrate specificity, regioselectivity and stereoselectivity of the enzyme can be controlled by varying the reaction medium (Gandhi *et al*., 2000). FA type specific lipases catalyze the release of a particular type of FA from the TAGs molecules. Acylglycerols specific lipases such as

potato acylhydrolase (patatin) are specific to monoacylglycerols (MAG) while *Penicillium roqueforti* are specific to TAGs. Non-specific lipase, such as that from *Candida rugosa*, can catalyze the release of free FAs from any position on the glycerol molecule (Diks and Bosley, 2000).

2.5.5. Microbial Lipases

Alloue *et al*. (2007) reported the use of selected commercial immobilized enzymes, Novozym 435, Lipozyme TL IM and Lipozyme IM 60, obtained, respectively, from *Candida antartica*, *Thermomyces lanuginosus* and *Rhizomucor miehei* for the synthesis of lipids and esters.

Inexpensive and nearly commercially developed immobilized lipase, Lipozyme TL IM, obtained from *Thermomyces lanuginosa*, has gradually gained interest in lipid research and in industry. Lipozyme TL IM is a food-grade granulated silica preparation of a microbial 1,3-specific lipase from *T*. *lanuginosa*, produced by submerged fermentation of a genetically modified *Aspergillus oryzae* microorganism. Lipase-catalyzed interesterification between FO and medium-chain TAGs showed that Lipozyme TL IM was stable in a 2-week continuous bioconversion process without any adjustment of water content (Yang *et al*., 2003). A screening of different immobilized lipases showed that Lipozyme TL IM had a higher activity as compared to that of Novozym 435 and Lipozyme IM 60 during the lipase-catalyzed acidolysis between soybean lecithin and caprylic acid under solvent-free conditions (Vikbjerg *et al*., 2006).

Lipozyme IM 20 is a 1,3-specific lipase for interesterification and ester synthesis. It is a lipase from *R*. *meihei*, immobilized on a macroporous ion-exchange resin. On the other hand, Novozym 435 is a lipase from *C*. *antarctica*, produced by submerged fermentation of a genetically modified *Aspergillus oryzae* microorganism and adsorbed on a macroporous resin; this enzyme exhibits broad substrate specificity and is particularly useful in the synthesis of esters and amides. Lipozyme IM 20 and Novozym 435 (Karboune *et al*., 2005; Sabally *et al*., 2005a; Sabally *et al*., 2006a; Sabally *et al*., 2006b; Safari *et al*., 2006; Karboune *et al*., 2008) as biocatalysts have been used in the production of phenolic lipids (PLs) in our laboratory. The enzymatic esterification of

dihydrocaffeic acid (DHCA) with linoleyl alcohol, using immobilized lipases (Lipozyme IM 20 and Novozym 435) was investigated in selected organic solvent media (OSM). Novozym 435 was found to be more efficient for catalyzing the esterification reaction (Sabally *et al*., 2005b). Similar findings were obtained with the enzymatic transesterification of 3,4-dihydroxyphenylacetic acid (DHPA) with FO in organic solvent media (Karam *et al*., 2009).

2.6. Biocatalysis in Non-Conventional Media

2.6.1. Generality

Non-conventional media can be classified as organic system and solvent-free system. In organic systems, the media is composed of substrates and organic solvents. On the other hand, in solvent-free media (SFM), one or more of the substrate(s) form the medium and no other solvent is required.

2.6.2. Biocatalysis of Enzymes in Organic Solvent Media

Lipases can catalyze esterifications and ester hydrolyses in several types of systems including reverse micellar, biphasic and organic systems (Yang and Russell, 1995).

In a reverse micellar system, enzyme molecules are solubilized in discrete hydrated reverse micelles, formed by surfactants, within a continuous phase of a non-polar organic solvent. Under appropriate conditions a reverse micellar solution is homogeneous, thermodynamically stable, and optically transparent (Yang and Russell, 1995). A large amount of enzymatic work has been carried out using reverse micelles composed of nanometer-sized dispersions of aqueous and/or polar material in a lipophilic organic continuum, formed by the action of amphiphilic molecules such as a surfactant (Moniruzzaman *et al*., 2007). Reverse micelles provide excellent lipase substrate contact due to their dynamic nature, enhanced thermal stability of lipase and a considerable interfacial area that enhances the catalytic activity of enzymes (Moniruzzaman *et al*., 2007).

On the other hand, a biphasic system is a system consisting of an enzyme-containing aqueous phase and an organic phase consisting of a water-immiscible organic solvent

(Yang and Russell, 1995). Schneider *et al*. (2009) reported that a useful method for the reduction of lipase denaturation is the use of a biphasic system (water/organic solvent), because the enzyme remains protected in the aqueous phase. Other advantages of the use of enzymes in biphasic systems instead of aqueous media are the solubilization of hydrophobic compounds, the possibility of shifting thermodynamic equilibrium towards the desired reaction and the possibility of re-using the separate phases to increase enzyme turnover numbers (Kraai *et al*., 2008).

In an organic solvent system, solid enzymes preparations (lyophilized or absorbed on an inert support) are suspended in an organic solvent in the presence of enough buffer to ensure activity in the reaction being studied (Yang and Russell, 1995). The use of enzymes, in particular lipases, in OSM rather than in aqueous ones has been the object of numerous studies (Akoh and Yee, 1998). Several advantages, including the shift in thermodynamic equilibrium in favor of synthesis over hydrolysis, increased solubility of non-polar substrates, elimination of hydrolytic side reactions, ease of enzyme and product recovery, increased enzyme thermostability and elimination of microbial contamination due to the low water activity (a_w) of organic solvents, have been suggested (Akoh and Yee, 1998).

2.6.3. Biocatalysis of Enzymes in Solvent-Free Media

The use of organic solvents in enzyme biocatalysis involves higher investment costs to meet safety requirements since they are toxic, hazardous and inflammable (Dossat *et al*., 2002). Hence, a solvent-free system presents several advantages over OSM; these include the elimination of risk of solvent-induced inactivation of biocatalyst as well as environmnental, safety and health issues (Yamane, 2005). Furthermore, the absence of solvent facilitates downstream processing, since fewer components would be present at the end of the reaction, hence, minimizing the production cost. In addition, solvent-free systems offer greater increased reactant concentrations and consequently volumetric productivity (Yamane, 2005). Work in our laboratory (Sorour, 2010; Sorour *et al*., 2012a; Sorour *et al*., 2012b) succeeded in the biosynthesis of PLs from flaxseed oil (FSO) and fish liver oil (FO) with 3,4 dihydroxyphenylacetic acid (DHPA) and dihydrocaffeic acid (DHCA), respectively in SFM.

2.6.4. Parameters Affecting Enzymatic Synthesis

2.6.4.1. Effect of Organic Solvent

The type of organic solvent employed can dramatically affect the reaction kinetics and catalytic efficiency of an enzyme, where the choice of a solvent to be used in biocatalyis is critical. Enzyme activity in organic solvent depends very much on the nature of the solvent since it can cause inhibition and activation of the enzyme (Akoh and Hee Kim, 2008). The polarity of the solvent is an important characterisitic that determines the effect of a solvent on the enzymatic catalysis. Solvent polarity, determined as Log *P* value, is measured by means of the partition coefficient (*P*) of a solvent between octanol and water. The catalytic activity of enzymes in solvent with Log $P < 2$ is usually lower than that of enzymes in solvent with Log $P > 2$; this is due to the fact that the hydrophilic or polar solvents can penetrate into the hydrophilic core of the protein and alter the functional structure (Akoh and Hee Kim, 2008). In addition, the organic solvents can strip off the essential water of the enzyme (Akoh and Hee Kim, 2008). On the other hand, hydrophobic solvents are less able to remove or distort the enzyme-associated water and are less likely to cause inactivation (Akoh and Hee Kim, 2008).

2.6.4.2. Effect of Phenolic Acids Structure

The structure of the phenolic compounds, which are hydroxylated and/or methoxylated derivatives of cinnamic, phenyl acetic and benzoic acids, can have an effect on the bioconversion yield (BY) (Guyot *et al*., 1997; Stamatis *et al*., 2001; Karboune *et al*., 2008; Sorour, 2010).

Guyot *et al*. (1997) investigated the effect of two families of phenolic compounds, the isomers of hydroxycinnamic and benzoic acids as well as the isomers of dihydroxybenzoic acid on the esterification yield, using Novozym 435; the results have shown that the presence of the two -OH groups on the benzene cycle inhibits the esterification of the acid function if the latter is conjugated with the cycle, either by direct bonding on the cycle, benzoic acid, or via a double bond, cinnamic acid.

Stamatis *et al*. (2001) investigated the effect of concentration of various hydroxylated derivatives of cinnamic acid and *o*- and *p*-coumaric acid as well as *o*- and *p*-hydroxylated derivatives of phenylacetic acid on the activity of lipase, from *C*. *antarctica*, in SFM; although the results confirmed that an increase in the aromatic acid concentration resulted in an increase in the reaction rate, the degree of esterification of *p*-coumaric acid was lower than that of hydroxylated derivatives of phenylacetic acid in a similar concentration range. These experimental findings suggest that the lipase inhibiting effect of electron donating substituent conjugated to the carboxylic groups in hydroxylated derivatives of cinnamic acid is strong.

Sabally *et al*. (2006b) investigated the enzymatic transesterification of selected PAs with TAGs, including trilinolein and trilinolenin in organic solvent media (OSM), and reported that the affinity of Novozym 435 was found to be greater for DHCA than that for ferulic acid; these authors suggested that the presence of both the methoxyl substituent and the double bond on the side of the aromatic ring of the ferulic acid could explain its lower affinity for the transesterification reactions with TAG.

Karboune *et al*. (2008) studied the effect of PA structure on the bioconversion yield (BY) of phenolic lipids (PLs) obtained by acidolysis of FSO with selected PAs, including hydroxylated and/or methoxylated derivatives of cinnamic, phenylacetic and benzoic acids in OSM, using Novozym 435 as biocatalyst. The overall findings showed that the BY of PL was dependent on the structural characteristics of PAs. The highest BY was obtained with cinnamic acid (74%). In addition, Karboune *et al*. (2008) concluded that the presence of *p*-OH groups on the benzene cycle of cinnamic acid derivatives may have an inhibitory effect on the lipase activity, since the BY decreased to 45 and 11%, respectively when *p*-coumaric and caffeic acids were used as substrates. The inhibitory effect of *p*-OH substituent was most likely due to their electronic donating effect rather than to their steric hindrance in the enzyme active site as the inhibition was much less significant (56%) in the presence of a double bond on the side chain conjugated with the aromatic ring of DHPA.

Sorour (2010) investigated the effect of the chemical structure of PAs on the transesterification of FSO/FO and selected PAs, including hydroxylated and/or methoxylated derivatives of cinnamic, phenylacetic and benzoic acids in SFM, using Novozym 435 as biocatalyst. The experimental findings showed that the effect of the structure of PAs on the BY of the PLs in SFM was of a less magnitude as compared to that in OSM (Karboune *et al*., 2008).

2.6.4.3. Effect of Reaction Temperature

Temperature changes can affect a wide range of parameters, including enzyme stability, enzyme affinity for the substrate and preponderance of competing reactions (Akoh and Hee Kim, 2008). In general, increasing the temperature increases the rate of interesterification; however, high temperature can reduce the reaction rates due to irreversible denaturation of the enzyme (Stamatis *et al*., 2001). Animal and plant lipases are usually less thermostable than those of microbial sources (Akoh and Hee Kim, 2008). The literature (Lue *et al*., 2005; Tsuzuki, 2005) reported that the optimal temperature for Novozym 435-catalyzed esterification reaction falls within the range of 45 to 60°C. Lue *et al*. (2005) found that an increase in enzymatic activity of Novozym 435 from 17.5 nmol g^{-1} min^{-1} at 35°C to a maximum of 189.95 nmol g^{-1} min^{-1} at 55°C; this increase was followed by a sharp decrease in activity at higher temperatures. Tsuzuki (2005) reported that the optimal reaction temperature for acidolysis reaction by lipase has been found to be 52°C.

2.6.4.4. Effect of pH

Lipases are catalytically active at certain pHs, depending on their origin and the ionization state of residues in their active sites (Akoh and Hee Kim, 2008). While lipases contain basic, neutral acidic residues, the residues in the catalytic site are only active in one particular ionization state. The pH optima for most lipases are over a wide range of acid and alkaline pHs from about 7 to 10 (Willis and Marangoni, 2008). Running an interesterification reaction with lipases at pH far from the optimum can lead to rapid inactivation of the enzyme (Willis and Marangoni, 2008). Studies on the effect of pH on the enzyme activity in OSM show that enzymes remember the pH of the last aqueous solution to which they were exposed (Willis and Marangoni, 2008). Consequently, the

optimum pH of an enzyme in OSM coincides with the pH optimum of the last aqueous solution it was exposed to; this phenomenon is called pH memory (Zacharis *et al*., 1999; Halling, 2000).

2.6.4.5. Effect of Enzyme Concentration

Normally, as the enzyme concentration increases, the reaction equilibrium will be shifted quickly towards the synthesis (Awang *et al*., 2004; Carrín and Crapiste, 2008). In addition, the presence of high enzyme concentration in the reaction medium may increase the probability of its collision with the substrate subsequently enhancing the reaction rate (Kumari *et al*., 2009); however, after reaching certain enzyme concentration, the BY was constant (Awang *et al*., 2004; Carrín and Crapiste, 2008). Awang *et al*. (2004) reported that an excess (> 0.2 g) of Novozym 435 did not increase the esterification yield of oleic acid with oleyl alcohol. In addition, Carrín and Crapiste (2008) reported that during the Lipozyme IM-catalyzed acidolysis of sunflower oil with palmitic acid and stearic acid mixture, the extent of palmitic and stearic acids incorporation was enhanced by increasing the amount of enzyme in the reaction; however, when the enzyme concentration was greater than 8% by weight of substrates, there was no significant increase in the esterification yield.

2.6.4.6. Effect of Agitation Speed

The agitation speed (AS) may decrease the boundary liquid layer surrounding the porous support, resulting in lower diffusional limitations (Almeida *et al*., 1998). Kumari *et al*. (2009) reported that carrying the reaction at the optimum AS can limit the external mass transfer limitations, in the case of immobilized enzymes, where the reactants need to diffuse from the bulk oil to the external surface of the enzyme particles and from there, subsequently to the interior pores of the catalyst. Sorour (2010) investigated the effect of AS on the BY of PLs synthesized from FO and DHCA; the results have shown that the BY increased significantly from 39 to 62.5% when the AS was increased from 50 to 150 rpm, before it was decreased to 44.8% at agitation speed of 250 rpm. The low BY could be attributed to insufficient agitation rate, a condition in which a hydrophilic layer of glycerol may be formed around the enzyme, limiting hence the mass transfer rate of the oil to the surface of the lipase (Sorour, 2010). In addition, the low BY observed with high

AS may be due to the attrition of the particles sticking to the wall or to the shearing of the enzyme molecules (Yadav and Devi, 2004; Kumari *et al*., 2009).

2.6.4.7. Effect of Water Activity

It is well-known that different enzymes require different amounts of water for their optimal activity (Zaks and Klibanov, 1985). Water activity (a_w) is an important parameter used for the characterization of the amount of water in the reaction system (Petersson *et al*., 2007). Although the enzyme needs a film of water to retain its activity, an excess of it results in undesired hydrolysis (Elfman-Borjesson and Harrod, 1999).

The properties of the enzyme are much more influenced by the amount of bound water than by the total water concentration (Petersson *et al*., 2007). It has been reported (Aldercreutz, 2008) that the variations in the activity of a biocatalyst are largely influenced with the thermodynamic water activity or relative humidity (a_w). Thermodynamic a_w can be measured via the vapor phase above the reaction mixture and can be expressed as the partial pressure of the solution over the partial pressure of pure water measured through the vapor phase (Aldercreutz, 2008).

The use of pairs of salt hydrates is a method used for the control of a_w. It is based on the fact that salt hydrates containing different numbers of water molecules are interconverted at fixed a_w (Elfman-Borjesson and Harrod, 1999; Aldercreutz, 2008). The salt hydrates pairs act as a buffer for the water activity control or for optimal water level. Aldercreutz (2008) reported that the a_w, at which lipases express 10% of their maximal activity, was 0.0 to 0.2. Lipases have consistently been reported to tolerate low a_w environments (Aldercreutz, 2008). Sabally *et al*. (2005a) indicated that Lipozyme IM 20 and Novozym 435 need only a small amount of water to maintain their conformation which is required for catalytic activity.

2.6.4.8. Effect of Molecular Sieve

Esterification generates water that can induce hydrolysis, which generally reduces the ester BY; molecular sieve has the capacity to remove water molecules, and this should shift the reaction equilibrium toward esterification; Li *et al*. (2007) indicated that the

reaction yield of the esterification of conjugated linoleic acid with L-carnitine was increased from 38.02% to 56.62 when 150 mg of 4A molecular sieves were used in SFM. From 150 to 200 mg, there was no significant change in the conversion rate. This could be explained by the fact that molecular sieves promote the lipase-catalyzed-synthesis reactions by dehydrating; however, excess of molecular sieves will capture the necessary water of enzyme, which may inhibit the enzyme activity. Karboune *et al*. (2005) reported that the addition of 10 mg/mL molecular sieves to the reaction mixture during the transesterification of cinnamic acid and at triolein ratios of 1:3 and 1:4.5 resulted, respectively, in 28 and 35% decreases in the maximum BY of cinnamoylated lipids.

2.7. Biosynthesis of Phenolic Lipids

2.7.1. Generality

For fats and oils, oxidation is one of the main causes of food deterioration. Oxidized lipids, when absorbed in mammals are considered as the main inducers of atherosclerosis. For decades, antioxidants have been added to food to control the oxidative process and for better food preservation (de Pinedo *et al*., 2007).

Because of their potential in promoting carcinogenesis, the overall demand for synthetic phenolic such as butylated hydroxytoluene (BHT) and butylated hydroxyanisole (BHA) continues to decrease (Lue *et al*., 2005). The development of natural antioxidants became an area of great interest (Karboune *et al*., 2005). In addition to their capacity to act as potential antioxidants, phenolic compounds exhibit a wide range of physiological properties, such as anti-allergenic, anti-artherogenic, anti-inflammatory, anti-microbial, antioxidant, anti-cancer, anti-viral, anti-thrombotic, cardioprotective and vasodilatory effects (Balasundram *et al*., 2006).

However, the use of phenolic acids (PAs) in fat and oil systems is limited by their hydrophilic nature (Stamatis *et al*., 2001). One way to improve or change the solubility and miscibility characteristics of phenolic compounds can be achieved upon their incorporation into TAGs or phospholipids (Akoh and Yee, 1998), which could result in the biosynthesis of novel biomolecules, phenolic lipids (PLs), that possess both nutritional, functional and health benefits (Karam *et al*., 2009).

In nature, PLs, are secondary metabolites that are mainly synthesized by plants, animals, fungi and bacteria, during normal development and in response to stress conditions such as infection, wounds and ultraviolet (UV) radiation. They are much diversified including both simple-ring phenols and their derivatives (Stasiuk and Kozubek, 2010). They can act as antioxidant, antigenotoxic, and cytostatic agents and have the ability to inhibit bacterial, fungal, protozoan, and parasite growth, which may depend on the interaction of PLs with proteins and/or on their membrane-disturbing properties.

The biosynthesis of PL esters may be accomplished through lipase-catalyzed esterification in OSM as an alternative to the conventional chemical processes, which do not meet the necessary requirements for food applications (Lue *et al*., 2005; Sabally *et al*., 2005b).

Research work, carried out in our laboratory, has succeeded in the enzymatic synthesis of structured PLs in OSM, including lipase-catalyzed esterification of fatty alcohols and PAs (Lue *et al*., 2005), and the transesterification of PAs with acylglycerol models (Sabally *et al*., 2005b; Safari *et al*., 2006) as well edible oils (EOs), including FSO and FO (Sabally *et al*., 2006a; Sabally *et al*., 2007; Karboune *et al*., 2008; Karam *et al*., 2009). However, a major drawback limiting the enzymatic synthesis of PLs in OSM at a large scale is the low volumetric productivity. One of the most promising approaches consists of using SFM (Dossat *et al*., 2002). Recently, the enzymatic synthesis of PLs using EOs including FSO (Sorour *et al*., 2012a,b) and FO (Sorour, 2010), was successfully carried out in SFM.

2.7.2. Optimization of the Bioprocess using Response Surface Methodology

Response surface methodology (RSM) is a collection of statistical and mathematical techniques useful for developing, improving and optimizing processes. It has also important application in the design, development, and formulation of new products, as well as in the improvement of existing product designs (Myers *et al*., 2009). The main advantages of RSM are the reduced number of experimental runs needed to provide sufficient information for statistically acceptable data, which results in lower reagent

consumption and considerably less laboratory work (Ferreira *et al*., 2007). It is a faster and a less expensive method for gathering research results than classical one-variable-at-a-time or full-factorial experimentation (Myers *et al*., 2009). RSM consists of an empirical modelization technique, which has been used to evaluate the relation between the experimental and the predicted results. Central composite rotatable design (CCRD) is generally considered the most popular design for response-surface optimization (Jeong and Park, 2006). It combines two-level fractional factorial, central points for which all the factors are at the zero or midrange value and axial points (Figure 2-5a). The Box Behnken designs (BBDs) (Figure 2-5b), which are a class of rotatable or nearly rotatable second-order designs based on three-level incomplete factorial designs, is an alternative to the CCRD (Ferreira *et al*., 2007). One distinguishing feature is that there are only three levels per factor whereas in CCRD there are five levels. Another important difference between the two designs is that the BBD has no points on the vertices of the cube. This is sometimes useful when these points are to be avoided due to engineering considerations. As compared to other response surface designs, BBD has demonstrated to be slightly more efficient than the central composite design but much more efficient than the three-level full factorial designs (Ferreira *et al*., 2007).

`

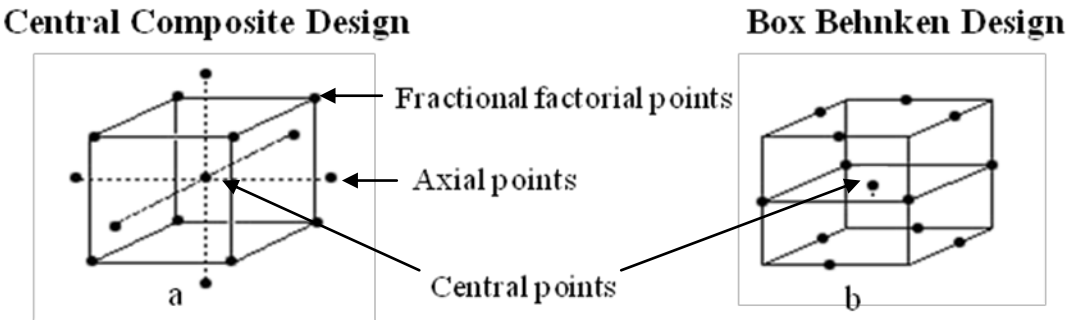

Figure 2-5. Response surface designs, including central composite design (a) and Box-Behnken design (b).

Zheng *et al*. (2009) reported the optimization of PLs synthesis in SFM using RSM, where feruloylated diacylglycerols (DAGs) were synthesized using Novozym 435 by the transesterification of ethyl ferulate intro triolein. In order to optimize the reaction

parameters, including reaction temperature, time, enzyme load, water activity and substrate molar ratio, RSM was applied and a total of 32 experiments were performed. The highest BY obtained was 73.9%.

Rodrigues and Ayub (2011) investigated the effects of substrate molar ratio, enzyme content, and the ratio of *Thermomyces lanuginosus* and *Rhizomucor meihei* in the mixture of the biocatalyst on the transesterification of soybean oil with ethanol, using the central composite design. Under the optimal conditions, the yields of conversion were 90% for transesterification.

Sorour (2010) reported the optimization of PLs in SFM using FO and DHCA. RSM was applied to optimize selected reaction parameters, including temperature, AS, enzyme and phenolic acid concentrations, a_w and Silica gel. The highest BY obtained under these conditions was 86.5%.

Zhang *et al*. (2010a) described the successful production of biodiesel from *Zanthoxylum bungeanum* seed oil with high free FAs by one-step heterogeneous acid-catalyzed esterification followed by heterogeneous alkali-catalyzed transesterification using BBD with three factors, including methanol to oil molar ratio, catalyst amount (%) and reaction time (h). Under the optimum conditions, the conversion to biodiesel reached above 96%.

Qv *et al*. (2011) explored the optimization of process conditions for the encapsulation of lutein, using BBD as statistical model. Under the optimal conditions, the highest encapsulation efficiency (EE) obtained was 85.32%.

2.8. Characterization of Phenolic Lipids

2.8.1. Structural Characterization

Gas-liquid chromatography (GLC) and high-performance liquid chromatography techniques (HPLC) are widely used for both separation and quantification of PLs. Structure elucidation is often achieved using thin–layer chromatography (TLC), a combination of GLC and HPLC with mass spectrometric analysis, and other techniques (Naczk and Shahidi, 2004).

Thin layer chromatography (TLC) is a chromatographic technique used to separate reaction mixtures. The reaction components of the acidolysis reaction between FSO and selected PAs were also separated by TLC on preparative Silica gel 60F plates, with fluorescent indicator (Karboune *et al*., 2008; Karam *et al*., 2009). On the other hand, the separation of lipids resulting from the lipase-catalyzed acidolysis between short chain FAs and triolein was carried on Silica gel 60 plates using chloroform/methanol/acetic acid (8:3:0.1 v/v) (Tsuzuki, 2005).

HPLC is now most widely used for both separation and quantification of phenolic compounds (Naczk and Shahidi, 2004). The separation of the reaction components of the acidolysis and esterification reaction for the synthesis of PLs was performed using a C18 reversed-phased column equipped with an ultraviolet diode array detector (UV-DAD) and a laser light-scattering detector (LLSD) (Safari *et al*., 2006) or an evaporative light scattering detector (ESLD) with an UV-DAD (Karboune *et al*., 2005) and UV-DAD (Lue *et al*., 2005; Sabally *et al*., 2006a; Sabally *et al*., 2006b; Karboune *et al*., 2008; Karam *et al*., 2009; Sorour, 2010).

Lipid analysis has been traditionally difficult by GLC, GLC/mass spectrometry (MS), and HPLC. Gas-chromatography (GC) or GC/MS requires tedious sample pretreatment and derivatization due to low volatility and thermal instability of lipid compounds (Cai and Syage, 2006).

The liquid chromatography/MS simplifies sample preparation procedure by requiring fewer cleanups and avoiding derivatization (Cai and Syage, 2006). Furthermore, liquid chromatography/MS offers higher sensitivity and provides chemical structure information. Electrospray ionization (ESI) and atmospheric pressure chemical ionization (APCI) are two widely used ionization techniques for analysis of polar and less polar compounds by liquid chromatography/MS, and these methods have been used for lipid analysis (Cai and Syage, 2006). However, the analysis of nonpolar compounds can often be difficult by ESI and APCI. Atmospheric pressure photoionization (APPI) is a recently introduced technique that extends the range of ionizable compounds. APPI is gaining its popularity mainly due to its ability to ionize those compounds that are often missed or are

not readily ionized by ESI and APCI (Cai and Syage, 2006). The molecular structures of phenolic lipids were characterized using HPLC interfaced to atmospheric pressure chemical ionization-mass spectrometry (APCI-MS) (Karboune *et al*., 2005; Sabally *et al*., 2006a; Sabally *et al*., 2006b; Safari *et al*., 2006; Karam *et al*., 2009; Sorour, 2010).

GLC is used for separating and analyzing compounds that can be vaporized without decomposition (Naczk and Shahidi, 2004). FAs composition of the FO and of the phenolic mono- and diacylglycerols (DAGs), recovered by the preparative TLC, was investigated using GLC. The FA methyl esters were subjected to GLC analysis, using a chromatography system equipped with a flame ionization detector (FID) and a splitless injector (Karam *et al*., 2009; Sorour, 2010).

Many lipid systems have been studied by Fourier transform infrared spectroscopy (FTIR) in order to determine several aspects including the degree and the form of unsaturation of the acyl groups as well as their length (Nilsson *et al*., 1991; Mitra and Bhowmik, 2000). The infrared region of the electromagnetic spectrum extends from 14,000 to 50 cm^{-1} and is divided into three areas; the far-infrared from 400 to 50 cm^{-1}; the mid-infrared region from 4,000 to 400 cm^{-1} and the near-infrared from 14,000 to 4,000 cm^{-1} (Guillén and Cabo, 1997). The mid-infrared spectroscopy has been commonly used for the structural characterization of EOs because some atoms display characteristic vibrational absorption frequencies in this infrared region of the electromagnetic spectrum (Guillén and Cabo, 1997; Vlachos *et al*., 2006). Vlachos *et al*. (2006) reported that FTIR was an effective analytical tool to determined extra virgin oil adulteration as well as to monitor the oxidation of corn oils samples during heating or/and exposure to ultraviolet radiation.

.

2.8.2. Antioxidant Capacity

Antioxidant capacity (AOC) is related to compounds capable of protecting a biological system against the adverse effects of processes or reactions involving ROS and RNS (Karadag *et al*., 2009). In complex heterogeneous foods and biological systems, many factors, including the partitioning properties of the antioxidants between lipid and aqueous phases, the oxidation conditions and the physical state of the oxidizable substrate affects the AOC of a compound to the extent that antioxidant protection significantly

changes according to the substrate used to conduct the evaluation (Karadag *et al*., 2009). In addition, the response of antioxidants to different radical or oxidant sources may be different (Prior *et al*., 2005).

On the basis of the inactivation mechanism involved, the major AOC methods are based on the ability of the antioxidants of hydrogen atom transfer (HAT) or electron transfer (ET) (Laguerre *et al*., 2007). The two major factors that determine the mechanism and efficiency of antioxidants are the bond dissociation energy and the ionization potential. ET and HAT mechanisms almost occur together in all samples and their difference can be made difficult (Karadag *et al*., 2009).

HAT-based methods tend to be more relevant to the radical chain-breaking AOC and they measure the classical ability of an antioxidant to scavenge free radicals by hydrogen donation to form stable compounds (Prior *et al*., 2005).

$$AH + X^{\bullet} \rightarrow XH + A^{\bullet} \qquad \ldots\ldots\ldots\ldots\ldots\ldots \text{(2-1)}$$

The relative reactivity in HAT methods is determined by the bond dissociation energy of the H-donating group in the potential antioxidant. The antioxidant reactivity is based on competition kinetics (Prior *et al*., 2005). While HAT reactions are usually quite rapid and typically completed in seconds to minutes, they tend to be solvent and pH dependent. In addition, the presence of reducing agents, including metals can lead to erroneously high apparent reactivity (Karadag *et al*., 2009).

On the other hand, ET-based methods detect the ability of a potential antioxidant to transfer one electron to reduce any compound, including metals, carbonyls and radicals (Prior *et al*., 2005).

$$AH + X^{\bullet} \rightarrow X^{-} + AH^{\bullet+} \qquad \ldots\ldots\ldots\ldots\ldots\ldots \text{(2-2)}$$

The relative reactivity in ET methods is based primarily on deprotonation and ionization potential. ET reactions are usually slow and can require long times to reach completion.

Consequently, the measure the relative percent decrease in product rather than kinetics or total AOC (Karadag *et al*., 2009).

When $AH^{\bullet+}$ has a sufficient lifetime, secondary reactions become a significant interference in assays and can even lead to toxicity or mutagenicity *in vivo*. ET assays are very sensitive to ascorbic and uric acids, which are important in maintaining plasma redox tone. Unfortunately, trace compounds and metals interfere with ET methods and can account for high variability and poor reproducibility *in vivo* assays (Prior *et al*., 2005).

The most commonly used methods include trolox equivalent antioxidant capacity (TEAC), ferric reducing antioxidant power (FRAP), oxygen radical absorbance capacity (ORAC), 2,2-diphenyl-1-picrylhydrazyl (DPPH). The following are examples of the some of the most frequently used simple *in vitro* models for the evaluation of total antioxidant activity (Tsao and Deng, 2004).

The DPPH assay is based on the measurement of the reducing ability of antioxidants toward $DPPH^{\bullet}$, one of the few stable organic nitrogen radicals. The percentage of remaining $DPPH^{\bullet}$ is proportional to the antioxidant concentration, and the concentration that causes a decrease in the initial $DPPH^{\bullet}$ concentration by 50% is defined as IC_{50} (Prior *et al*., 2005). Although the $DPPH^{\bullet}$ assay is considered to be a simple and rapid one, its use to measure AOC is associated with many drawbacks mainly the radical itself does not bear any similarity to the highly reactive and transient peroxyl radicals, involved in the lipid peroxidation and its absorbance is decreased by light, oxygen and solvent type (Karadag *et al*., 2009).

The antioxidant activity of potato peel extract using free radical method was found to be comparable to butylated hydroxytoluene (BHT), potato peel extract showed excellent antioxidant activity as determined by its radical scavenging activity of DPPH (Kanatt *et al*., 2005). In addition, cinnamic acid, DHCA and their ethyl esters have shown to have radical scavenging activity towards the free radical $DPPH^{\bullet}$; however, their PL esters demonstrated a lower scavenging activity than that with the PA component, but very

close to that of the α-tocopherol (Karboune *et al*., 2005; Sabally *et al*., 2006b; Sabally *et al*., 2006a; Sabally *et al*., 2007; Karam *et al*., 2009; Sorour, 2010). Choo *et al*. (2009) reported that based on the ratio of a substrate to DPPH concentration, the lipophilized products, obtained by the lipase-catalyzed transesterification of FSO with ferulic acid and not with cinnamic acid, were able to provide an enhanced AOC for the FSO.

The oxygen radical absorbance capacity (ORAC) method is becoming widely used for assessing AOC in biological samples and food (Prior *et al*., 2003). The ORAC method is based on the inhibition of a peroxyl-radical induced oxidation initiated by thermal decomposition of azo-compounds, like 2,2'-azobis(2-amidinopropane) dihydrochloride (AAPH) (Prior *et al*., 2003). The protective effect of an antioxidant in ORAC assay is measured by the net area under the curve (AUC) of the sample compared to that of blank ($AUC_{sample}-AUC_{blank}$) and stands for lag time, initial rate, and total inhibition in a single value (Karadag *et al*., 2009).

ORAC assay has several advantages including the capability of employing different radical generators or oxidants as well as following the reaction for extended time avoiding underestimation of AOC. In addition, it operates well for both antioxidants that exhibit distinct lag phase and those that have no lag phase (Karadag *et al*., 2009). On the other hand, one of the original limitations of this method is due to its inability to determine both hydrophilic and lipophilic antioxidants (Huang *et al*., 2002). Huang *et al*. (2002) developed a method for lipophilic antioxidants using randomly methylated β-cyclodextrin (RMCD) as a solubility enhancer. Prior *et al*. (2003) validated the use of ORAC assay for lipophilic antioxidants using RMCD in plasma or serum. Another limitation is that the ORAC reaction is temperature sensitive (Karadag *et al*., 2009). Zheng and Wang (2002) studied the activity-structure relationships of flavonoids and PAs, using the ORAC assay of selected berry crops and suggested that the contribution of individual phenolics to the total AOC is generally dependent on their structures and the content in the berries.

However, none of these *in vitro* assays do reflect the cellular physiological conditions and do consider the bioavailability and the metabolism issues (Liu and Finley, 2005). While

animal models and human studies are the best methods for determining the actual efficacy of antioxidants in the body, they tend to be expensive and are not suitable for initial screening antioxidant screening in foods (Liu and Finley, 2005). The cellular antioxidant activity (CAA) assay was developed to measure the antioxidant activity of antioxidants, dietary supplements and foods in cell culture (Song *et al*., 2010). The CAA assay utilizes 2',7'-dichlorofluorescin diacetate (DCFH-DA) as a probe in cultured human HepG2 liver cancer cells. Non-polar DCFH-DA is taken by the cells by passive diffusion and deacetylated to form the polar 2',7'-dichlorofluorescin (DCFH) which is trapped within the cells which is easily oxidized to the fluorescent dichlorofluorescein (DCF). This method measures the ability of compounds to prevent the formation of DCF by 2,2'-azobis (2-amidinopropane)-generated peroxyl radicals in human hepatocarcinoma HepG2 cells. The decrease in cellular fluorescence when compared to the control cells indicated the AOC of the compounds (Song *et al*., 2010). Song *et al*. (2010) reported that the CAA values correlated significantly with the total phenolic content and this method is more biologically representative than the popular chemistry AOC measures.

2.8.3. Methods for Measuring Lipid Oxidation

2.8.3.1. Generality

Numerous analytical methods are available for the measurement of lipid oxidation in foods. These methods can be classified into five groups depending on what they measure and includes the absorption of oxygen, the loss of initial substrates, the formation of free radicals as well as primary and secondary oxidation products (Dobarganes and Velasco, 2002).

2.8.3.2. Measurement of Primary Oxidation Products

2.8.3.2.1. Generality

Analytical methods for measuring hydroperoxides (HPs) in fats and oils can be classified as those measuring the total amount of HPs and those based on chromatographic technique. The latter provides detailed information on the structure and the amount of specific HPs present in a certain oil sample (Dobarganes and Velasco, 2002). The peroxide value (PV) is an indicator of the initial stages of oxidation. It represents the total HP content and is one the most common quality indicators of fats and oils during

production and storage. The most frequently used methods for the determination of PV are the iodometric titration and ferric ion complex spectrophotometry methods (Shahidi and Zhong, 2005).

2.8.3.2.2. Iodometric Titration

Traditionally, the iodometric titration method has been the preferred method for the measurement of hydroperoxides (HPs) as PV. It is based on the oxidation of iodide ion (I^-) by HPs. The PV is reported as milliequivalents of oxygen per kilogram of sample (meq/kg) (Dobarganes and Velasco, 2002). However, this method is associated with many drawbacks; the procedure is time-consuming and labor intensive and this technique requires a large amount of sample and generates a significant amount of waste. Lack of sensitivity, possible interferences and difficulties in determining the endpoints are also other limitations (Shahidi and Zhong, 2005). To overcome these disadvantages, techniques including potentiometric endpoint determination and spectrophotometric determination have been proposed (Dobarganes and Velasco, 2002).

2.8.3.2.3. Ferric Iron Complexes

To overcome several of the drawbacks associated with the traditional iodometric titration method, chemical methods based on the oxidation of ferrous ion (Fe^{2+}) to ferric ion (Fe^{3+}) in an acidic medium and the formation of iron complexes have been developed (Shantha and Decker, 1994). These methods spectrophotometrically measure the ability of lipid HPs to oxidize Fe^{2+} to Fe^{3+}, which are complexed by either thiocyanate in the International Dairy Federation (IDF) method or xylenol orange in the ferrous oxidation-xylenol orange (FOX) methods (Hornero-Méndez *et al*., 2001).

The ferric thiocyanate is a red-violet complex that shows strong absorption at 500-510 nm (Dobarganes and Velasco, 2002). The ferric thiocyanate method for PV determination in edible oils is simple, reproducible and considered more sensitive than the standard iodometric titration method (Shahidi and Zhong, 2005). It has been used to measure lipid oxidation in milk products, fats, oils and liposomes (Dobarganes and Velasco, 2002). However, pigments including carotenoids, present in the oil, can cause strong interferences since they absorb in the same wavelength region used to determine PV. To

overcome this problem, Hornero-Méndez *et al*. (2001) modified the Shantha and Decker method by using diethyl ether to extract the pigments after oxidation reaction has completed, so that it could be applied to samples with high carotenoid content (Hornero-Méndez *et al*., 2001).

The ferrous oxidation of xylenol orange forms a blue-purple complex that shows maximum absorption at 550-600 nm. This method, originally developed to detect very low levels of HP in tissues, is rapid and inexpensive. It is not sensitive to ambient oxygen or light and there is a good agreement that exists between the results obtained with the FOX assay as compared to the iodometric method (Dobarganes and Velasco, 2002). However, accurate measurements require knowledge of the nature of peroxides present in the sample and careful control of the conditions used because of the apparent molar absorption coefficient is dependent on many factors, including the amount of sample, the solvent used and the source of xylenol orange (Shahidi and Zhong, 2005).

2.8.3.3. Measurement of Secondary Oxidation Products

2.8.3.3.1. Generality

The primary oxidation products of lipids, HPs, tend to be relatively stable at room temperature in the absence of metals. However, in the presence of metals and high temperature, they breakdown to a wide range of secondary oxidation products, including aldehydes, ketones, alcohols, hydrocarbons, volatile organic acids and epoxy compounds (Choe and Min, 2006). Methods for assessing secondary oxidation products tend to focus on a single compound or group of compounds. The thiobarbituric acid (TBA) test and *p*-anisidine value (*p*-AnV) will be discussed below.

2.8.3.3.2. TBA Test

The TBA test is considered one of the most extensively used methods for the detection of the oxidation of fat-containing foods. As a result of the degradation of PUFAs, malonaldehyde (MA), a minor component of FAs with three or more double bonds is formed. In this assay, the MA reacts with TBA to form a pink complex that is measured at 530-535 nm. The extent of oxidation is reported as the TBA value which is expressed as of MA equivalents per kilogram sample or as micromoles of MA equivalents per gram

of sample (Shahidi and Zhong, 2005). Despite the fact that the TBA assay lacks sensitivity and specificity, it provides a good mean for evaluating lipid oxidation, especially on a comparative basis. The main limitation arises from the ability of several compounds to react with the TBA reagent and hence contributing to an overestimation of the intensity the color of the complex (Heras *et al*., 2003).

2.8.3.3.3. *p*-Anisidine Value

The *p*-anisidine value (*p*-AnV) method measures the content of aldehydes, mainly 2-alkenals and 2,4-alkadienals, which are generated during the decomposition of HPs. The reaction of the p-anisidine reagent with aldehydes under acidic conditions gives yellowish products that absorb at 350 nm (Doleschall *et al*., 2002). The color is quantified and converted to *p*-AnV which is defined as the absorbance of a solution resulting from the reaction of 1 g of fat in isooctane solution (100 mL) with *p*-anisidine (0.25% in glacial acetic acid) (Shahidi and Zhong, 2005). In this assay, the unsaturated aldehydes absorb more strongly at this wavelength than saturated aldehydes making this test more sensitive to unsaturated aldehydes (Gordon, 2001; Shahidi and Zhong, 2005). Guillén and Cabo (2002) reported that *p*-AnV may be only comparable within the same oil type because initial AnV varies among oil sources. For instance, oils with high levels of PUFAs might have higher AnV even when fresh (Shahidi and Zhong, 2005). In bulk oils, *p*-AnV is more commonly used than the TBA assay. In addition, *p*-AnV is less frequently used in North America but widely used in Europe as part of the Totox number, which combines both PV and *p*-AnV as follows:

$$\text{Totox value} = 2\text{PV} + p\text{-AnV} \qquad \ldots\ldots\ldots\ldots\ldots\ldots \quad (2\text{-}3)$$

However, Totox value has no scientific basis because it is a combination of two indicators with different dimensions (Shahidi and Zhong, 2005).

2.9. Encapsulation of Bioproducts

2.9.1. Generality

In encapsulation, components, referred to as the core, are packaged within a secondary material (referred to as the wall material or the encapsulant) and delivered in small

particles (Sanguansri and Augustin, 2006). The size of particles formed through encapsulation may be classified as macro (> 5000 μm), micro (1.0-5000 μm) and nano (< 1.0 μm). Capsules below 1.0 μm in size are frequently referred to as nanocapsules, which are often made by very specialized nanoencapsulation methods (Jafari *et al*., 2008).

2.9.2. Microencapsulation of Edible Oils

Krill oil (KO) contains highly unsaturated lipids, EPA ($C_{20:5}$ *n*-3) and DHA ($C_{22:6}$ *n*-3) as well as astaxanthin, which are prone to oxidative degradation (Bustos *et al*., 2003). In addition, the incorporation of KO in foods is limited because of its low solubility in the hydrophilic media (Liu *et al*., 2010).

Microencapsulation could be an effective method for the oxidative stabilization of EOs and is used for the protection and the delivery of functional lipids in food applications (Champagne and Fustier, 2007). Microencapsulation could be defined as the technology of packaging solid, liquid or gaseous materials in small capsules which may release their contents at controlled rates over prolonged periods of time (Champagne and Fustier, 2007).

A wide range of natural or synthetic materials can be selected for the encapsulant materials depending on the desired properties of the final microcapsule. The encapsulant materials, used for food products, are more restricted to natural food components such proteins, sugars, starches, gums, lipids, cellulosic material and other ingredients that have Generally Regarded as Safe (GRAS) status; these materials include cyclodextrin, chitosan and low-molecular weight emulsifiers (Champagne and Fustier, 2007).

There are several methods that can be used for microencapsulation, where each one of them depends on the required format and inherent properties of the bioactive core and the encapsulant materials used (Champagne and Fustier, 2007). Current technologies used in the food industry for the *n*-3 microencapsulation include spray-dried emulsions, complex coacervation, gravity flow dry blending, co-extrusion, fluid bed coating and liposomes (Barrow *et al*., 2007).

For several decades, microencapsulation by spray-drying has been applied in the food industry and is still the predominating technology as it is rather inexpensive, straightforward, the machinery are available, it has the ability to handle heat-sensitive materials and the microcapsules have good keeping qualities (Drusch *et al*., 2006b). However, this technology is associated with several limitations, including large particle size, low oil payload (<30%), high surface oil. Spray-dried emulsions have some success in short shelf-life products such as bread but have not been successful in a broad range of food products due to their poor sensory and stability characteristics (Barrow *et al*., 2007).

On the other hand, Ocean Nutrition Canada's MEG-3 powder, produced using complex coacervation, is the most successful powder in terms of performance in a variety of food products (Barrow *et al*., 2007) Complex coacervation involves the electrostatic attraction between two biopolymers of opposing charges (Liu *et al*., 2010). As compared to other technologies, complex coacervation has been successfully commercialized, since it offers several advantages including higher payload (normally at least 60%), traces of surface oil (≤ 0.02%) and a relatively thick outer shell (Barrow *et al*., 2007).

The microcapsules, obtained by coacervation, can be divided into mononuclear microcapsules, which are formed when a given oil is encapsulated by coacervates, and multinuclear microcapsules that are formed by the aggregation of multiple mononuclear ones (Dong *et al*., 2007). Spherical multinuclear microcapsules have been found to possess better controlled-release characteristics than their mononuclear counterparts (Dong *et al*., 2007; Dong *et al*., 2011).

The literature (Prata *et al*., 2008; Liu *et al*., 2010; Dong *et al*., 2011; Qv *et al*., 2011) reported that the gelatin-gum arabic is the most investigated system in the formation of complex coacervation, where its use as a delivery matrix has many advantages including its abundance, biodegradability and oxygen impermeability (Liu *et al*., 2010). Because of the dietary and religious customs limitations, which may prevent the use of porcine gelatin, kosher-certified beef gelatin and fish gelatin can be used as alternatives (Karim and Bhat, 2008).

During the complex coacervation process, the formed coacervates are usually cross-linked and hardened by the addition of a chemical agent (Prata *et al*., 2008). Glutaraldehyde is a chemical agent used in protein cross-linking, and promotes covalent binding between amino groups, which is irreversible and resistant to extreme conditions of pH and temperature. However, glutaraldehyde presents high toxicity preventing its use in food products (Alvim and Grosso, 2010). Other alternatives include transglutaminase which promotes cross-linking among proteins resulting in the formation of intra and intermolecular ε-(γ-glutamyl) lysine bonds (Alvim and Grosso, 2010) and genipin. Genipin is a naturally occurring cross-linking agent that may be obtained from its parent compound, geniposide, which may be isolated from the fruits of *Gardenia jasminoides Ellis* whose cytotoxicity, feasibility and biocompatibility is well studied (Sung *et al*., 1999).

Bustos *et al*. (2003) evaluated chitosan as a microencapsulation material for the oxidative stabilization of Antarctic krill oil (KO) in microparticulate aquaculture feed, using the emulsification-ionotropic gelation method. When compared to oil/water dispersion, the results show that long-chain PUFAs were not significantly stabilized in the chitosan microcapsules. The stabilizing effect was more important on astaxanthin pigments than on PUFAs and degradation was slower in the microcapsules prepared with low molecular weight chitosan.

Drusch *et al*. (2006b) investigated the microencapsulation of FO, with 33% *n*-3 FAs, by its spray-drying in a matrix of *n*-octenylsuccinate-derivatized starch with either glucose syrup or trehalose; the results showed that there were no differences between the various matrices used in the physicochemical properties as determined by measurement of particle size, oil droplet size, true density and Brunauer–emmett–teller (BET) surface. In addition, trehalose was found to be more suitable as wall material for microencapsulation than glucose syrup, since the results showed that the lipid oxidation decreased upon storage at low relative humidity (Drusch *et al*., 2006b).

Kolanowski *et al*. (2006) investigated the effect of spray drying on oxidative stability of dried microencapsulated FO, coated with modified cellulose; these authors showed that

spray drying did not significantly protect FO against oxidation in comparison to bulk FO; these authors also reported that modified celluloses, especially methylcellulose can be used as an alternative material for FO microencapsulation.

Qv *et al*. (2011) explored the optimization of process conditions for the encapsulation of lutein, using BBD as statistical model; the authors reported that pH had a significant linear and quadratic effects on the EE of lutein since it controls the balance of macromolecules charges hence influencing the intensity of the electrostatic interactions driving the formation of complexes between the two biopolymers. In addition, the encapsulation of lutein improved its ability to resist to light and temperature.

Liu *et al*. (2010) carried out the optimization of the encapsulation of FSO using complex coacervation, in the absence of cross-linking agent. The formed microcapsules had an EE of 84% and showed a protective effect against the production of primary and secondary oxidative products as compared to the bulk oil after storage 25 days at room temperature. In addition, the microcapsules had sufficient stability to maintain their structure in the absence of a cross-linker.

Alvim and Grosso (2010) investigated the influence of the type of reticulation, including glutaraldehyde as well as transglutaminase and the drying process, including spray-drying and freeze-drying on the release properties of a mixture of paprika oleoresin and soybean oil encapsulated by complex coacervation. Lyophilized capsules without cross-linking were able to maintain their integrity, whereas only cross-linked samples kept their structure after spray drying.

CHAPTER III

STATEMENT OF CHAPTER III LINKAGE

Although the method of analysis of phenolic lipids (PLs), obtained with fish and flaxseed oils, has already been developed and established in our laboratory, the presence of high levels of phospholipids in krill oil (KO) required further development for such methodology. Chapter III covers the development of a high-performance liquid chromatography (HPLC) method for the separation of a complex mixture of triacylglycerols (TAGs) and phospholipids of KO as well as its esterified PLs. In addition, the synthesized PLs molecules were characterized, using Fourier transform infrared spectroscopy (FTIR) as well as mass spectrometry (MS).

CHAPTER III

CHROMATOGRAPHIC SEPARATION OF SYNTHESIZED PHENOLIC LIPIDS FROM KRILL OIL AND DIHYDROXYPEHNYL ACETIC ACID

3.1. Abstract

The separation and characterization of novel biomolecules, phenolic lipids (PLs), obtained by the enzymatic transesterification in organic solvent-free media (SFM) of krill oil (KO) with 3,4-dihydroxyphenylacetic acid (DHPA) were investigated. The experimental findings showed that by increasing the polarity of the gradient eluent and by decreasing the solvent strength of the mobile phase, from methanol (MeOH) to acetonitrile (ACN), a higher resolution was obtained. The use of a shorter column and smaller particle packing size resulted in an enhancement of the efficiency, with decreases in both separation time and solvent consumption. Overall, the evaporative light-scattering detector (ELSD) showed better repeatability of the resolution (R), theoretical plate number (n), plates per meter (N) and the retention time (RT) values as compared to that of the ultraviolet (UV) detection at 210 and 280 nm. In terms of detection and repeatability, ELSD was shown to be a more appropriate tool for the quantitative analysis of the components of KO and its esterified PLs than UV detection. Fourier transform infrared spectroscopy (FTIR) analysis tentatively confirmed the nature of the separated compounds. In addition, the structural analyses of novel biomolecules by high-performance liquid chromatography-mass spectrometry-atmospheric pressure chemical ionization/electrospray ionization (HPLC-MS-APCI/ESI) suggested the formation of two phenolic monoacylglycerols (MAGs).

3.2. Introduction

Fish oils (FOs) are the major sources of eicosapentaenoic acid (EPA, $C_{20:5}$ *n*-3) and docosahexaenoic acid (DHA, $C_{22:6}$ *n*-3) in the diet. However, increasing consumption rate and declining resources of fish have necessitated the search for new sources (Tou *et al*., 2007). KO is distinct from other marine oils in containing up to 40% of phospholipids.

Although phenolic acids (PAs) are commonly known as natural antioxidants (Balasundram *et al*., 2006) and have been described to have various other biological activities (Stasiuk and Kozubek, 2010), their hydrophilic nature limits their solubility in hydrophobic medium and consequently reduces their potential use in fats and oils (Sabally *et al*., 2006a). The incorporation of PAs into unsaturated lipids could result in the biosynthesis of novel biomolecules, PLs, with potential functional, nutritional and health benefits (Karam *et al*., 2009). Research work in our laboratory (Karam *et al*., 2009; Sorour, 2010) showed that the enzymatic transesterification of endogenous edible oil (EO) with PA models resulted in PLs of variable polarities.

Although the method of analysis of PLs, obtained with fish (FO) and flaxseed (FSO) oils, has been developed already and established in our laboratory (Sabally *et al*., 2006a; Karam *et al*., 2009), the presence of high levels of phospholipids in KO required further development for such methodology. Hence, the development of an analytical method for the separation and characterization of the components of such complex is essential to unravel the lipid profiles of PLs (Peterson and Cummings, 2006).

The use of new column technologies with smaller particle sizes often enables faster separation with the same or similar resolution (Zweigenbaum *et al*., 1999; Chen and Kord, 2009) and significant waste reduction (Chen and Kord, 2009; Welch *et al*., 2010). In order to minimize cost and waste disposal problems, decreasing solvent consumption is becoming increasingly important.

The aim of the present work was to develop and to validate a well repeatable and efficient solvent-saver separation method for the characterization of a complex mixture of KO components as well as for those of esterified PLs, obtained by its enzymatic transesterification with selected PAs.

3.3. Materials and Methods

3.3.1. Separation of Krill Oil Components and Its Esterified Phenolic Lipids

3.3.1.1. High-Performance Liquid Chromatography Analysis

The high-performance liquid chromatography (HPLC) separation of KO components as well as those of esterified PLs was carried out, using a 32 Karat software version 8.0 (Model 126, Beckman Instruments Inc., San Ramon, CA) equipped with an autosampler (Model 507), with dual detection systems of UV/VIS-diode array detector (DAD-Model 168), and an evaporative light-scattering detector (ELSD, Model 2000; Alltech Associates, Inc., Deerfield, IL). A sample of 5 μL was injected into the system using the appropriate loading loop. Organic solvents of HPLC grade were purchased from Fisher Scientific (Fair Lawn, N.J.).

3.3.1.2. Short-Term Repeatability and Comparison of Gradient HPLC Methods

Short-term repeatability is characterized by the relative standard deviation (RSD) of a series of consecutive measurements made under the same experimental conditions, using the same products within few hours (Kele and Guiochon, 1999). The US Food and Drug Administration (FDA) recommends that a coefficient of variation (CV), also known as RSD, of 15% of the nominal value represents an acceptable degree of repeatability in bioanalytical methods for drugs (Gika *et al*., 2008). The repeatability of the gradient reversed-phase HPLC (RP-HPLC) methods for the separation of KO and its esterified PLs was investigated. Samples were withdrawn at 0 and 24 h period of incubation and submitted to HPLC analysis in triplicate trials using three different gradient RP-HPLC methods (Table 3-1). The retention time (RT) and the peak area, the resolution (R), the number of theoretical plates (n) as well as the plates per meter (N) were recorded for each analysis.

3.3.2. Transesterification Reaction in Solvent-Free Medium

3.3.2.1. Transesterification Trials

Lipase-catalyzed transesterification of krill oil (KO) was carried out according to a modification of the method developed in our laboratory (Sabally *et al*., 2006a; Sorour, 2010), using 3,4-dihydroxyphenylacetic acid (DHPA) as the PA substrate (Sigma Chemical Co.). High-potency KO, extracted from *Euphausia superba*, was generously

Table 3-1. Characteristics of the different methods, used for reversed-phase gradient high-performance liquid chromatography (RP-HPLC), for the separation of krill oil and its esterified phenolic lipids.

Method	Column	RT (min)[b]	Relative elution (%)[c] A[d]	B[d]	C[d]	Flow rate (mL/min)	IV (µL)[e]	N_2 (mL/min)[f]	T (°C)[g]	SC (mL)[h]	Pressure (Ksi)[i]
I	Zorbax[a]	10	100	0	-	1.00	5	1.6	60	45	0.76
		20	40	60	-	1.00					
		35	0	100	-	1.00					
		35	100	0	-	1.00					
		45	100	0	-	1.00					
II	Zorbax[a]	15	-	0	100	1.00	5	1.7	70	70	0.47
		45	-	40	60	1.00					
		60	-	100	0	1.00					
		60	-	0	100	1.00					
		70	-	0	100	1.00					
III	Zorbax[j]	9	-	0	100	0.43	5	1.7	50	46	0.53
		27	-	40	60	0.43					
		36	-	100	0	0.43					
		36	-	0	100	0.43					
		46	-	0	100	0.43					

[a]The used column was Agilent Zorbax SB (StableBond)-C18 (250x4.6 mm, 5 µm).
[b]Retention time of solutes in min.
[c]Relative percent of the solvent in the gradient elution system.
[d]Solvent A was methanol, B was isopropanol and C was acetonitrile.
[e]The injected volume of the sample in µL.
[f]Flow of nitrogen in the evaporative light-scattering detector (ELSD).
[g]Temperature in Celsius of the drift tube and the exhaust of the ELSD.
[h]Total solvent consumption per run in mL.
[i]Column drop pressure of system with 100% of solvent A for Method I and Solvent C for Method II and III, where ksi is a unit of pressure that refers to kilopound per square inch.
[j]The used column was Agilent Zorbax SB-C18 (150x3.0 mm, 3.5 µm).

obtained from Enzymotec Ltd (Morristown, N.J.). Immobilized lipase from *Candida antarctica* (Novozym 435) with an activity of 10,000 propyl laurate units, PLU, per g solid enzyme, was purchased from Novozymes Nordisk A/S (Bagsværd, Denmark). Prior to each enzymatic reaction, a stock solution of PA (143 mM) was freshly prepared in 2-butanone. Aliquot of the PA stock solution was mixed with KO to acquire a final concentration of 10 mM, with 7% butanone in the reaction mixture. The reaction mixture was homogenized, using a Corning tissue grinder pestle (Corning Inc., Lowell, MA). Using well-defined conditions, including a reaction volume (2 mL), Novozym 435 concentration (40 mg solid enzyme/mL; 400 PLU) with continuous shaking at 150 rpm, in an orbital incubator shaker (New Brunswick Scientific Co., Inc., Edison, N.J.), the enzymatic reaction was initiated by the addition of the enzymatic preparation to the reaction mixture. Transesterification reactions were run in duplicates with concomitant control trials containing all reaction components except the enzyme; the reaction mixtures were withdrawn at specific time intervals over the course of 2 days of the reaction. Recovered samples were flushed with a gentle stream of nitrogen and stored at −80ºC for further analysis. The sample to be subjected to HPLC analysis was prepared by the recovery of 8 µL from the reaction mixture and was solubilized in 100 µL isopropanol (IPA) and 52 µL acetonitrile (ACN) by sonication, using the sonicator® ultrasound processor for 10 sec (Model XL2020, Heat Systems, Inc., Farmingdale, N.Y.).

3.3.2.2. Recovery of Selected Separated Fractions

To identify the phospholipids of KO and PLs, obtained by the enzymatic transesterification reaction, selected fractions were recovered after injection in the HPLC. Elution of the injected sample was carried out by a gradient system of using ACN as solvent (A) and IPA as solvent (B) and Zorbax SB (StableBond)-C18 reversed-phase column (150x3.0 mm, 3.5 µm; Agilent Technologies, Santa Clara, CA). The elution was initiated by an isocratic flow of 100% of solvent A for 9 min, followed by 18 min gradient to 60 and 40% of solvent A and B, respectively, then to 100% of solvent B for 9 min period, and followed with an equilibration period of 10 min. The flow rate was 0.43 mL/min and detection was performed simultaneously at 210 and 280 nm as well as with ELSD. The fractions were collected and concentrated, using a Thermo Savant Automatic

Environmental Speedvac System (Model AES1010; Thermo Scientific, Fair Lawn, N.J.). After concentration, the separated fractions were re-injected into the HPLC system for confirmation.

3.3.3. Characterization of Krill Oil Components and Its Esterified Phenolic Lipids

3.3.3.1. FTIR

One µL volume of each recovered purified fraction was solubilized in acetonitrile (ACN) and repeatedly applied and evaporated onto the attenuated total reflectance (ATR) crystal to form a thin-layer and immediately scanned at room temperature. Similarly, sufficient amounts of the standard L-α-phosphatidylcholine (PtdCho) from egg yolk, Type XVI-E (Sigma Chemical Co., St-Louis, MO), was placed on the ATR crystal and immediately scanned at room temperature. Infrared spectra were recorded on a Bruker Alpha-P spectrometer (Bruker Optic GmbH, Ettlingen, Germany), equipped with a deuterated triglycine sulfate (DTGS) detector, a temperature controlled single bounce diamond ATR crystal and a pressure application device for solid samples. A total of 32 scans at 4 cm^{-1} resolution were co-added. Processing of the FTIR data was performed using Bruker OPUS software.

3.3.3.2. Mass Spectrometry Analysis

The purified fractions of phospholipids present in KO and esterified PLs, obtained by the lipase-catalyzed transesterification reaction of KO and selected PAs, were analyzed and characterized by HPLC interfaced to atmospheric pressure ionization-mass spectrometry (API-MS), with an atmospheric pressure chemical ionization (APCI) and/or electrospray ionization interface (ESI). The separation of biomolecules was performed with Zorbax SB-C18 column, using a mixture of MeOH:ACN (5:7, v/v) as solvent C and IPA containing 0.1% formic acid as solvent D. The elution was initiated by an isocratic flow of 100% of solvent C for 3 min period, followed by 9 min gradient to 100% of solvent D and maintained for 6 min, followed with a 2 min gradient to 100% solvent C and maintained for 6 min.

The LC-API-MS system (ThermoFinnigan, San Jose, CA) consisted of the Surveyor Plus liquid chromatograph coupled to the LCQ Advantage ion-trap with the Xcalibur®

System Control Software (Version 1.3) for data acquisition and processing. The MS was operated in positive ion mode, with collision induced dissociation energy of 10 V. The ESI source was operated with a capillary temperature of 260°C, a source voltage of 4.5 kV and the sheath and auxiliary gases N_2 at 25 and 4, respectively (arbitrary unit). The APCI source was operated with a capillary temperature of 150°C, a source temperature of 400°C, a source voltage of 6.0 kV and a source current of 5.0 µA, with the sheath and auxiliary gases N_2 at 35 and 15, respectively.

3.4. Results and Discussion

3.4.1. Method Development and Optimization

3.4.1.1. Preliminary Trials using High-Performance Liquid Chromatography

Table 3-1 shows a summary of the three Methods (I, II and III) investigated in this study for the separation of krill oil (KO) and its esterified phenolic lipids (PLs). Preliminary trials were carried out with Method I which had previously been developed in our Laboratory for the separation of the esterified PLs from fish liver oil (FO) (Sorour, 2010). Hence, the separation ability and column efficiency of Methods II and III were compared to those obtained with Method I.

Table 3-2 summarizes the repeatability of the retention time (RT), the resolution (R), the numbers of theoretical plates (n) and plates per meter (N) and peak areas for the components of the initial reaction mixture of DHPA and phospholipids of KO as well as the enzymatic transesterification reaction of the mixture after 24 h of incubation, using Method I and II, monitored simultaneously with UV at 210 nm and with ELSD. The experimental findings (Table 3-2) demonstrate that the mean relative standard deviation (RSD) of retention times for Method I, which is calculated as the standard deviation of triplicate samples divided by their mean multiplied by 100, obtained with UV and ELSD are small and similar. For Method I, the mean retention times of the peaks for the components of the enzymatic transesterification mixture showed better repeatability of 0.50 and 0.55% as compared to that of the components of the initial reaction mixture with 1.58 and 1.95% for UV and ELSD, respectively. These results could be due to certain variations in the temperature of the column.

Table 3-2. Comparison of Methods I[a], II[a] and III[a], used for the analysis of the components of the initial reaction mixture of 3,4-dihydroxyphenylacetic acid, the phospholipids of krill oil as well as the enzymatic transesterification reaction mixture after 24 h of incubation.

Reaction Time (h)	Detection mode / Method	RT RSD (%)[b]	R	R RSD(%)[b]	(n)[d]	(N)[e]	RSD (%)[b]	Peak area RSD (%)[b]
	UV/280 nm[g]							
0[f]	I	0.47[h]	ND[i]	ND[i]	270[h]	1,079[h]	16.36[h]	ND[i]
	II	0.58	ND[i]	ND[i]	ND[i]	ND[i]	ND[j]	ND[i]
	III	0.45	ND[i]	ND[i]	ND[i]	ND[i]	ND[j]	ND[i]
24[j]	I	0.47[h]	ND[i]	ND[i]	253[h]	1,012[h]	23.24[h]	ND[i]
	II	3.30	ND[i]	ND[i]	ND[i]	ND[i]	ND[i]	ND[i]
	III	0.69	ND[i]	ND[i]	ND[i]	ND[i]	ND[i]	ND[i]
	UV/210 nm[g]							
0[f]	I	1.58[h]	0.92[h]	15.07[h]	3,544[h]	14,175[h]	20.43[h]	ND[i]
	II	2.75	1.05	7.25	5,942	23,786	30.48	3.41[h]
	III	1.53	0.98	7.10	4,808	32,044	14.89	3.40
24[j]	I	0.50[h]	0.88[h]	13.06[h]	2,875[h]	11,501[h]	25.28[h]	ND[i]
	II	0.38	1.02	3.72	5,464	21,857	13.01	5.85[h]
	III	0.63	0.94	4.66	5,163	34,421	11.27	5.69
	ELSD[k]							
0[f]	I	1.95[h]	0.88[h]	12.19[h]	2,899[h]	11,596[h]	20.58[h]	ND[i]
	II	2.15	1.64	6.75	3,818	26,655	19.23	10.71[h]
	III	1.51	1.23	1.89	4,240	28,267	4.40	9.08
24[j]	I	0.55[h]	0.88[h]	14.22[h]	3,062[h]	12,249[h]	14.95[h]	ND[i]
	II	0.31	0.95	5.68	5,639	22,555	14.77	14.63[h]
	III	0.54	0.91	4.28	3,189	21,262	26.56	10.11

[a]Refer to Table 1 for gradient reversed-phase high performance liquid chromatography (RP-HPLC) program; the peaks used for measuring the retention time (RT), peak resolution (R), number of theoretical plates (n) and plate per meter (N) for Methods I, II and III are shown in Figures 3-1, 3-2 and 3-3, respectively.

[b]Relative standard deviation (RSD) was calculated as the standard deviation of triplicate samples divided by their mean multiplied by 100.

[c]Resolution (R) which is equal to the distance between the peak centers of two adjacent peaks divided by the average bandwidth.

[d]Number of theoretical plates (n) was calculated as 16 multiplied by the square foot of the retention time of the component divided by the width of the base.

[e]Plates per meter (N) is expressed as the number of theoretical plates per unit of length.

[f]Components of the initial reaction mixture at time 0 h.

[g]The detection was performed using UV/VIS diode array detector (DAD) Model 168 (Beckman Instruments Inc., San Ramon, CA).

[h]Mean of triplicate samples.

[i]Not determined, because the peak area was below the detection limit or not repeatable.

[j]Components of the enzymatic reaction mixture after 24 h of reaction.

[k]Evaporative light-scattering detector (ELSD) was Model 2000 (Alltech Associates Inc., Deerfield, IL).

Reuhs and Rounds (2010) reported that an increase of 1°C in column temperature will normally decrease the retention time (RT) by 1 to 2%. Moreover, the results (Table 3-2) indicate that both UV and ELSD detectors were approximately as good in repeating the RT. On the other hand, for Method I, in both mixtures, at t_0 and t_{24} and for both detections, UV and ELSD, the mean resolution (R) was lower than 1, with repeatability higher than 10%. In all cases, the values of n are above 2,000; however, the repeatability was quite poor, with values above 15%. Consequently, the peaks were not well resolved, which did compromise their analysis and their quantification. Although the column was acceptable in terms of its efficiency (>2,000), the repeatability was poor and therefore further development of this methodology was needed.

Figure 3-1 shows an HPLC chromatogram of the reaction components of lipase-catalyzed transesterification of KO with DHPA, monitored at UV 210 and 280 nm as well as with ELSD, using Method I (Table 3-1). Chromatograms of the reaction mixture of KO and DHPA at time 0 are shown in Figures 3-1A, 3-1B and 3-1C. whereas those of 3-1A', 3-1B' and 3-1C' represent those after 24 h of reaction. The results (Fig. 3-1) demonstrate that the new peaks a', b', c' and d', eluted in the region r_1 of 2.094 to 3.721 min (Fig. 3-1B') and those of 2.280 to 3.881 min (Fig. 3-1C'), were monitored with UV at 210 nm and with ELSD, respectively; however, as shown in Figures 3-1B and 3-1C, KO already contains compounds that correspond to peaks a, b, c and d, which eluted in the same region. The results (Fig. 3-1) depict a significant peak overlap and co-elution between peaks of a, b, c and d and those of a', b', c' and d', which render the analysis of the multi-components in the mixture a difficult task. This phenomenon of overlap was not reported when the transesterification of FO with DHPA in solvent-free medium (SFM) was subjected to HPLC analysis, using the same Method I (Sorour, 2010). The overlaps and the co-elutions are probably due to the high content of phospholipids (40%) in KO which results in PLs of close nature, polarity and molecular weight. These findings are in agreement with those results reported by Dolan *et al*. (1999) who suggested that the important cause of poorly resolved individual peaks is the presence of compounds in the sample of similar molecular structure.

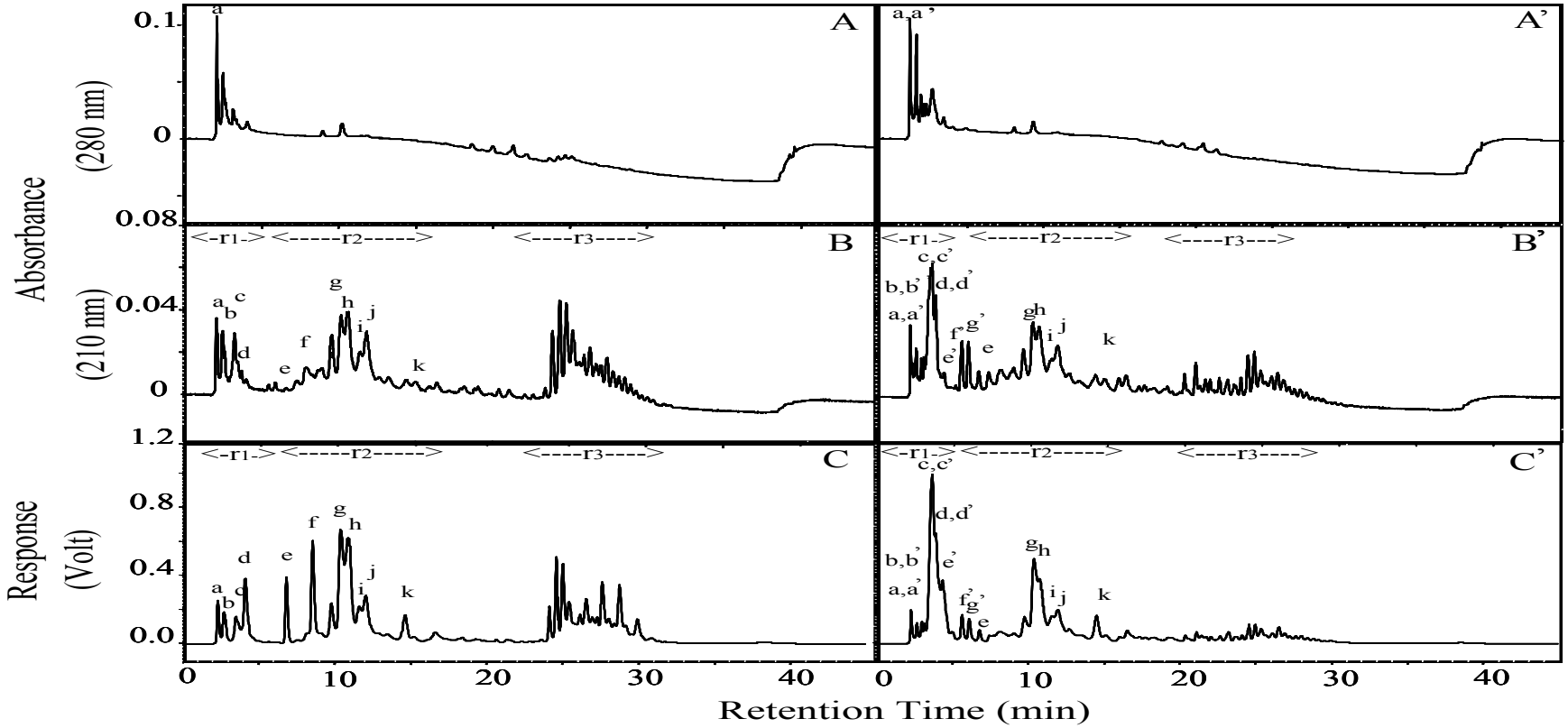

Figure 3-1. HPLC chromatograms of the components of the initial reaction mixture of 3,4-dihydroxyphenylacetic acid (DHPA) with krill oil (KO) (A, B and C) as well as the enzymatic transesterification reaction mixture (A', B' and C'), monitored at 280/210 nm and with the evaporative light-scattering detector (ELSD), respectively using Method I (refer to Table 3-1). Peaks a, b, c, d, e, f, g, h, i, j and k were the components of KO at time 0, whereas peaks a', b', c', d', e' and f' are the novel products that appeared after 24 h of reaction. The abbreviations r_1, r_2 and r_3 are referring to regions 1, 2 and 3, respectively.

In order to resolve the peak overlap and the co-elution issues and to allow a better separation between the peaks of the newly synthesized products and the components of krill oil, further development of Method I was needed.

3.4.2. Optimization of HPLC Separation

In order to obtain a well repeatable and efficient separation of the lipid components of KO as well as those of the esterified PLs, several parameters, including the solvent strength and the solvent polarity gradient, the appropriate column and the modes of detection were investigated.

3.4.2.1. Effect of Polarity and Solvent Strength of the Gradient on the Retention Time

In order to determine the appropriate elution gradient program that will result in better band spacing and resolution, initial work was carried out with the use of solvent gradient systems and RP column (Method I). As illustrated in Table 3-1, for Method I, the elution was initiated by an isocratic flow of 100% of solvent A methanol (MeOH) for 10 min, followed by a 10 min gradient to 40 and 60% of solvent A and solvent B isopropanol (IPA), respectively, then to 100% of solvent B for 15 min period, which is followed by an equilibration period of 10 min. The overall findings suggest that by increasing the ratio of solvent A in the gradient system, the elution of late-eluting compounds (region r_3), with RT between 24 to 30 min was delayed. Consequently, they were better separated from compounds (regions r_1 and r_2) than early eluted with RT between 0 and 15 min. It was found that a gradient of 40 and 60% of solvent A and B resulted in the best spacing between early and late eluting solutes. These results could be explained by the fact that the mixture contains compounds of different polarities and by increasing the ratio of MeOH and decreasing that of isopropanol (IPA) in the gradient, the polar compounds were eluted earlier (r_2) and the non-polar compounds (r_3) were longer retained resulting hence in more spacing between the two regions. These results are in agreement with the RP column where the retention of the solutes is due to the hydrophobic interactions with the non-polar stationary phase and are eluted in order of decreasing polarity (Reuhs and Rounds, 2010). In addition, the overall findings indicate, that the longer the gradient time, the better the peak spacing and the least the peak width. However, it was important to determine the adequate time that could provide a better separation without any significant

increase in the run time. Hence, increasing the gradient time from 10 min to 30 min was adequate to obtain satisfactory results.

3.4.2.2. Effect of Solvent Strength of the Mobile Phase on the Selectivity and Resolution

Although the initial HPLC separation with an isocratic system of solvent A resulted in a rapid elution of the polar components within the first 10 min, poor peak spacing and resolution (R <1) were obtained (Fig. 3-1; Table 3-2). The use of different ratios of methanol (MeOH) and acetonitrile (ACN) has been investigated. A change in the ratio from 100 to 50% of solvent A (MeOH), with a polarity index of 5.1 and a concomitant increase in ACN ratio, with a polarity index of 5.8, resulted in an increase in the retention time (RT) and band spacing, but with little improvement in resolution (R). Similarly, the results are in agreement with those reported by Snyder *et al*. (1979) who indicated that starting the gradient with a mobile phase of higher strength could result in shorter retention times, narrower and taller bands as well as poorer resolution. In order to decrease the strength of solvent A, MeOH was substituted by ACN, which resulted in an increase in retention time, better band spacing and resolution. These results are in agreement with the principle that the sample retention can be controlled by varying the solvent strength of the mobile phase (Reuhs and Rounds, 2010). Since the strength of the solvent is inversely proportional to its polarity, the use of a more polar solvent ACN improved the separation in terms of RT and R. In order to improve the resolution and to decrease the peak width, the isocratic flow was increased by 5 min. A mobile phase of 100% ACN and an increase in the isocratic elution program by 5 min resulted in much better separation of the initial mixture of DHPA with KO (Figs. 3-2A, 3-2B and 3-2C as well as Fig. 3-3A, 3B and 3C) as well as the enzymatic transesterification reaction mixture (Fig. 3-2A', 3-2B' and 3-2C' as well as Fig. 3-3A', 3-3B'and 3-3C'). For both detectors, UV and ELSD, as well as for both mixtures at time 0 and 24 h using Method II, the resolution (R) improved significantly as compared to that obtained in Method I. In most cases, the mean R values (Table 3-2) were slightly above or very close to 1. The baseline resolution of PA (peak # 1) and all phospholipids (peaks # 2, 3, 4, 5 and 6) in KO were achieved.

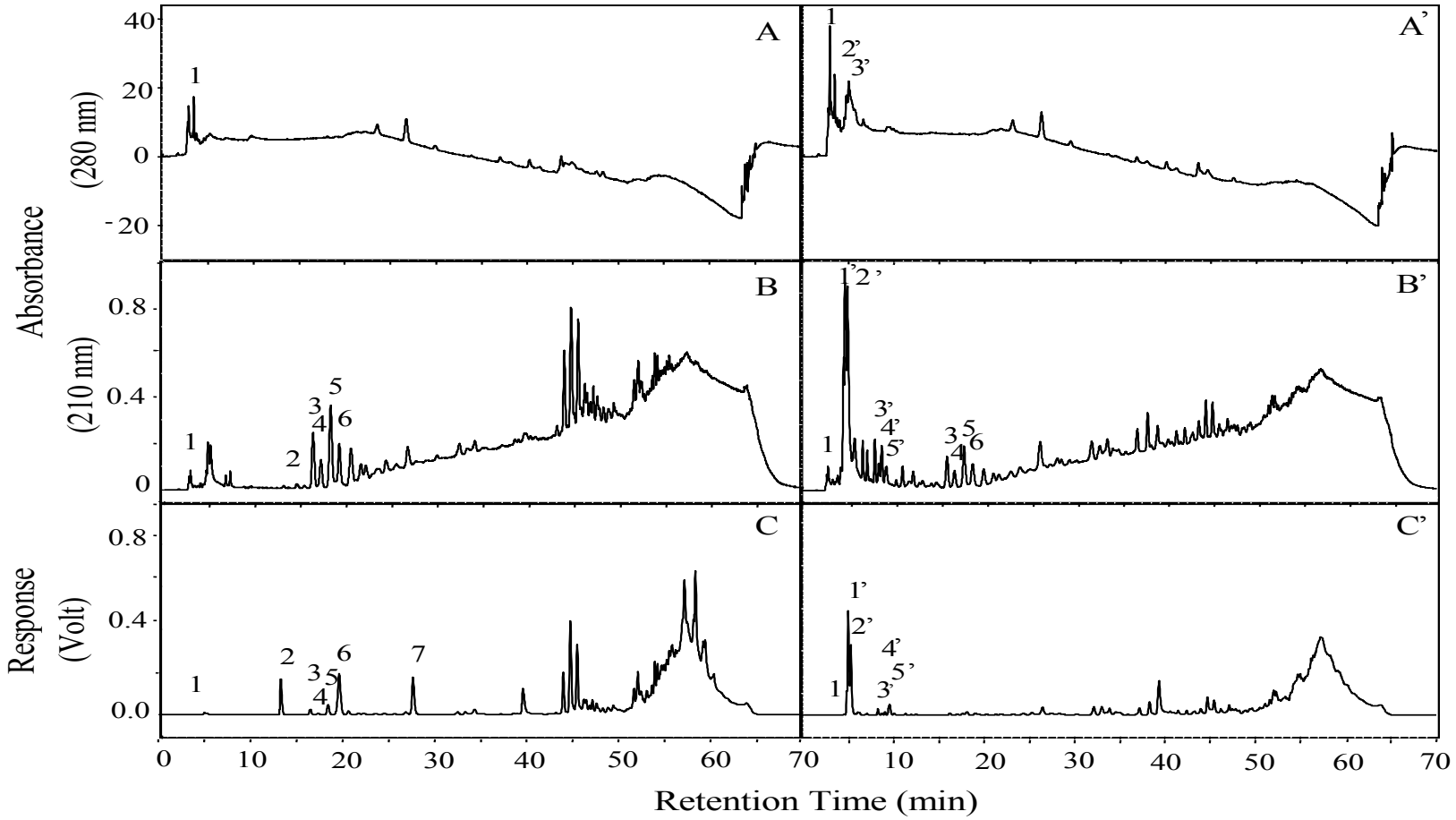

Figure 3-2. HPLC chromatograms of the components of the initial reaction mixture of 3,4-dihydroxyphenylacetic acid (DHPA) with krill oil (KO) (A, B and C) as well as the enzymatic transesterification reaction mixture (A', B' and C'), monitored at 280/210 nm and with the evaporative light-scattering detector (ELSD) respectively, using Method II (Table 3-1). Peak numbers were tentatively characterized as follows: DHPA (peak # 1), phenolic lipids (peaks # 1', 2', 3', 4'and 5') and the phospholipids of KO (peaks # 2, 3, 4, 5, 6 and 7).

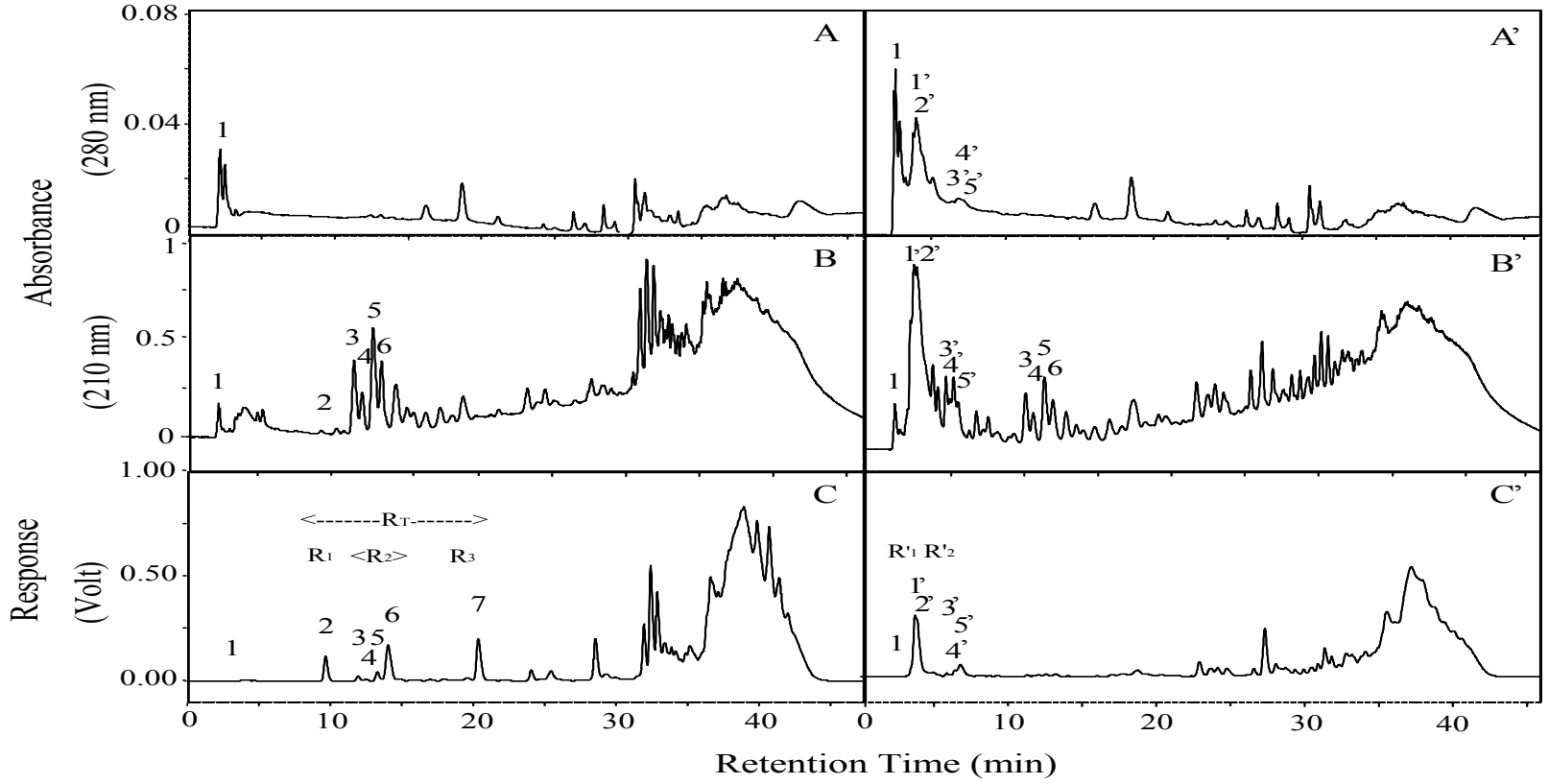

Figure 3-3. HPLC chromatograms of the components of the initial reaction mixture of 3,4-dihydroxyphenylacetic acid (DHPA) with krill oil (KO) (A, B and C) as well as the enzymatic transesterification reaction mixture (A', B' and C'), monitored at 280/210 nm and with the evaporative light-scattering detector (ELSD), respectively, using Method III (Table 3-1). Peak numbers were tentatively characterized as follows: DHPA (peak # 1), phenolic lipids (peaks # 1', 2', 3', 4'and 5') and phospholipids of KO (peaks # 2, 3, 4, 5, 6 and 7). The abbreviations R_1, R_2, R_3, R_T, R'_1 and R'_2 are referring to the regions selected for peaks recovery.

Figures 3-2A', 3-2B' and 3-2C' as well as Figures 3-3A', 3-3B' and 3-3C' depict no significant peak elution between the synthesized PLs (peaks # 1', 2', 3', 4' and 5') and the phospholipids of KO (peaks # 2, 3, 4, 5, 6 and 7) nor that DHPA (peak # 1). Peaks # 1' and 2' were not completely separated. These results could be explained by the fact that the synthesized PLs are very close in polarity, molecular weight and nature, and hence it could be difficult to achieve complete separation which is in agreement with what was reported by Dolan *et al*. (1999). For Method II, column efficiency evaluated, by number of theoretical plates (n) and plates per meter (N) values, was improved significantly as compared to those in Method I.

3.4.2.3. Effect of Column Length and Particle Size

The effects of column length and particle size on solvent consumption, efficiency and resolution were investigated. The optimized gradient RP-HPLC program (Method II) is illustrated in Table 3-1. Although the separation obtained in Method II was better than that in Method I, the run time was relatively longer (70 min instead of 45 min), with higher consumption of solvent (Table 3-1). Figures 3-2 and 3-3 depict the gradient reversed-phase separation of the two different columns of 250 and 150 mm packed, respectively, with two different particle sizes of Zorbax SB-C18, 5 and 3.5 μm. Table 3-2 also summarizes the mean RT, R, n and N and peak area values for the components of the initial components of the reaction mixture of DHPA and phospholipids of KO as well as the enzymatic transesterification reaction mixture after 24 h of reaction using Method III and monitored, simultaneously, with UV at 210 nm and ELSD.

For the components of the initial reaction mixture, the mean R was decreased by 6.7 and 25% for Method III as compared to that in Method II with UV at 210 nm and with ELSD, respectively. While for components of the enzymatic transesterification mixture, the mean R was decreased by 7.84 and 4.21% for Method III as compared to Method II for UV detection at 210 nm and with ELSD, respectively. With the exception of the resolution obtained for the analysis of KO components and DHPA with ELSD, using smaller packing particle size (3.5 μm), the results (Table 3-2) show that there was no major change in the resolution as compared to that obtained with Method II. These experimental findings are in agreement with those obtained by Kirkland *et al*. (1994) who

reported that in comparison with a conventional column (150x4.6 mm) of 5 μm particles where the separation of antibiotics was performed in half the time and without significant loss in separation resolution, using a smaller particle (3.5 μm) column Zorbax SB-C_8 (80 x 4.6 mm). Similar findings were also reported by Zweigenbaum et *al*. (1999) with the use of a Mac-Mod Rapid resolution cartridge (2.1x15 mm) packed with 3.0 μm particles of Zorbax SB-C18 when a mixture of six benzodiazepines was obtained in less than 25 sec with some coelution. For column comparison purpose, the plates per number of two Zorbax columns of different dimensions were calculated. The results (Table 3-2) depict that the overall number of plates per meter for Zorbax SB-C18 (150x3.0 mm, 3.5 μm) were higher than those for Zorbax SB-C18 (250x4.6 mm, 5 μm), hence indicating a higher column efficiency. In addition, these findings are in agreement with the equation reported by Chen and Kord (2009) who demonstrated that small particles could lead to significant improvement in column efficiency.

$$N = L / H = L / 2d_p \quad \text{(3-1)}$$

where, N is the efficiency, L is the column length, H is the plate height and dp is the particle size.

Using Method III (Table 3-1), the solvent consumption was reduced by 71.7% as compared to that for Method II. The experimental findings are in agreement with the equations, developed by Chen and Kord (2009) that indicates that smaller particles of inner column diameter and shorter stationary phases could lead to a decrease in the mobile phase consumption. Likewise, Welch *et al*. (2010) reported that significant solvent saving can be obtained simply by changing the column dimensions and by reducing the retention time. In addition, the reduction of the flow rate to almost half contributed to a significant reduction in the amount of solvent consumed per run. However, as the particle size of the column decreases, the column backpressure increases with the inverse square of the particle diameter (Neue *et al*., 1999). Hence, using the same column length, the pressure would go up by a factor of 2.0 for a 3.5 μm particle versus a 5.0 μm one. Since the flow rate of 1 mL/min used in Method III was lowered almost by half as compared to that in Method II (Table 3-1), no significant change in the pressure was observed between the two methods.

Using Zorbax SB-C18 column (150x3.0 mm, 3.5 μm), the separation time of the components of the initial reaction mixture of DHPA with krill oil as well as for those of the enzymatic transesterification reaction mixture was reduced by 34.3%, without a major loss of resolution. Method III could be considered as a more rapid, efficient, cost-effective and a green chemistry method as compared to Method II, and hence it was used for further investigation.

3.4.3. Comparative Analyses using UV-DAD Detection and ELSD

3.4.3.1. Sensitivity and Detection of UV-DAD as Compared to ELSD

Figures 3-2 and 3-3 demonstrate the different chromatograms of HPLC analysis of the initial components of the reaction mixture of DHPA with KO as well as those of the enzymatic transesterification reaction mixture, using UV-DAD detector at 280 and 210 nm as well as with ELSD for Method II and III, respectively (Table 3-1). For Methods II and III, DHPA (peak # 1) absorbed with UV at 280 and 210 nm; however, little response was seen in ELSD. In addition, most phospholipids peaks (# 2 , 3, 4, 5 and 6) showed no absorbance with UV at 280 nm, but a response with ELSD and with UV at 210 nm , with the exception of peaks # 2 and 7, that showed little or no absorbance at 210 nm (Figs. 3-3-2A, 3-2B and 3-2C as well as Figs. 3-3A, 3-3B and 3-3C). Although the UV detection lacks specific absorption peaks, the experimental findings could be explained by the fact that most phospholipids absorb UV in the region of 190 to 210 nm (Peterson and Cummings, 2006). The strong absorption at 210 nm may be related to the presence of unsaturated bonds and functional groups, such as carbonyl, carboxyl and amino groups (Peterson and Cummings, 2006). As opposed to UV, the response of ELSD is independent of the nature of the compound whether it contains unsaturated conjugated double bonds or functional groups as long as they condense as liquids (Stolyhwo *et al*., 1985). Hence, although peaks # 2 and 7 (Figs. 3-2B and 3-2C as well as Figs. 3-3B and 3-3C) showed response in ELSD, there was little or no absorbance in UV at 210 nm. Stolyhwo et *al*. (1985) reported that using laser-scattering detector, the quantitative analysis of oils and fats can be determined directly from the peak areas and without the need of calibration by either internal or an external standard. Consequently, the use of ELSD in quantitative analysis could be more accurate as compared to that of UV and it

was used as the mode of detection for further investigation. Phenolic lipids (peaks # 1', 2', 3', 4' and 5') from Figures 3-2 and 3-3, showed UV absorbance at 280 and 210 nm as well as with ELSD for Method I. The experimental findings may confirm that the synthesized novel products could be the PLs, since they absorbed with UV at 280 and 210 nm as well as with ELSD. In addition, using Method II (Table 3-2), ELSD showed better or similar mean resolution of 1.64 and 0.95 for the components of the initial reaction as well as those of the enzymatic transesterification mixtures versus 1.05 and 1.02 for UV detection, respectively. Similar results were obtained using Method III (Table 3-2), with ELSD showing better or similar mean resolution of 1.23 and 0.91 versus 0.98 and 0.94 for the components of the initial reaction as well as those of the enzymatic transesterification mixtures. In addition, in most cases, the mean RSD for the ELSD showed better repeatability of resolution as compared to that of UV. On the other hand, the number of plates per meter (N) was not affected significantly by the method of detection although the repeatability was sometimes poor.

3.4.3.2. Repeatable Separation

Tables 3-2 and 3-3 show the repeatability of the retention time as well as the peak area of the components of the initial mixture of DHPA and phospholipids of KO, using Methods II and III, respectively, monitored with UV at 210 and 280 nm as well as with ELSD. The repeatability of the retention time as well as the peak area of the components of the enzymatic transesterification reaction mixture of DHPA, phospholipids of KO and PLs after 24 h of reaction, using Methods II and III, are shown in Table 3-2, respectively, monitored with UV at 210 and 280 nm as well as with ELSD. The peak areas reported for the different compounds and the two detection methods cannot be compared in any meaningful ways because the individual responses are compound specific and detection-method specific (Chen *et al*., 2000). On average, for Method II, the UV-detected peak areas showed better repeatability, with a mean RSD of 3.41% for the components of the initial reaction mixture (Table 3-2) and 5.85% for those of the enzymatic transesterification (Table 3-2) versus 10.71 and 14.63%, respectively, for ELSD. As compared to Method II, the ELSD-detected peak areas in Method III resulted in better mean RSDs of 9.08 and 10.11% for the components of the initial reaction mixture (Table

3-2) as well as for those of the enzymatic transesterification reaction (Table 3-2), respectively; however, the UV-detected peak areas still showed better repeatability. These results could be explained by the fact that UV detection is dependent on the presence of a chromophore and therefore it is not an accurate tool for the quantification (Stolyhwo *et al*., 1985). Two major components of the initial mixture (peaks # 2 and 7) were not detected. On the other hand, the RSD of the retention time for both Methods I and II showed better repeatability in ELSD as compared to that for UV. For Method II, the mean RSDs for ELSD was 2.15% for the initial components of the reaction mixture (Table 3-2) and 0.31% for those of the enzymatic transesterification reaction mixture (Table 3-2) versus 2.75 and 0.38%, respectively for UV detection at 210 nm. Similar results (Table 3-2) were obtained with Method III, with 1.51% for the initial components of the reaction mixture and 0.54% for those of the enzymatic transesterification reaction mixture versus 1.53 and 0.63% for UV detection at 210 nm.

3.4.4. FTIR Analysis

In order to tentatively identify the phospholipids of KO and PLs, further analysis by Fourier transform infrared spectroscopy (FTIR) of the purified eluted peaks from the regions of R_T, R_1, R_2 and R_3 (Fig. 3-3) of the components of the initial reaction mixture at time 0 was carried out. The infrared absorbance of the purified eluted fraction peaks was compared to that of the standard L-α-phosphatidylcholine from egg yolk (Fig. 3-4).

Figure 3-4 shows that the FTIR spectra of the purified eluted fraction peaks from the regions RT (Fig. 3-4-IA), R_1 (Fig. 3-4-IB), R_2 (Fig. 3-4-IC) and R_3 (Fig. 3-4-ID) were very similar to that of the phospholipid standard. As reported earlier, peaks # 2 and 7, recovered from regions R_1 and R_3, did show little or no absorbance at UV 210 nm (Figs. 3-3B and 3-3B') but responded with ELSD (Figs. 3-3C and 3-3C'). As compared to the FTIR spectra of peaks eluted in the regions RT and R_2, peaks # 2 and 7 seem to lack the absorption band 1 at 3,027 cm^{-1}, which could be due to an aromatic carbon-hydrogen bond (Mitra and Bhowmik, 2000). This band could be the chromophore responsible for the absorbance at UV 210 nm. The similar spectra to L-α-phosphatidylcholine, from egg yolk, confirm that the eluted peaks in the region RT could be indeed the phosphatidylcholine.

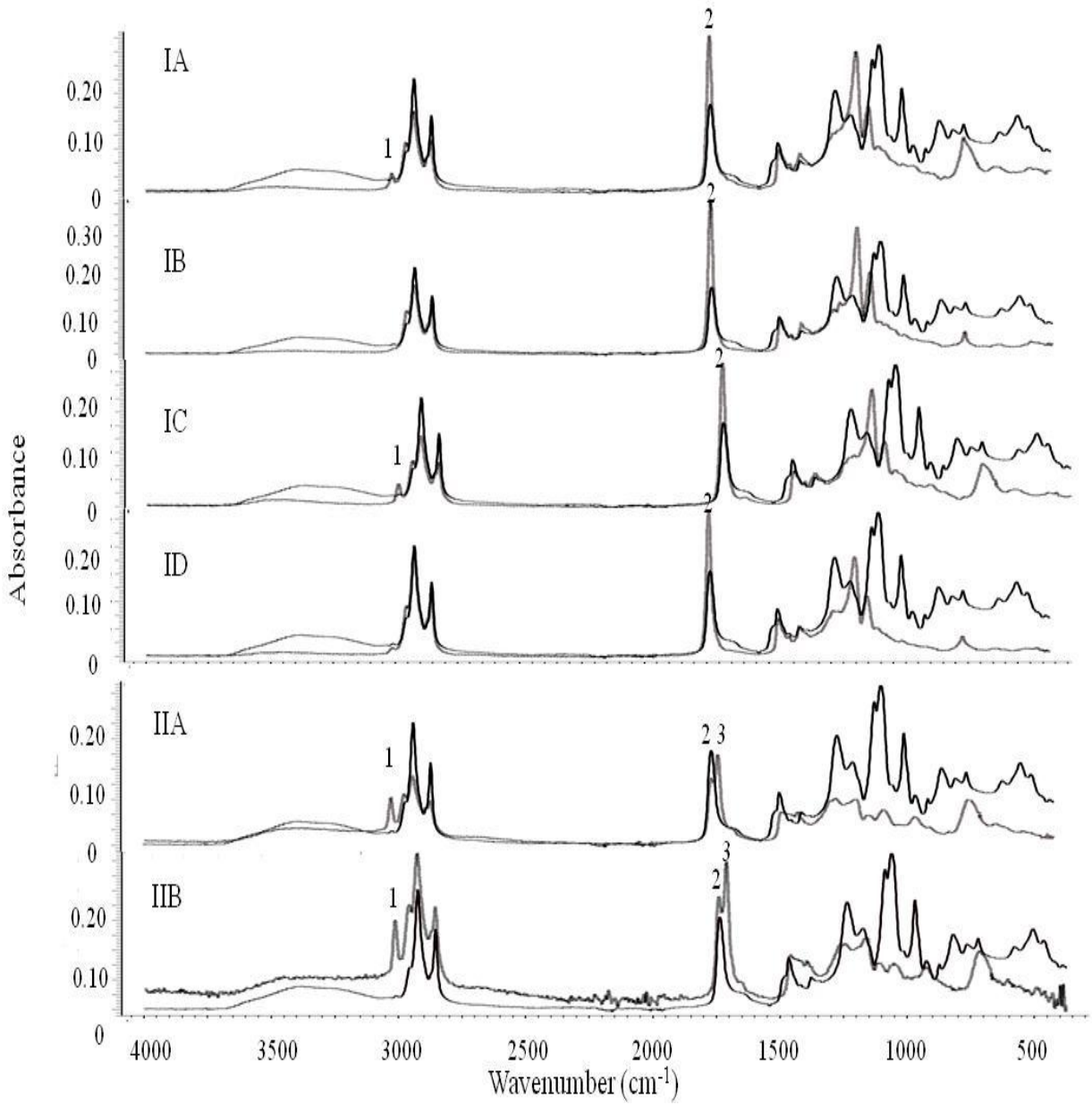

Figure 3-4. Overlaid Fourier transform infrared spectroscopy (FTIR) spectra of the purified eluted fraction peaks from the regions RT (IA), R_1 (IB), R_2 (IC) and R_3 (ID) of the components of the initial reaction mixture at time 0 (clear line), (Figures 3-3A, 3-3B and 3-3D) and from the regions R'_1 (IIA) and R'_2 (IIB) of the components of the enzymatic transesterification reaction (clear line), (Figures 3-3A', 3-3B' and 3-3C') as well as L-α-phosphatidylcholine from egg yolk (dark line).

Figure 3-4 shows also the purified eluted peaks from regions R'_1 (Fig. 3-4-IIA) and R'_2 (Fig. 3-4-IIB) of the components of the enzymatic transesterification reaction (Figs. 3-3A', 3-3B' and 3-3C') as compared to that of those of L-α-phosphatidylcholine from egg yolk. As compared to the phosphatidylcholines (PtdCho) in region R_T, the results (Figs 4II-A and 4-IIB) showed that the absorbance band 1 at 3,027 cm^{-1} was increased dramatically; this increase could be due to the incorporation of the DHPA molecule into the PtdCho. In addition, a new absorption band (3) at 1,735 cm^{-1} appeared in the C=O stretching region of the spectra; this absorption band could be due to the formation of ester carbonyls (Nilsson *et al*., 1991). These findings are in agreement with those reported by Nilsson *et al*. (1991), who suggested that the infrared absorption of the two ester carbonyls of dioleylphosphatidylcholine has its maximum intensity at 1,735 cm^{-1}. The significant increase in the band absorption at 3,027 cm^{-1} and the presence of two carbonyl esters in the region of 1,600 to 1,700 cm^{-1} (bands 2 and 3) suggest that the recovered eluted peaks from the regions R'_1 and R'_2 of the components of the enzymatic transesterification reaction could be the synthesized PLs.

3.4.5. Structural Characterization of Phospholipids in Krill Oil and Phenolic Lipids

Figure 3-3 shows the elution profile of the initial reaction mixture of DHPA with KO (Figs. 3-3A, 3-3B and 3-3C) at time 0 as well as the enzymatic transesterification reaction mixture (Figs. 3-3A',3-3B' and 3-3C'), monitored at 280/210 nm and with ELSD using Method III. Peak # 1, which absorbed mainly at 280 nm, was characterized as DHPA. The peaks (# 2, 3, 4, 5, 6 and 7) were tentatively identified as phospholipids species by FTIR (Figs. 3-4-IA, 3-4-IB, 3-4-IC and 3-4-ID). In order to characterize the molecular structure of these molecules, the purified eluted peaks from the regions R_T (Fig. 3-3) were subjected to further analyses by HPLC/APCI-MS. The identified molecular species are listed in Table 3-3. In addition to the complex matrixes of phospholipids of KO (Winther *et al*., 2011), the analysis of an enriched krill oil (high-potency grade) made the identification of the peaks even more challenging. Since APCI is known as a less soft ionization technique than ESI, a consistent fragmentation pattern characterized by the loss of phosphocholine head (PO_4Choline) with a molecular ion of m/z 166 was obtained.

Table 3-3. Characterization of lyso-phosphatidylcholines (lyso-PtdCho) and phosphatidylcholines (PtdCho) in krill oil in the purified fraction (Fig. 3-3C, R_T), using atmospheric pressure chemical ionization.

Peak # [a]	RT (min)[b]	Mass [M]	m/z [M - PO_4Choline]$^{+c}$ [M - FA- PO_4Choline]$^{+d}$	Proposed structure
2	5.3	493.4	327.1[c]	16:1 lyso-PtdCho
5	6.3	825.5	661.3[c]	(20:5 - 20:5) PtdCho
6	6.7	851.6	687.3[c]	(20:5 - 22:6) PtdCho
7	7.7	813.6	355.2[d] 383.2[d]	(18:1 - 20:1) PtdCho

[a]With reference to Figures 3-3B and 3-3C.

[b]Retention time of solutes in min.

[c]The mass [M] minus phosphocholine group.

[d]The mass [M] minus fatty acid minus phosphocholine group.

The loss of the phosphocholine head has been already reported by Le Grandois *et al*. (2009) when analyzing phospholipid species by LC-ESI-tandem mass spectrometry. The analysis of peak # 2 resulted in a molecular ion of m/z 327.1 $[M - PO_4Choline]^+$, which suggests a 16:1 lyso-phosphatidylcholine (lyso-PtdCho), whereas the analysis of peak # 5 showed a molecular ion of m/z 661.3 $[M - PO_4Choline]^+$ which correspond to 20:5 - 20:5 PtdCho. On the other hand, the fragmentation of peak # 6 produced a molecular ion of m/z 687.3 $[M- PO_4Choline]^+$ that could represents a 20:5 - 22:6 PtdCho. The analysis of peak # 7 showed two molecular ions of m/z 355.2 and 383.2 [M - fatty acid-$PO_4Choline]^+$, which suggests a 18:1 - 20:1 PtdCho. The structures proposed for peaks # 1 and 7 could explain the reasons behind their lack of absorption in UV, because of the absence of chromophore. Although the characterization of phospholipid molecular species in KO were recently reported (Le Grandois *et al*., 2009; Winther *et al*., 2011), it is the first time and as the authors are aware the experimental data provides the identification of such species in a commercial KO of high-potency grade (Enzymotec Ltd); The overall results suggest that the experimental findings obtained in our laboratory are in agreement with those reported in literature (Le Grandois *et al*., 2009; Winther *et al*., 2011).

Two predominant peaks (# 1'and 2') (Figs. 3-3B' and 3-3C') were tentatively identified as phenolic lipids by FTIR (Figs. 3-4IIA, 3-4IIB). In order to characterize the molecular structure of these molecules, the purified eluted peaks from the regions R'_1 and R'_2 (Fig. 3C') were subjected to further analyses by HPLC-APCI/ESI-MS. However, the analysis of peaks # 1' and 2', using APCI, resulted in molecular ions of m/z 377.2 and 403.2 $[M – DHPA + H_2O]^+$ (Table 3-4) which correspond to 20:5 and 22:6-glycerol, respectively. In order to confirm the UV absorbance and the FTIR spectra that showed the characteristics of PLs, further analysis was carried out using ESI. The analysis of peaks # 1' and 2', using ESI, showed molecular ions of m/z 546.4 and 574.5 $[M + H_2O]^+$, which correspond, respectively, to a monoeicosapentaenonyl dihydroxyphenylacetic and a monodocosahexaenonyl dihydroxyphenylacetic acids. As compared with ESI, the analysis with APCI resulted in a fragmentation pattern characterized by the loss of DHPA.

Table 3-4. Characterization of phenolic lipids in the purified fractions (Fig. 3-3C, R'_1 and R'_2), using atmospheric pressure chemical ionization (APCI) and electrospray ionization (ESI).

	APCI		ESI			
Peak#[a]	RT[b] (min)	m/z $[M - DHPA + H_2O]^+$	RT[b] (min)	m/z $[M + H_2O]^+$	Mass [M]	Proposed structure[c]
1’	2.8	377.17	2.5	546.4	527.3	DHPA - 20:5
2’	2.9	403.17	2.5	574.5	553.3	DHPA - 22:6

[a]With reference to Figures 3-3B’ and 3-3C’.

[b]Retention time of solutes in min.

[c]3,4 dihydroxyphenylacetic acid linked to glycerol backbone.

The identification of various molecules species carried out throughout this study did not take into account the position of the fatty acid on the glycerol moiety. In summary, the HPLC/APCI-MS analyses suggest the formation of two phenolic monoacylglycerols (MAGs), obtained by the transesterification of phospholipids in KO with DHPA in solvent-free media. This is the first report on the biosynthesis of PLs from phospholipids. Previous work performed in our laboratory succeeded in the characterization of PLs obtained by the transesterification of flaxseed oil (FSO)(Sabally *et al*., 2006a) and fish oil (FO) (Karam *et al*., 2009), which they contain normally triacylglycerols (TAGs), but not phospholipids.

3.5. Conclusion

A new HPLC method was developed for the separation of a complex mixture of TAGs and phospholipids of KO as well as the esterified PLs. Two detectors, including ELSD as well as UV and two SB-C18 Zorbax columns of different dimensions and packing particle size has been investigated, where the results showed that using a shorter column and smaller particle size, the separation time of the initial reaction and the enzymatic transesterification mixtures was significantly reduced, without a major loss in resolution. In addition, the solvent consumption was decreased dramatically. As a whole, ELSD was shown to be a more appropriate tool for the quantitative analysis of the components of KO and its esterified PLs as compared to UV. FTIR and MS analyses confirmed the nature of the separated compounds.

CHAPTER IV

STATEMENT OF CHAPTER IV LINKAGE

As a result of the development of the high-performance liquid chromatography (HPLC) method, used for the separation of the component of krill oil (KO) and its esterified phenolic lipids (PLs) and described in Chapter III, the evaporative light-scattering detector (ELSD) was selected as the appropriate detection and quantitative method. Chapter IV covers the experimental findings related to the optimization of the synthesis of PLs, obtained by the transesterification of KO and selected phenolic acid (PA) models, in solvent-free medium, using the response surface methodology (RSM).

CHAPTER IV

LIPASE-CATALYZED TRANSESTERIFICATION OF KRILL OIL AND 3,4-DIHYDROXYPHENYL ACETIC ACID IN SOLVENT-FREE MEDIUM USING RESPONSE SURFACE METHODOLOGY

4.1. Abstract

The optimization of the enzymatic transesterification in solvent-free medium (SFM) of krill oil (KO) with selected phenolic acids (PAs), using two immobilized lipases, was investigated. The use of Novozym 435 with 3,4-dihydroxyphenylacetic acid (DHPA) resulted in the highest bioconversion yield (BY). The central composite rotatable design (CCRD) was used to evaluate the effects of the PA concentration (PAC) and lipase concentration (LC) as well as the agitation speed (AS) on the BY of phenolic lipids (PLs). The initial findings indicated that the stationary point was a saddle point. To overcome this saddle point, sequential experiments have been carried out at fixed PAC, with LC and AS as the two independent variables. For the models with PAC, fixed at 10 and 20 mM, the results revealed that LC had a significant quadratic effect (P <0.05) on the %BY, whereas a significant linear effect was only obtained at PAC fixed at 20 mM. The AS had a significant quadratic effect (P <0.05) on the %BY only for the model with PAC fixed at 10 mM. At fixed PAC of 20 mM, the response surface model predicted a BY of 75%, using a LC of 62 mg/mL and an AS of 154 rpm. The subsequent verification experiment carried out under these conditions confirmed the validity of the prediction.

4.2. Introduction

The long-chain omega-3 fatty acids (*n*-3 FAs) eicosapentaenoic acid (EPA) and docosahexaenoic acid (DHA) have been widely recognized in the modulation of risk of a variety of human diseases (Kidd, 2007). Although fish and fish oils (FOs) are the major dietary sources of EPA and DHA, the sustainability of such source is uncertain (Blanco *et al*., 2007), which has led to the emergence of a new source of these long-chain *n*-3 FAs on the market, krill oil (KO). In addition to having an important biomass and being rich in naturally-occurring antioxidants including astaxanthin, KO is distinct from other marine oils in that most of the EPA and DHA are linked to phospholipids (Massrieh,

2008). On the other hand, phenolic acids (PAs) are another group of compounds that have been shown to exhibit a wide range of physiological properties and biological activities, such as antioxidant and antimicrobial capacities (Balasundram *et al*., 2006; Stasiuk and Kozubek, 2010). However, their hydrophilic nature limits their solubility in the hydrophobic medium and consequently reduces their potential use in edible fats and oils (Stamatis *et al*., 2001). The incorporation of phenolic antioxidants into unsaturated lipids could result in the biosynthesis of novel biomolecules, PLs, that possess both functional and nutritional benefits (Karam *et al*., 2009).

Research work, carried out in our laboratory, has succeeded in the enzymatic synthesis in organic solvent media (OSM) of structured PLs with enhanced antioxidative and solubility properties (Lue *et al*., 2005; Sabally *et al*., 2006a; Sabally *et al*., 2006b; Safari *et al*., 2006; Sabally *et al*., 2007; Karboune *et al*., 2008; Karam *et al*., 2009). However, the low volumetric productivity is a major drawback limiting the enzymatic synthesis of PLs in OSM at a large scale. One of the most promising approaches to enhance volumetric productivity consists of using solvent-free medium (SFM) (Dossat *et al*., 2002). Recently, work in our laboratory (Sorour, 2010) succeeded in the enzymatic synthesis of PLs using edible oils (EOs), including flaxseed (FSO) and fish liver oils (FO) in SFM.

Although the optimization of a bioprocess for the biosynthesis of PLs, obtained with using FO and FSO, was already developed in our laboratory (Lue *et al*., 2005; Sabally *et al*., 2006a; Sabally *et al*., 2006b; Safari *et al*., 2006; Sabally *et al*., 2007; Karboune *et al*., 2008; Karam *et al*., 2009; Sorour, 2010), the reported study is the first in which the PLs were synthesized by using KO. KO is not only rich in polyunsaturated fatty acids (PUFAs), but also in amphipathic compounds, the phospholipids (Massrieh, 2008). It would therefore be of interest to investigate the effects of phospholipids on the dynamics of the transesterification as well as on the lipase efficiency and its affinity.

In order to investigate the individual, combined and cumulative effects of the various factors in a given study, response surface methodology (RSM) is considered an effective statistical technique (Myers *et al*., 2009). Central composite rotatable design (CCRD) is

generally the most appropriate design for response surface optimization (Jeong and Park, 2006). Its main advantage is the reduced number of experimental runs needed to obtain sufficient information for statistically acceptable results. The CCRD is considered a faster and less expensive method than the one-variable-at-a-time and full-factorial experimentation (Myers *et al*., 2009). The use of RSM for optimizing the lipase-catalyzed synthesis of esters has been recently reported (Aybastler and Demir, 2010; Rodrigues and Ayub, 2011). Although the maximization of the response is of interest in most cases, a saddle point, which is neither a maximum nor a minimum, can be encountered (Baş and Boyacı, 2007).

The aim of our work was to optimize the biosynthesis of novel biomolecules, PLs, from KO and DHPA, using RSM. The effects of several reaction parameters, including the PA concentration (PAC), lipase concentration (LC) and agitation speed (AS) and the relationships between them have been investigated. In addition, we show how RSM and sequential experiments can be used to overcome a saddle point in order to meet the objective of maximization of the bioprocess.

4.3. Materials and Methods

4.3.1. Materials

Commercial immobilized lipases, including a non-specific one, Novozym 435, from *Candida antartica* with an activity of 10,000 propyl laurate units (PLU) per g solid enzyme and a 1,3-specific one Lipozyme TL IM from *Thermomyces lanuginose* with an activity of 20,000 units per g solid enzyme, were purchased from Novozymes A/S (Bagsværd, Denmark). 3,4-dihydroxyphenylacetic acid (DHPA) and dihydrocaffeic acid (DHCA) were purchased from Sigma Chemical Co. (St-Louis, MO). High-potency krill oil extracted from *Euphausia superba* was generously provided by Enzymotec Ltd. (Morristown, NJ, USA). Organic solvents of high-performance liquid chromatography (HPLC) grade were obtained from Fisher Scientific (Fair Lawn, N.J.).

4.3.2. Transesterification Reaction in Solvent-Free Medium

4.3.2.1. Screening of Selected Biocatalysts and Phenolic Acid Models

The selection of the appropriate biocatalyst and phenolic acids (PAs) for the transesterification reaction was investigated by using Novozym 435 and Lipozyme TL IM as well as DHPA and DHCA. Aliquots of reaction medium were withdrawn over a 48-h incubation period. The selection of the biocatalyst was determined in well-defined conditions, including reaction volume (2 mL), enzyme amount (20 and 40 mg solid enzyme/mL (400 PLU) for Lipozyme TL IM and Novozym 435, respectively), agitation speed (AS; 150 rpm) and reaction temperature (60°C).

4.3.2.2. Transesterification Trials

Lipase-catalyzed transesterification of krill oil (KO) was carried out with a modification to the method developed in our laboratory (Sabally *et al*., 2006a; Sorour, 2010), using DHPA and DHCA as substrates. Prior to each enzymatic reaction, a stock solution of PA was freshly prepared in 2-butanone. Aliquot of the PA stock solution was mixed with KO to obtain a final concentration between 3 and 37 mM, with 7% butanone in the reaction mixture. The reaction mixture was homogenized, using a Corning tissue grinder pestle (Corning Inc.; Lowell, MA). The enzymatic reaction was initiated with the addition of a variable amount of Novozym 435 (43-77 mg solid enzyme /mL) to the reaction mixture (2 mL), with continuous shaking (140-309 rpm) in an orbital incubator shaker (New Brunswick Scientific Co., Inc.; Edison, N.J.). Transesterification reactions were run in duplicate, with concomitant control trials containing all reaction components except the enzyme; samples from the reaction mixtures were withdrawn at specific time intervals over the course of the 48-h reaction. The recovered samples were flushed with a gentle stream of nitrogen and stored at −80ºC for further analyses. For HPLC analysis, 8 µL from the recovered reaction mixture was solubilized in 100 µL isopropanol (IPA) and 52 µL acetonitrile (ACN), and homogenized by sonication using the sonicator® ultrasound processor (Model XL2020, Heat Systems, Inc.; Farmingdale, N.Y.).

4.3.3. Characterization of the Components of Krill Oil and Its Esterified Phenolic Lipids

4.3.3.1. High-Performance Liquid Chromatography Analysis

HPLC separation of the components of KO and those of its esterified PLs was carried out with a Zorbax SB-C18 reversed-phase column (150x3.0 mm, 3.5 μm) purchased from Agilent Technologies (Santa Clara, CA), using the 32 Karat software version 8.0 (Model 126, Beckman Instruments Inc.; San Ramon, CA) equipped with an autosampler (Model 507) with dual detection systems of a UV/VIS-diode array detector (DAD-Model 168) and an evaporative light scattering detector (ELSD, Model 2000; Alltech Associates, Inc.; Deerfield, IL). A sample of 5 μL was injected into the system, using the appropriate loading loop. The elution was initiated with an isocratic flow of 100% of acetonitrile (ACN, solvent A) for 9 min, followed by an 18-min gradient up to 60 and 40% of solvent A and isopropanol (IPA, solvent B), respectively, then to 100% of solvent B for a 9-min period, followed with an equilibration period of 10 min with 100% of solvent A. The flow rate was 0.43 mL/min and the detection was performed with ELSD. The bioconversion yield (BY) of phenolic lipids (PLs) was calculated as the peak area of total PLs, monitored with ELSD after 24 h of reaction, divided by the sum of the peak area of phospholipids at time 0 and that of total PLs after 24 h of reaction, multiplied by 100.

4.3.4. Experimental Design

In order to optimize the bioprocess for the biosynthesis of PLs, after choosing the most appropriate enzyme and PA, a 'five-level-by-three-factor' central composite design was used (Myers *et al*., 2009). The treatment combinations were constructed from eight factorial points, six axial points and one central point. Duplicate reactions were carried for all designed points except the central one, which was replicated six times, resulting in a total of 34 treatments. To minimize the effect of unexplained variability in the observed responses that could be due to extraneous factors, all reactions were carried in a randomized order. The variables and their coded and uncoded values are presented in Table 4-1.

Table 4-1. Process variables and their levels, used in the central composite rotatable design.

Variable	Name	Coded levels				
		- 1.682	- 1	0	+ 1	+ 1.682
x_1	Phenolic acid concentration (mM)	3.18	10	20	30	36.82
x_2	Lipase concentration (mg/mL)	43.18	50	60	70	76.82
x_3	Agitation speed (rpm)	140.91	175	225	275	309.09

The response Y was the percent of BY) (%), and a quadratic polynomial regression model was used to predict it:

$$Y = \beta_0 + \Sigma \beta_i x_i + \Sigma \beta_{ii} x_i^2 + \Sigma\Sigma \beta_{ij} x_i x_j \quad \ldots\ldots\ldots\ldots\ldots\ldots (4\text{-}1)$$

where β_0, β_i, β_{ii}, and β_{ij} are the intercept, linear, quadratic, and bilinear regression coefficient terms, respectively, while x_i and x_j denote independent variables (Myers *et al*., 2009). The procedures RSREG and GLM (with the SS3 option) of the statistical analytical system SAS 9.1 were used for multiple regression analysis, canonical analysis, and analysis of variance. Response surface plots were generated with SAS 9.1 ADX Interface for Design of Experiments.

4.4. Results and Discussion

4.4.1. Optimization of the Bioprocess for the Biosynthesis of Phenolic Lipids

4.4.4.1. Selection of the Appropriate Biocatalyst and Phenolic Acid

Figure 4-1 shows the HPLC chromatograms of the components of the acidolysis of KO with 3,4-dihydroxyphenylacetic acid (DHPA), catalyzed by Novozym 435 and monitored with ELSD, with initial reaction mixture at time 0 (A) and after 24 h (B). Peak numbers were identified as DHPA (peak # 1) with a retention time (RT) of 2.419 min, phenolic lipids (peaks # 1', 2', 3', 4' and 5') with RT of 3.729, 3.802, 5.861, 6.301 and 6.772 min, respectively, and phospholipids of KO (peaks # 2, 3, 4, 5, 6 and 7) with RT of 9.279, 11.456, 11.970, 12.734, 13.446 and 19.538 min, respectively. As reported recently by our group (Aziz *et al*., 2012b), the structural analyses of the synthesized phenolic lipids (PLs) suggested the formation of two phenolic monoacylglycerols (MAGs), resulting from the transesterification by lipase in SFM of the phospholipids present in KO and the DHPA. However, in order to determine the appropriate biocatalyst and phenolic acid, selected commercial immobilized lipases including Novozym 435 from *Candida antarctica* and Lipozyme TL IM from *Thermomyces lanuginose* as well as phenolic acids, 3,4-dihydroxyphenylacetic acid (DHPA) and dihydrocaffeic acid (DHCA) were investigated.

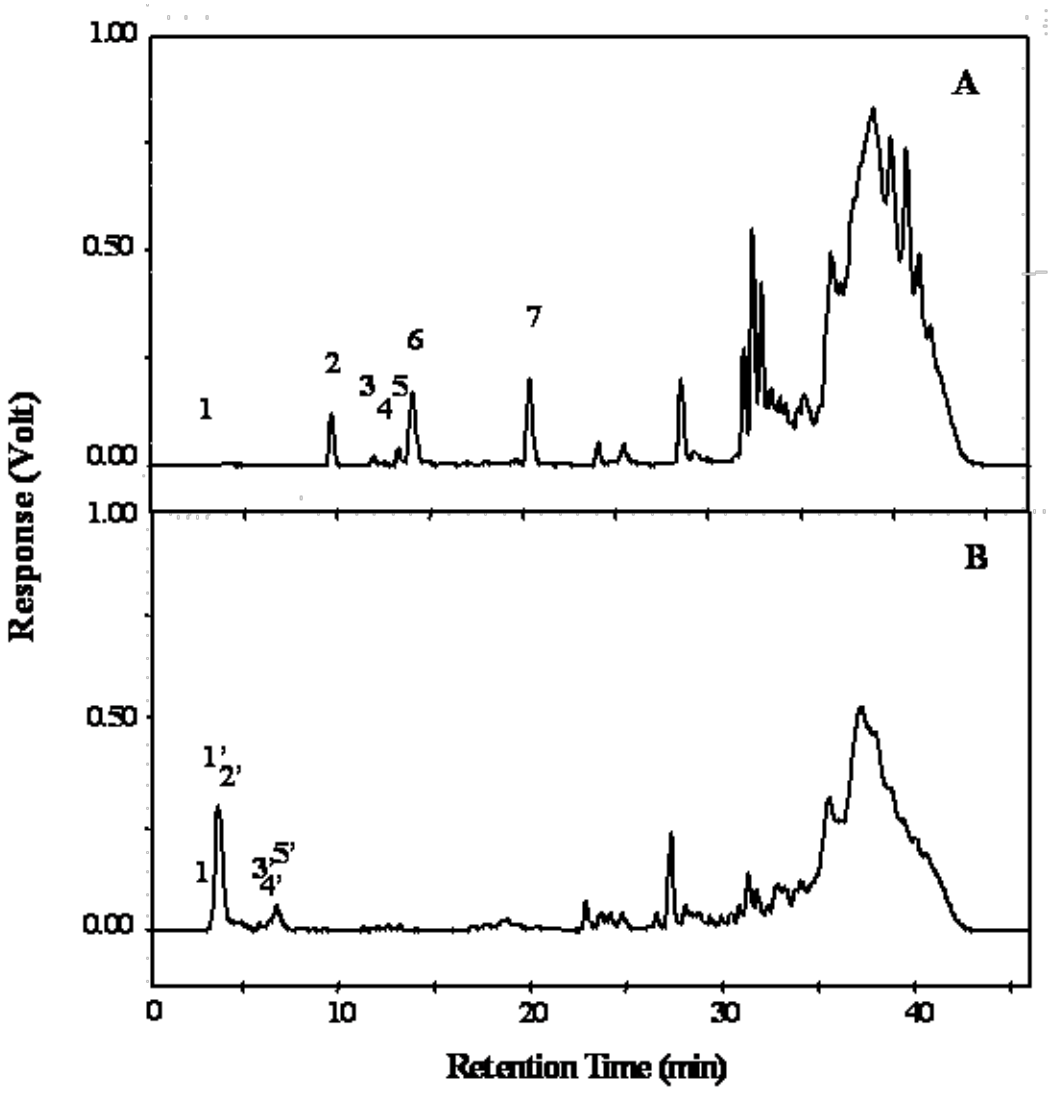

Figure 4-1. HPLC chromatograms of the components of the acidolysis of krill oil (KO) with 3,4-dihydroxyphenylacetic acid (DHPA), catalyzed by Novozym 435, monitored with ELSD, with initial reaction mixture at time 0 (A) and after 24 h (B). Peak numbers were identified as follow: DHPA (peak #1), phenolic lipids (peaks # 1', 2', 3', 4'and 5') and phospholipids of KO (peaks # 2, 3, 4, 5, 6 and 7).

Figure 4-2 shows the time course of the acidolysis of KO with DHPA and DHCA, catalyzed by either Novozym 435 or Lipozyme TL IM in SFM, over the 48-h reaction period. For both enzymes, the time course of the enzymatic synthesis was initiated after 9 h of reaction, where the transesterification was favored over hydrolysis. For Novozym 435, with DHPA and DHCA as substrates, the trend of the enzymatic reaction was similar. There was a gradual increase in the BY to a maximum of 56.79% (24 h) and 47.46 % (18 h), respectively, before its decrease to 46.15 and 40.46% after 36 h; this decrease may be due to a shift in the thermodynamic equilibrium of the reaction towards hydrolysis and/or to the acyl migration, as a result of an increase in the concentration of free fatty acids (Karboune *et al*., 2005; Vikbjerg *et al*., 2005). Although the reaction rate was slower for lipase-catalyzed transesterification in OSM of fish liver oil (FO) with DHCA and DHPA (Sabally *et al*., 2007; Karam *et al*., 2009) as well as in SFM with DHPA (Sorour, 2010), a similar trend to that in Figure 4-2 was observed. For Lipozyme TL IM, there was no significant difference in the BY between the two PAs after 18 h of reaction, with a maximum BY of 47.78 and 45.38% for DHPA and DHCA, respectively; the time course for Lipozyme TL IM followed a trend similar to that for Novozym 435. Nevertheless, the experimental data obtained with Lipozyme TL IM (Fig. 4-2) showed lower reproducibility; this could be attributed to the non-uniformity of the circular granular size of the Lipozyme TL IM immobilized lipase that could affect the lipase and substrate interaction at the interface. Valencia *et al*. (2010) reported that the size distribution of the enzyme particles has an important effect on the performance, which may result in high variability of the predicted values. Overall, the highest BY was obtained with Novozym 435 and DHPA after 24 h of reaction. The difference in the catalytic efficiency between the two biocatalysts could be due to the differences in their affinity and regioselectivity towards the phospholipids of the KO as well as the PAs, DHPA and DHCA (Stamatis *et al*., 1999). Likewise, Karam *et al*. (2009) showed that Lipozyme IM-20 catalyzed acidolysis of DHPA with fish liver oil resulted in a maximum BY of 14.1% after 10 days of reaction, whereas with Novozym 435 as biocatalyst, the maximum BY of 64.8% was obtained after 8 days of reaction.

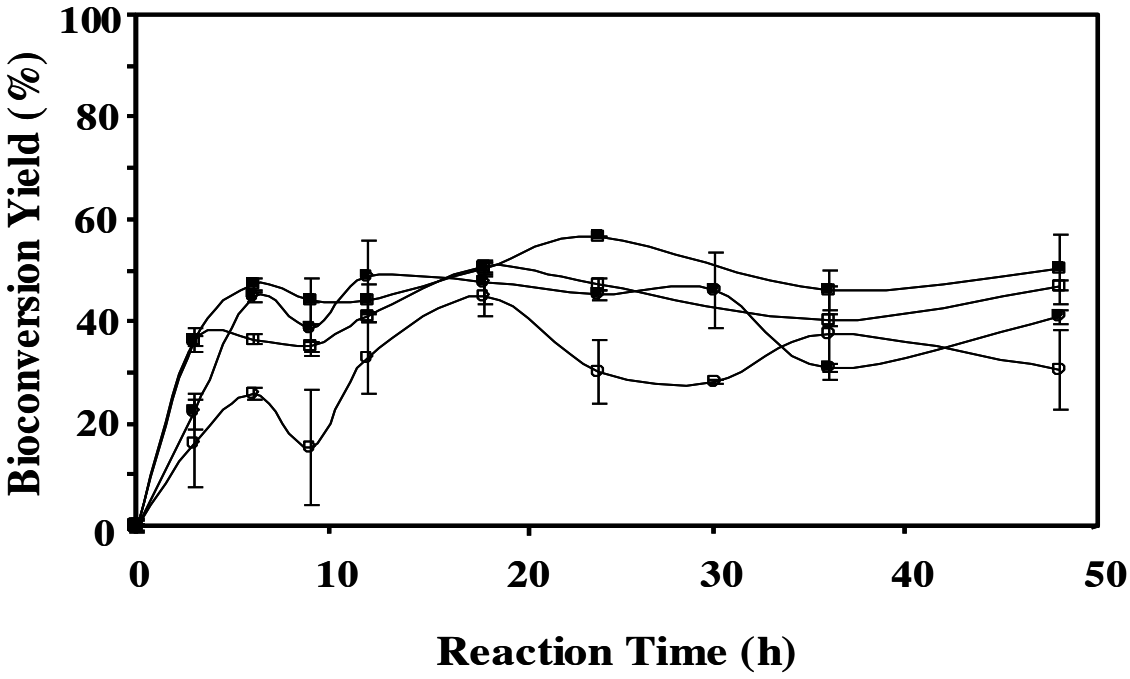

Figure 4-2. Time course for the acidolysis reaction of krill oil with dihydroxyphenylacetic acid (DHPA), catalyzed by Novozym 435 (■) and by Lipozyme TL IM (●) as well as with dihydrocaffeic acid (DHCA) catalyzed by Novozym 435 (□) and by Lipozyme TL IM (○) in solvent-free medium.

The reaction time for the acidolysis in SFM of KO (24 h) was much shorter than that for FO and flaxseed oil, where the highest BY was obtained after 7 days of reaction (Sorour, 2010); the shorter reaction time could be explained by the fact that the enzyme has better affinity for phospholipids than that for triacylglycerols (TAGs), which could be due to their viscosity and polarity (Vikbjerg *et al*., 2005). Based on the experimental findings, Novozym 435 as well as DHPA were used for further investigation, using a 24 h reaction time.

4.4.4.2. Model Fitting and ANOVA

Throughout this study, the CCRD was used for the optimization of the enzymatic synthesis in SFM of PLs from KO and DHPA, with three factors (x_1: PAC; x_2: LC; x_3: AS) and five levels, considering all three factors together or only two of them at a time for a given value of the third one; the actual and coded values of the factors, together with the corresponding BY (%) experimental data, are reported in Table 4-2. The response surface analysis (Table 4-3) shows that the transesterification of KO and DHPA in SFM was most suitably described with the following quadratic polynomial model:

$$Y = 56.82 - 1.16\,x_1 + 5.52\,x_2 + 3.94\,x_3 + 5.51\,x_1^2 - 0.93\,x_1x_2 - 7.59\,x_1x_3 - 4.73\,x_2^2 + 1.27\,x_2x_3 - 6.57\,x_3^2 \quad \text{(4-2)}$$

where Y = BY (%), and x_1, x_2 and x_3 are the coded values of PAC, LC and AS, respectively.

The regression model for %BY above was highly significant, with a coefficient of determination ($R^2 = 0.9$). The response surface analysis (Table 4-3) for the optimization of the biosynthesis of PLs showed that the predicted model was very adequate ($P < 0.0001$). The lack-of-fit *F*-value of 0.69 was non-significant, with an associated *P*-value much higher than 0.05. These results imply that the model represents well the responses within the selected ranges for the reaction parameters.

Table 4-2. Central composite rotatable second-order design (CCRD), experimental data for 5 levels-3-factors response surface analysis.

Run	DHPA (mM)[a] x_1	Lipase (mg/mL)[b] x_2	Agitation speed (rpm) x_3	BY (%)[c] y
1	36.82[d] (1.682)[e]	60.00[d] (0.000)[e]	225.00[d] (0.000)[e]	60.39
2	3.18 (-1.682)	60.00 (0.000)	225.00 (0.000)	64.91
3	20.00 (0.000)	43.18 (-1.682)	225.00 (0.000)	45.54
4	10.00 (-1.000)	50.00 (-1.000)	175.00 (-1.000)	45.42
5	10.00 (-1.000)	70.00 (1.000)	275.00 (1.000)	64.76
6	10.00 (-1.000)	70.00 (1.000)	175.00 (-1.000)	56.67
7	20.00 (0.000)	60.00 (0.000)	140.91 (-1.682)	46.48
8	20.00 (0.000)	60.00 (0.000)	225.00 (0.000)	56.74
9	20.00 (0.000)	60.00 (0.000)	225.00 (0.000)	54.32
10	20.00 (0.000)	60.00 (0.000)	309.09 (1.682)	54.10
11	20.00 (0.000)	43.18 (-1.682)	225.00 (0.000)	48.21
12	20.00 (0.000)	76.82 (1.682)	225.00 (0.000)	55.31
13	10.00 (-1.000)	70.00 (1.000)	275.00 (1.000)	64.51
14	30.00 (1.000)	70.00 (1.000)	275.00 (1.000)	58.49
15	10.00 (-1.000)	70.00 (1.000)	175.00 (-1.000)	53.60
16	30.00 (1.000)	50.00 (-1.000)	175.00 (-1.000)	50.22
17	3.18 (-1.682)	60.00 (0.000)	225.00 (0.000)	60.11
18	30.00 (1.000)	70.00 (1.000)	275.00 (1.000)	56.25
19	20.00 (0.000)	60.00 (0.000)	140.91 (-1.682)	43.52
20	20.00 (0.000)	60.00 (0.000)	225.00 (0.000)	57.97
21	10.00 (-1.000)	50.00 (-1.000)	175.00 (-1.000)	49.75
22	20.00 (0.000)	76.82 (1.682)	225.00 (0.000)	57.83
23	30.00 (1.000)	70.00 (1.000)	175.00 (-1.000)	59.71
24	10.00 (-1.000)	50.00 (-1.000)	275.00 (1.000)	58.89
25	30.00 (1.000)	70.00 (1.000)	175.00 (-1.000)	54.87
26	30.00 (1.000)	50.00 (-1.000)	275.00 (1.000)	47.71
27	20.00 (0.000)	60.00 (0.000)	225.00 (1.000)	58.25
28	20.00 (0.000)	60.00 (0.000)	225.00 (1.000)	57.69
29	30.00 (1.000)	50.00 (-1.000)	275.00 (1.000)	50.95
30	10.00 (-1.000)	50.00 (-1.000)	275.00 (1.000)	54.32
31	30.00 (1.000)	50.00 (-1.000)	175.00 (-1.000)	54.51
32	20.00 (0.000)	60.00 (0.000)	225.00 (0.000)	56.23
33	36.82 (1.682)	60.00 (0.000)	225.00 (0.000)	62.47
34	20.00 (0.000)	60.00 (0.000)	309.09 (1.682)	55.46

[a]Concentration of the phenolic acid, 3,4 dihydroxyphenylacetic acid, in mM.

[b]Concentration of the lipase Novozym 435 in mg solid enzyme/mL, with an activity of 10,000 propyl laurate unit/g solid enzyme.

[c]Bioconversion yield (BY) in percent was calculated as the peak area of total phenolic lipids, monitored with ELSD, after 24 h of reaction, divided by the sum of that of phospholipids at time 0 and that of total phenolic lipids after 24 h of reaction, multiplied by 100.

[d]Actual experimental amounts.

[e]Actual experimental amounts in coded values.

Table 4-3. Response surface analysis[a] and model coefficients of first and second orders.

Source	Number of degree of freedom	Type III Sum of squares	Mean square	*F*-value	*P*-value
x_1	1	7.249	7.249	1.64	0.2124[c]
x_2	1	60.966	60.966	13.80	0.0011[b]
x_3	1	109.499	109.499	24.79	<.0001[b]
x_1*x_1	1	85.681	85.681	19.40	0.0002[b]
x_1*x_2	1	1.724	1.724	0.39	0.5381[c]
x_1*x_3	1	115.230	115.230	26.09	<.0001[b]
x_2*x_2	1	63.156	63.156	14.30	0.0009[b]
x_2*x_3	1	3.236	3.236	0.73	0.4005[c]
x_3*x_3	1	121.515	121.515	27.51	<.0001[b]
Model	9	936.583	104.065	23.56	<.0001[b]
(Linear)	3	457.561	152.521	34.53	<.0001[b]
(Quadratic)	3	358.832	119.611	27.08	<.0001[b]
(Cross Product)	3	120.190	40.063	9.07	0.0003[b]
Error	24	106.010	4.417	_	_
(Lack of fit)	5	16.324	3.265	0.69	0.6359[c]
(Pure Error)	19	89.686	4.720	_	_
Total	33	1042.593	_	_	_

[a]The phenolic lipids bioconversion yield has been investigated using three independent variables; phenolic acid concentration x_1 (3-37 mM), lipase concentration x_2 (43-77 mg solid enzyme/mL) and agitation speed x_3 (141-309 rpm), and it was calculated as the peak area of total phenolic lipids, monitored with ELSD, after 24 h of reaction divided by the sum of that of phospholipids at time 0 and that of total phenolic lipids after 24 h of reaction, multiplied by 100.

[b]Significant at less than 0.05 level.

[c]Not significant at higher than 0.05 level.

4.4.4.3. Effect of Variables on the Bioconversion Yield of Phenolic Lipids

Among the three independent variables, LC (x_2) and AS (x_3) have the most significant linear and quadratic effects on the BY of PLs, with *t*-test values of 4.98, 3.72 and –3.78, –5.25, respectively (Table 4-3). On the other hand, PAC showed a significant quadratic effect (*t*-test value = 4.40) and a significant bilinear one when combined with AS ($x_1 * x_3$; *t*-test value = –5.11). Note that a *t*-test value with a positive sign indicates that in the response surface model, an increase in this variable has a positive (increasing) effect on the BY of PLs, while a negative sign indicates a negative (decreasing) effect on the BY when the corresponding variable increases. No other combined effects were found to be statistically significant.

Figure 4-3 shows the effects of PAC, LC and AS, taken two by two, on the enzymatic synthesis by Novozym 435 of phenolic lipids. In the two-dimensional response surface plots (Figs. 4-3A, 3B and 3D), the factors that have not been displayed were fixed at their central value. The analysis (Table 4-3) indicates that LC and AS have important linear and quadratic effects on the BY of phenolic lipids. In view of Fig. 4-3C, at fixed PAC of 20 mM, there was an increase in both AS and LC that led to a concomitant linear increase, followed by a quadratic increase in the BY up to a certain limit. As expected, the presence of higher enzyme concentration in the reaction medium may have increased the probability of its collision with the substrate, and subsequently enhanced the rate of the reaction (Kumari *et al*., 2009). Furthermore, in the case of immobilized enzymes, AS can minimize the external mass transfer limitations by allowing the reactants to diffuse from the bulk liquid to the external surface of the enzyme particles and from there, subsequently to the interior pores of the catalyst (Kumari *et al*., 2009). However, further increase in LC and AS was associated with a concomitant decrease in the BY of phenolic lipids. Results similar to those of Figure 4-3C were also reported by Sorour (2010) for the transesterification in SFM of fish liver oil (FO), with DHCA as substrate. The same results (Fig. 4-3C) are also in agreement with those of Hadzir *et al*. (2001), who reported that a decrease in the enzyme activity, at high concentration, may be due to the hindrance of its active site.

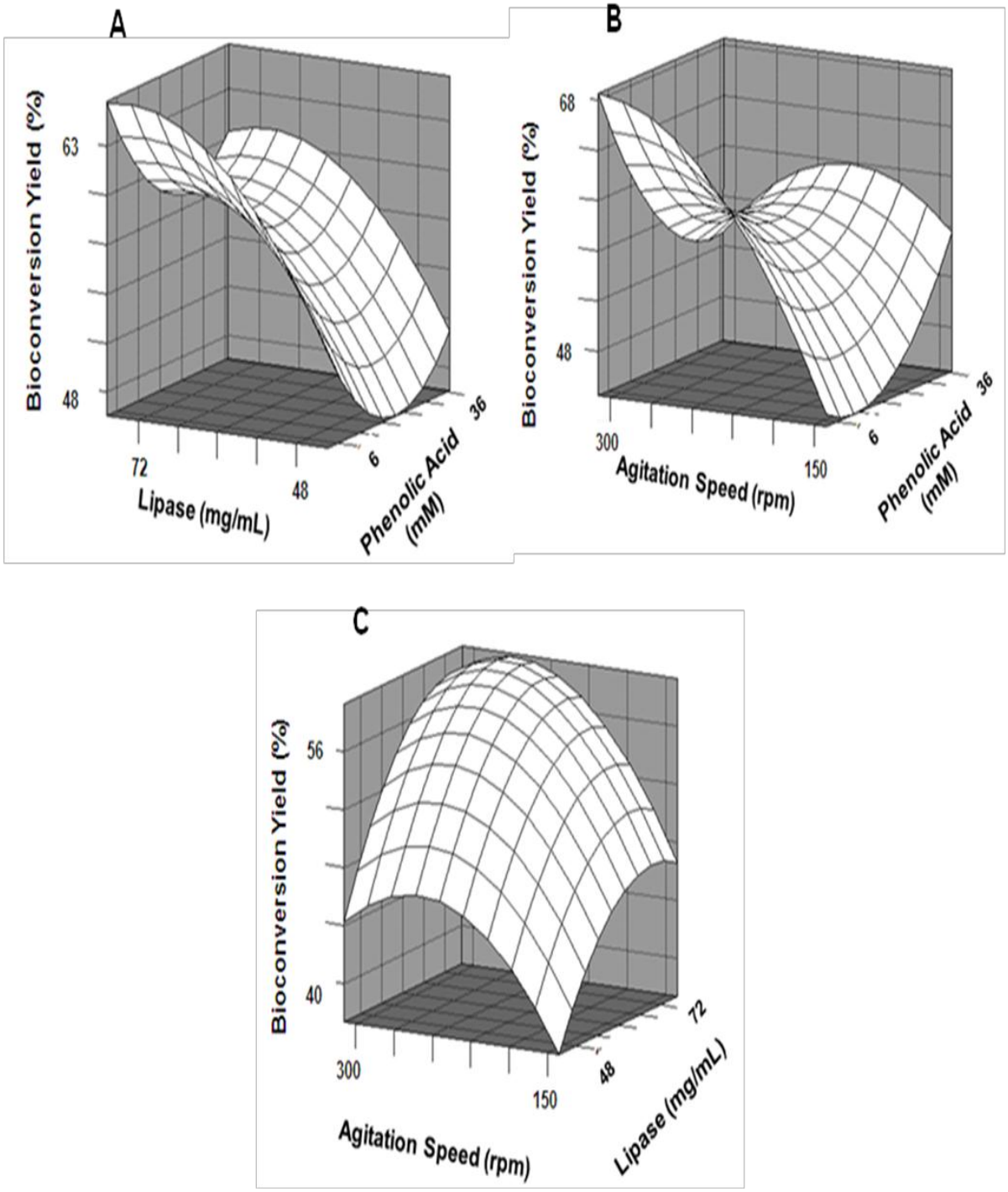

Figure 4-3. Response surface plots showing the effects of lipase concentration versus phenolic acid concentration (A), agitation speed versus phenolic acid concentration (B) and agitation speed versus lipase concentration (C) on the enzymatic synthesis of phenolic lipids by Novozym 435.

Similarly, the decrease in the BY of PLs could be attributed to a shift in the reaction thermodynamic equilibrium towards hydrolysis (Karboune *et al*., 2005) or to a mass transfer limitation, caused by a high concentration of the enzyme (Vikbjerg *et al*., 2005). On the other hand, Yadav and Devi (2004) and Kumari *et al*. (2009) indicated that there was no further increase or decrease in conversions with high AS, which may be due to the attrition of the particles sticking to the wall or to the shearing of the enzyme molecules.

In addition, the results (Tables 4-2 and 4-3) showed that PAC had no significant linear effect on the BY of PLs. At fixed AS of 225 rpm (Fig. 4-3A) and LC of 60 mg/mL (Fig. 3B), an increase in PAC from 3.18 to 20 mM resulted in a slight decrease in the BY, from an average of 62.51 to 56.57% (Fig. 4-3A). However, further increase of PAC to 36.82 mM resulted in a slight increase of BY to 61.43% (Fig. 4-3A). These experimental findings indicate that the variation in PAC, within the investigated range of 3.18 to 36.82 mM, did not have an important linear effect, but rather a quadratic one on BY. Vikbjerg *et al*. (2005) reported that for the lipase-catalyzed acidolysis reaction in SFM between soybean phosphatidylcholine (PtdCho) and caprylic acid, an increase in the substrate molar ratio of the fatty acid decreased its incorporation into PtdCho, whereas its incorporation into lyso-phosphatidylcholine (Lyso-PtdCho) was increased. Since KO contains both Lyso-PtdCho and PtdCho (Winther *et al*., 2011; Aziz *et al*., 2012b), the effect of PAC on BY (Figs. 4-3A and 4-3B) could have the same trend (Vikbjerg *et al*., 2005).

Furthermore, the analysis of the response surface plots (Table 4-3, Fig. 4-3B) also showed that the interaction between PAC and AS was negative and significant. At fixed LC of 60 mg/mL, an increase of AS, from 140.91 to 225 rpm, resulted in increases of BY from 43.52 to 56.86% (Table 4-2, Fig. 4-3B). On the contrary, an increase of PAC, from 3.18 to 20 mM, resulted in a decrease of BY from an average of 62.51 to 56.57%. The literature (Dossat *et al*., 2002; Lue *et al*., 2005; Kumari *et al*., 2009) indicated that AS increases the diffusion of the reactants to the interfacial area of the enzyme and thus, their availability for the reaction, by reducing external mass transfer limitations. The negative sign of the bilinear effect coefficient for PAC and AS could be attributed to the opposite

effects of PAC and AS on BY. Similarly, Vikbjerg *et al*. (2005) reported that the substrate molar ratio of caprylic acid to phospholipids had a decreased effect on the lipase-catalyzed acidolysis in SFM. Our experimental results (Table 4-3, Fig. 4-3B) are in agreement with those of Sorour *et al*. (2010), who indicated that the enzymatic synthesis of PA from FO and DHCA was decreased when the PAC concentration was increased.

4.4.4.3.1. Canonical Analysis and the Presence of a Saddle Point

To examine more closely the overall shape of the response surfaces and to characterize the nature of the stationary point, canonical analysis was performed on the matrices of second derivatives of the predicted quadratic polynomial surfaces; second derivatives are calculated to determine whether the first derivatives have vanished at a maximum, a minimum or a saddle point. Canonical analysis is a mathematical method that decomposes square matrices, such as matrices of second derivatives, into so-called "eigenvalues" and "eigenvectors". When all eigenvalues are negative, the stationary point is a maximum; when they are all positive, it is a minimum; and a mixture of negative and positive eigenvalues corresponds to a saddle point. Depending on the direction, the response may increase or decrease when moving away from a saddle point (Carlson and Carlson, 2005).

The response surfaces showing the effects of PAC, LC and AS, taken two by two, on the enzymatic synthesis of phenolic lipids are displayed in Figures 4-3A, 4-3B and 4-3C. When PAC is combined with LC and AS, the response increases, or decreases from the center of the surface, depending on the direction (Figs. 4-3A and 4-3B). Such saddle-shaped surfaces reflect the opposite effect of PAC on BY, compared to LC and AS; this can also be seen from the mixed positive and negative signs of estimated coefficients in Equation 4-2.

Although the maximization of the BY of PLs was of interest, the stationary point was a saddle point, which does not correspond to a unique optimum for the response (Baş and Boyacı, 2007). Hence, using PAC (x_1), LC (x_2) and AS (x_3) as independent variables, a maximum BY could not be obtained. Nevertheless, the canonical analysis revealed that a maximum point could be obtained when LC (x_2) and AS (x_3) are used

as independent variables, that is, by excluding PAC (x_1) or by working at a given value of PAC. Indeed, the response, once averaged over the experimental values of PAC considered in the initial three-factor-by-five-level CCRD, is a concave surface, with a maximum point (Fig. 4-3C). The resulting predicted response at the stationary point is then 61% of BY, obtained with 67.8 mg/mL of LC and 248 rpm of AS.

4.4.4.4. Optimization of the Transesterification Reaction, using Sequential Experiments

To further explore the response surface methodology and to overcome a saddle point, two independent variables, namely LC (x'_1) and AS (x'_2), were used at fixed PAC of 10, 20 and 30 mM, which corresponded to the coded levels of –1, 0 and 1 in the initial three-factor-by-five-level CCRD. The uncoded and coded values of the new independent variables are presented in Table 4-4. The response to be predicted (Y) remained %BY. The experimental data obtained in the sequence of three experiments are given in Table 4-5.

4.4.4.4.1. Model Fitting and ANOVA

Based on the *P*-values reported in Table 4-6 for the models with PAC fixed at 10 and 20 mM, the transesterification of KO and DHPA in SFM was most suitably described with a quadratic polynomial model. For the model with PAC fixed at 30 mM, none of the linear, quadratic and bilinear effects were found to be statistically significant, or even close. The R^2 values for the different models are also reported in Table 4-6.

More specifically, the analyses of variance and error performed for the optimization of the biosynthesis of PLs indicate that the models with PAC fixed at 10 and 20 mM were adequate, with *P*-values of 0.0004 and <0.0001 (Table 4-6). All three models show no significant lack of fit; in other words, the three models represent well the relationships between the response and the reaction parameters within the selected ranges. The equations of predicted models, using coded values for the two-factor-by-five-level CCRD with PAC fixed at 10, 20 and 30 mM, are reported in Table 4-7.

Table 4-4. Process variables and their levels used in the central composite rotatable design for the three models with 3,4-dihydroxphenylacetic acid (DHPA) fixed at 10, 20, and 30 mM.

		Coded levels				
Variables	Name	-1.414	-1	0	+1	+1.414
x'_1	Lipase concentration (mg/mL)	45.86	50	60	70	74.14
x'_2	Agitation speed (rpm)	154.29	175	225	275	295.71

Table 4-5. Central composite rotatable second-order design (CCRD), experimental data for 5 levels-2-factors response surface analysis.

Run	Lipase conc. (mg/mL)[a] x'_1	Agitation speed (rpm) x'_2	Observed BY[b] (%) for fixed DHPA[c] conc. 10 mM	20 mM	30 mM
1	70.00[d] (1.000)[e]	175.00[d] (-1.000)[e]	59.06[b]	69.41[b]	45.00[b]
2	70.00 (1.000)	275.00 (1.000)	63.78	64.35	54.00
3	45.86 (-1.414)	225.00 (0.000)	53.29	29.10	43.40
4	50.00 (-1.000)	275.00 (1.000)	55.42	34.63	37.10
5	50.00 (-1.000)	275.00 (1.000)	45.14	35.50	36.60
6	60.00 (0.000)	225.00 (0.000)	60.00	66.78	34.90
7	60.00 (0.000)	154.29 (-1.414)	51.92	75.20	42.00
8	74.14 (1.414)	225.00 (0.000)	56.93	57.96	42.10
9	60.00 (0.000)	295.71 (1.414)	54.70	64.90	44.50
10	74.14 (1.414)	225.00 (0.000)	60.67	56.45	40.80
11	45.86 (-1.414)	225.00 (0.000)	50.10	22.00	34.80
12	60.00 (0.000)	225.00 (0.000)	61.20	72.44	42.80
13	60.00 (0.000)	225.00 (0.000)	64.75	71.14	46.40
14	70.00 (1.000)	275.00 (1.000)	64.98	68.82	45.10
15	60.00 (0.000)	225.00 (0.000)	59.90	68.00	46.40
16	60.00 (0.000)	154.29 (-1.414)	51.31	73.90	45.70
17	60.00 (0.000)	225.00 (0.000)	60.90	73.98	35.20
18	70.00 (1.000)	175.00 (-1.000)	58.86	69.66	49.50
19	60.00 (0.000)	295.71 (1.414)	57.63	69.90	40.70
20	50.00 (-1.000)	175.00 (-1.000)	52.03	46.40	36.50
21	50.00 (-1.000)	175.00 (-1.000)	54.38	42.57	34.10

[a]Concentration of the lipase Novozym 435 in mg solid enzyme/mL, with an activity of 10,000 propyl laurate unit/g solid enzyme.

[b]Observed bioconversion yield (BY) in percent was calculated as the peak area of total phenolic lipids, monitored with ELSD, after 24 h of reaction divided by the sum of that of phospholipids at time 0 and that of total phenolic lipids after 24 h of reaction, multiplied by 100.

[c]3,4 dihydroxyphenylacetic acid.

[d]Actual experimental amounts.

[e]Actual experimental amounts in coded values.

Table 4-6. The t- and *P*-values of second-order response surface methodology design with x'_1 and x'_2 as independent variables[a] at fixed concentrations of 10, 20 and 30 mM of 3,4 dihydroxyphenylacetic acid (DHPA).

	Fixed DHPA concentration (mM)					
	t-value			*P*-value		
Source	10	20	30	10	20	30
x'_1	2.01	14.50	0.32	0.0625[c]	< .0001[b]	0.7531[c]
x'_2	1.64	-0.87	-0.66	0.1212[c]	0.3974[c]	0.5206[c]
$x'_1 * x'_1$	-2.70	-15.34	-0.20	0.0166[b]	< .0001[b]	0.8412[c]
$x'_1 * x'_2$	1.97	1.45	0.11	0.0678[c]	0.168	0.9152[c]
$x'_2 * x'_2$	-3.42	-0.32	0.76	0.0038[b]	0.7565[c]	0.4566[c]
R^2	0.7508	0.9728	0.3766			
Model				0.0004[b]	< .0001[b]	
(Linear)				0.0004[b]	< .0001[b]	
(Quadratic)				0.0067[b]	< .0001[b]	
Error						
(Lack of fit)				0.1555[c]	0.1177[c]	0.1579[c]

[a]The phenolic lipids bioconversion yield has been investigated using two independent variables lipase concentration x'_1 (46-74 mg solid enzyme/mL) and agitation speed x'_2 (154-296 rpm) at fixed values of phenolic acid concentration, and it was calculated as the peak area of total phenolic lipids, monitored with ELSD, after 24 h of reaction divided by the sum of that of phospholipids at time 0 and that of total phenolic lipids after 24 h of reaction, multiplied by 100.

[b]Significant at less than 0.05 level.

[c]Not significant higher than 0.05 level.

Table 4-7. Equations of predicted models using coded values for the 2-factors-5-levels CCRD[a] with 3,4-dihydroxyphenyacetic acid concentration fixed at 10, 20 and 30 mM.

Fixed phenolic acid concentration (mM)	Equations of predicted models
10	% BY[b] (Y) = $61.35 + 5.29\ x'_1 + 1.58\ x'_2 - 5.03\ x'_{1*}x'_1 + 4.17\ x'_{1*}x'_2 - 6.39\ x'_{2*}x'_2$
20	% BY[b] (Y) = $70.47 + 17.91\ x'_1 - 3.97\ x'_2 - 30.22\ x'_{1*}x'_1 + 3.23\ x'_{1*}x'_2 - 0.62\ x'_{2*}x'_2$
30	% BY[b] (Y) = $41.14 + 4.95\ x'_1 + 0.37\ x'_2 - 0.62\ x'_{1*}x'_1 + 0.37\ x'_{1*}x'_2 + 2.33\ x'_{2*}x'_2$

[a]Central composite rotatable design.

[b]The phenolic lipids bioconversion yield (%BY) has been investigated using two independent variables lipase concentration x'_1 (46-74 mg solid enzyme/mL) and agitation speed x'_2 (154-296 rpm) at fixed values of phenolic acid concentration, and it was calculated as the total peak area of phenolic lipids, monitored with ELSD, after 24 h of reaction divided by the sum of that of phospholipids at time 0 and that of total phenolic lipids after 24 h of reaction, multiplied by 100.

4.4.4.4.2. Effects of Selected Parameters on the Bioconversion Yield of Phenolic Lipids

For the two models with PAC fixed at 10 and 20 mM (Table 4-6), LC had a significant quadratic effect on BY, whereas a significant linear effect was obtained only when PAC was fixed at 20 mM. Figures 4-4A and 4-4B show the individual effects of LC and AS as well as their combined effect on the enzymatic synthesis of PLs, with PAC fixed at 10 mM and 20 mM, respectively. At PAC maintained constant at 20 mM, LC exhibits a trend (Fig. 4-4B) similar to the one reported earlier (Section 4.4.4.3.) for the "five-level-by-three-factor" central composite design (Tables 4-2 and 4-3; Fig. 4-3); this consisted of linear and quadratic increases in the BY, with increasing LC, up to a certain limit before it decreases. On the other hand, LC shows a different trend when PAC is fixed at 10 mM (Fig. 4-4A); in this case, only the quadratic effect of the enzyme concentration has an important effect on the BY of phenolic lipids, which could be attributed to the lower value of PAC (i.e., 10 mM, coded –1).

For all three models, AS has no significant linear effect on the BY of PLs (Table 4-6, Fig. 4-4). Increasing AS from 154 to 296 rpm (Table 4-6) results in no major difference in BY, with 51.1 instead 56.2% and 74.5 instead 67.4% for the models with PAC fixed at 10 and 20 mM, respectively. These experimental findings are in agreement with those of Laudani *et al*. (2006), who investigated the influence of AS on the esterification of oleic acid with 1-octanol, using Lipozyme RM IM. These authors reported that within the range of 200 to 1,200 rpm of AS, there was no relevant change in BY, and therefore suggested this was likely due to the absence, at high AS, of external mass transfer limitations. On the contrary, Sorour (2010) reported that the BY of phenolic lipids obtained by the transesterification of fish liver oil and DHCA in SFM was increased from 39.0 to 62.5% when AS was increased from 50 to 150 rpm, before its decrease to 44.8% at AS of 250 rpm. The difference between our experimental findings (Tables 4-5 and 4-6) and those reported by Sorour (2010) may be due to the presence of phospholipids in KO, which could act as emulsifiers and would hence limit the mass transfer. Indeed, the range of AS investigated by Sorour (2010) was lower where the mass transfer limitation was more significant.

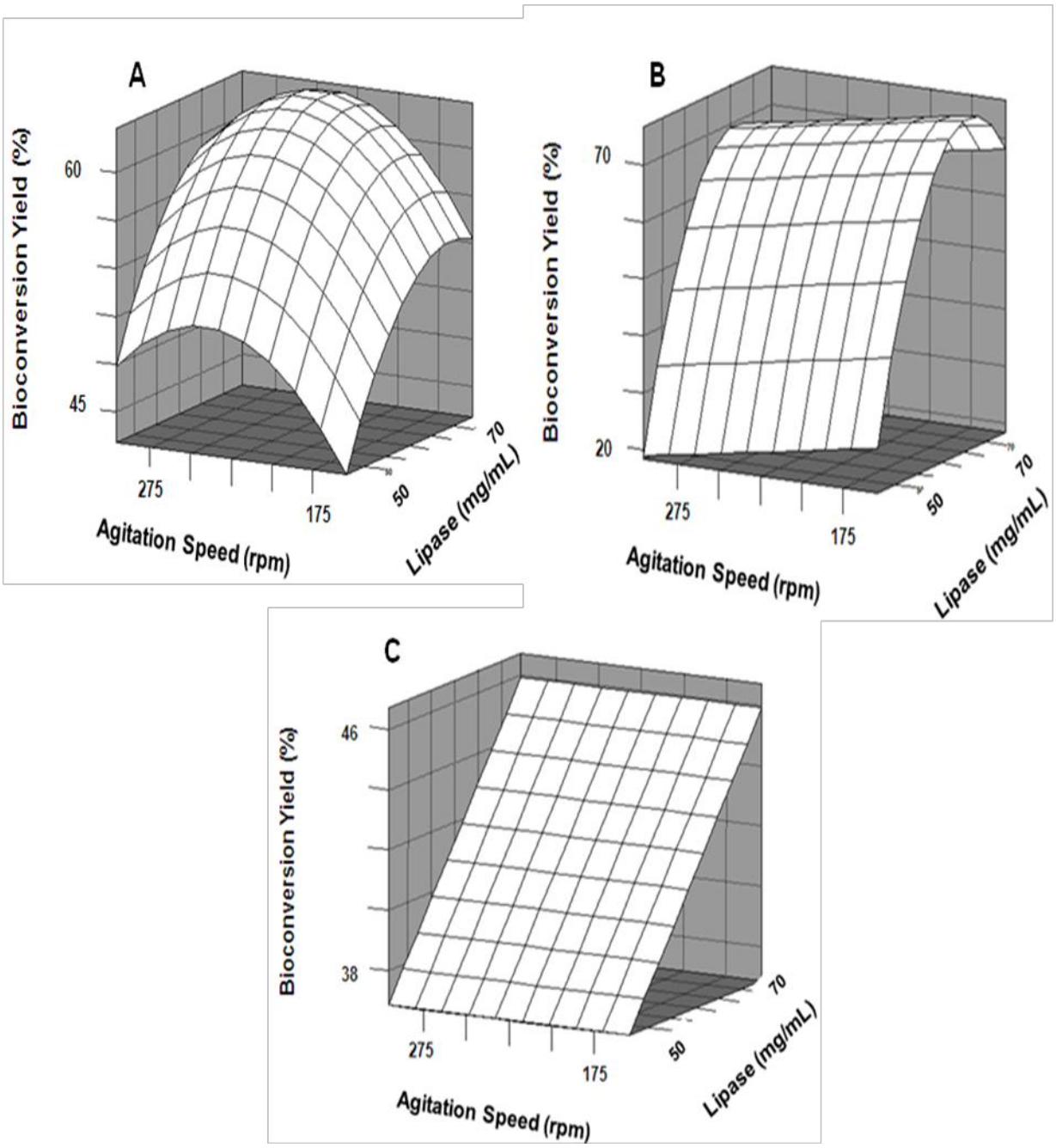

Figure 4-4. Response surface plots showing the effects of phenolic acid and lipase concentrations as well as their interactions on the enzymatic synthesis of phenolic lipids by Novozym 435, when the phenolic acid concentrations were fixed at 10 mM (A), 20 mM (B) and 30 mM (C).

Among the three models tried with a fixed value of PAC, only the quadratic effect of AS ($x'_2{}^2$) was found to be significant when PAC was fixed at 10 mM. At the lower value of PAC (10 mM), AS could have favored the diffusion of the substrate to the enzyme active site, and thus increased its availability for the reaction (Dossat *et al*., 2002; Lue *et al*., 2005; Kumari *et al*., 2009). None of the three models, investigated in our study, showed a significant interaction between LC and AS.

4.4.4.4.3. Canonical Analysis and Optimal Conditions

Canonical analysis was performed on the predicted models. The response surfaces illustrating the individual effects of LC (x'_1) and AS (x'_2) and their combined effects on the enzymatic synthesis of PLs at fixed PAC of 10, 20 and 30 mM are displayed in Figure 4-4.

Figure 4-4A shows that the response could be maximized when PAC was fixed at 10 mM; using 69.4 mg solid enzyme/mL with an AS of 249 rpm, the predicted value of BY at the stationary point was 63%. The response surface illustrating the effects of LC and AS and their interaction on the enzymatic synthesis of PLs, with PAC fixed at 20 mM, is shown in Figure 4-4B; the stationary point is a maximum with a predicted BY of 77%, obtained with 62 mg solid enzyme/mL and an AS of 23 rpm. However, the orbital incubator shaker used throughout our study was limited to a minimum AS of 50 rpm; since AS was found to have no significant effect on BY (Table 4-6; Fig. 4-4B), an AS of 154 rpm was used thereafter. At fixed PAC of 20 mM, the response surface model predicted a BY of 75%, using 62 mg solid enzyme/mL and an AS of 154 rpm. By fixing the PAC while letting LC and AS vary, the saddle point was overcome and the BY was significantly increased from 61 to 75%. However, the response surface was linear when PAC was fixed at 30 mM (Fig. 4-4C), and the predicted value at the stationary point was 50.6%. The increase of PAC from 10 to 30 mM (Table 4-6; Fig. 4-4C) resulted in a 24.4% decrease in the enzymatic bioconversion of phenolic lipids. These findings are in agreement with those of Sorour (2010), who indicated that increasing the DHPA concentration from 20 to 60 mM resulted in a 10% decrease in the BY of PLs in SFM, using flaxseed oil (FSO) and DHPA as substrates; similar findings were also obtained

when PAC was increased from 10 to 30 mM, with FO and DHCA in SFM. The literature (Dossat *et al*., 2002; Yadav and Devi, 2004) indicated that some lipase-catalyzed esterification or transesterification reactions can be inhibited by an excess of alcohol or acid, or both substrates; this inhibition could be explained by the fact that in the substrate-enzyme complex [ES], the substrate would associate to the enzyme binding site. However, as the concentration of the substrate is increased, more substrate molecules will attempt to bind to the enzyme at the same site, thus making the [ES] complex ineffective.

4.4.4.4.4. Model Validation

The optimal conditions found for the lipase-catalyzed transesterification reaction were 62 mg/mL of LC and 154 rpm of AS, at fixed PAC of 20 mM. In these conditions, the value of BY predicted by the model was 75%. Accordingly, the validation of the proposed model was conducted under these conditions, and was carried out with three repetitions. The mean BY thus obtained was 75.8%, with a standard deviation of 1.52%, supporting a strong correlation between the experimental results and the statistical predictions of the model.

4.5. Conclusion

An efficient process for the biosynthesis in solvent-free media (SFM) by a commercial lipase (Novozym 435) of PLs, was obtained by the transesterification of KO and DHPA. The central composite rotatable design (CCRD) was successfully used for the optimization of this process. The presence of phospholipids in KO may have a major effect on the dynamics of the transesterification in terms of enzyme efficiency and affinity. The experimental findings indicated that the PAC had an opposite effect to that of lipase as well as agitation speed; it was therefore essential to keep the PAC constant throughout the models to achieve a higher bioconversion. The verification experiment, carried out under the optimal conditions, confirmed the validity of the prediction process.

CHAPTER V

STATEMENT OF CHAPTER V LINKAGE

A process for the enzymatic synthesis of phenolic lipids (PLs), obtained from krill oil (KO), was optimized using the central composite rotatable design (CCRD) (Chapter IV). Chapter V covers the determination of the antioxidant capacity and the oxidative stability of the esterified EOs containing PLs obtained from the transesterification of selected edible oils (EOs), including krill, flaxseed and fish liver oils with phenolic acids (PAs).

CHAPTER V

ANTIOXIDANT CAPACITY AND OXIDATIVE STABILITY OF SELECTED EDIBLE OILS CONTAINING PHENOLIC LIPIDS

5.1. Abstract

The research work was aimed at the determination of the antioxidant capacity (AOC) and the oxidative stability of esterified EOs containing phenolic lipids (PLs), obtained by the lipase-catalyzed transesterification of phenolic acids (PAs) with selected edible oils (EOs), including flaxseed (FSO), fish liver (FO) and krill (KO) oils. The statistical analyses (Tukey's test at P <0.05) revealed that the difference in AOC between that of the EOs and their esterified products, including esterified FSO (EFSO) and esterified krill oil (EKO) was significant (P <0.05). To evaluate the storage stability, the EOs and their esterified products were subjected to two oxidation treatments. The experimental findings showed that all PLs had higher oxidative stability when they were subjected to light, oxygen and agitation at 50ºC as compared to that of the EOs; however, only the esterified fish oil (EFO) showed a significant difference in its peroxide value (PV), when the esterified oils were placed in the dark at 25ºC. Overall, the phenolic mono- and diacyglycerols present in the EOs have shown to be potential antioxidants in improving the oxidative stability of the oil and enhancing its AOC.

5.2. Introduction

Over the last two decades, there has been growing evidence supporting the nutritional benefits of omega-3-polyunsaturated fatty acids (*n*-3-PUFAs), in particular eicosapentaenoic acid (EPA, $C_{20:5}$ *n*-3) and docosahexaenoic acid (DHA, $C_{22:6}$ *n*-3), for human health (Aziz *et al*., 2012b). Although, fish and fish oils (FOs) are the major dietary sources of these *n*-3-PUFAs, the uncertainty of their sustainability has led to the emergence of a new supply on the market, krill oil (KO) (Blanco *et al*., 2007). In addition to the marine products, other alternatives such as algal oils could also provide promising sources for EPA and DHA (Lenihan-Geels *et al*., 2013). On the other hand, flaxseed oil (FSO), is considered a rich source of α-linolenic acid (ALA, $C_{18:3}$ *n*-3) and could be used as the precursor of metabolically-derived EPA and DHA (Kasote, 2013).

In the presence of air, heat, light and oxidizing agents, *n*-3-PUFAs are readily oxidized resulting in the formation of oxidized products (Choe and Min, 2009). Oxidized fatty acids can lead to the destruction of essential fatty acids (EFAs), with the formation of rancid flavors and toxic compounds that could play a role in the development of atherosclerosis (Choe and Min, 2009; Ahmed *et al*., 2011). Considerable efforts have been made to make the food products, which are rich in *n*-3-PUFAs, more stable during food processing and storage (Shahidi and Zhong, 2010). Although phenolic acids (PAs) are commonly known as natural antioxidants, they possess other biological activities (Zheng and Wang, 2002); however, their hydrophilic nature limits their solubility in the hydrophobic media and consequently reduces their potential uses in fats and oils (Sorour *et al*., 2012a).

Research work carried out in our laboratory (Sorour, 2010; Aziz *et al*., 2012a; Sorour *et al*., 2012a) has succeeded in the enzymatic synthesis, in solvent-free media (SFM), of structured phenolic lipids (PLs), using the PAs, dihydrocaffeic acid (DHCA) and 3,4-dihydroxyphenylacetic acid (DHPA), as well as selected edible oils (EOs), including FSO, FO and KO. The structural analyses of these PLs showed the formation of various mono- and diacylglycerols (DAGs) containing one or more molecules of *n*-3 FAs and a PA (Sorour, 2010; Aziz *et al*., 2012a; Sorour *et al*., 2012a). In addition to their health benefits, these PLs could have a wide range of applications including their incorporation in cosmetics, in dietary supplement and as ingredients in pharmaceuticals (Feltes *et al*., 2013).

The aim of the present work was to assess, *in vitro*, the antioxidant properties of PLs in relationship to their structures and to investigate their effectiveness in preventing the oxidative deterioration of EOs. The evaluation of the AOC of PLs was performed with the use of oxygen radical absorbance capacity (ORAC), whereas the oxidative stability of the EOs and their corresponding structured PLs was determined by measuring the peroxide value (PV) and the *p*-anisidine value (*p*-AnV). The overall objective was to provide an insight on the AOC of the main sources of *n*-3-PUFAs and their esterified PLs as well as their stability.

5.3. Materials and Methods

5.3.1. Chemicals and Instrumentation

Fluorescein sodium, 2,2'-azobis (2-methylpropionamidine) dihydrochloride (AAPH), 6-hydroxy-2,5,7,8-tetramethylchroman-2-carboxylic acid (Trolox), 3,4-dihydroxyphenylacetic acid (DHPA), dihydrocaffeic acid (DHCA), salt pairs and potassium iodide were purchased from Sigma Chemical Co. (St-Louis, MO). Commercial immobilized lipase, Novozym 435, from *Candida antartica* with an activity of 10,000 propyl laurate units (PLU) per g solid enzyme, was purchased from Novozymes A/S (Bagsværd, Denmark). Potassium phosphate monobasic (KH_2PO_4), potassium phosphate dibasic (K_2HPO_4), *p*-anisidine (99%), glacial acetic acid and organic solvents of high-performance liquid chromatography (HPLC) grade were obtained from Fisher Scientific (Fair Lawn, N.J.). Randomly methylated β-cyclodextrin (RMCD) (Trappsol) (Pharmacy grade) was obtained from Cyclodextrin Technologies Development Inc. (High Springs, FL). Sodium thiosulfate was purchased from Ricca Chemical Company (Arlington, TX). Silica gel was purchased from Silicycle (Quebec City, Qc). Redox buffer solution (No. 51340065), DM140-SC platinum electrode A and titration beakers were purchased from Mettler-Toledo Inc. (Columbus, OH). Mixture of methylated FA mixture standards (# 538) for gas-liquid chromatography (GLC) analysis was purchased from Nu-Check-Prep, Inc. (Elysian, MN); it is composed mainly of methylated myristate (6%), palmitate (16%), palmitoleate (5%), stearate (8%), oleate (13%), eicosapentaenoate (10%), docosahexaenoate (12%) and tricosanoate (8%).

5.3.2. Edible Oils

Cold-pressed Organic flaxseed oil (FSO) was generously obtained from Arista Industries, Inc. (Wilson, CT); its FA composition was determined (Sorour *et al*., 2012a) as follow: $C_{16:0}$ (4.75 ±7.1%), $C_{18:0}$ (3.50 ±12%), $C_{18:1}$ *n*-9 (18 ±7.9%), $C_{18:2}$ *n*-6 (16.50 ±4.3%) and $C_{18:3}$ *n*-3 (57.70 ±9.2%). On the other hand, fish liver oil (FO), from *Gadus morrhua*, was purchased from Sigma Chemical Co.; it is composed (Sorour, 2010) mainly of $C_{16:0}$ (10.5 ±2.7%), $C_{18:1}$ *n*-9 (16.5 ±5.2%), $C_{20:1}$ *n*-9 (11.0 ±2.5%) $C_{20:5}$ *n*-3 (11.5 ±2.5%), $C_{22:1}$ *n*-11 (8.5 ±1.5%), and C22:6 n-3 (12.0 ±3.2%). High-potency krill oil (KO), extracted from *Euphausia superba*, was generously obtained from Enzymotec Ltd. (Morristown, N.J.).

5.3.3. Transesterfication Trials

The transesterification trials for the synthesis of esterified flaxseed oil (EFSO), fish oil (EFO) and krill oil (EKO) were carried out according to the procedures described previously by Sorour *et al*. (2012a), Sorour (2010) and Aziz *et al*. (2012a), respectively. Prior to each enzymatic reaction, a stock solution of PA was freshly prepared in 2-butanone. An aliquot of the PA stock solution was mixed with the edible oils (EOs) to give a final concentration of 7% butanone in the reaction mixture. The enzymatic reaction was initiated by the addition of the enzyme preparation to the reaction mixture. The optimized transesterification conditions for the investigated PLs are listed in Table 5-1.

5.3.4. Phenolic Lipids

The phenolic lipids (PLs), obtained from the transesterification of FSO with DHPA, were characterized as monoacylglycerol (MAG) dihydroxyphenylacetate (monolinolenyl dihydroxypheynyl acetate) and diacylglycerol dihydroxyphenylacetates, including dioleyl-, dilinolenyl-, linoleyl linolenyl-, oleyl linolenyl- and oleyl linoleyl dihydroxyphenyl acetates (Sorour *et al*., 2012a). On the other hand, the characterization of the PLs, obtained from the transesterification of FO with DHCA, resulted in dihydrocaffeoylated MAGs, including monooleyl-, monoeicosapentaenoyl- and monodocasahexaenoyl dihydrocaffeates, as well as dihydrocaffeoylated DAGs, including dieicosapentaenoyl-, eicosapentaenoyl docosahexaenoyl- and didocosahexaenoyl dihydrocaffeates (Sorour, 2010). The lipase-catalyzed transesterification of the phospholipids, present in KO, with DHPA resulted in the formation of two phenolic MAGs, monoeicosapentaenoyl- and monodocosahexaenoyl 3,4-dihydroxyphenylacetates (Aziz *et al*., 2012b).

5.3.5. Determination of Relative Fatty Acid Composition of Krill Oil

The FA composition of the KO and the two phenolic MAGs, resulting from the transesterification of the phospholipids present in KO with DHPA, was determined by GLC, according to the method established in our laboratory (Sorour *et al*., 2012a).

Table 5-1. Optimized transesterification conditions for the investigated esterified edible oils containing phenolic lipids.

Esterified oils/ Conditions	Esterified flaxseed oil (EFSO)[a]	Esterified fish oil (EFO)[b]	Esterified krill oil (EKO)[c]
T (°C)	55	50.0	60
Phenolic acid (mM)	20	20.9	20
Novozym 435 (mg/mL)[d]	40	51.2	62
Agitation speed (rpm)	150	160	154
Incubation time (days)	7	7	1
Silica gel (mg/mL)	N/A	3.45	N/A
Water activity[e]	N/A	0.5	N/A
Phenolic acid	DHPA[f]	DHCA[g]	DHPA
Bioconversion yield (%)	65.4[h] (0.1)[i]	86.5[h] (1.8)[i]	75.8[j] (1.52)[i]

[a]The conditions for the transesterification of EFSO with DHPA (Sorour *et al*., 2012a).

[b]The conditions for the transesterification of FO with DHCA (Sorour, 2010).

[c]The conditions for the transesterification of KO with DHPA (Aziz *et al*., 2012a).

[d]Concentration of the lipase Novozym 435 in mg solid enzyme/mL, with an activity of 10,000 propyl laurate unit/g solid enzyme.

[e]Water activity was controlled using salt hydrate pairs (Sorour, 2010).

[f]3,4-dihydroxyphenylacetic acid.

[g]Dihydrocaffeic acid.

[h]The bioconversion yield in percent was calculated as the total peak area of phenolic lipids, detected at 280 nm, divided by the peak area of the residual phenolic acid and that of total phenolic lipids, multiplied by 100.

[i]Relative standard deviation was calculated from the standard deviation of duplicate samples divided by their mean, multiplied by 100.

[j]The bioconversion yield (BY) in percent was calculated as the peak area of total phenolic lipids, monitored with ELSD, after 24 h of reaction, divided by the sum of that of phospholipids at time 0 and that of total phenolic lipids after 24 h of reaction, multiplied by 100.

The mixture of methylated FA standards (# 538) was used for the identification of the relative FA composition. The recovery of phenolic monoacylglycerols (MAGs) by HPLC was carried out according to the method of Aziz *et al*. (2012b). The methylation of FAs in the phenolic MAGs was carried out in duplicates.

5.3.6. Determination of the Antioxidant Capacity

The AOC of selected products, including PAs, EOs and their esterified products containing phenolic lipids, was determined according to a modification of the method of ORAC of Dávalos *et al*. (2003) for the hydrophilic antioxidants and that of Prior *et al*. (2003) for the lipophilic ones. All reaction mixtures were prepared in duplicate. Five calibration solutions, using Trolox of a wide range of concentrations (6.25, 12.5, 25 and 50 μM), were carried out for each ORAC assay. The fluorescence measurement, using a Fluorimeter SFM 25 (Kontron Instruments Ltd; Watford, U.K.), was recorded every min until equilibrium was reached. The 485-P excitation and 520-P emission filters were used. The temperature of the samples in the cells was maintained during the reading at 37°C, using a recirculator water-bath (Haake; Karlsruhe, Germany).

5.3.6.1. Hydrophilic ORAC Assay

The reaction was carried out in potassium phosphate buffer solution (75 mM, pH 7.4), where the final reaction mixture was 2 mL. The mixture of the antioxidant (222 μL) and 1,333 μL of fluorescein (FL), for a final concentration of 70 nM solutions, was pre-incubated at 37°C for 15 min in a reciprocal shaking water-bath (Model 25, Precision Scientific Inc.; Chicago, IL); a volume of 1.4 mL of this solution was introduced in a fluorescence optical cell (Hellma GmbH & Co. KG; Müllheim, Germany). An amount of 0.6 mL of 2,2'-azobis(2-amidinopropane) dihydrochloride (AAPH) solution, with a final concentration of 12 mM, was added rapidly. Blank trials of FL and AAPH, using the phosphate buffer instead of the antioxidant solution, were performed for each assay. All dilutions of the PAs were made with the phosphate buffer.

5.3.6.2. Lipophilic ORAC Assay

For the lipophilic antioxidant assay, the fluorescein solution and AAPH were prepared and added in the same manner as that for the hydrophilic assay described previously. The

7% randomly methylated β-cyclodextrin (RMCD), prepared in a mixture of acetone/water (1:1, v/v), was used to dissolve the Trolox standards and to dilute the EOs and their esterified products. A blank (FL + AAPH), using 7% RMCD instead of the antioxidant solution, was performed for each assay.

5.3.6.3. Calculation of Area Under Curve (AUC)

For each product, the antioxidant curves of fluorescence reading versus time were plotted. The area under curve (AUC) was calculated with SigmaPlot (Windows Version 11), using trapezoidal rule as:

$$AUC = \sum_{i=0}^{n-1} [y_i (x_{i+1} - x_i) + 0.5 (y_{i+1} - y_i)(x_{i+1} - x_i)] \quad \text{(5-1)}$$

where x = time in min, y = fluorescence reading and i = number of readings.

The net AUC was obtained by subtracting that of the blank from that of the sample. Regression equations between the net AUC and the antioxidant concentration were calculated for all samples. Linear regression was used in the range of 6.25 to 50 µM Trolox. Data was expressed as micromolar of Trolox equivalents (TE) per micromolar of product (µM TE/µM).

5.3.7. Determination of the Oxidative Stability of Selected Products

To determine the storage stability of the selected EOs and their esterified products, the samples were subjected to two different treatments. In the first treatment, each oil or its esterified products was introduced in the clear titration beaker (CTB) and wrapped with aluminum foil before its placement in a Precision gravity convection incubator (Economy Model 2EG, Thermo Scientific Inc.; Fair Lawn, N.J.), set at room temperature. The second treatment consisted of an accelerated oxidation, where the oils and their esterified products were placed in CTBs and subjected to light in an orbital incubator shaker (New Brunswick Scientific Co., Inc.; Edison, N.J.) at 55°C, with an agitation speed of 150 rpm. To assess the oxidative stability, the experiments were run in triplicate for each given reaction product, with concomitant control trials, using the corresponding oils. The samples were withdrawn and analyzed at selected interval times of 0, 1, 3 and 7 days.

5.3.7.1. Determination of Peroxide Value

The peroxide value (PV) of the selected EOs and their esterified products, considered as an indicator of the primary oxidation products, was measured according to a modification of the International Union of Pure and Applied Chemistry standard method, code # 2.501 (1987). Three g of sample was dissolved in 20 mL of a mixture of acetic acid/chloroform (3:2, v/v), followed by the addition of 1 mL of saturated potassium iodide. The mixture was stirred for 30 sec, with 40% stirring speed scale of a Nuova hot plate stirrer (Model SP18424, Barnsted Thermolyne; Boulevard Dubuque, IA). The sample was then flushed with a gentle stream of nitrogen and was kept in the dark for 5 min before its dilution with 50 mL of deionized water and its subjection to titration with a 0.01 N of sodium thiosulfate ($Na_2S_2O_3$) solution, The potentiometry was monitored with the use of Mettler-Toledo DL58 automated titrator (Mettler-Toledo Inc.; Columbus, OH), using LabX® Software. The equivalent point was determined by measuring the redox change, with the use of DM140-SC platinum electrode A, which was calibrated prior to its use with a Redox buffer solution. For the mode of measurement as well as for the recognition, termination and evaluation conditions of the equivalent point, the method 91016 and that 91015 of Mettler Toledo was used for the sample and the blank, respectively. The peroxide value was calculated as:

$$\text{meq } O_2\text{/ kg oil} = (S\text{-}B) \times N \times 1000\text{/ mass of sample (g)} \quad \text{(5-2)}$$

where, B = volume of titrant (mL) of the blank; S = volume of titrant (mL) of the sample, and N = the normality of $Na_2S_2O_3$.

5.3.7.2. Determination of Secondary Oxidation Products

To monitor the secondary oxidation products of the investigated EOs and their esterified products, their *p*-anisidine value (*p*-AnV) was determined according to the AOCS Official Method #Cd 18-90 (AOCS, 2009). The *p*-AnV was calculated as:

$$p\text{-AnV} = 25 \times (1.2\ As\text{-}Ab)\text{/mass of sample (g)} \quad \text{(5-3)}$$

where, the As and Ab, were the absorbance at 350 nm of the fat solution, after and before its reaction with the *p*-anisidine reagent, respectively.

5.3.8. Statistical Analyses

All experiments were analyzed as a completely randomized design, using PROC GLM of the Statistical Analysis System SAS 9.1 (SAS institute Inc.; Cary, N.C.). Multiple comparisons of mean values were done by Tukey's honest significance test at $P < 0.05$.

5.4. Results and Discussion

5.4.1. Fatty Acid Composition of KO and Its Esterified PLs

In order to determine the relative FA composition of KO, the oil was subjected to GLC analysis. The experimental results showed that the predominant fatty acids in KO were $C_{14:0}$ (2.42 ±3.08%), $C_{16:0}$ (16.76 ± 1%), $C_{18:1}$ *n*-9 (5.04 ±0.87%), $C_{18:2}$ *n*-6 (1.61 ±1.84%), $C_{20:5}$ *n*-3 (19.14 ±2.94%), $C_{22:6}$ *n*-3 (12.41 ±4.12%). Aziz *et al*. (2012b) reported that the major phospholipids of KO are palmitoleyl lyso-phosphatidylcholine and many phophatidylcholines, including didocosahexaenoyl-, dieicosapentaenoyl- and oleic docosahexaenoyl phosphatidylcholines. On the other hand, the two phenolic MAGs, obtained from the lipase-catalyzed transesterification of DHPA and the phospholipids present in KO, were methylated and subjected to GLC analysis. The experimental results indicated the presence of one major peak for each phenolic MAGs, a $C_{20:5}$ *n*-3 and a $C_{22:6}$ *n*-3, respectively. These findings are in agreement with those reported by Aziz *et al*. (2012b), where the two phenolic MAGs were characterized as the monoeicosapentaenoyl- and the monodocosahexaenoyl 3,4-dihydroxyphenylacetate.

5.4.2. Antioxidant Capacity of Selected Products

Using 2,2-diphenyl-1-picrylhydrazyl ($DPPH^{\bullet}$) as the stable radical, PLs demonstrated a relative radical scavenging activity close to that of α-tocopherol (Sorour, 2010). Although the $DPPH^{\bullet}$ assay is considered to be a simple and rapid one for measuring the AOC, it has many drawbacks, mainly due to the fact that the radical itself does not bear any similarity to the highly reactive and transient peroxyl radicals, involved in the lipid peroxidation (Prior *et al*., 2003). The radical scavenging capacity of KO could not be determined with the DPPH colorimetric assay and this may be due to the chromogenic red-orange color of KO, conferred with the presence of astaxanthin (Massrieh, 2008). On the other hand, the oxygen radical absorbance capacity (ORAC) provides a controllable

source of peroxyl radicals that could be considered as an appropriate model for the reaction of antioxidants with lipids in both food and physiological systems (Prior *et al*., 2003); the ORAC method could be considered, hence, as a suitable approach for the evaluation of AOC of the investigated EOs and their esterified products.

5.4.2.1. ORAC Assay and Kinetic Oxidation of Fluorescein

The ORAC assay measures the chain-breaking AOC of hydrophilic and lipophilic antioxidants by peroxyl radicals, which are the most abundant ones in biological systems (Prior *et al*., 2003). Table 5-2 shows the Trolox calibration curves of the net area under curve (AUC) versus concentration. The coefficient of determination (R^2) was >0.99.

The results (Table 5-3) indicated that all the investigated products showed a good linear antioxidant response (>0.99) in function of their concentrations. For each product, the solutions of concentrations, obtained within the linearity range, provided the same ORAC value.

Figure 5-1 depicts the fluorescence decay curves, induced by 2,2'-azobis(2-amidinopropane) dihydrochloride (AAPH), in the presence of the selected PAs as well as the EOs and their esterified products. The results show differences in the shape of the ORAC curves, mainly between the hydrophilic and lipophilic antioxidants. For the investigated PAs (Fig. 5-1A), the ORAC curves show initially a slow rate of fluorescein oxidation before it became dramatic with time. On the other hand, for the lipophilic assays (Figs. 5-1B and 5-1C), there was no lag phase and the fluorescence emission disappeared approximately exponentially from the beginning of the reaction. These findings are in agreement with the shape of the ORAC curves reported by Bisby *et al*. (2008), who suggested that the differences in the lag phase could result from the equilibrium between the antioxidants and the fluorescein radicals, where the shape of the lag phase could be determined by the equilibrium constant. Figure 5-2 shows the rank order for the AOC of the investigated products, which could be related to their composition. The literature (Choe and Min, 2009; Shahidi and Zhong, 2010) indicated that the presence of phenolics, carotenoids and anthocyanins components in food and food products are important indicators of high AOC.

Table 5-2. Linearity of Trolox calibration curves for hydrophilic and lipophilic oxygen radical absorbance capacity (ORAC) assays (net area under curve (AUC) versus concentration).

ORAC assay	slope[a]	intercept[b]	R^{2c}
Hydrophilic	0.2996	1.1490	0.9951
Lipophilic	0.1533	5.1624	0.9970

[b]The slope quantifies the steepness of the line. It is expressed in the units of Y-axis divided by the units of X-axis.

[c]Represents the Y value of the line when X equals zero.

[d]R^2 is a measure of the goodness-of-fit of the data to a straight line.

Table 5-3. Trolox equivalents[a] and linear ranges of products, including selected phenolic acids as well as edible oils and their esterified products containing phenolic lipids.

Products	Trolox equivalents (TE)[a]	Concentration range (μM)	slope[b]	intercept[c]	R^{2d}
Hydrophilic phenolic acids					
DHPA[e]	5.24 (1.038)[f]	7.5 - 15	2.0718	+31.680	0.9961
DHCA[g]	5.57 (0.559)	7.5 - 15	3.9644	+16.204	0.9963
Lipophilic edible oils					
Flaxseed oil	0.257 (0.014)	50 - 200	0.2609	-0.5124	0.9964
Fish liver oil	0.043 (0.004)	500 - 2000	0.0371	+4.9112	0.9997
Krill oil	0.114 (0.024)	200 - 750	0.0668	+20.238	0.9980
Esterified edible oils					
Flaxseed oil	1.98 (0.246)	30 - 40	3.6981	-59.315	0.9987
Fish liver oil	0.12 (0.014)	350 - 500	0.1926	-32.193	1
Krill oil	0.90 (0.140)	35 - 50	1.2548	-11.877	0.9922

[a]Expressed as μM of TE/μM product. Results are presented as the mean n=3.
[b]The slope quantifies the steepness of the line. It is expressed in the units of Y-axis divided by the units of X-axis.
[c]Represents the Y value of the line, when X equals zero.
[d]R^2 is a measure of the goodness-of-fit of the data to a straight line.
[e]3,4-dihydroxyphenylacetic acid.
[f]Standard deviation of triplicate samples.
[g]Dihydrocaffeic acid.

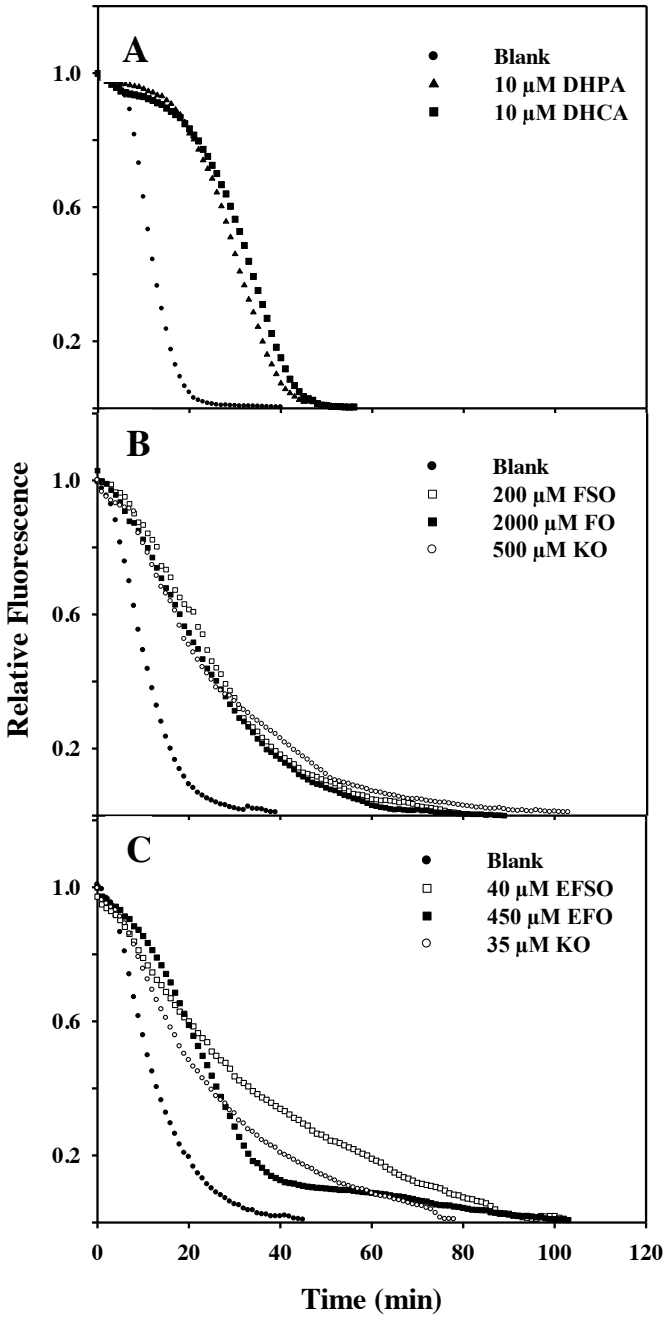

Figure 5-1. Fluorescein fluorescence decay curve induced by AAPH, in the presence of (A) selected phenolic acids (PAs) 3,4-dihydroxyphenylacetic acid (DHPA) and dihydrocaffeic acid (DHCA), (B) edible oils including flaxseed (FSO), fish (FO) and krill oils (KO) (B), and (C) esterified FSO (EFSO), esterified FO (EFO) and esterified krill oil (EKO).

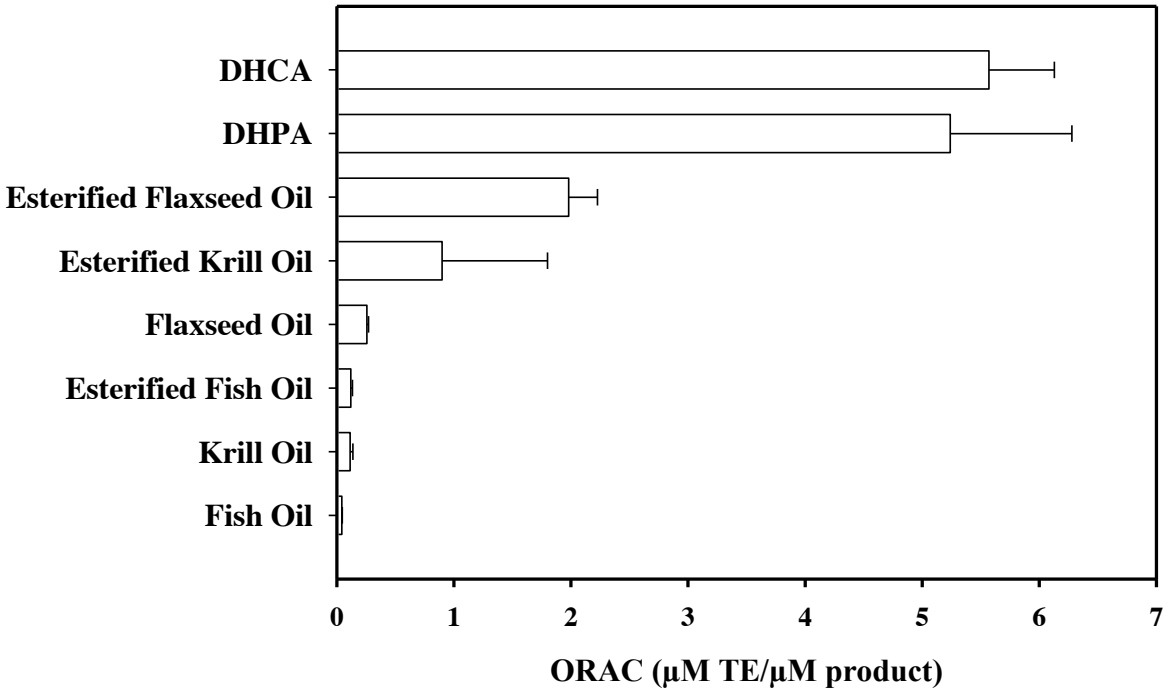

Figure 5-2. Rank order for the antioxidant capacity of selected phenolic acids, edible oils and their esterified products.

5.4.2.2. Determination of AOC of the Selected Phenolic Acids

The experimental findings (Fig. 5-2 and Table 5-3) indicated that DHCA showed the highest ORAC values (5.57±0.559 μM Trolox equivalent (TE)/μM product), followed by that for DHPA (5.24±1.038 μM TE/μM product). However, the statistical analyses (Tukey's test) showed that there was no significant difference (P >0.05) between the AOC of the two investigated phenolic acids (PAs). Likewise, Sorour (2010) and Sorour *et al*. (2012a) investigated the radical scavenging activity of selected PAs, including DHCA, DHPA as well as caffeic and sinapic acids, toward the stable free radical $DPPH^{\bullet}$, and reported that the most potent radical scavenger was DHCA, followed closely by DHPA. Similarly, Sroka and Cisowski (2003) investigated the radical scavenging activity of selected PAs against H_2O_2 as well as $DPPH^{\bullet}$ and reported that the degree of antioxidant activity of PAs was pending on the number of -OH, bonded to the aromatic ring; the model of an *ortho* substitution of the –OH group at the aromatic ring seems to be adequate for the DPPH scavenging activity of PAs. On the other hand, Zheng and Wang (2002) studied the activity-structure relationships of flavonoids and PAs, using the ORAC assay of selected berry crops and suggested that the contribution of individual phenolics to the total AOC is generally dependent on their structures. The experimental findings (Fig. 5-2, Table 5-3) suggest that the scavenging activity of DHCA and DHPA may be due to the presence of a side chain attached to the aromatic ring by a single bond, which could allow the phenyl group to have a certain flexibility to rotate as well as to having two –OH groups that would increase the resonance stabilization through the formation of quinone (Sroka and Cisowski, 2003). In comparison to DHPA, DHCA has an additional methylene bridge $-CH_2$ on the side chain, attached to the aromatic ring, which may increase its flexibility to rotate; this may explain the slight difference in AOC between DHCA and DHPA, in the present study.

5.4.2.3. Determination of AOC of the Selected Edible Oils

Among the investigated EOs, flaxseed oil (FSO) demonstrated the highest AOC (Table 5-3), with 0.257±0.014 μM TE/μM product. The AOC of FSO could be attributed to the constituents of the oil, including *n*-3 FAs and phytoestrogenic lignans, which could play

an important role in the free radical scavenging and singlet oxygen quenching (Kasote, 2013). The experimental findings (Table 5-3) are in agreement with those reported by Hu *et al*. (2007), who indicated that the flaxseed lignan secoisolariciresinol diglucoside (SDG) and its aglycone secoisolariciresinol (SECO) were effective antioxidants against DPPH•; these authors attributed the antioxidant activity to the 3-methoxy-4-hydroxyl substituents of SDG and SECO. Likewise, Bhatia *et al*. (2007) reported that the radioprotective FSO against the radiation-induced hepatotoxiciy in mice could be due to the antioxidant action of the lignans.

On the other hand, the results (Table 5-3) shows that KO exhibited 2.5-fold of the AOC as compared to that of FO. Although both FO and KO are rich sources of *n*-3-PUFAs, including EPA and DHA, KO contains up to 40% of phospholipids, mainly phosphatidylcholines (Massrieh, 2008; Aziz *et al*., 2012b). The mechanism for the antioxidative effect of phospholipids has not yet been elucidated in detail; however the polar group present in the nitrogen-containing phospholipids, including phosphatidylcholine and phosphatidylethanolamine, could play an important role in the AOC under most conditions (Choe and Min, 2009). Lyberg *et al*. (2005) reported that phosphatidylcholine, which contains long-chain *n*-3-PUFAs, protected DHA from oxidation; hence, their presence in KO may have acted as antioxidants. In addition, KO contains endogenous antioxidants, including astaxanthin, vitamins E and A as well as a bioflavonoid, similar to 6,8-di-C-glucosyl luteoloin (Massrieh, 2008). The mechanism of synergism of α-tocopherol, with carotenoid and phospholipids, has been reported by Choe and Min (2009); hence, the association between these endogenous antioxidants and the phospholipids may confer an antioxidant potency for the KO (Deutsch, 2007; Massrieh, 2008). This association could explain the higher AOC obtained with KO as compared to that with FO. The lower AOC (0.043±0.004 μM TE/μM product), obtained with FO (Table 5-3) could indicate that this oil is highly susceptible to oxidation, which may be due to the high number of 1,4-pentadiene system in its long-chain PUFAs and to the lack of endogenous antioxidants which are lost during the FO processing.

5.4.2.4. Determination of ORAC Value for the Esterified Edible Oils

For a better understanding of the structure-activity relationship, the chemical structures of phenolic lipids (PLs), obtained from FSO (Sorour *et al*., 2012a), FO (Sorour, 2010) and KO (Aziz *et al*., 2012b), were characterized and evaluated for their AOC as previously indicated in the Materials section 5.3.4.

The experimental findings (Table 5-3) show that the esterified flaxseed oil (EFSO), containing mono- and DAGs-PLs, exhibited an 8-fold increase in its AOC, with a significant difference (P <0.05), as compared to that of the unmodified oil (Table 5-3); these results (Table 5-3) are in agreement with those of Choo *et al*. (2009), who reported that based on the ratio of a substrate to DPPH concentration, the lipophilized products, obtained by the lipase-catalyzed transesterification of FSO with ferulic acid and not with cinnamic acid, were able to provide an enhanced AOC for the FSO. On the other hand, the modification of the lipid profile of the FSO as a result of an increase in the relative proportion of phenolic MAGs and DAGs could have increased the antioxidant effectiveness of the FSO. Similarly, Cho *et al*. (2010) reported that a functional oil, containing DAGs and MAGs, has been shown to have a strong anti-atherosclerotic effect in a mouse model, with the MAG being responsible for an enhanced antioxidant effect. In addition, Platt *et al*. (2005) developed DAG-rich oils containing high unsaturated FAs with added phytosterols, which were able to reduce the blood cholesterol and serum triacylglycerols (TAGs) level. On the other hand, the presence of 3,4-dihyroxyphenyl acetoylated lipids in FSO could have improved its radical scavenging capacity, as compared to the unmodified oil, by the donation of a hydrogen atom from its -OH groups to the chemically unstable peroxyl radicals generated in the ORAC assay (Prior *et al*., 2003; Sroka and Cisowski, 2003). Although Karboune *et al*. (2008) and Sorour *et al*. (2012a) reported that the esterification of the -COOH of DHPA to a mono- or DAG moiety reduced its radical scavenging ability, the 3,4-dihydroxyphenyl acetoylated lipids demonstrated a scavenging capacity against $DPPH^{\bullet}$ half of that of α-tocopherol, indicating hence their potential as antioxidants.

The esterified krill oil (EKO) exhibited an 8-fold increase in its AOC, with a significant difference (P <0.05), as compared to that of the unmodified oil. On the basis of the MS

spectrometry analyses, the lipase-catalyzed transesterification of the phospholipids present in KO with DHPA resulted in the formation of two phenolic MAGs (Aziz *et al*., 2012b). The presence of MAGs, rich in EPA and DHA, as well as PA could have enhanced the AOC of KO (Feltes *et al*., 2013). Similarly, Cho *et al*. (2010) reported that MAG-containing oleic acid demonstrated antioxidant, antidiabetic and antiatherogenic effects, both *in vitro* and in cells. In addition, a synergism between the α-tocopherol and the PLs could also explain the experimental findings, reported in Table 5-3 (Deiana *et al*., 2002).

Although EFO exhibited 2.5-fold of AOC as compared to that of FO, the statistical analyses showed no significant difference (P >0.05). Sorour (2010) reported the characterization of dihydrocaffeoylated MAGs and DAGs, obtained from the transesterification of FO with DHCA. Despite the presence of MAG- and DAG-PLs as well as DHCA, the efficiency of the radical scavenging capacity of EFO did not increase significantly as compared to that of the unmodified oils. On the contrary, Sorour (2010) reported that dihydrocaffeoylated lipids showed the highest radical scavenging activity, where only 27.3 μM was required to reduce 50% of the initial amount of $DPPH^{\bullet}$ as compared to that of 34.4 μM for α-tocopherol. The difference between the results reported by Sorour (2010) and the experimental findings presented in this study (Table 5-3) may be due to the fact that the PLs were recovered from the oil prior to measuring its radical scavenging capacity against DPPH, whereas, in our case the AOC was measured using the mixture containing FO and dihydrocaffeoylated lipids, taking into account the role of other minor components. Feltes *et al*. (2013) reported that FO contains high number of 1,4-pentadiene system and lacks the endogenous antioxidants, which may play a synergistic effect with the phenolic-MAGs and DAGs (Choe and Min, 2009).

5.4.3. Oxidative Stability of Selected Products

Peroxide value (PV) is a measure of the concentration of peroxide and hydroperoxide (HPs), formed in the initial stages of lipid oxidation; it is widely used as an index of the rancidity of the oil (Ahmed *et al*., 2011). Since KO contains astaxanthin, which provide the oil with its chromogenic characteristic red-orange color, it was difficult to determine the PV by the colorimetric iodine method (Massrieh, 2008). Hence, a redox

potentiometric method was used to evaluate the PV (Saad *et al*., 2006). Figure 5-3, which depicts the potentiometric titration curves for the selected edible oils (EOs), including flaxseed (FSO), fish (FO) and krill (KO) oils, shows that equivalent point was determined using the first derivative of the data.

In the presence of metals and high temperature, the primary oxidation products of lipids tend to breakdown into a wide range of secondary oxidation products, including aldehydes and ketones (Choe and Min, 2006). The *p*-anisidine value (*p*-AnV) measures the content of aldehydes, generated during the decomposition of HPs, and it is considered as a reliable indicator for the oxidative rancidity in fats and oils (Shahidi and Zhong, 2005).

To determine the oxidative stability, the unmodified EOs and their esterified products were subjected to two different treatments. The effects of both treatments on the peroxide and the *p*-AnV of FSO, FO and KO and their esterified products are displayed in Figures 5-4 and 5-5, respectively. For both treatments, each given oil and its esterified products showed different trends for the increase in PV and *p*-AnV as compared to those of the other oils and their esterified products. These results (Figs. 5-4 and 5-5) could be due to the fact that the composition of the investigated oils and their esterified products is different (Massrieh, 2008; Feltes *et al*., 2013; Kasote, 2013). The experimental findings (Fig. 5-4) are in agreement with those reported by Nielsen *et al*. (2004), who suggested that the lipid-type, primarily their degree of unsaturation, significantly affects the oxidative stability of oils. In addition, the presence of minor components in fats and oils could also affect their oxidative stability by acting as antioxidants or as pro-oxidants (Shahidi and Zhong, 2010).

5.4.3.1. Effect of First Treatment on Primary Oxidation Products

Among the investigated edible oils (EOs), only fish oil (Fig. 5-4B) showed a significant increase (P <0.05) in its primary oxidation products, after its subjection to the first treatment (0 to 7 days), as compared to that of the unmodified oils. The PV for FO increased, from 2.743 at day 0 to 18.205 meq O_2/kg oil at day 7.

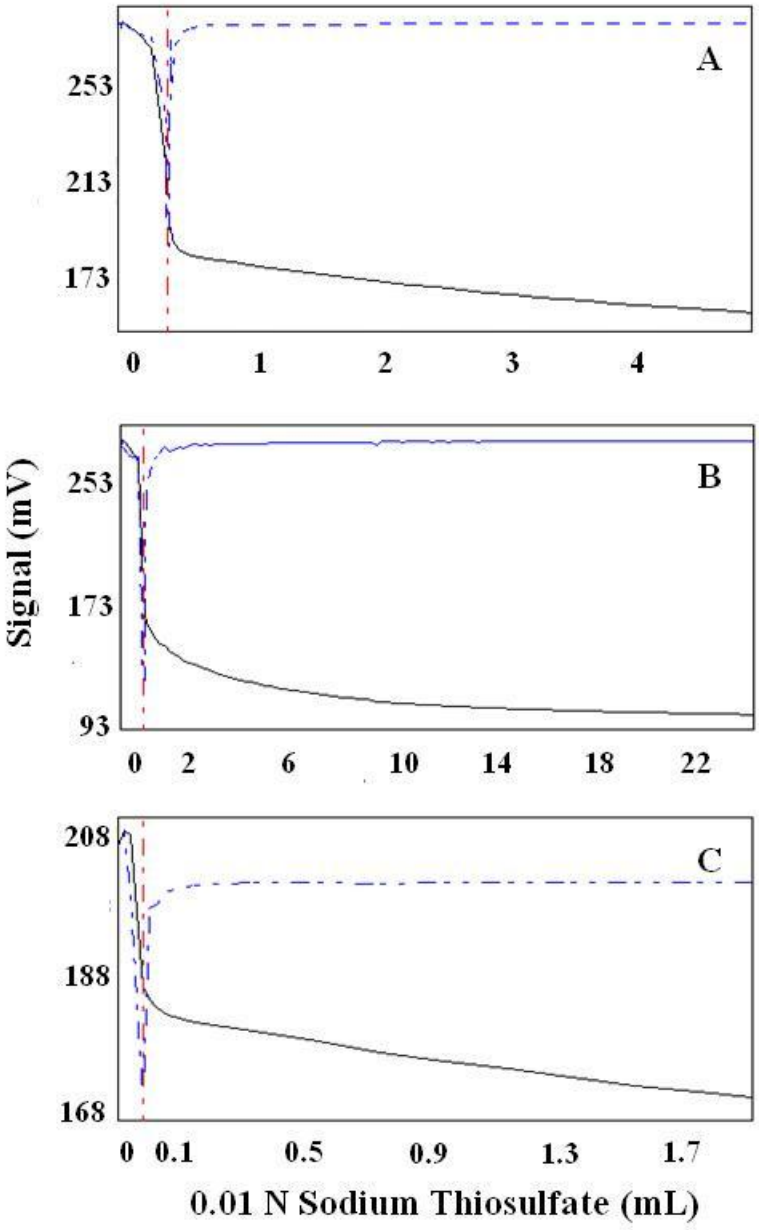

Figure 5-3. Titration curves (—) for the selected edible oils at time 0, including (A) flaxseed (FSO), (B) fish oil (FO) and (C) krill oil as well as their first derivatives (----).

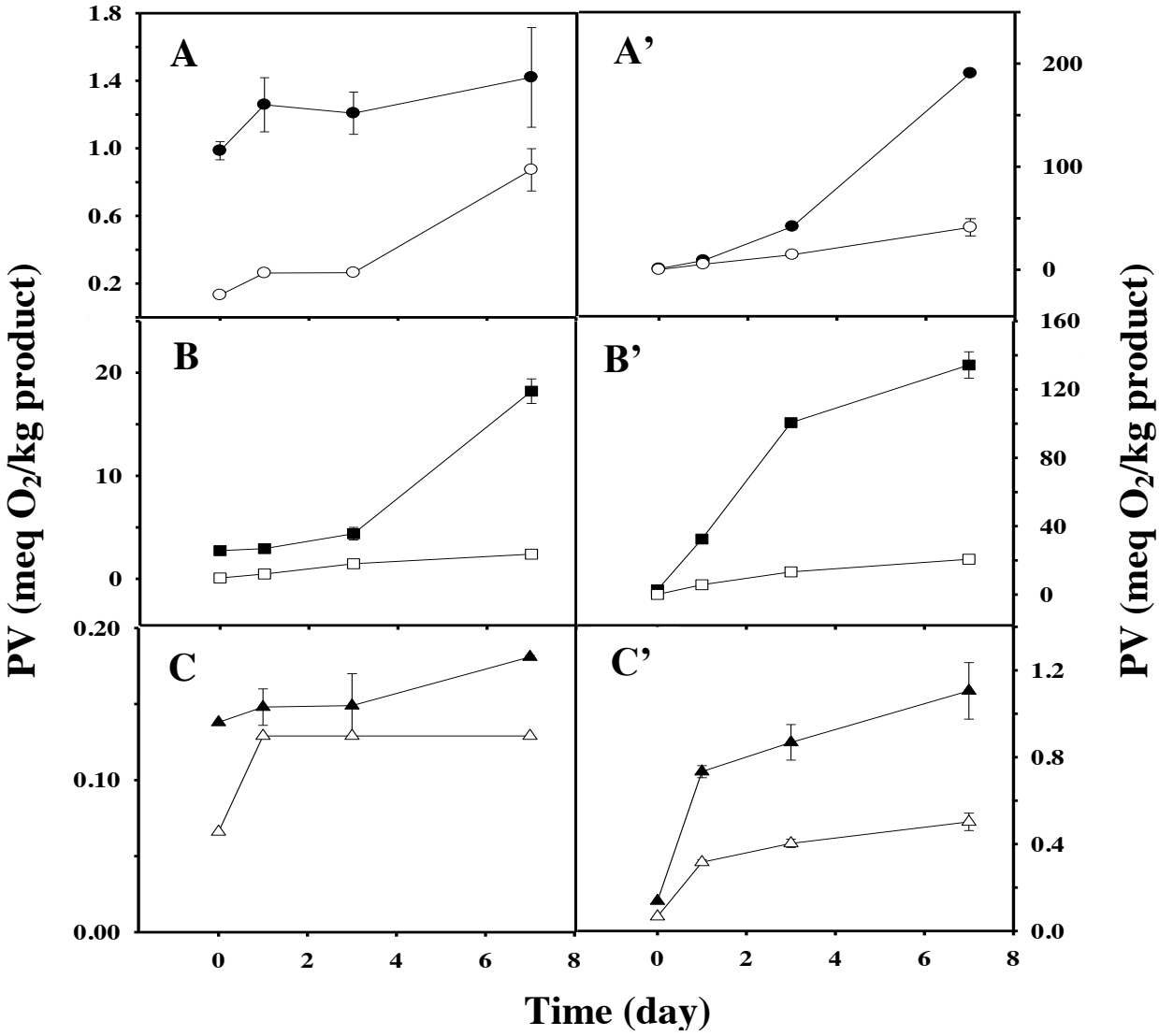

Figure 5-4. Effects of the type of treatment on the peroxide value of selected edible oils, flaxseed oil (FSO - ●), fish oil (FO - ■) and krill oil (KO - ▲) as well as their esterified products, including esterified flaxseed oil (EFSO - ○), esterified fish oil (EFO - □) and esterified krill oil (EKO - Δ). First treatment (A, B and C), where the samples were introduced into clear titration beakers (CTBs), wrapped with aluminum foil and then placed in a convection incubator set at room temperature of 25ºC. Second treatment (A', B' and C'), where the samples were introduced into CTBs and placed in an orbital incubator shaker at 55ºC, with an agitation speed of 150 rpm and exposed to light.

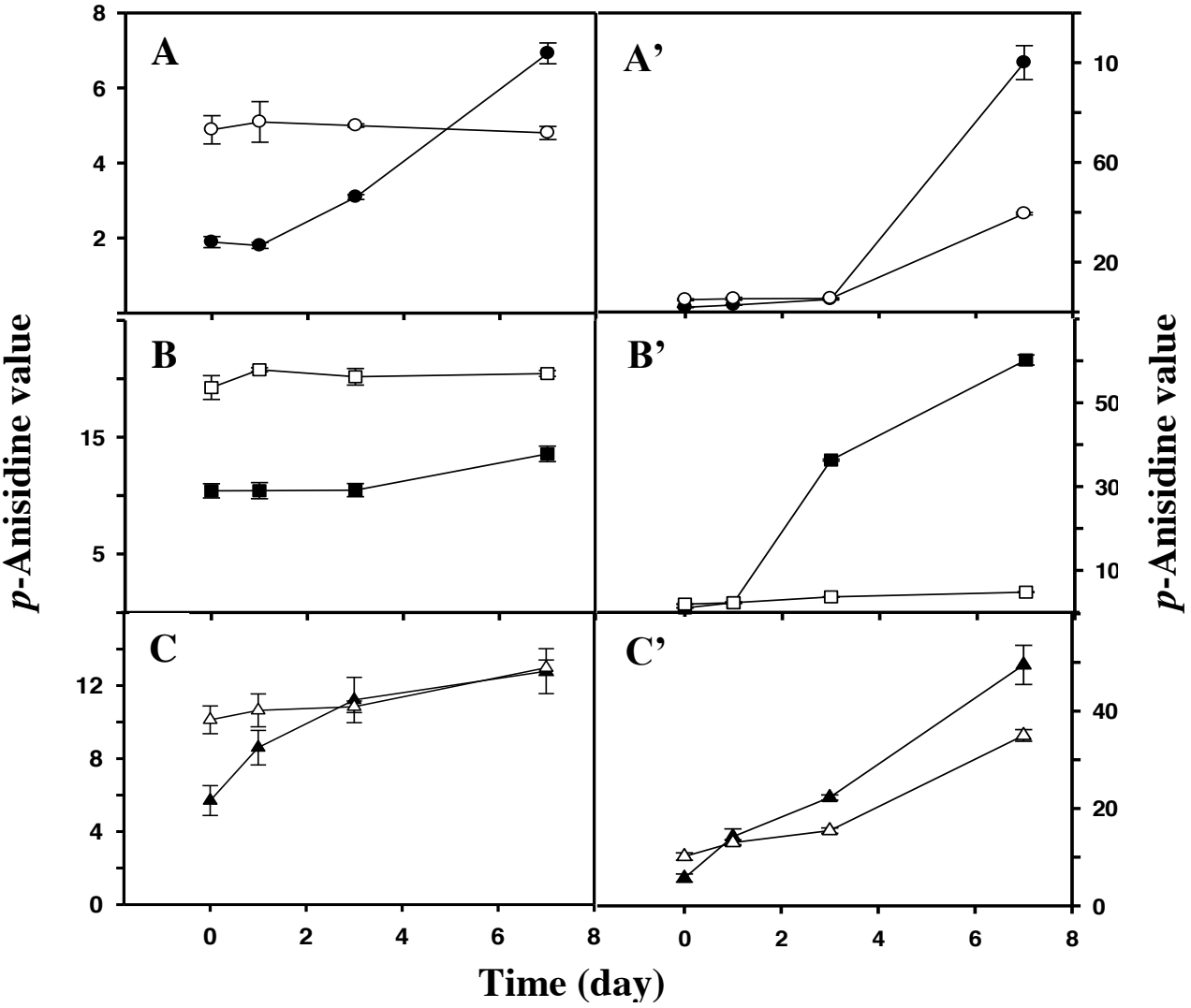

Figure 5-5. Effects of the type of treatment on the *p*-anisidine value of selected edible oils, flaxseed oil (FSO - ●), fish oil (FO - ■) and krill oil (KO - ▲) as well as their esterified products, including esterified flaxseed oil (EFSO - ○), esterified fish oil (EFO - □) and esterified krill oil (EKO - Δ). First treatment (A, B and C), where the samples were introduced into clear titration beakers (CTBs), wrapped with aluminum foil and then placed in a convection incubator set at room temperature of 25ºC. Second treatment (A', B' and C'), where the samples were introduced into CTBs and placed in an orbital incubator shaker at 55ºC, with an agitation speed of 150 rpm and exposed to light.

Sorour (2010) reported similar results, when FO was subjected to the same treatment where the PV was 17.4 meq O_2/kg oil after 7 days of storage at 25ºC. The high degree of unsaturation of FAs and the lack of endogenous antioxidants in FO could explain the significant difference in its oxidation as compared to other EOs, when it was stored in open container at 25ºC (Feltes *et al*., 2013). The high degree of unsaturation of FAs and the lack of endogenous antioxidants in FO could explain the significant difference in its oxidation as compared to other EOs, when it was stored in open container at 25ºC (Feltes *et al*., 2013).

Although KO is rich in long-chain PUFAs, the DHA and EPA are mainly esterified to its phospholipids component, and this may have enhanced its oxidative stability as compared to that of FO. These findings (Figs. 5-4B and 5-4C) are in agreement with those of Lyberg *et al*. (2005), who reported that the formation of HPs of DHA, was almost completely avoided by the incorporation of DHA into either a phosphatidylcholine or a phosphatidylethanolamine, where the phospholipid completely prevented the oxidation of the DHA molecule at carbon atoms 4, 7, 8, and 11. Similarly, Song *et al*. (1997) demonstrated that phospholipids could provide better protection for DHA than TAGs and ethyl esters, containing DHA, in bulk systems at 25°C. On the other hand, the statistical analyses revealed that none of the investigated EOs (Figs. 5-5A, 5-5B and 5-5C) showed a significant difference (P >0.05) in *p*-AnV, when they were stored in open containers at 25ºC for a period of 7 days. These findings are in agreement with those of Choe and Min (2006), who reported that the HPs, tend to be relatively stable at room temperature and in the absence of metals.

After 7 days of subjecting the esterified EOs to the first treatment, the statistical analyses revealed that the difference in the PV and *p*-AnV was not significant (P >0.05) as compared to that of their corresponding oils, with the exception of PV for EFO (Fig. 5-4B). The naturally-occurring antioxidants in FSO and KO may have provided a protection against the oxidation of long-chain PUFAs, comparable to that of the PLs. On the other hand, the EFO was less prone to oxidation than the unmodified FO, and this may be due to the presence of the phenolic mono- and DAGs in the EFO. While the esterified oils containing PLs showed higher initial *p*-AnV as compared to their

corresponding oils, the statistical analyses indicated that the difference was not significant (P >0.05). The higher initial *p*-AnV (Fig. 5-5) could be due to the oxidation that occurred during the transesterification or to the difference in the esterifed oil composition as compared to the unmodified oils (Shahidi and Zhong, 2005).

5.4.3.2. Effect of Second Treatment on Secondary Oxidation Products

The results (Figs. 5-4A', 5-4B' and 5-4C' and Figs. 5-5A', 5-5B' and 5-5C') indicate that there was a significant increase (P <0.05) in the PV and *p*-AnV for all investigated EOs and their esterified products, after their subjection to the second treatment during a period of 0 to 7 days. The PV for FSO, FO and KO increased from 0.986, 2.777, 0.138, at day 0 to 190.575, 123.444, 1.105 meq O_2/kg oil at day 7, respectively, whereas that for EFSO, EFO and EKO, there was an increase, from 0.132, 0.095, 0.066 at day 0 to 41.240, 20.664 and 0.502 meq O_2/kg PV at day 7, respectively. On the other hand, the *p*-AnV for FSO, FO and KO increased from 1.890, 10.401 and 5.699, at day 0 to 100, 601.98 and 49.479 at day 7, respectively; there was also an increase in the *p*-AnV, from 4.880, 19.245 and 10.120 at day 0 to 39.346, 48.098 and 35.025 at day 7 for EFSO, EFO and EKO, respectively. In addition, the experimental data (Figs. 5-4 and 5-5) revealed that the oxidation of all EOs, subjected to the second treatment, was significantly higher (P <0.05) when it was compared to that of their esterified products. The presence of MAGs- and DAGs dihydroxyphenylacetates in FSO and KO and dihydrocaffeoylated MAGs- and DAGs in FO (Sorour, 2010; Aziz *et al*., 2012b; Sorour *et al*., 2012a) may have provided protection for the unsaturated lipids against the formation of HPs and their degradation into secondary oxidation products. These results are in agreement with those obtained by Siriwardhana *et al*. (2004), who reported that the FO, enriched in *Hizikia fusiformis* methanolic, significantly (P <0.05) reduced the PV and the thiobarbituric acid-reactive substances (TBARS) formation as compared to those for FO alone. Likewise, the EFO, synthesized by the transesterification of FO with DHCA, showed less susceptibility to oxidation, where the PV was significantly (P <0.05) less than that for the unmodified FO (Sorour, 2010). Similarly, Wang *et al*. (2011) reported that FO, supplemented with carnosic acid, which is the primary phenolic diterpene compound found in rosemary leaves, was effective in restraining FO oxidation.

Among the investigated products, KO and its esterified products showed the least trend of oxidation after their subjection to light, temperature and oxygen (Figs. 5-4 and 5-5); this trend may be due to the presence of naturally occurring antioxidants, including astaxanthin, vitamin E, vitamin A and a bioflavonoid, which could provide a synergic protection for the oil against oxidation. The mechanism of synergism of *α*-tocopherol with carotenoid and phospholipids has been reported by Choe and Min (2009). In addition, Deiana *et al*. (2002) indicated that α-tocopherol seems to have a synergistic antioxidant effect in its association with some phenolic compounds for the prevention of oxidation of olive oil.

5.5. Conclusion

The ORAC assay was shown to be a suitable method for the evaluation of the antioxidant capacity in phenolic acids (PAs), edible oils (EOs) and their esterified products. The use of a redox potentiometric method for the evaluation of peroxide value (PV) was successful for all investigated products. Although the highest AOC was obtained with FSO and its esterified products, KO and its esterified products showed the least trend of oxidation after their exposure to light, temperature and oxygen. In addition, the synergistic interaction between the endogenous antioxidants and PLs could explain the enhanced stability of FSO, KO and their esterified products as compared to that of FO and EFO. The overall experimental findings indicated that the esterified edible oils containing PLs demonstrated an enhanced chain-breaking AOC and a less susceptibility to oxidation after their subjection to relatively high temperature incubation in the presence of light and oxygen as compared to those of the unmodified oils.

CHAPTER VI

STATEMENT OF CHAPTER VI LINKAGE

Chapter VI describes the effects of the most significant microencapsulation parameters on the morphology and the encapsulation efficiency (EE) of gelatin-gum arabic microcapsules, via complex coacervation of KO, using Box-Behnken as the statistical model. In addition, the physicochemical properties of the optimized microcapsules in the absence of a cross-linker were also studied.

CHAPTER VI

MICROENCAPSULATION OF KRILL OIL USING COMPLEX COACERVATION

6.1. Abstract

The research work was aimed at the development of a process to yield gelatin-gum arabic multinuclear microcapsules of krill oil (KO), via complex coacervation. Initial screening trials were performed to determine the parameters that have the most significant effects on the encapsulation efficiency (EE) of KO. On the basis of the experimental results of the screening trials, a three-level-by-three factor Box-Behnken design was used to evaluate the effects of the ratio of the core material to the wall (RCW), with x_1 of 1.25:1 to 1.75:1, the stirring speed (SP), with x_2 of 2 to 4, over a scale of 10 and the pH, with x_3 of 3.8 to 4.2, on the EE. The experimental findings indicated that x_3 has the most significant linear and quadratic effects on the EE of KO and a bilinear one with x_1, whereas x_2 did not have any effect. To overcome the saddle point, the quadratic model was reduced to the most significant variables. The optimal conditions for a 92% of EE were: 1.75:1 for RCW, 3.8 for pH and 3 for SP. The microcapsules, formed by complex coacervation and without any cross-linking agent, were multinucleated, circular in shape and had sufficient stability to maintain their structure.

6.2. Introduction

Krill oil (KO) offers a new abundant source of omega-3-polyunsaturated fatty acids (*n*-3-PUFAs) on the market (Massrieh, 2008), in particular eicosapentaenoic acid (EPA, $C_{20:5}$ *n*-3) and docosahexaenoic acid (DHA, $C_{22:6}$ *n*-3), which are widely recognized for their nutritional and health benefits (Kidd, 2007). As compared to other marine oils, KO contains up to 40% of phospholipids and diverse naturally-occurring antioxidants mainly astaxanthin, which confers to the oil its characteristic orange color (Deutsch, 2007; Massrieh, 2008). However, its incorporation in foods products is limited because of its low solubility in the hydrophilic medium (Liu *et al*., 2010) and to its oxidative instability (Bustos *et al*., 2003). Microencapsulation is considered as an effective method for the oxidative stabilization of edible oils (Bustos *et al*., 2003) and it is used for the protection and the delivery of functional lipids in food applications (Champagne and Fustier, 2007).

Complex coacervation involves the electrostatic attraction between two biopolymers of opposing charges (Liu *et al*., 2010). As compared to other technologies, the complex coacervation has been successfully commercialized, since it offers several advantages including higher payload, traces of surface oil and a relatively thick outer shell (Barrow *et al*., 2007). The microcapsules, obtained by coacervation, can be divided into mononuclear, which are formed when a given oil is encapsulated by coacervates, and multinuclear that are formed by the aggregation of multiple mononuclear ones (Dong *et al*., 2007). Spherical multinuclear microcapsules have been found to possess better controlled-release characteristics than their mononuclear counterparts (Dong *et al*., 2007; Dong *et al*., 2011). The literature (Prata *et al*., 2008; Liu *et al*., 2010; Dong *et al*., 2011; Qv *et al*., 2011) reported that the gelatin (GE)-gum arabic (GA) is the most investigated system in the formation of complex coacervation, where its use as a delivery matrix has many advantages including its abundance and its biodegradability (Liu *et al*., 2010). Because of the dietary and religious customs limitations, which may prevent the use of porcine gelatin, beef-hide gelatin was used (Karim and Bhat, 2008).

In order to investigate the individual, combined and cumulative effects of various factors, response surface methodology (RSM) is considered an effective statistical technique because of its many advantages, mainly by limiting the number of experimental runs (Myers *et al*., 2009). Box-Behnken designs (BBDs) are a class of rotatable or nearly rotatable second-order designs based on three-level incomplete factorial designs; BBD has demonstrated to be slightly more efficient than the central composite design, but much more efficient than the three-level full factorial designs (Ferreira *et al*., 2007).

The aim of the present work was to investigate the effects of the most significant process parameters on the morphology and the EE of GE-GA microcapsules, via complex coacervation of krill oil (KO), using the BBD as statistical model. In addition, the physicochemical properties of the optimized microcapsules in the absence of a cross-linker were also studied.

6.3. Materials and Methods

6.3.1. Materials

Beef-hide gelatin Kosher-certified (GE, Type B, 250±10 Bloom, 12.0% moisture) was obtained from Vyse Gelatin Company (Schiller Park, IL). Gum arabic (GA) was purchased from ACP Chemicals Inc. (Montreal, Qc). High-Potency KO, extracted from *Euphausia superba*, was generously obtained from Enzymotec Ltd (Morristown, N.J.). Ammonium hydroxide, ethanol, glacial acetic acid and organic solvents of high-performance liquid chromatography (HPLC) grade were purchased from Fisher Scientific (Fair Lawn, N.J.).

6.3.2. Optimization of Krill Oil Microencapsulation Process

6.3.2.1. Preparation of Microcapsules

The coacervated particles were produced according to a modification of the methods of Dong *et al*. (2007) and Liu *et al*. (2010). Solutions of GE powder (1% w/v, 45±3°C) were prepared by its dispersion in 50 mL of deionized water (Milli-Q, Millipore Corporation; Billerica, MA) under constant agitation at a scale of 3 over 10 for 10 min, using an electrically powered overhead stirrer (Caframo Stirrer; Wiarton, ON). Solutions of GA (1% w/v, 45±3°C) were also prepared in a similar manner. The microencapsulation was carried out in a double-jacketed reactor linked to a circulator-water bath (ThermoScientific; Neslab EX-7, Newington, N.H.) to maintain a constant temperature of 45±3°C. All operation steps were prepared at 45°C, unless otherwise indicated. An amount of 2 g of KO was emulsified into 50 mL of GE dispersion (20,500 rpm, 3 min), using a PowerGen 125 high-shear homogenizer (KIA; Wilmington, N.C.). The homogenization took place at room temperature, using the pre-heated mixture and the emulsion was placed back into the double-jacketed reactor to maintain the temperature. The GA solution (50 mL) was then added dropwise, using a Pasteur pipette (Wheaton; Millville, N.J.) to the GE-stabilized emulsion for a final volume of 100 mL (pH 5.37). The emulsion was then stirred for an additional 5 min, followed by an acidification to pH 4.0 by the dropwise addition of 10% (v/v) acetic acid to induce the complex coacervation. The mixture was allowed to cool slowly to room temperature over a 2 h period of time, under constant mechanical stirring, at a scale of 3 over 10. The particle suspension was

slowly cooled further, with continuous stirring, to 10°C, using an ice-bath. The stirring was then halted to allow the phase separation, where the upper aqueous-rich phase was removed and the lower coacervate one rich with the entrapped oils layer was recovered and stored at 4°C for further analyses.

6.3.2.2. Screening Single Factor Experiments

In order to identify the parameters that have the most significant effects on the EE of KO, initial screening trials were performed. The investigated parameters, include the homogenization rate (11,500, 14,500, 20,500 and 30,000 rpm), the ratio of the core material to the wall (RCW) of 1:1, 1.5:1, 2:1, 2.5:1 and 3:1, the concentration of wall materials (CWM) of 0.5, 1, 1.5 and 2% w/v, the pH of 3.4, 3.7, 4.0 and 4.3 and the stirring speed (SP) of 2, 3, 4 and 5, over a scale of 10. The response was the %EE of krill oil.

6.3.2.3. Determination of the Encapsulation Efficiency of KO

6.3.2.3.1. Determination of the Surface Oil

The determination of the surface oil on the wet capsules was carried out according to the method of Drusch *et al*. (2006a), where an amount of wet microcapsules was filtered (Whatman #41) to yield 500 mg of drained ones. Fifteen mL of petroleum ether (B.P. 36-60ºC) was added and the surface oil was extracted at room temperature from the samples by shaking (90 rpm, 15 min) the mixture, using an orbital incubator shaker (New Brunswick Scientific Co., Inc., Edison, N.J.). The upper organic phase was recovered and concentrated, using a Thermo Savant Automatic Environmental Speedvac System (Model AES1010; Thermo Scientific, Fair Lawn, N.J.). The amount of surface oil was determined gravimetrically.

6.3.2.3.2. Determination of Total Oil Content

Total oil content, including encapsulated and surface, of the wet capsules was determined according to a modification of the methods of Drusch *et al*. (2006a) and Liu *et al*. (2010). A defined amount of the wet microcapsules was filtered (Whatman #41) to yield 500 mg of drained ones, which were then suspended into 3 mL of deionized water and placed in the orbital incubator shaker (300 rpm, 15 min, 65°C). One mL of 14.8 N ammonium

hydroxide solution was added to the mixture and the shaking was monitored for an additional 15 min; the mixture was then cooled to room temperature.

Four mL of ethanol, petroleum ether and hexane were successively added and the samples were agitated in the orbital incubator shaker (300 rpm, 2 min, 25°C). This mixture was then centrifuged (IEC Central CL2; International Equipment Co., Needham Heights, MA) at 1,000 rpm. The extraction was repeated with the use of 2.5 mL of each solvent. The upper layer was recovered and the combined organic phases were concentrated, using the Thermo Savant Automatic Environmental Speedvac System. Total oil content was determined gravimetrically.

6.3.2.3.3. Determination of Encapsulation Efficiency

Percent encapsulation efficiency (EE) was determined as:

$$[\%EE = (\text{Total oil-Surface oil})/\text{Total oil}) \times 100] \quad \ldots\ldots \quad (6\text{-}1)$$

For each batch, the determination of EE was performed in triplicate.

6.3.2.4. Experimental Design

On the basis of the experimental findings of single trials, a "three-level-by-three-factor" Box-Behnken was used in order to optimize the EE of KO. The treatment combinations were constructed from 12 factorial points and 5 central points. Duplicate reactions were carried out for all designed points except the central one, resulting in 29 treatments. All reactions were carried in a randomized order to minimize the effect of unexplained variability in the observed responses that could result from extraneous factors.

The variables as well as their coded and uncoded values are presented in Table 6-1. The investigated response Y was the percent of EE. A quadratic polynomial regression model was used for predicting the Y-variable. The response surface model proposed for Y was:

$$Y = \beta_0 + \Sigma\, \beta_i x_i + \Sigma\, \beta_{ii} x_i^2 + \Sigma\Sigma\, \beta_{ij} x_i x_j \quad \ldots\ldots\ldots\ldots\ldots \quad (6\text{-}2)$$

where, β_0, β_i, β_{ii}, β_{ij} are the intercept, linear, quadratic and interaction regression coefficient terms, respectively, and x_i and x_j are the independent variables (Myers *et al*.,

2009). The data were analyzed, using Design Expert program (State-Ease Inc., Version 7.1.4, Statistics Made Easy, Minneapolis, MN). The RSREG and GLM/ss3 procedures of the statistical analytical system (SAS 9.2) were used for canonical analysis.

6.3.3. Physicochemical Properties of Optimized KO Microcapsules

Using the optimized conditions, a portion of the microcapsules was lyophilized (Labconco Co.; Model 79480, Kansas City, MO) and stored at 4°C. The morphology of the optimized wet and lyophilized microcapsules was monitored on a Hemocytometer (Hausser Scientific, Horsham, PA), using a stereomicroscope (Model SZX12, Olympus America Inc; Melville, N.Y.) equipped with a QICAM 12-bit camera (QImaging Corporation; Surrey, B.C.). The particle diameters and the size distribution were measured, using a Malvern Mastersizer 2000 equipped with a wet dispersion accessory, Hydro 2000S (Malvern Instruments Ltd; Worcestershire, U.K.). The water activity (a_w) was measured at 25ºC by a Novasina AW SPRINT TH-500 system (Axair Ltd.; Pfaffikon, Switzerland), using the humidity reference points. The moisture content was determined, using a vacuum oven, according to the AOAC method (1990). All measurements were carried out in triplicate.

Table 6-1. Process variables and their levels, used in the Box-Behnken design.

Variables	Name	Coded levels		
		- 1	0	+ 1
x_1	Ratio of core material to wall	1.25:1	1.50:1	1.75:1
x_2	Stirring speed (over a scale of 10)	2	3	4
x_3	pH	3.8	4.0	4.2

6.4. Results and Discussion

6.4.1. Optimization of the Krill Oil Microencapsulation Process

6.4.4.1. Screening Single Factor Trials

In order to identify the parameters that have the most significant effects on the encapsulation efficiency (EE) of KO and to determine the appropriate levels of single factors, initial screening trials were performed.

6.4.4.1.1. Effect of the Homogenization Rate on the Emulsion Stability and the Morphology of the Microcapsules

Figure 6-1 depicts the effect of the homogenization rates on the morphology and stability of GE-KO emulsions. The experimental results indicated that, with homogenization rates of 11,500 (Fig. 6-1a) and 14,500 rpm (Fig. 6-2a), free oil was prevalent. Similar findings were reported by Liu *et al*. (2010) for the encapsulation of flaxseed oil (FSO) within GE-GA matrix via complex coacervation, at low homogenization rates. As the homogenization rate increased (Figs. 6-1c and 6-1d), smaller but more homogenous droplets were obtained. These findings could be the results of the higher mechanical energy and droplet surface area in the system (Liu *et al*., 2010). Although the size of the emulsion droplets was the smallest (Fig. 6-1d) at the homogenization rate of 30,000 rpm, the higher mechanical energy resulted in the creation of a foam layer. Lemetter *et al*. (2009) reported that above certain limit, air can be incorporated in the system, creating hence a foam layer, in which the capsules are no longer subjected to shear; in order to prevent foaming formation, a maximum level of shear is required.

Figure 6-2 demonstrates the GE-GA coacervates, monitored by a stereomicroscope, as a function of the homogenization rate. Under the experimental process parameters, the formed microcapsules consisted of mononuclear capsules surrounding a single large oil droplet (Fig. 6-2). In addition, Figure 6-2 shows that the homogenization rate affected the shape and the stability of the microcapsules. At a homogenization rate of 11,500 (Fig. 6-2a) and 14,500 (Fig. 6-2b) rpm, the microcapsules were irregular in shapes, which could be a consequence of the heterogeneous size of the emulsion droplets (Figs. 6-1a and 6-1b).

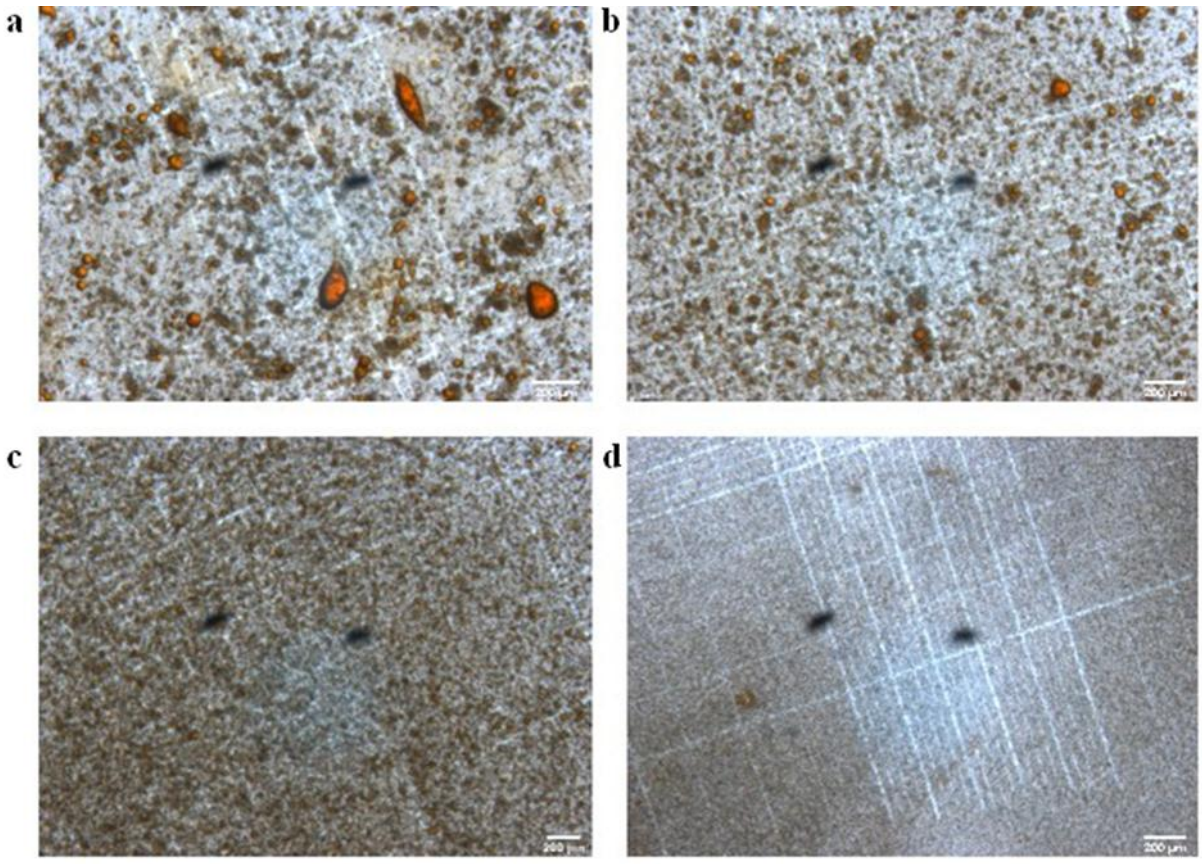

Figure 6-1. Gelatin-krill oil emulsions observed by the stereomicroscope as a function of homogenization rate of (a) 11,500 rpm, (b) 14,500 rpm, (c) 20,500 rpm and (d) 30,000 rpm. Coarcervates were formed at a constant ratio of the core material to the wall of 2:1, concentration of wall materials of 1%, pH of 4 and a stirring speed of 3 out of a scale of 10.

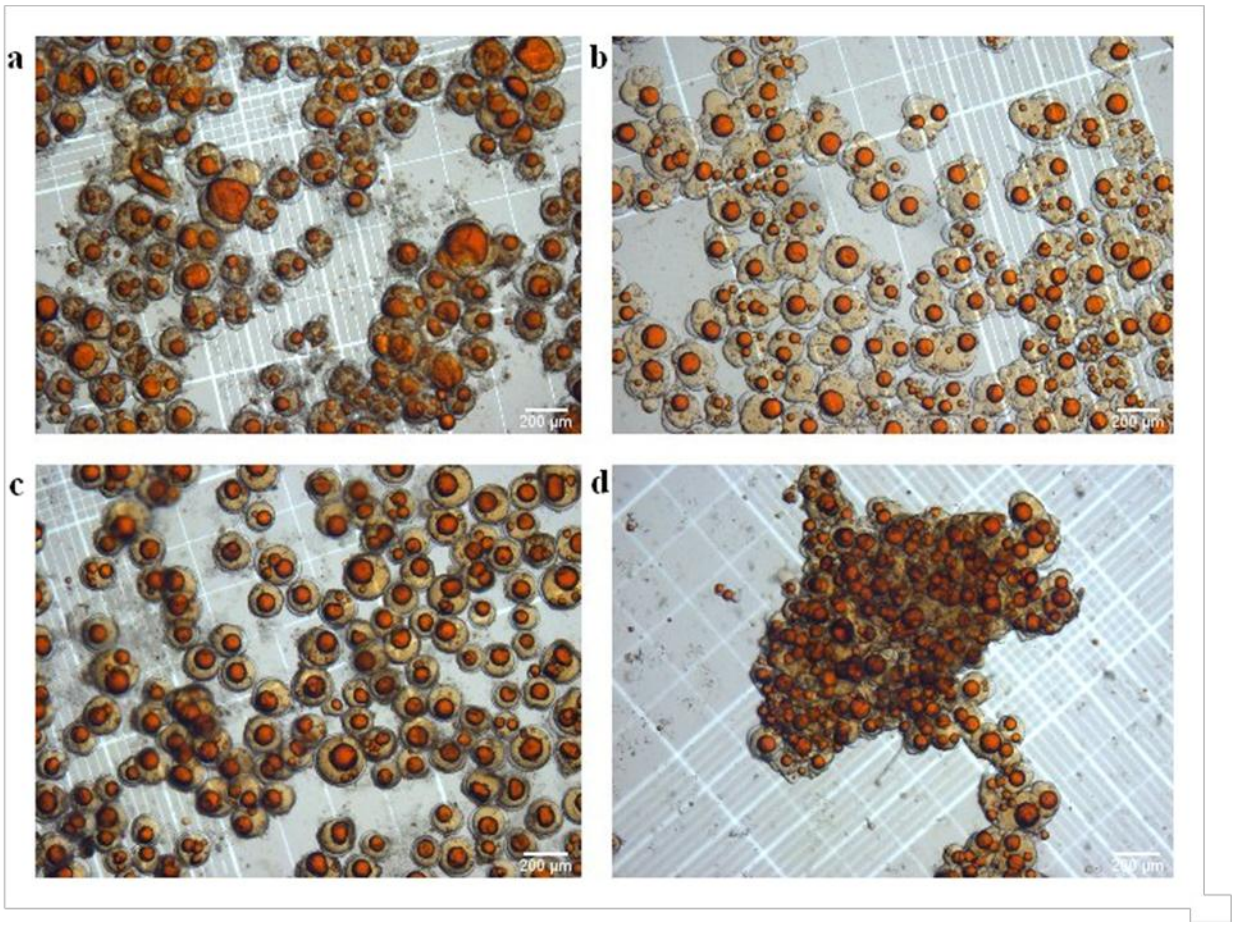

Figure 6-2. Gelatin-gum arabic coacervates observed by the stereomicroscope as a function of homogenization rate of (a) 11,500 rpm, (b) 14,500 rpm, (c) 20,500 rpm and (d) 30,000 rpm. Coarcervates were formed at a constant ratio of the core material to the wall of 2:1, concentration of wall materials of 1%, pH of 4 and a stirring speed of 3 out of a scale of 10.

These experimental findings (Fig. 6-2) could be explained by the Stokes law of oil, which depicts that the droplet size of the emulsion could affect its stability (Drusch *et al*., 2012). At a homogenization rate of 20,500 rpm, the microcapsules were circular in shape and consisted of mononuclear capsules; however, at a higher homogenization rate, the aggregation of the capsules was obtained as a result of the rupturing of the capsules membrane. Liu *et al*. (2010) reported that the possible exposure of the entrapped core could allow for increased hydrophobic interactions and clustering of neighboring capsules.

At homogenization rate of 20,500 rpm (Fig. 6-2c), the EE of wet microcapsules was 69.2±0.27. However, other rates resulted by their breaking and by the release of their content, which made it difficult to estimate their EE; this breakdown could be the result of the instability of the emulsion (Drusch *et al*., 2012). Based on these findings, the homogenization rate of 20,500 rpm was selected for further investigations.

6.4.4.1.2. Effect of RCW on the Morphology of the Microcapsules

Figure 6-3 represents the GE-GA coacervates, monitored by a stereomicroscope, as a function of the ratio of the core material to the wall (RCW). The experimental findings indicated that the RCW had an influence on the internal structure of the microcapsules. With a RCW lower than 2:1, the microcapsules were multinuclear with multiple small oil droplets, entrapped within the GE-GA capsules and they were circular in shape (Figs. 6-3a and 6-3b). With a RCW of 2:1 and higher (Figs. 6-3c, 6-3d and 6-3e), the microcapsules were mononucleated, with a single oil droplet core entrapped in the hydrocolloid shell. The microcapsules, with a RCW of 2:1 and 2.5:1, were circular in shape, whereas those with a RCW of 3:1 were irregular. Dong *et al*. (2007) indicated that with the increase in RCW, the morphology of microcapsules encapsulating peppermint oil changed from spherical to irregular (Fig. 6-3e). In addition, the size of the microcapsules was increased with the rise in RCW, both in mononuclear (Figs. 6-3a and 6-3b) and multinuclear capsules (Figs. 6-3c, 6-3d and 6-3e). These findings are in agreement with those of Dong *et al*. (2007), who reported that when the RCW was increased from 1:1 to 2:1, the mean particle size, increased from 53 to 73 μm, and

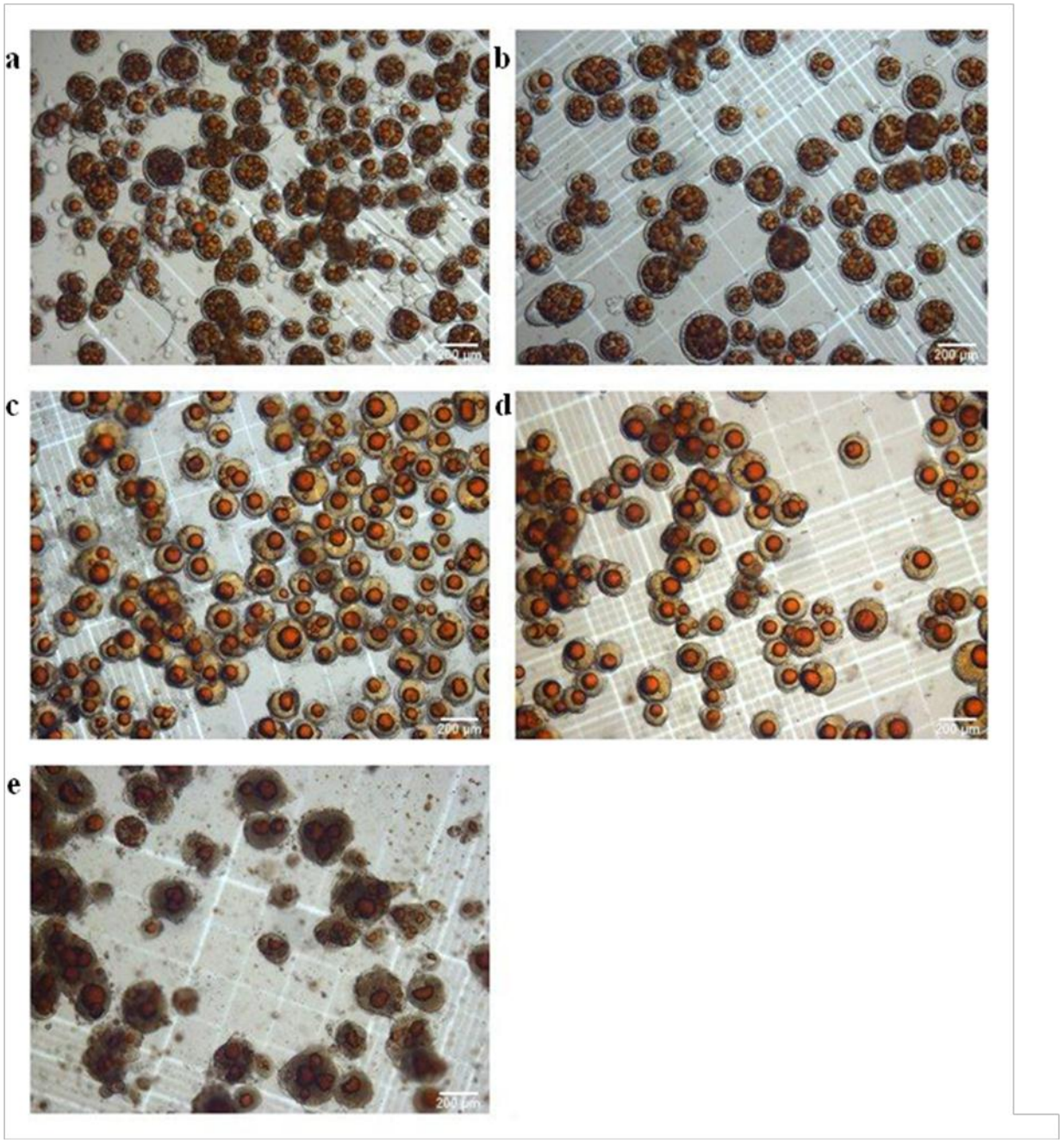

Figure 6-3. Gelatin-gum arabic coacervates observed by the stereomicroscope as a function of the ratio of the core material to the wall of (a) 1:1, (b) 1.5:1, (c) 2:1, (d) 2.5:1 and (e) 3:1. Coacervates were formed at a constant homogenization rate of 20,500 rpm, concentration of wall materials of 1%, pH of 4 and a stirring speed of 3 out of a scale of 10.

continued to increase at a RCW of 3:1 and 4:1. On the other hand, the results (Fig. 6-3) show that the multinuclear microcapsules were bigger in size as compared to their mononuclear counterparts. In comparison with the small oil-containing microcapsules, the large and medium size microcapsules could be more suitable for controlled core release properties (Lee and Rosenberg, 1999).

KO EE of wet microcapsules reached 69.2±0.27% and 84.0±0.48% with a RCW of 2:1 and 1.5:1, respectively. The multinuclear capsules showed better stability and less susceptibility to breakage; this could explain the higher EE, obtained with the multinucleated ones. The literature (Yeo *et al*., 2005; Dong *et al*., 2007; Liu *et al*., 2010; Dong *et al*., 2011) indicated that the multinuclear microcapsules are generally recognized as having better controlled release properties than the mononuclear designs, and they can release the core material slowly even when the wall of the microcapsules is completely destroyed. In contrast, the mononuclear microcapsules with reservoir type structure can release all of the core material very quickly even when the microcapsule wall is only partly destroyed (Dong *et al*., 2007).

In the absence of cross-linking agents, it was necessary to investigate whether the microcapsules would keep their integrity after their lyophilization. Figure 6-4 demonstrates the lyophilized GE-GA coacervates, monitored by the stereomicroscope, as a function of RCW. The results depicted that the multinuclear microcapsules (Fig. 6-4a) maintained more adequately their structure as compared to their mononuclear counterparts (Fig. 6-4b). Likewise, Alvim and Grosso (2010) indicated that the lyophilization process maintained the wall integrity of the multinucleated capsules of a mixture of paprika oleoresin and soybean oil, even without a cross-linker. The lyophilization of the mononucleated capsules resulted by their breakdown and the release of their content; these findings are in agreement with those of Alvim and Grosso (2010) who reported that the lyophilization can cause the disintegration of the capsule wall, which may affect the size of the particle and consequently the core release properties.

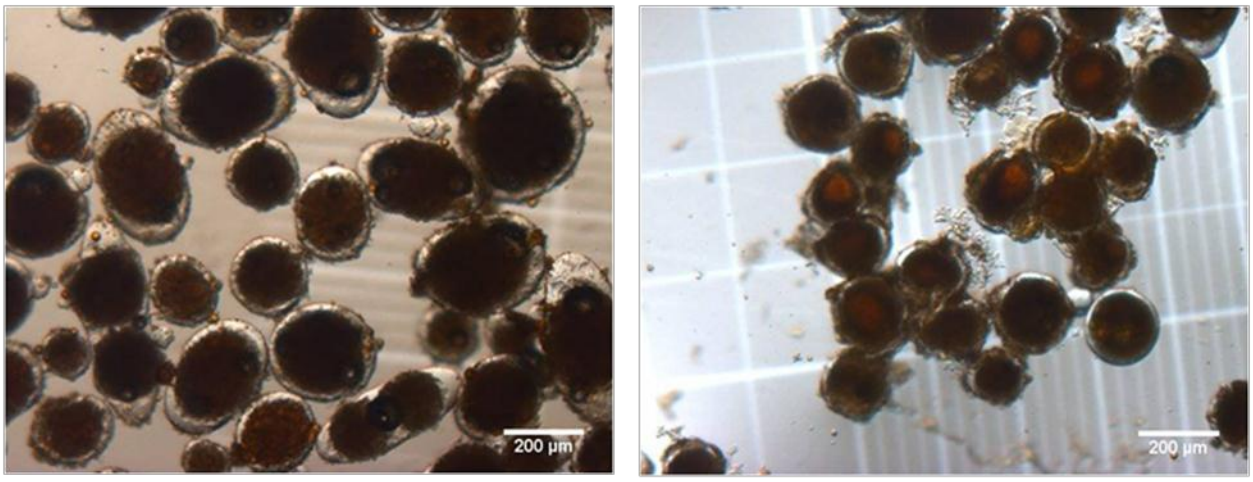

a b

Figure 6-4. Lyophilized gelatin-gum arabic coacervates observed by the stereomicroscope as a function of the ratio of the core material to the wall: (a) 1.5:1 and (b) 2:1.

The literature (Prata *et al*., 2008; Liu *et al*., 2010; Dong *et al*., 2011; Qv *et al*., 2011) reported that the multinuclear microcapsules are believed to have better release core properties as compared to their mononuclear counterparts. Based on the experimental findings, a ratio of core material to wall (RCW) of 1:5:1 was selected for further studies.

6.4.4.1.3. Effect of CWM on the Morphology of the Microcapsules

The effect of the concentration of wall materials (CWM) on the morphology of the microcapsules was investigated (Fig. 6-5). The results show that less free coacervates were formed with a CWM of 0.5 and 1% as compared to that with higher one. These findings are in agreement with those of Yeo *et al*. (2005), who reported that reducing the concentrations of GE and GA solutions decreased the frequency of the free coacervates. Figure 6-5a shows that with a CWM of 0.5%, the microcapsules were multinuclear of irregular shape and big in size. Yeo *et al*. (2005) indicated that the microcapsules, prepared with the most diluted polymer solution (0.5%), formed a significant amount of aggregates, where the size could not be reliably measured. As the CWM increased, from 0.5 to 2%, the microcapsules became smaller. Similarly, Liu *et al*. (2010) reported that the size of aggregated capsule clusters decreased substantially as the biopolymer level was raised from 1 to 2%. In addition, with a CWM higher than 1%, the capsules were mononuclear. The experimental findings (Fig. 6-5) show that the CWM could influence the internal structure as well as the morphology of the microcapsules. Likewise, the CWM affected the number of core aggregates in a microcapsule, when the flavor oil was encapsulated using complex coacervation method (Yeo *et al*., 2005). In summary, the use of a CWM of 1% resulted in the formation of spherical multinucleated capsules and such concentration was selected for further studies.

6.4.4.1.4. Effect of pH on the Properties of Coacervates

The effect of pH on the properties of coacervates, which are formed by the interaction of two biopolymers with opposite charge, was investigated. At a pH lower than 4.0, the experimental results (Figs. 6-6a and 6-6b) show that the formed microcapsules were of irregular shapes.

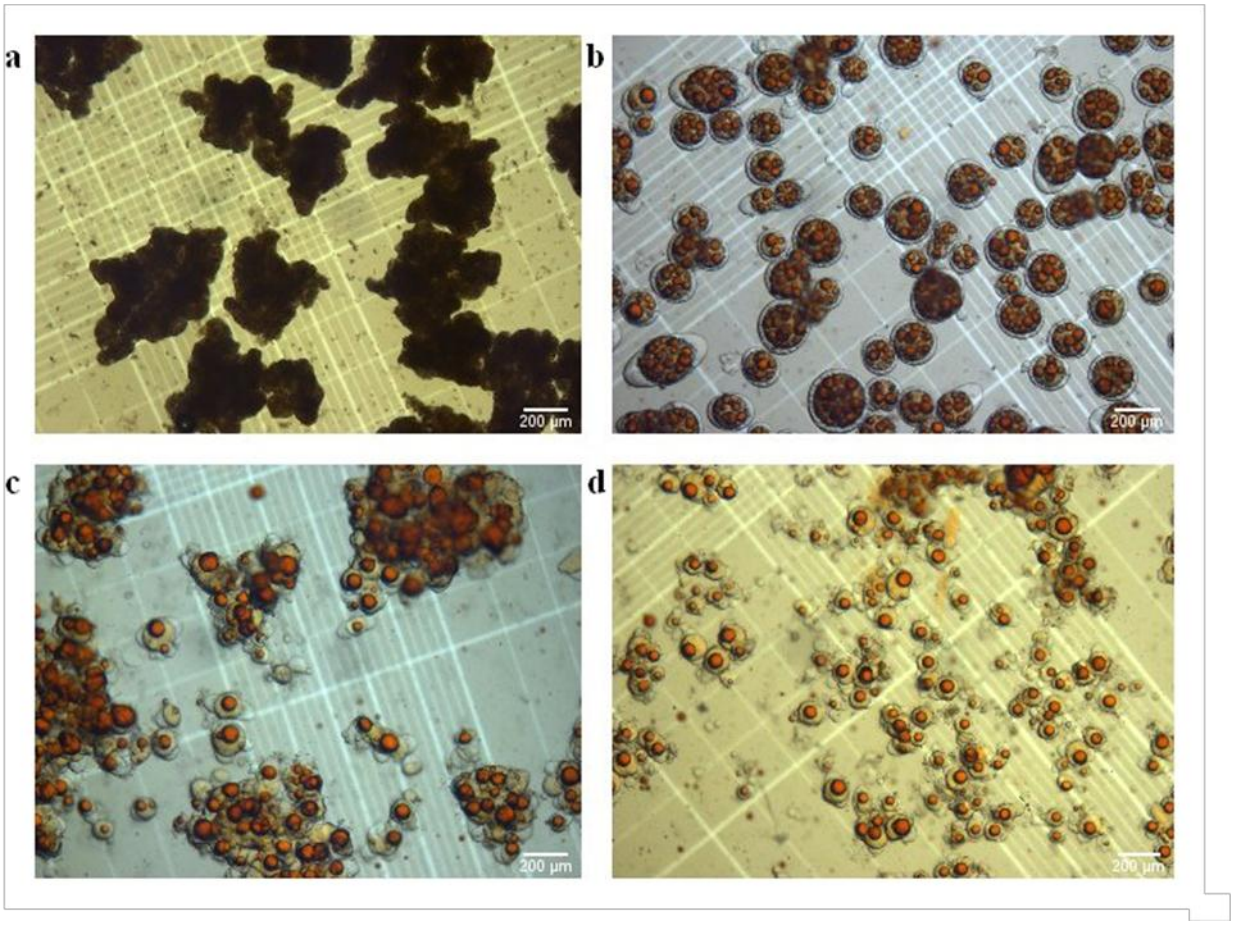

Figure 6-5. Gelatin-gum arabic coacervates observed by the stereomicroscope as a function of the concentration of wall materials of (a) 0.5%, (b) 1.0%, (c) 1.5% and (d) 2.0%. Coarcervates were formed at a constant ratio of the core material to the wall of 1.5:1, pH of 4, homogenization rate of 20,500 rpm and a stirring speed of 3 out of a scale of 10.

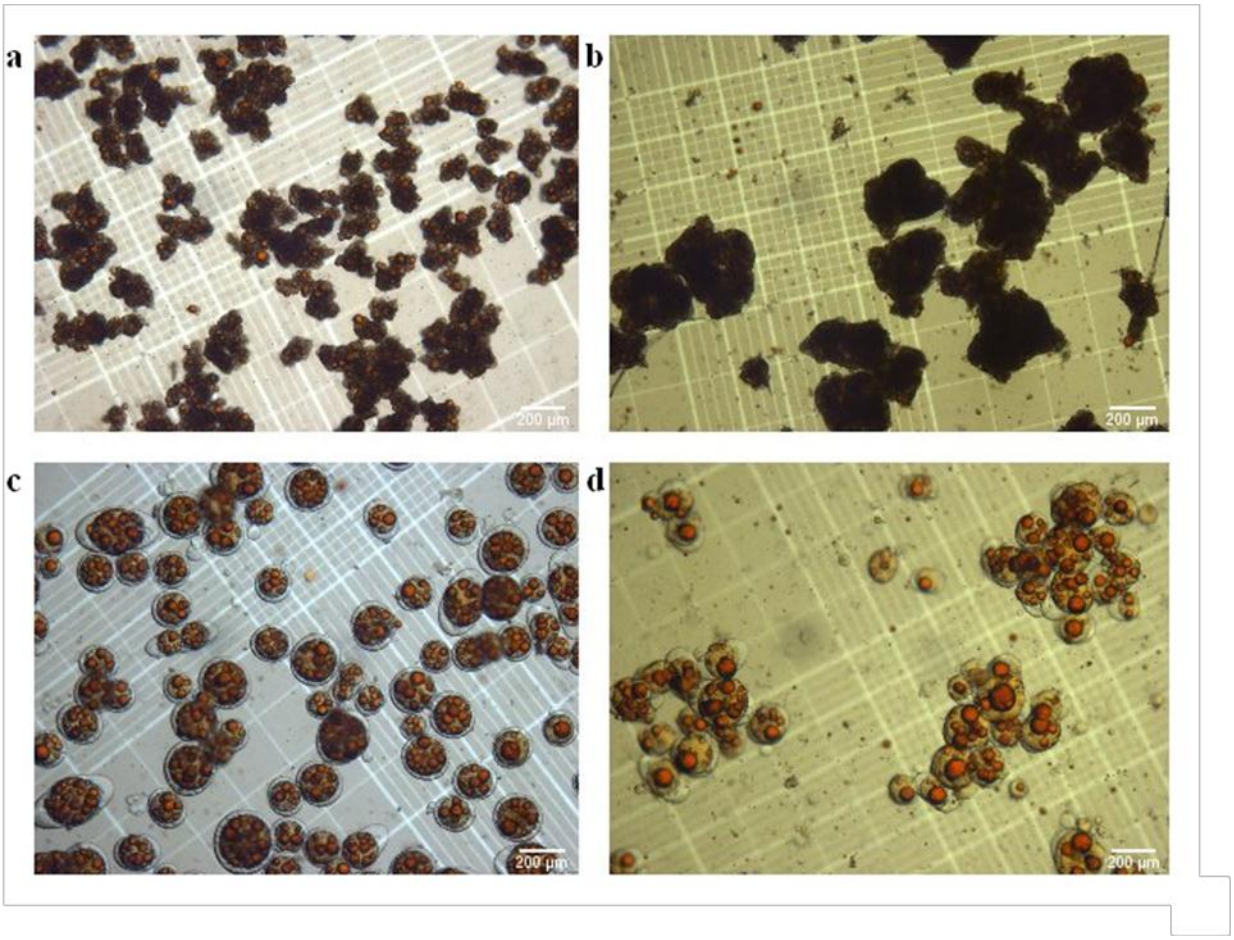

Figure 6-6. Gelatin-gum arabic coacervates observed by the stereomicroscope as a function of pH of (a) 3.4, (b) 3.7, (c) 4.0 and (d) 4.3. Coarcervates were formed at a constant ratio of the core material to the wall of 1.5:1, concentration of wall materials of 1%, homogenization rate of 20,500 rpm and a stirring speed of 3 out of a scale of 10.

Similarly, Dong *et al*. (2007) indicated that when the pH value was lower than 3.7, both the quantity and viscosity of coacervates started to decrease, where the spherical multinuclear became irregular at pH 3.4. In addition, at pH 4.0 (Fig. 6-6c), the spherical multinuclear capsules were formed. These results could be explained by the fact that as the pH decreased, the GE tended to take more positive charges and to interact with GA to form coacervates of high viscosity. Consequently, the mononuclear microcapsules were easier to collide with each other and accumulated into larger size multinuclear microcapsules (Fig. 6-6c). Since the spherical multinuclear capsules are of interest, the pH of 4.0 was considered for further investigations.

6.4.4.1.5. Effect of SP on the Morphology of the Microcapsules

Figure 6-7 demonstrates the effect of stirring speed (SP) on the morphology of the microcapsules. With a SP of 2 out of 10, the microcapsules of larger size and of high oil content were formed. Similarly, Dong *et al*. (2007) reported that with a lower SP, a lot of emulsion droplets floated upward and accumulated into the multinuclear microcapsules, with a larger size and a higher oil content. Figure 6-7 shows that as the SP increased, the size of the microcapsules decreased and the proportion of mononuclear capsules increased. Lemetter *et al*. (2009) indicated that as the rotation speed increased, the mean diameter of a capsule decreased; in addition, with a higher SP, much more mononucleated capsules were present in the dispersion and the remaining multinucleated ones were quite small. The higher the turbulence level, caused by high SP, the smaller was the contact time between the two oil droplets and the less likely they will merge together to form a spherical structure enclosing two oil droplets (Lemetter *et al*., 2009); this could explain the increase in the proportion of mononuclear capsules in Figures 6-7c and 6-7d. The EE of KO was 84.0±0.48, 75.9±0.74 and 65.0±9.45% for SP of 3, 4 and 5, respectively. The decrease in the EE could be explained by the increase in the proportion of the mononuclear capsules with the increase in SP, which tend to be more vulnerable to breakage (Yeo *et al*., 2005; Dong *et al*., 2011).

6.4.4.2. Box-Behnken Design

The appropriate levels of single factors, obtained from the single factor trials, were as follow: 1:25-1.75 for RCW, 2 to 4 for SP and 3.8 to 4.2 for pH.

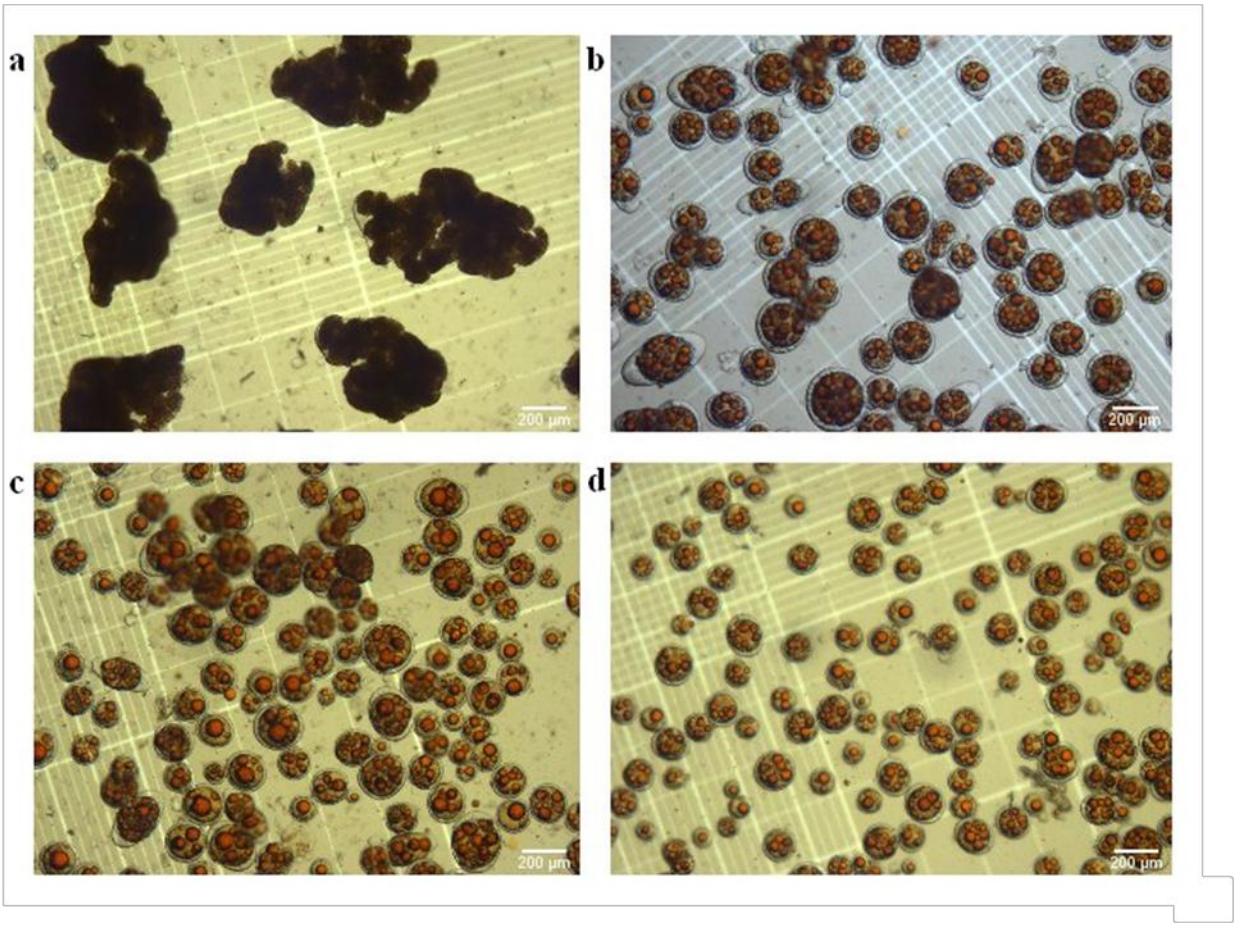

Figure 6-7. Gelatin-gum arabic coacervates observed by the stereomicroscope as a function of stirring speed of (a) 2, (b) 3, (c) 4 and (d) 5. Coarcervates were formed at a constant ratio of the core to the wall ratio of 1.5:1, concentration of wall materials of 1%, homogenization rate of 20,500 rpm and pH of 4.

On the basis of these results and taking into consideration that the encapsulation efficiency (Y) as response value of RCW (x_1), stirring speed (x_2) and pH value (x_3), the experiments were arranged according to a Box-Behnken design (BBD). The levels of the three variables are listed in Table 6-1.

6.4.4.2.1. Model Fitting and Validation

Throughout this study, the BBD was used for the optimization of the EE of KO, using the complex coacervation. The actual and coded values of the factors, together with the corresponding EE (%) experimental data, are reported in Table 6-2. The response surface analysis (Table 6-3) shows that the EE of KO was most suitably described with the following quadratic polynomial model:

$$Y = 81.17 + 1.22\,x_1 - 1.44\,x_2 - 11.75\,x_3 + 3.34\,x_1^2 - 1.95\,x_1x_2 - 10.33\,x_1x_3 - 3.91\,x_2^2 - 3.89\,x_2x_3 - 10.13\,x_3^2 \quad \text{…….. (6-3)}$$

where, Y = EE (%), and x_1, x_2 and x_3 are the coded values of RCW, SP and pH value, respectively.

The response surface analysis (Table 6-3) for the optimization of the EE of KO showed that the predicted model was adequate (P = 0.0002). The lack-of-fit F-value of 3.06 was non-significant, with an associated P-value much higher than 0.05. These results may imply that the model could well represent the responses, within the selected ranges for the reaction parameters.

6.4.4.2.2. Effects of Variables on the EE of KO

Among the three independent variables, the pH value (x_3) had significant linear and quadratic effects on the encapsulation efficiency (EE) of krill oil (KO) (Table 6-3), with P-value of <.0001 and 0.0036, respectively. On the other hand, RCW showed a significant bilinear effect when it was combined with pH value ($x_1 * x_3$; P-value =0.0018). SP (x_2) was found to have no significant linear, bilinear or quadratic effect on the EE of KO. In addition, no other combined effects were found to be statistically significant.

Table 6-2. Box-Behnken second-order design, experimental data for 3 levels-3-factors response surface analysis.

Run	RCW[a] x_1	Stirring speed[b] x_2	pH x_3	EE (%)[c] y
1	1.25[d] (-1)[e]	2[d] (-1)[e]	4.0[d] (0)[e]	74.43
2	1.25 (-1)	2 (-1)	4.0 (0)	78.66
3	1.25 (-1)	4 (1)	4.0 (0)	76.76
4	1.25 (-1)	4 (1)	4.0 (0)	72.16
5	1.75 (1)	2 (-1)	4.0 (0)	90.34
6	1.75 (1)	2 (-1)	4.0(0)	90.93
7	1.75 (1)	4 (1)	4.0 (0)	84.64
8	1.75 (1)	4 (1)	4.0 (0)	76.90
9	1.50 (0)	2 (-1)	3.8 (-1)	81.80
10	1.50 (0)	2 (-1)	3.8 (-1)	74.44
11	1.50 (0)	2 (-1)	4.2 (1)	64.45
12	1.50 (0)	2 (-1)	4.2 (1)	47.37
13	1.50 (0)	4 (1)	3.8 (-1)	75.30
14	1.50 (0)	4 (1)	3.8 (-1)	96.92
15	1.50 (0)	4 (1)	4.2 (1)	45.16
16	1.50 (0)	4 (1)	4.2 (1)	51.56
17	1.25 (-1)	3 (0)	3.8 (-1)	85.92
18	1.25 (-1)	3 (0)	3.8 (-1)	64.50
19	1.75 (1)	3 (0)	3.8 (-1)	88.84
20	1.75 (1)	3 (0)	3.8 (-1)	92.26
21	1.25 (-1)	3 (0)	4.2 (1)	78.03
22	1.25 (-1)	3 (0)	4.2 (1)	79.69
23	1.75 (1)	3 (0)	4.2 (1)	51.49
24	1.75 (1)	3 (0)	4.2 (1)	54.29
25	1.50 (0)	3 (0)	4.0 (0)	85.61
26	1.50 (0)	3 (0)	4.0 (0)	83.96
27	1.50 (0)	3 (0)	4.0 (0)	82.13
28	1.50 (0)	3 (0)	4.0 (0)	78.77
29	1.50 (0)	3 (0)	4.0 (0)	81.70

[a]Ratio of the core material to the wall.

[b]Stirring speed over a scale of 10.

[c]Encapsulation efficiency (EE) in percent was calculated as the difference between the total oil minus the surface oil divided by total oil, multiplied by 100.

[d]Actual experimental amounts.

[e]Actual experimental amounts in coded values.

Table 6-3. Analysis of variance of the regression parameters.

Source	Number of degree of freedom	Type III Sum of squares	Mean square	*F*-value	*P*-value
x_1	1	23.86	23.86	0.37	0.5505[c]
x_2	1	33.12	33.12	0.51	0.4826[c]
x_3	1	2207.59	2207.59	34.18	<.0001[b]
x_1*x_1	1	77.77	77.77	1.20	0.2862[c]
x_1*x_2	1	30.26	30.26	0.47	0.5019[c]
x_1*x_3	1	853.26	853.26	13.21	0.0018[b]
x_2*x_2	1	106.30	106.30	1.65	0.2150[c]
x_2*x_3	1	120.75	120.75	1.87	0.1875[c]
x_3*x_3	1	714.42	714.42	11.06	0.0036[b]
Model	9	4207.36	467.48	7.24	0.0002[b]
Error	19	1227.17	64.59	_	_
(Lack of fit)	3	447.44	149.15	3.06	0.0584[c]
(Pure Error)	16	779.72	48.73	_	_
Total	28	5434.53	_	_	_

[a]The encapsulation efficiency of krill oil has been investigated using three independent variables; ratio of the core material to the wall x_1 (1.25:1-1.75:1), stirring speed x_2 (2-4 over a scale of 10) and pH x_3 (3.8-4.2) and it was calculated as the difference between the total oil minus the surface oil divided by the total oil, multiplied by 100.

[b]Significant at less than 0.05 level.

[c]Not significant at higher than 0.05 level.

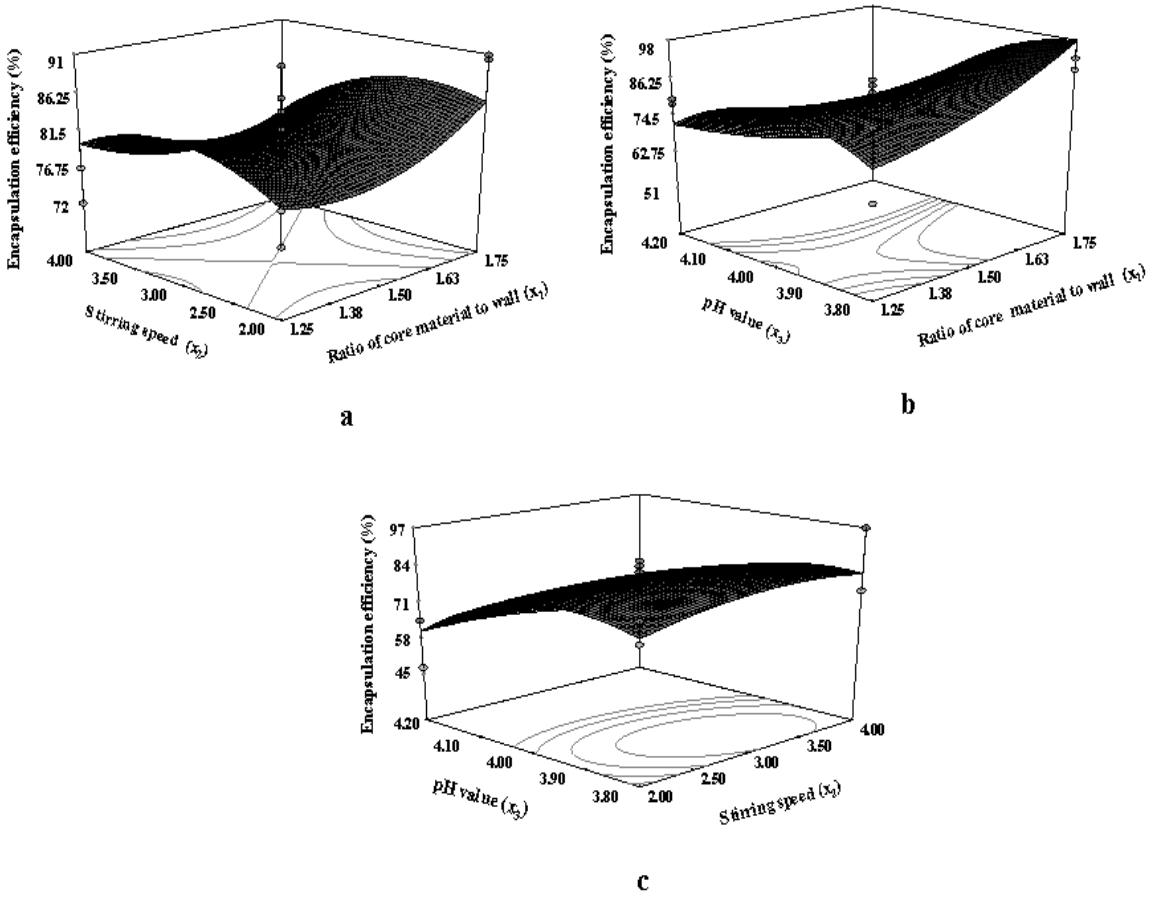

Figure 6-8. Response surface and contour plots showing the effects of stirring speed versus the ratio of the core material to the wall (RCW), pH versus RCW, stirring speed versus pH.

Figure 6-8 shows the effects of RCW, pH and SP values, taken two by two, on the EE of KO. In the two-dimensional response surfaces (Figs. 6-8a, 6-8b and 6-8c), the factors that have not been displayed were fixed at their central value. The statistical analysis (Table 6-3) indicates that the RCW has an important bilinear effect with pH on the EE of KO. As the RCW increased (Fig. 6-3b), the EE increased linearly over all the investigated ranges. Dong *et al*. (2007) reported that as the RCW increased, the formed coacervates were enough to encapsulate more core material.

On the other hand, as the pH increased, the response was increased linearly and up to a certain limit, followed by linear and quadratic decreases. These findings could be explained by the fact that with the increase in pH, GE took less positive charges and interacted less strongly with the GA, decreasing hence the EE of KO (Dong *et al*., 2007). In addition, the results (Table 6-3) show that the pH had significant linear and quadratic effects on the EE of KO. Similarly, Qv *et al*. (2011) explored the optimization of process conditions for the encapsulation of lutein, using Box-Behnken as the statistical model; the authors reported that pH had a significant linear and quadratic effects on the EE of lutein, since it controls the balance of macromolecules charges and therefore influencing the intensity of the electrostatic interactions driving the formation of complexes between the two biopolymers.

The results (Table 6-3) show that SP had no effect on the EE. These results are in agreement with those of Dong *et al*. (2007), who reported that when the SP was increased, from 200 to 400 rpm, the yield of microcapsules remained constant. In addition, Lemetter *et al*. (2009) indicated that during the shell gelation, the SP was critical to avoid coalescence that could affect the morphology and the size of the microcapsules rather than their EE.

6.4.4.2.3. Canonical Analysis and the Presence of a Saddle Point

To examine more closely the overall shape of the response surfaces and to characterize the nature of the stationary point, canonical analysis was performed on the matrices of the second derivatives of the predicted quadratic polynomial surfaces. The second derivatives

were calculated to determine whether the first derivatives have been vanished at a maximum, minimum or saddle point.

Canonical analysis is a mathematical method that decomposes square matrices, such as matrices of second derivatives, into so-called “eigenvalues” and “eigenvectors”. When all eigenvalues are negative, the stationary point is a maximum; when they are all positive, it is a minimum; and a mixture of negative and positive eigenvalues corresponds to a saddle point. Depending on the direction, the response may increase or decrease when moving away from a saddle point (Carlson and Carlson, 2005).

The response surfaces showing the effects of RCW, SP and pH value, taken two by two, on the EE of KO are displayed in Figure 6-8. When RCW was combined with the SP and the pH, the response increased, or decreased from the center of the surface, depending on the direction (Figs. 6-8a and 6-8b). Such saddle-shaped surfaces reflect the opposite effect of RCW on EE, as compared to SP and pH; this can also be seen from the mixed positive and negative signs of estimated coefficients in Equation #6-3.

Although the maximization of the EE of KO was of the objective, the stationary point was a saddle point, which does not correspond to a unique optimum for the response (Baş and Boyacı, 2007). Hence, using RCW (x_1), SP (x_2) and pH (x_3) as independent variables, a maximum EE could not be obtained. Nevertheless, the canonical analysis revealed that a maximum point could be obtained when the SP (x_2) and RCW (x_3) are used as independent variables, that is, by excluding RCW (x_1). Indeed, the response, once averaged over the experimental values of RCW considered in the initial three-factor-by-three-level BDD, is a concave surface, with a maximum point (Fig. 6-8c).

6.4.4.3. Response Surface Reduced Quadratic Model

In order to explore the response surface methodology and to overcome a saddle point, the response surface quadratic model was reduced by removing the non-significant variables, including the linear (x_2), bilinear (x_1*x_2, x_2*x_3) and quadratic (x_2^2) effects of stirring speed (SP). The analysis of variance for the response surface reduced quadratic model is displayed in Table 6-4.

Table 6-4. ANOVA for response surface reduced quadratic model[a].

Source	Number of degree of freedom	Type III Sum of squares	Mean square	*F*-value	*P*-value
Model	4	3811.85	952.96	14.09	<.0001[b]
x_1	1	23.86	23.86	0.35	0.5580[c]
x_3	1	2207.59	2207.59	32.65	<.0001[b]
x_1*x_3	1	853.26	853.26	12.62	0.0016[b]
x_3*x_3	1	727.14	727.14	10.75	0.0032[b]
Error	24	1622.68	67.61	_	_
(Lack of fit)	8	842.95	105.37	2.16	0.0901[c]
(Pure Error)	16	779.72	48.73	_	_
Total	28	5434.53	_	_	_

[a]The encapsulation efficiency of krill oil has been investigated using two independent variables; ratio of the core material to the wall x_1 (1.25:1-1.75:1) and pH x_3 (3.8-4.2) and it was calculated as the difference between the total oil minus the surface oil divided by the total oil, multiplied by 100.

[b]Significant at less than 0.05 level.

[c]Not significant at higher than 0.05 level.

6.4.4.3.1. Model Fitting and ANOVA

The analyses of variance and error (Table 6-4), performed for the optimization of the encapsulation efficiency (EE) of KO, showed that the predicted model was adequate (P <0.0001). The lack-of-fit F-value of 2.16 was non-significant, with an associated P-value much higher than 0.05. These results could imply that the model represents well the relationships between the response and the reactions parameters, within the selected ranges. As indicated previously, the pH value (x_3) had the most significant linear and quadratic effects on the EE of KO, with a P-value of <.0001 and 0.0032, respectively. On the other hand, RCW showed a significant bilinear effect, when it was combined with the pH value ($x_1 * x_3$; P-value = 0.0016). The equation of predicted model, using coded values for the two-factor-by-three-level BBD, as follows:

$$Y = 80.82 + 1.22\, x_1 - 11.75\, x_3 - 10.33\, x_1 x_3 - 10.07\, x_3^2 \quad \text{(6-4)}$$

where, Y = EE (%), and x_1 and x_3 are the coded values of RCW and pH value, respectively

6.4.4.3.2. Canonical Analysis

Canonical analysis was performed on the reduced quadratic predicted model. The response surface, illustrating the individual effects of RCW (x_1) and pH (x_3) and their combined effects on the EE of KO, is displayed in Figure 6-9. The response, once averaged over the experimental values of SP, considered in the initial two-factor-by-three-level BDD, is a concave surface with a maximum point.

6.4.4.3.3. Model Validation

The optimal conditions for the EE of KO were 1.75:1 for RCW, 3 out of scale of 10 for SP and 3.8 for pH. Under these conditions, the value of EE predicted by the model was 94%. Accordingly, the validation of the proposed model was conducted and carried out with three repetitions. The mean of 92% for EE, with a standard deviation of 0.16%, supports a strong correlation between the experimental results and the statistical predictions of the model.

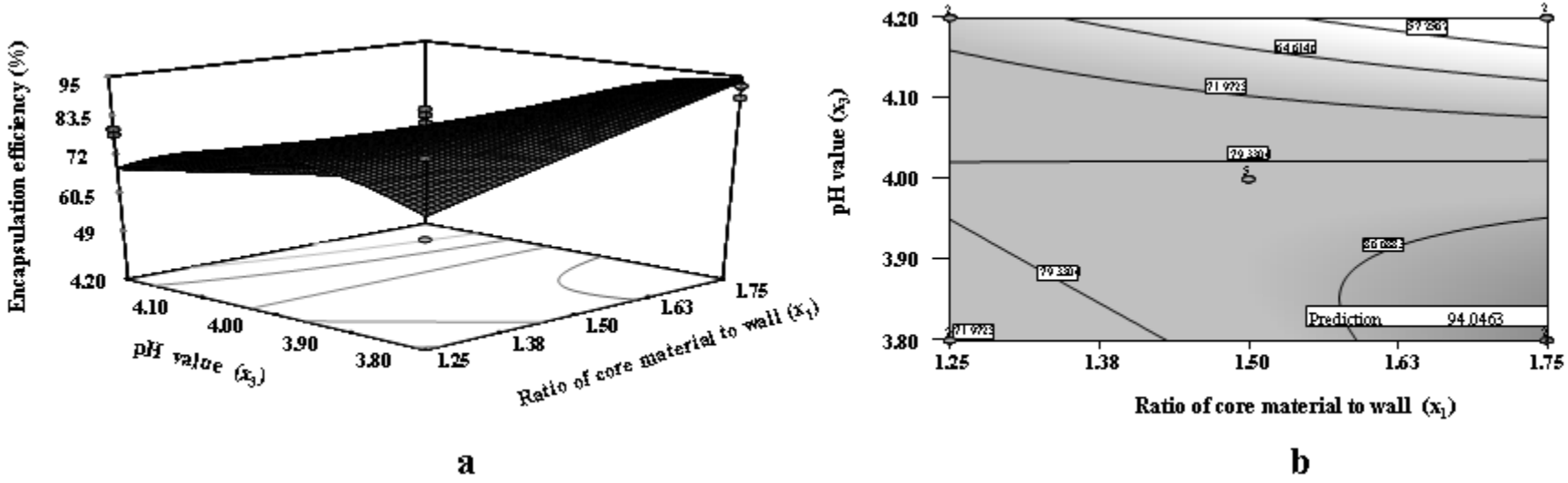

Figure 6-9. Response surface (a) and contour plot (b) showing the effect of pH versus ratio of the core material to the wall (RCW).

6.4.2. Physicochemical Properties of the Optimized KO Microcapsules

Using three measurements, the particle size distribution of the optimized multinuclear microcapsules (Fig. 6-10) exhibited a normal narrow one with the same curve shape, suggesting hence a good reproducibility. The results also show that the volume median diameter d (0.5) was 285.207 μm, which suggests that 50% of the distribution was either higher or lower than this value. In addition, 10% of the microcapsules had a volume diameter d (0.1), lower than 197.443 μm while 90% of them had a volume diameter d (0.9) of 412.515 μm. These findings indicate that the microcapsules, obtained under the optimum conditions, had a good homogeneity.

The lyophilization of the GE-GA, with the entrapped KO, resulted by a free-flowing red-orange powder, with low moisture content of 0.19±0.005% and a a_w of 0.197±0.00. Liu *et al*. (2010) reported similar results for the lyophilized microcapsules, with entrapped FSO of low moisture content of 3.17 ±0.08% and with a_w of 0.18±0.00. Qv *et al*. (2011) indicated that the microcapsules of encapsulated lutein had a water content of 3.12%; these authors suggested that the low moisture content and the a_w are beneficial for the prevention of the oxidation of food products. Klaypradit and Huang (2008) reported that the maximum moisture content for most dried food products is 3-4%, with a a_w close to 0.3.

The KO EE reached 92 ± 0.16%, with low amounts of oil extracted from the surface. The %EE of the designed capsules are comparable to others in literature (Yeo *et al*., 2005; Alvim and Grosso, 2010; Liu *et al*., 2010; Qv *et al*., 2011), when complex coacervation was used as method of encapsulation.

To investigate whether the microcapsules will keep their integrity after drying, the optimized microcapsules were subjected to lyophilization. Figure 6-11 demonstrates a stereomicroscope view of KO microcapsules, prepared under the optimal conditions, before and after lyophilization. Figure 6-11b shows that the capsules maintained their wall integrity after lyophilization despite the absence of cross-linking agents. These findings are in agreement with those reported in literature for multinucleated microcapsules (Alvim and Grosso, 2010; Liu *et al*., 2010).

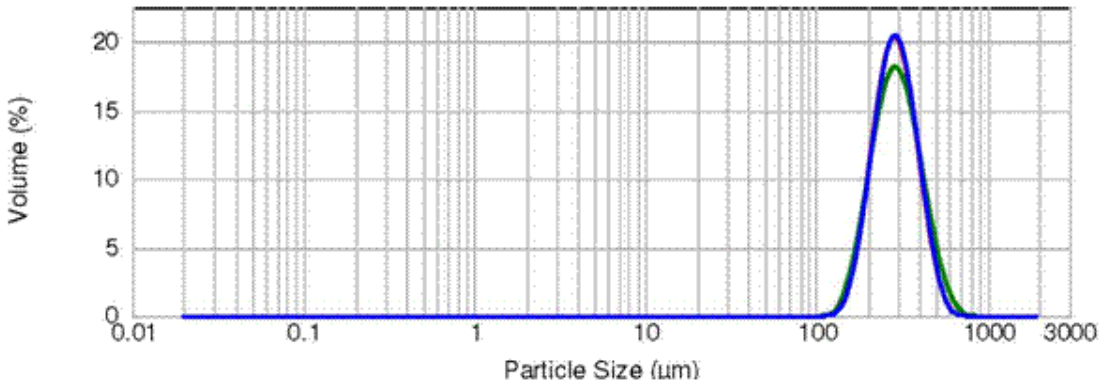

Figure 6-10. Particle size distribution of the krill oil microcapsules prepared under the optimal conditions.

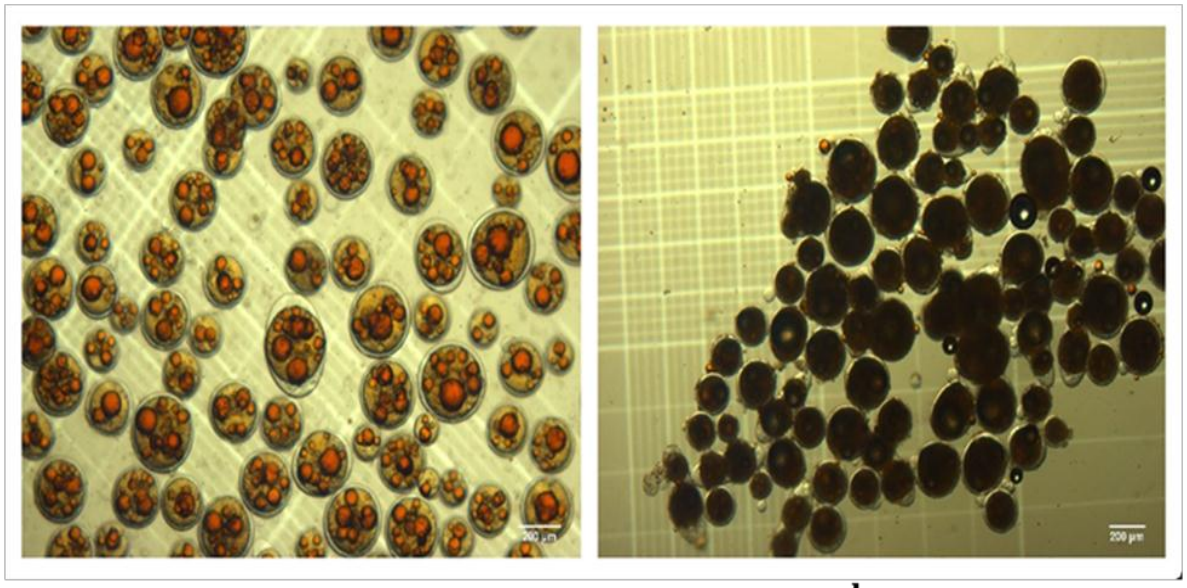

a b

Figure 6-11. Stereomicroscope view of krill oil microcapsules prepared under the optimal conditions obtained: (a) before lyophilization and (b) after lyophilization.

6.6. Conclusion

Using complex coacervation, the Box-Behnken design was successfully used for the optimization of the EE of KO. The chromogenic red-orange color of KO, conferred by astaxanthin, facilitated the stereomicroscopic visualization of the entrapped oil without the need of a lipid-soluble dye. The EE and the stability of the microcapsules were influenced by their internal structure, which can be obtained by adjusting the RCW and the SP. The verification experiment, carried out under the optimal conditions, confirmed the validity of the prediction process. This encapsulation design could contribute to the use of krill oil as a nutraceutical product in food systems.

CHAPTER VII

STATEMENT OF CHAPTER VII LINKAGE

Using complex coacervation, Chapter VII reports on the encapsulation of the esterified krill oil (EKO) and on the effects of the presence of the PA and PLs, in the esterified oil, on the encapsulation efficiency (EE) and morphology of the GE-GA microcapsules. The effects of pH (5.8 up to 8.5) of GE and with the use of two emulsification devices, including the high-shear homogenizer and the ultrasonic liquid processor, on the EE and the size of the microcapsules were also investigated. In addition, the storage and the oxidative stability of the microcapsules as well as their physicochemical properties were evaluated.

CHAPTER VII

MICROENCAPSULATION OF ENZYMATICALLY ESTERIFIED KRILL OIL USING COMPLEX COACERVATION

7.1. Abstract

The research work was aimed at the microencapsulation of the enzymatically esterified krill oil (EKO) with 3,4-dihydroxyphenylacetic acid (DHPA), via complex coacervation. The storage and oxidative stability of the EKO microcapsules as well as their physicochemical properties were assessed. The experimental findings showed that the presence of DHPA and the phenolic lipids (PLs) in the EKO affected the stability of the gelatin (GE)-EKO emulsion. To improve the stability of EKO, the effects of the pH of GE and the type of emulsification device, including the high-shear homogenizer (HSH) and the ultrasonic liquid processor (ULP), on the encapsulation efficiency (EE) and the size of the microcapsules were investigated. Overall, the ULP was found to be more appropriate device for the emulsification of the EKO into GE, as compared to the HSH. In addition, the capsules prepared at a pH 8.0 for the GE showed higher storage stability, with significantly (P <0.05) lower peroxide value as compared to those obtained at pH of 6.5. The microencapsulation of EKO was effective in delaying the development of oxidation products during a storage period of 25 days at room temperature.

7.2. Introduction

Krill oil (KO), extracted from *Euphausia superba*, offers a new abundant source of eicosapentaenoic acid (EPA, $C_{20:5}$ *n*-3) and docosahexaenoic acid (DHA, $C_{22:6}$ *n*-3) on the market, with a biomass estimated between 500 to 2,500 million (Martin, 2007). As compared to other marine oils, KO contains a high proportion of omega-3 polyunsaturated fatty acids (*n*-3-PUFAs) bound to phospholipids and diverse naturally-occurring antioxidants, mainly astaxanthin (Deutsch, 2007; Massrieh, 2008). However, the limited incorporation of KO in food products is due to its low solubility in the hydrophilic medium (Liu *et al*., 2010) and to its oxidative instability (Bustos *et al*., 2003). On the other hand, phenolic acids (PAs) are commonly known as natural antioxidants (Balasundram *et al*., 2006) and have other biological activities (Stasiuk and Kozubek,

2010). Nevertheless, their hydrophilic nature limits their solubility in the hydrophobic media and consequently reduces their potential use in edible fats and oils (Karam *et al*., 2009).

The enzymatic incorporation of phenolic antioxidants into unsaturated lipids could result in the synthesis of novel biomolecules, phenolic lipids (PLs) that could possess both functional and nutritional benefits; recently, a process for the synthesis of PLs, obtained from the lipase-catalyzed transesterification of KO with 3,4-dihydroxyphenylacetic acid (DHPA) in solvent-free media (SFM), was optimized (Aziz *et al*., 2012a).

The entrapment of PLs within micron-sized particles could be an effective approach for their protection and delivery into food systems (Liu *et al*., 2010). Complex coacervation involves the electrostatic attraction between two biopolymers of opposing charges (Lemetter *et al*., 2009). Research work carried out in our laboratory has succeeded in the optimization of a process to yield gelatin (GE)-gum arabic (GA) multinuclear microcapsules of KO via complex coacervation, using Box-Behnken as statistical design (Chapter VI).

The aim of the present work was to encapsulate the enzymatically esterified krill oil (EKO), via complex coacervation. The effects of the presence of the DHPA and PLs, in the esterified oil, on the encapsulation efficiency (EE) and on the morphology of the GE-GA microcapsules were investigated. The effects of the pH of GE (5.8 to 8.5) as well as of selected emulsification devices, including the high-shear homogenizer (HSH) and the ultrasonic liquid processor (ULP), on the EE and the size of the microcapsules were also studied. In addition, the storage and the oxidative stability of the microcapsules as well as their physicochemical properties were evaluated.

7.3. Materials and Methods

7.3.1. Materials

Beef-hide gelatin (GE) Kosher-certified (Type B, 250±10 Bloom, 12.0% moisture, 5±0.42 isoelectric point "IP") was obtained from Vyse Gelatin Company (Schiller Park, IL). Gum arabic (GA) was purchased from ACP Chemicals Inc. (Montreal, Qc). High-

Potency KO, extracted from *Euphausia superba*, was generously obtained from Enzymotec Ltd (Morristown, N.J.). Commercial immobilized lipase, Novozym 435, from *Candida antartica* with an activity of 10,000 propyl laurate units (PLU) per g solid enzyme, was purchased from Novozymes A/S (Bagsværd, Denmark). Barium chloride dehydrate and 3,4-dihydroxyphenylacetic acid (DHPA) were purchased from Sigma Chemical Co. (St-Louis, MO). Ammonium hydroxide, sodium hydroxide, ethanol, glacial acetic acid, hydrochloric acid, *p*-anisidine (99%), ferrous sulfate, ammonium thiocyanate, organic solvents of high-performance liquid chromatography (HPLC) grade and a standard solution of 1,000 ppm Fe^{3+}, prepared in 3% HCl, were purchased from Fisher Scientific (Fair Lawn, N.J.).

7.3.2. Microencapsulation of Esterified Krill Oil (EKO)

7.3.2.1. Transesterification of EKO

Lipase-catalyzed transesterification of KO was carried out according to the procedure described previously by Aziz *et al*. (2012a). Prior to each enzymatic reaction, a stock solution of 3,4-dihydroxyphenylacetic acid (DHPA) was freshly prepared in 2-butanone. An aliquot of the DHPA stock solution was mixed with KO to give a final concentration of 7% butanone in the reaction mixture. The enzymatic reaction was initiated by the addition of 620 PLU of Novozym 435, obtained by the suspension of 62 mg dry enzyme per mL to the reaction mixture containing 20 mM of DHPA, with continuous shaking in an orbital incubator shaker (154 rpm, 24 h, 60ºC). The transesterification trials were run in duplicates.

7.3.2.2. Preparation of Microcapsules

The coacervated particles were obtained according to a modification of the method, developed in our laboratory (Chapter VI), for the formation of complex coacervation Solution of gelatin powder (GE, 1% w/v, 45±3°C) was prepared by its dispersion in deionized water (Milli-Q, Millipore Corporation; Billerica, MA) under constant agitation of 400 rpm, using an overhead Caframo Petite Digital Stirrer (Caframo Ltd; Model BCD250, Wiarton); their pH was adjusted, from 5.8 to 8.5, by the dropwise addition of 0.25 N sodium hydroxide solution. Solution of gum arabic (GA, 1% w/v, 45±3°C) was also prepared in a similar manner as for the GE, but their pH was not adjusted. The

microencapsulation was carried out in a double-jacketed reactor linked to a circulator-water bath (ThermoScientific; Neslab EX-7, Newington, N.H.) to maintain a constant temperature of 45±3°C. A defined amount of EKO was emulsified into GE according to a ratio of the core material to the wall (RCW) of 1.25:1, using a PowerGen 125 homogenizer (KIA; Wilmington, N.C.) as well as a sonicator ultrasonic liquid processor (Misonix Incorporated, Model XL2020; Farmingdale, N.Y.). Using the high-shear homogenizer (HSH), the EKO was emulsified into GE at room temperature and at 20,500 rpm for 5 min, followed by another 5 min at 30,000 rpm. On the other hand, using the ultrasonic liquid processor (ULP), the emulsification was carried out in an ice-bath. The pulsar mode was used, where the ultrasonic energy was delivered in pulsed cycles of 30 sec ON, followed by 30 sec OFF for a total time of 270 sec. The GA solution was added dropwise to the GE-stabilized emulsion, using a Pasteur pipette (Wheaton; Millville, N.J.). The emulsion was stirred at 45±3°C for an additional 5 min, followed by an induction of the complex coacervation, obtained by an acidification to pH 4.0 by the dropwise addition of 10% (v/v) acetic acid. The mixture was allowed to cool slowly to room temperature over a 2 h period of time, but under constant mechanical stirring at 400 rpm. The particle suspension was then slowly cooled further, with continuous stirring, to 10°C, using an ice-bath. The stirring was then halted to allow the phase separation, where the upper aqueous-rich phase was removed and the lower coacervate one, rich with the entrapped oils layer, was recovered and stored at 4°C for further analyses.

7.3.3. Effects of the pH of GE and the Emulsification Devices on the EE and the Size of the Microcapsules

The effects of the pH of GE (5.8 to 8.5) and emulsification device (HSH and ULP) on the encapsulation efficiency (EE) and the size of the capsules were investigated. All microencapsulation experiments were carried out in duplicates.

7.3.3.1. Effects of the pH of GE and the Emulsification Devices on the EE

7.3.3.1.1. Determination of the Surface Oil

Surface oil on the wet capsules was determined according to the procedure described previously (Chapter VI). After the addition of 15 mL of petroleum ether (B.P. 36-60ºC), the surface oil was extracted at room temperature from the drained microcapsules by

shaking (90 rpm, 15 min) the mixture in an orbital incubator shaker (New Brunswick Scientific Co., Inc., Edison, N.J.). The amount of surface oil was determined gravimetrically.

7.3.3.1.2. Determination of Total Oil Content

Total oil content, including encapsulated and surface, of the wet capsules was determined according to the procedure described previously (Chapter VI). Briefly, a defined amount of drained microcapsules were suspended in the deionized water and mixed by shaking using an orbital incubator shaker. This step was followed-up by the addition of 14.8 N ammonium hydroxide solution, with further agitation. The extraction of oil was then carried out successively with ethanol, petroleum ether and hexane. The mixture (drained capsules plus solvents) was agitated and centrifuged, where the upper organic phases were combined, recovered and concentrated. Total oil content was determined gravimetrically.

7.3.3.1.3. Determination of Encapsulation Efficiency

Percent encapsulation efficiency (EE) was determined as:

$$[\%EE = (\text{Total oil-Surface oil})/\text{Total oil}) \times 100] \quad \ldots\ldots \quad (7\text{-}1)$$

For each batch, the determination of EE was performed in triplicate.

7.3.3.2. Effects of the pH of GE and the Emulsification Devices on the Size of the Capsules

In order to investigate the effects of the pH of GE and the type of emulsification device on the size of the capsules, aliquots were withdrawn at various stages of the complex coacervation process, including emulsification as well as the addition of GA, 10% acetic acid and cooling. The morphology of the aliquots was monitored on a Hemacytometer (Hausser Scientific; Horsham, PA), using a stereomicroscope (Model SZX12, Olympus America Inc; Melville, N.Y.) equipped with a camera QICAM 12-bit camera (QImaging Corporation; Surrey, B.C.). The particle diameters were measured using ImageJ Analysis Software (ImageJ 1.45S; Wayne Rasband, National Institutes of Mental Health, Bethesda, MD).

7.3.4. Effects of the pH of GE on the Oxidation of EKO Microcapsules and Their Storage Stability

On the basis of the experimental findings reported in section 7.4.1., the peroxide value (PV) and the *p*-anisidine value (*p*-AnV) were determined on the immediately formed capsules of esterified krill oil (EKO), prepared with the ultrasonic liquid processor (ULP), with a pH value of GE of 6.5 and 8.0. In addition, the storage stability of these EKO microcapsules at 4 and 25ºC was investigated over a period of 25 days. The extraction of the EKO from the capsules followed the same procedure used for the total oil determination.

7.3.4.1. Effects of the pH of GE on the Oxidation of EKO During Encapsulation

A well defined amount of wet microcapsules was filtered (Whatman #41) to yield 500 mg of drained microcapsules. The primary and secondary oxidation products of the extracted EKO, obtained with a pH value of GE of 6.5 and 8.0, were determined immediately after encapsulation, using the modified international dairy federation (IDF) method (Hornero-Méndez *et al*., 2001) and by measuring the *p*-anisidine value (*p*-AnV) (AOCS, 2009), respectively.

7.3.4.1.1. Determination of Peroxide Value

The peroxide value (PV) of the free and encapsulated EKO was measured according to the modified IDF method (Hornero-Méndez *et al*., 2001). For calibration, a set of solutions of increasing Fe^{3+} concentration (0 to 10 μg/mL) was prepared by using a stock solution of Fe^{3+} of 10 μg/mL. The peroxide value was calculated as:

$$\text{PV (mequiv peroxide/kg sample)} = (A_{sm} - A_{bl})/ (55.84 \times 2 \times m \times W_{sm}) \quad (7\text{-}2)$$

where, A_{sm} and A_{bl}, were respectively, the absorbances at 470 nm of the sample and the blank, which were both corrected by subtracting their absorbances at 670 nm; *m* is the slope of the Fe^{3+} calibration plot; 55.84 is the atomic weight of Fe; 2 is the factor to convert milliequivalents of Fe (mequiv Fe) into milliequivalents of peroxide (mequiv peroxide) and W_{sm} is the sample weight in g.

7.3.4.1.2. Determination of *p*-Anisidine Value

To monitor the secondary oxidation products of the free and encapsulated EKO, *p*-AnV was determined according to the AOCS Official Method Cd 18-90 (AOCS, 2009). The *p*-AnV was calculated as:

$$p\text{-AnV} = 25 \times (1.2\ As\text{-}Ab)/\text{mass of sample (g)} \quad \ldots\ldots\ldots\ldots\ldots\ldots\ldots\ldots \quad (7\text{-}3)$$

where, the As and Ab, were the absorbance at 350 nm of the fat solution, after and before its reaction with the *p*-anisidine reagent, respectively.

7.3.4.2. Storage Stability of EKO Microcapsules

7.3.4.2.1. Determination of Retention Rate

The retention rate of the EKO microcapsules was calculated according to the following equation:

$$RR\ (\%) = C_A/C_B \times 100 \quad \ldots\ldots\ldots\ldots\ldots\ldots\ldots\ldots\ldots\ldots\ldots\ldots\ldots\ldots\ldots\ldots\ldots\ldots\ldots\ldots \quad (7\text{-}4)$$

where, RR was the retention rate, C_A and $C_{B,}$ were respectively, the EKO content in microcapsules after and before the defined time of storage.

7.3.4.2.2. Effects of the pH of GE and the Storage Temperature on the Stability of EKO Microcapsules

A defined amount of wet microcapsules was filtered to yield 500 mg of drained microcapsules, which were stored in screw-cap test tubes, wrapped with aluminum foil, at 4 and 25ºC for a total period of 25 days. The stability determination was carried out every 5 days, using a separate test tube. Three replicates were measured on duplicate batches of capsules.

7.3.5. Oxidative Stability of EKO and its Encapsulated Form

The oxidative stability of the free and encapsulated EKO was investigated during the storage at room temperature, over a total period of 25 days. The EKO capsules were lyophilized. The free and encapsulated EKO were stored within nitrogen-flushed amber glass screw-cap vials. Oxidative measurement was carried every 5 days, using a separate vial of EKO and capsules. The determination of the PV and *p*-AnV followed the same

procedures as those used for the evaluation of the oxidation of the EKO during encapsulation.

7.3.6. Physicochemical Properties of Free and Encapsulated EKO

Using the optimized conditions, a portion of the microcapsules was lyophilized (Freeze-dryer, Model 79480, Labconco Co.; Kansas City, MO) and stored at 4°C. The morphology of the optimized wet and lyophilized microcapsules was monitored on a Hemacytometer, using the stereomicroscope; the particle diameters were measured by using the ImageJ software. All measurements were carried out in triplicate.

7.3.7. Statistical Analyses

The statistical analyses were performed, with the use of SigmaPlot for Windows-Version 12. One Way Analysis of Variance test (ANOVA) was used to determine the differences among several groups, followed by the Holm-Sidak test for pairwise comparisons. For One Way ANOVA, a difference was considered significant at $P < 0.05$. For the Holm-Sidak test, each P value was compared to a critical level that was dependent upon the significance level of the test, the rank of the P value, and the total number of comparisons. A P value less than the critical level indicated that there was a significant difference between the corresponding two groups. Statistical analyses were applied to data from duplicate batches of prepared capsules and for each batch, assays were performed in triplicate.

7.4. Results and Discussion

7.4.1. Microencapsulation of EKO

7.4.1.1. Effects of Core Materials and Emulsification Devices on the Morphology and Stability of the Emulsion

The optimization of a process to yield GE-GA multinuclear microcapsules of krill oil (KO) via complex coacervation, was investigated previously (Chapter VI). Preliminary trials were carried out to encapsulate the esterified krill oil (EKO), obtained from the transesterification of KO with DHPA, using the established complex coacervation method described in Chapter VI.

Figure 7-1 depicts the GE-KO and GE-EKO emulsions observed by the stereomicroscope, using the high-shear homogenizer (HSH) and the ultrasonic liquid processor (ULP). When KO was emulsified into GE, the experimental findings (Fig. 7-1a) show that a stable homogenous emulsion was obtained at a homogenization rate of 20,500 rpm. However, when the EKO was emulsified into GE, under the same conditions, small particles of irregular shapes were formed at the emulsification stage and floated at the surface of the mixture, resulting hence into two separate phases. As compared to the GE-KO emulsion (pH= 6.12±0.05), the GE-EKO emulsion was more acidic (pH= 5.36±0.12), which is close to the isoelectric point (IP) of GE (pH= 5.0±0.42); the acidic environment in combination with the shearing, created by the HSH (Burden, 2008), could have favored the interaction of GE with the PLs in the esterified oil. These results are in agreement with those of Zhang *et al*. (2010b), who indicated that the PAs react with GE to form C-N covalent bonds and can act as cross-linking linkages. Likewise, Strauss and Gibson (2004) reported that plant-derived PAs and flavonoids can react, under oxidizing conditions, with the side chains of GE to form covalent cross-links. Despite increasing the homogenization rate from 20,500 to 30,000 rpm and carrying another trial with a combination of 20,500 and 30,000 rpm (Fig. 7-1b), there was little improvement in the emulsion stability. This limit could be related to the homogenizer properties, including its geometry and its energy input (Lemetter *et al*., 2009).

In order to improve the emulsion stability, the use of the ultrasonic liquid processor (ULP) as an emulsification device was investigated. Figure 7-1c shows that the emulsion, obtained with this device was homogenous, stable and free of particles. These findings could be due to the fact that the ultrasonicator applies shock waves using differential pressure, which may have prevented the interactions between the GE and the PLs, resulting hence in a stable homogeneous emulsion (Burden, 2008).

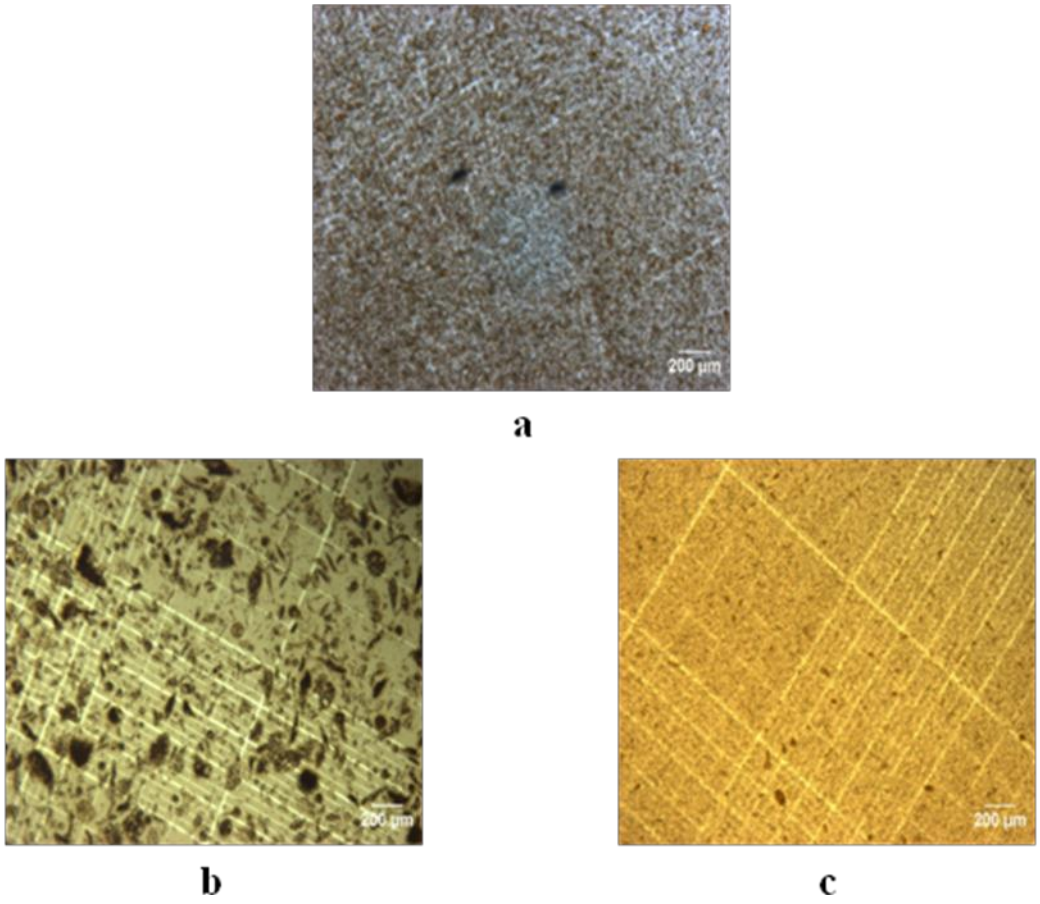

Figure 7-1. Gelatin-krill oil (a) and gelatin-esterified krill oil (b & c) emulsions observed by the stereomicroscope using the high-shear homogenizer (a & b) and the ultrasonic liquid processor (c), as emulsification devices

.

7.4.1.2. Effect of pH of GE and Emulsification Device on the Size of Microcapsules

In order to investigate the effects of pH of GE and emulsification device on the size of the capsules, aliquots were withdrawn at various stages of the complex coacervation, including emulsification, as well as the addition of GA, 10% acetic acid and cooling. For both emulsification devices, Table 7-1 displays the size of the microcapsules at the investigated pH range of 5.8 to 8.5. Figures 7-2, 7-3 and 7-4 are the stereomicroscopic views for the various stages of the complex coacervation process where the pH of GE was 5.8, 6.5 and 8.0, respectively.

The experimental findings (Table 7-1) indicate that the HSH, with a wide range of pH (5.8 to 8.5) for GE, resulted by a statistically insignificant difference (P >0.05) in the size of the EKO microcapsules. Figures 7-2a, 7-3a and 7-4a show that the change in pH of GE did not improve with the emulsion. The irregular particles (Figs. 7-2b, 7-3b and 7-4b), formed in the absence of acetic acid at the emulsification stage, were agglomerated together into bigger capsules, with a concomitant increase in size until the capsules were hardened. The formation of the capsules before the addition of acetic acid could be explained by the fact that after the addition of the GA to the GE-EKO emulsion, the pH was dropped from 5.36±0.12 to 4.87±0.1; at this pH, the GE was cationically charged allowing it hence to interact with GA, where the heterogeneous size of the emulsion particles affected their stability. Consequently, the particles were more likely to break and to cluster with neighboring particles resulting hence into bigger capsules. Liu *et al*. (2010) reported similar findings, where the aggregation of the capsules was obtained as a result of the rupturing of the capsules membranes. In addition, Drusch *et al*. (2012) indicated that according to the Stokes law of oil, the droplet size of the emulsion affects its stability.

Table 7-1. Effect of the pH of gelatin & the emulsification devices on the size of the microcapsules.

	Homogenizer[b]		Ultrasound[f]	
pH[a]	Size of capules (μm)[c]	RSD (%)[e]	Size of capsules (μm)[c]	RSD (%)[e]
5.8	626 (127)[d]	17.69	608 (121)[d]	19.92
6.5	708 (16)	2.21	457 (22)	4.81
7.0	705 (72)	10.19	477 (47)	9.90
7.5	594 (10)	1.70	417 (3)	0.65
8.0	677 (12)	1.85	408 (6)	1.54
8.5	ND[g]	ND[g]	515 (12)	2.30

[a]pH of gelatin was increased from 5.8 to8.5 by the addition of 0.25 N of sodium hydroxide solution.

[b]The high-shear homogenizer consisted of a PowerGen 125. Phenolic lipids were emulsified into gelatin (1% w/v) at 20,500 rpm for 5 min followed by another 5 min at 30,000 rpm.

[c]Images of microcapsules on a hemocytometer, were captured by a QICAM 12-bit camera linked to stereomicroscope. The diameter of the microcapsules was measured using ImageJ analysis software. For each sample, 400 capsules were measured to have a representative sampling of the microcapsules.

[d]Standard deviation of duplicate samples.

[e]Relative standard deviation (RSD) was calculated as the standard deviation of duplicate samples divided by their mean multiplied by 100.

[f]The ultrasound consisted of a sonicator ultrasonic liquid processor. The pulsar mode was used, where ultrasonic energy was delivered in pulsed cycles. The pulse ON time was set at 30 sec followed by a pulse off time of 30 sec for a total processing time of 270 sec.

[g]Not determined.

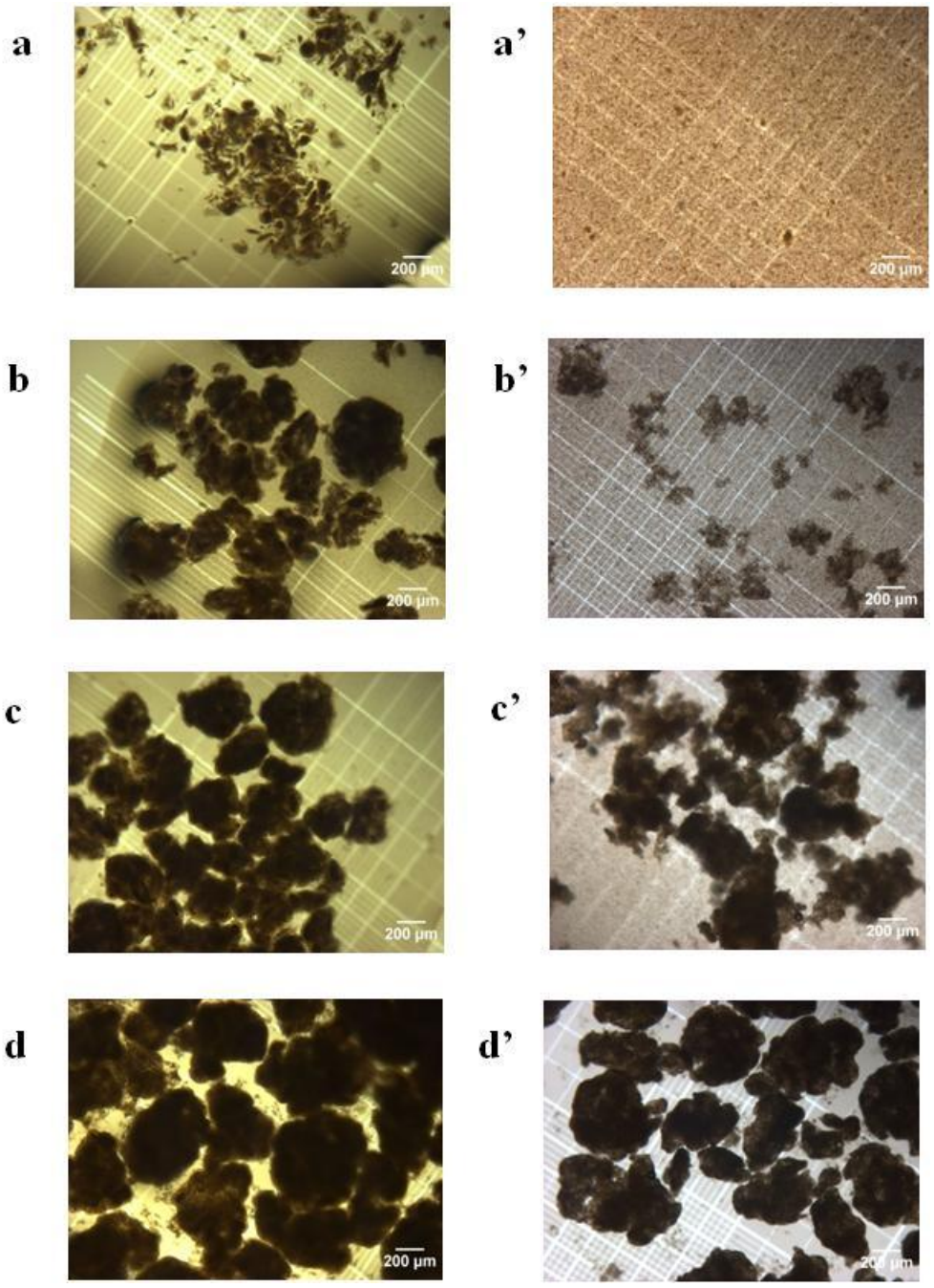

Figure 7-2. Stereomicroscopic view for the various steps of the complex coacervation process, including emulsification (a & a') as well as the addition of gum arabic (b & b'), 10% acetic acid (c & c') and cooling (d & d') using unmodified pH of gelatin (5.8) and the high-shear homogenizer (a, b, c & d) and the ultrasonic liquid processor (a', b', c' & d').

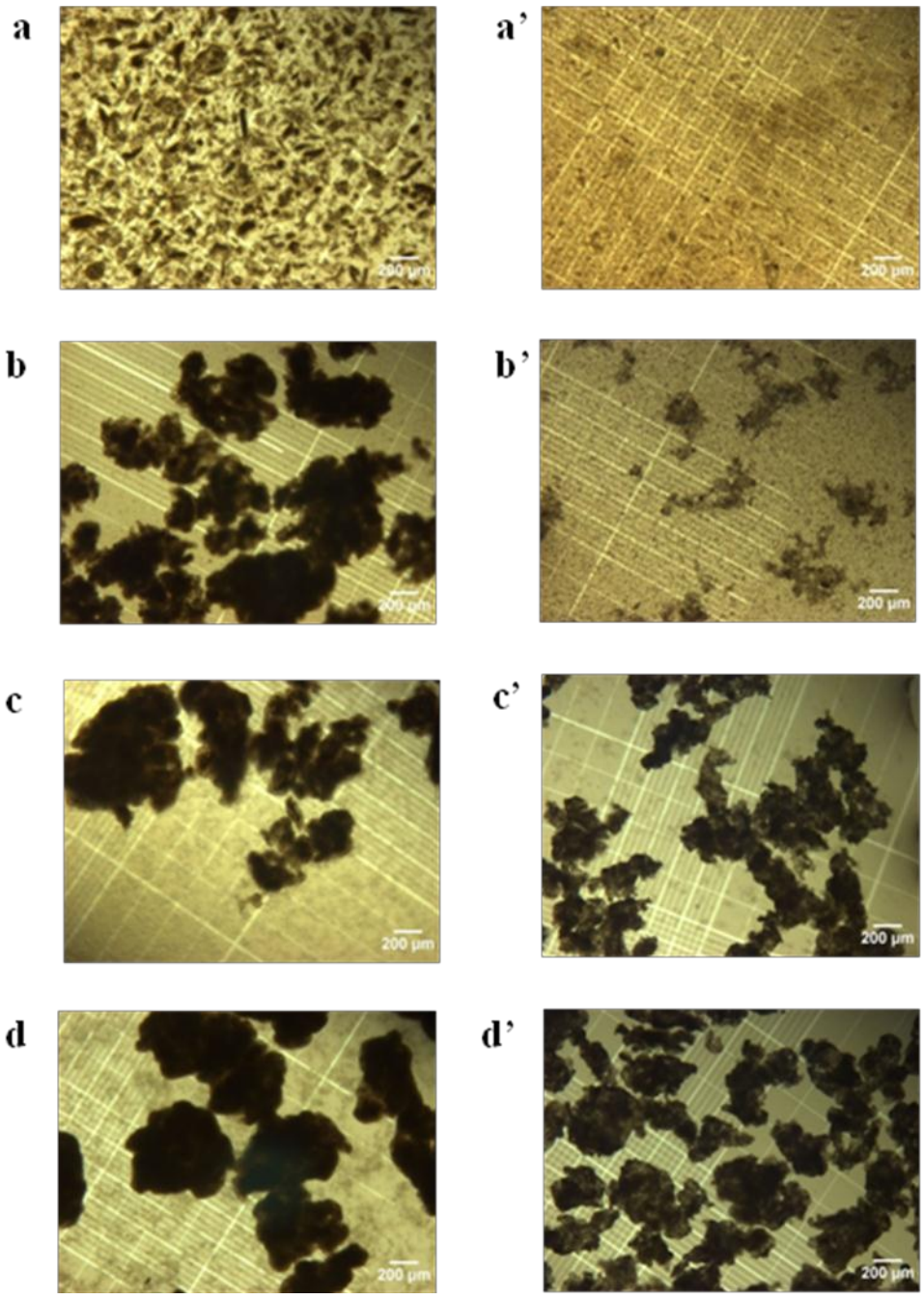

Figure 7-3. Stereomicroscopic view for the various steps of the complex coacervation process, including emulsification (a & a') as well as the addition of gum arabic (b & b'), 10% acetic acid (c & c') and cooling (d & d') using pH of gelatin adjusted to 6.5 and the high-shear homogenizer (a, b, c & d) and the ultrasonic liquid processor (a', b', c' & d').

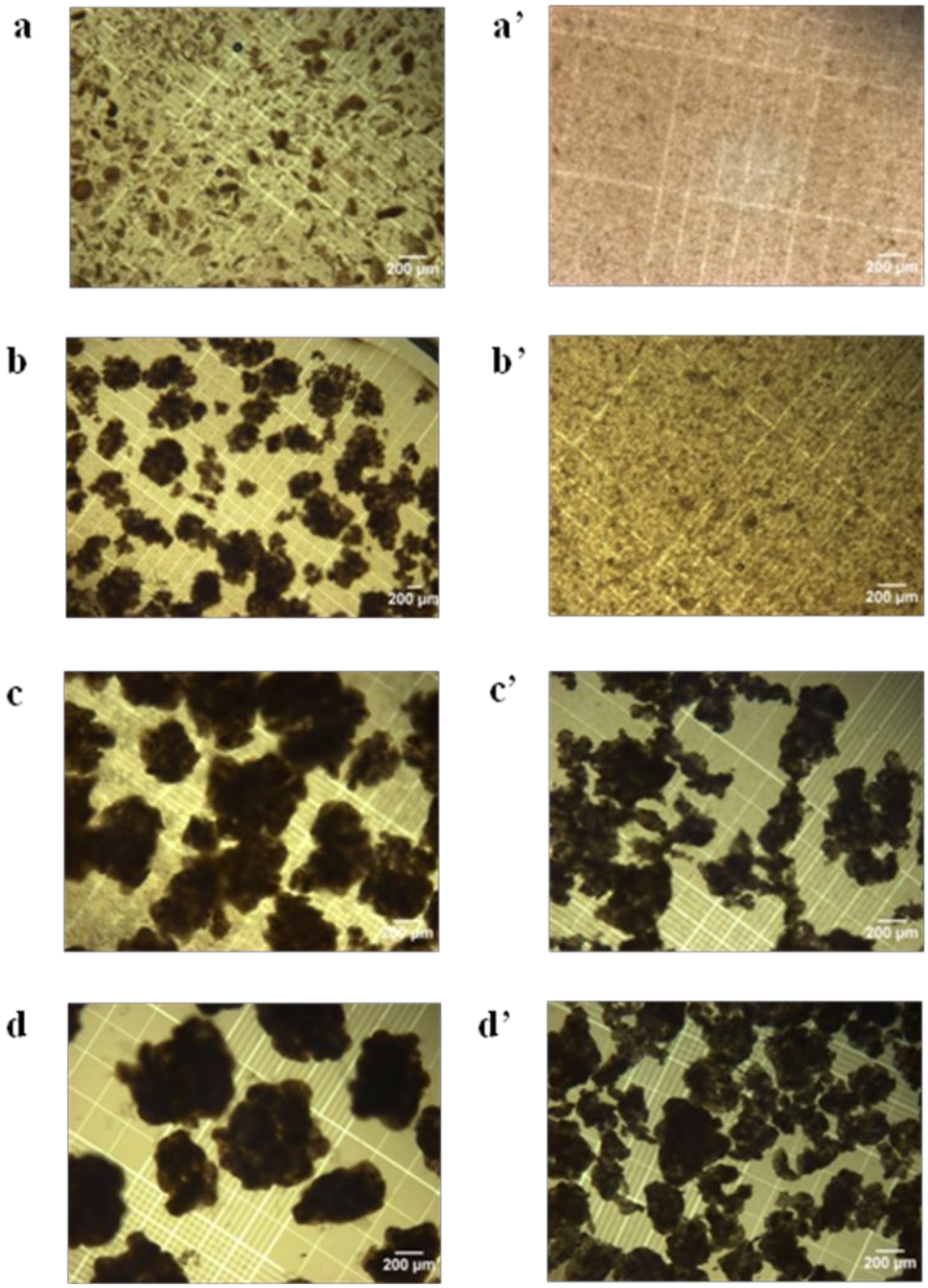

Figure 7-4. Stereomicroscopic view for the various steps of the complex coacervation process, including emulsification (a & a') as well as the addition of gum arabic (b & b'), 10% acetic acid (c & c') and cooling (d & d') using pH of gelatin adjusted to 8.0 and the homogenizer (a, b, c & d) and the ultrasonic liquid processor (a', b', c' & d').

On the other hand, using the ULP and varying the pH of GE, there was no statistically significant difference in the size (P >0.05) of the EKO microcapsules; however, the overall difference in the size of the microcapsules was significantly lower (P <0.05) than that with the HSH. These findings (Table 1) could be explained by the fact that unlike HSH, the ULP resulted in a stable and homogenous emulsion (Figs. 7-2a', 7-3a' and 7-4a'). Figures 7-2b', 7-3b' and 7-4b' show that as the pH of GE increased, there was a potential decrease in the electrostatic interactions between GA and the GE-EKO droplets, limiting hence the formation of GE-GA particles before the addition of acetic acid. These findings are in agreement with the principle that, in order for the GE to be able to interact with the GA, it has to become cationically charged which only occurs at pH below its IP (Lemetter *et al*., 2009).

7.4.1.3. Effect of pH of GE and Emulsification Device on the Encapsulation Efficiency of Microcapsules

The effects of the type of emulsification device and pH of GE on the stability of the EKO microcapsules, and consequently on their encapsulation efficiency (EE) were investigated (Fig. 7-5). Using the HSH, at unmodified pH of GE of 5.8, the formed capsules were susceptible to breakage, which made the determination of the EE difficult (Fig. 7-5); this could be a consequence of the heterogeneous nature and the instability of the emulsion (Drusch *et al*., 2012). In addition, Soottitantawat *et al*. (2003) indicated that the emulsion droplet size had a significant effect on the retention of volatile compounds, encapsulated by spray-drying.

The experimental findings (Fig. 7-5) indicate that using the high-shear homogenizer (HSH) and varying the pH of GE, there was a statistically significant difference (P <0.05) in the EE of EKO. Figure 7-5 shows that using the HSH, the EE of EKO gradually increased as the pH increased from 5.8 to 7.5, followed by a decrease at a pH of 8.0.

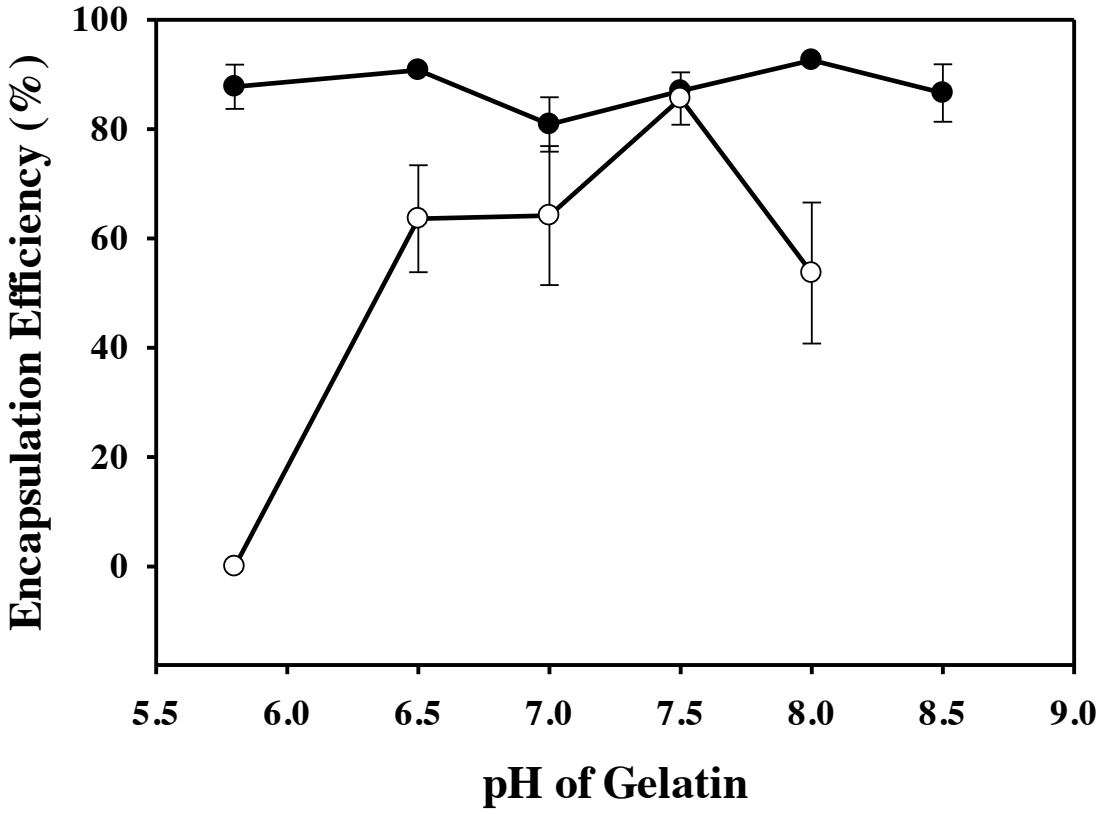

Figure 7-5. Effects of the pH of gelatin & emulsification devices, including the high-shear homogenizer (○) and the ultrasonic liquid processor (●) on the encapsulation efficiency of esterified krill oil (EKO).

These findings are in agreement with those of Strauss and Gibson (2004), who reported that the cross-linking between the PAs and GE resulted in the creation of a rigid framework when the pH was moved away from the isoelectric point (IP); this could explain the highest EE obtained at pH 7.5 of 85.5±4.78% (Fig. 7-5). These findings (Fig. 7-5) are also in agreement with those of Zhang *et al*. (2010b), who reported that the reactivity of the PAs with GE can be controlled by varying the pH of the GE and that the rigid covalent cross-links can be formed between PAs with GE, under alkaline conditions.

On the other hand, using the ultrasonicator and varying the pH of GE, there was no statistically significant difference in the EE (P >0.05) of the EKO microcapsules (Fig. 7-5). The results indicated that EE in the investigated range of pH of GE (5.8 to 8.5) was between 80.86±4.97 and 92.58±0.38. It is well understood that the pH controls the balance of the molecules charges and therefore, the intensity of the electrostatic interactions, driving the formation of complexes (Qv *et al*., 2011). Since the ultrasonication technique did not favor the cross-linking of GE with the PAs and PLs, in the esterified oil, at the emulsification stage (Figs. 7-2a', 7-3a' and 7-3a'), the pH of GE had no influence on the EE of the EKO microcapsules. As compared to the HSH, the microcapsules of EKO, prepared with the ULP, had high EE over a wider range of pH of GE and they were smaller in size (Fig. 7-5). Hence, the ULP was found to be a more appropriate device for the emulsification of the EKO into GE and it was used for further investigations.

7.4.2. Effect of pH of GE on the Oxidation of EKO Microcapsules and their Storage Stability

7.4.2.1. Effect of pH of GE on the Oxidation of EKO During Encapsulation

To investigate the effect of pH of GE on the oxidation of EKO microcapsules during encapsulation, primary and secondary oxidation products in the extracted oil were determined, using the modified IDF method and *p*-AnV, respectively.

Figure 7-6A shows that using the traditional IDF method to determine the peroxide value (PV), an overlap between the Fe^{3+}-thiocyanate complex and the EKO spectra was

majorly due to the presence of carotenoids in the EKO, mainly astaxanthin, that could interfered with the absorbance of the Fe^{3+}-thiocyanate complex (Fig. 7-6B). To avoid such interference and without a loss in sensitivity, Honero-Méndez *et al*. (2001) extracted the carotenoids with an organic solvent, before performing the spectrophotometric method for the determination of PV. Figure 7-6C shows that the absorbance spectrum of the Fe^{3+} thiocyanate complex is now free from interference from the carotenoids in the EKO, with a maximum absorption at 470 nm. These findings (Fig. 7-6) are in agreement with those reported by Honero-Méndez *et al*. (2001) for the determination of the PV in food lipids of high carotenoid content. Figure 7-7 shows the calibration plot of Fe^{3+} standard plot for the quantification of the PV by the modified IDF method, with a slope (*m*) of 0.0651 and a correlation coefficient of $R^2 = 0.998$. Overall, these results show a good linearity over the used range of concentration.

The effect of the pH of GE on the oxidation of EKO, during encapsulation, was also investigated. The results (data not shown) showed that the EKO extracted from the microcapsules, prepared with GE of pH 6.5, had a PV of 0.739±0.035 and a *p*-AnV of 10.165±0.219. On the other hand, the EKO extracted from the microcapsules, prepared with GE of pH 8.0, had a PV of 0.481±0.010 and a *p*-AnV of 9.812±0.283. While there was no significant difference ($P > 0.05$) in the *p*-AnV between the two trials, the statistical analyses revealed that there was a significant one ($P < 0.05$) in the PV. These results are in agreement with those of Jacobsen *et al*. (2001), who indicated that the PV and the total volatiles were generally increased with the decrease in pH of the mayonnaise, enriched with 16% of fish oil; these authors suggested that the increase in oxidation could be explained by the fact that the low pH promotes the breakage of the iron bridges between the egg yolk proteins at the oil-water interface, making the Fe ions more accessible as oxidation initiators. Likewise, Horn *et al*. (2011) reported that there was a tendency toward a faster progression in lipid oxidation at low pH as compared to that at higher one in 70% fish oil-in-water emulsion, prepared with protein.

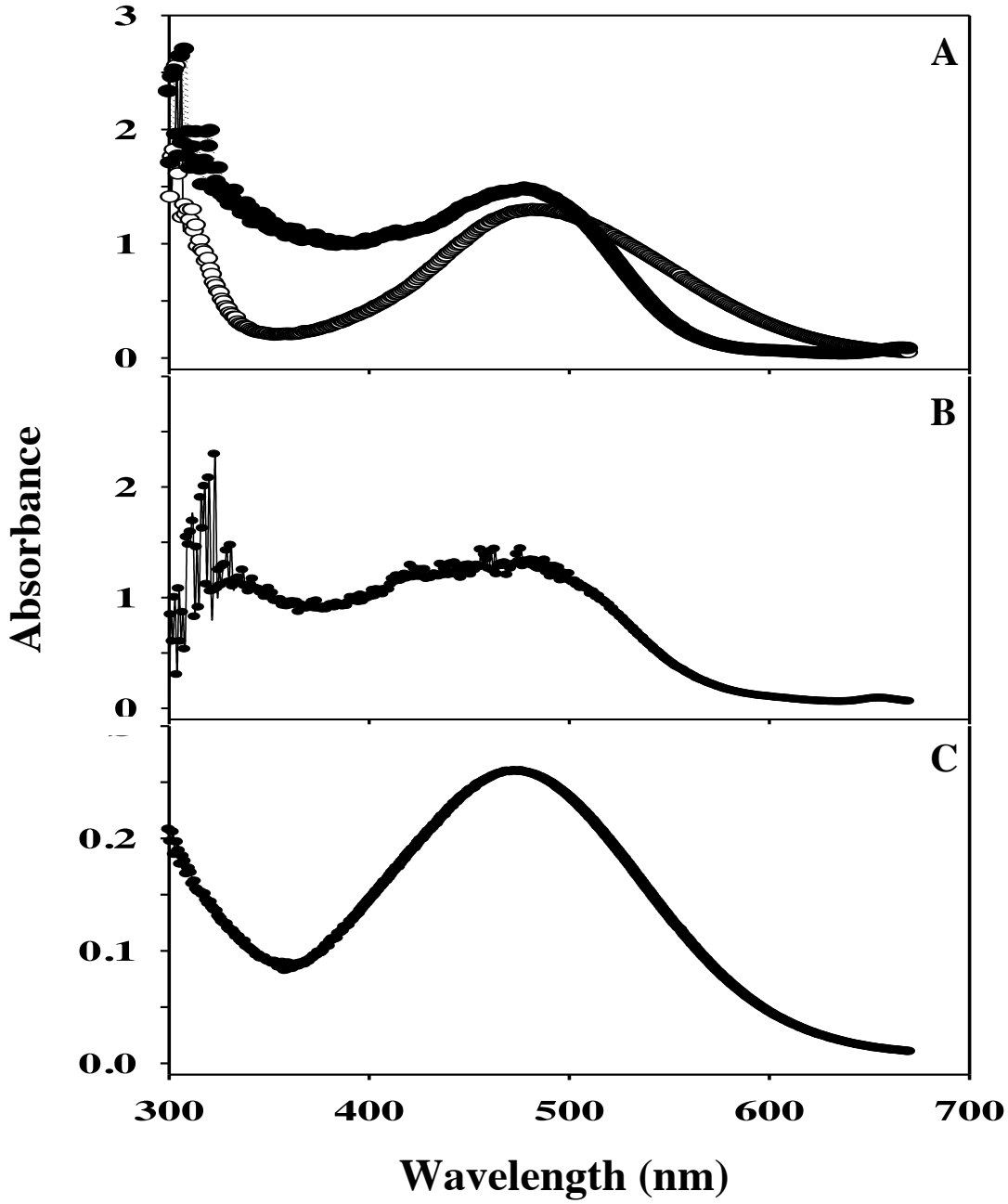

Figure 7-6. Ultraviolet-visible spectra of (A) esterified krill oil (EKO) (○) and Fe^{3+}-thiocyanate complex (●) in chloroform /acetic acid (2:3); (B) Fe^{3+}-thiocyanate complex added to phenolic lipids sample vs. a blank consisting of the same sample in chloroform/acetic acid (2:3); (C) Fe^{3+}-thiocyanate complex in the modified International Dairy Foundation (IDF) aqueous phase after elimination of the carotenoids from the EKO samples.

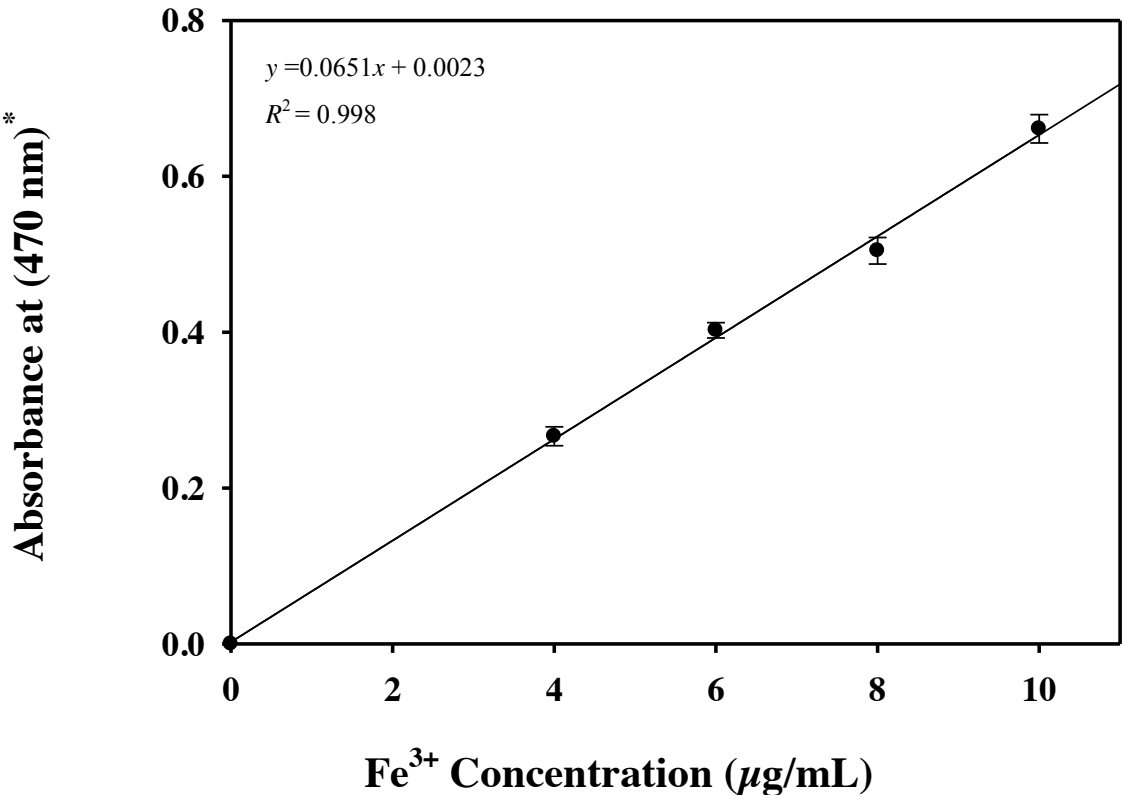

Figure 7-7. Standard Fe^{3+} calibration plot for the quantification of the peroxide value (PV) by the modified International Dairy Foundation (IDF) method.*Absorbances were corrected by subtracting at 670 nm.

7.4.2.2. Storage Stability of EKO Microcapsules

In order to investigate the effects of pH of GE and the storage temperature on the stability of EKO microcapsules, capsules prepared with the ultrasonic liquid processor (ULP) at pH of GE of 6.5 and 8.0 were stored in screw-cap test tubes and wrapped with aluminum foil at 4 and 25ºC for a total period of 25 days. Figure 7-8 depicts the effects of storage temperatures on the stability of the EKO microcapsules prepared at a pH 6.5 and 8.0, respectively, of the GE

Figure 7-8A shows that the capsules, prepared with pH of GE of 6.5, demonstrated a significant decrease (P <0.05) in the retention rate (RR), to 50.83 and 60.50% at 25 and 4°C, respectively after 25 days of storage. For the microcapsules prepared, with pH of GE of 8.0 (Fig. 7-8B), there was a significant decrease (P >0.05) in RR to 76.61 and 83.43% after 5 days of storage at 25 and 4°C, respectively, and this remained unchanged afterwards. On the contrary, Qv *et al*. (2011) reported that the RR of lutein was 92.86 and 90.16% at 4 and 25°C, respectively; the high stability could be explained by the fact that unlike the lutein capsules, no cross-linker was used in the case of EKO.

After 25 days, for both trials and for both temperatures, the statistical analyses (P <0.05) revealed that the capsules stored at 4°C showed higher stability as compared to that for those stored at 25°C. These findings could be due to the fact that the GE hardens at temperatures below its gelling point (<10°C), hence increasing the stability of the capsules (Lemetter *et al*., 2009). In addition, Qv *et al*. (2011) indicated that the RR of lutein decreased with the increase in temperature.

Overall, the capsules prepared with pH of GE of 8.0 showed better storage stability (P <0.05) as compared to that of those prepared with pH of 6.5. These findings could be explained by the fact that the lower pH may make the capsules more susceptible to breakage (Horn *et al*., 2011). In addition, the literature (Strauss and Gibson, 2004; Zhang *et al*., 2010b) indicated that the formation of rigid linkages is favored under alkaline conditions.

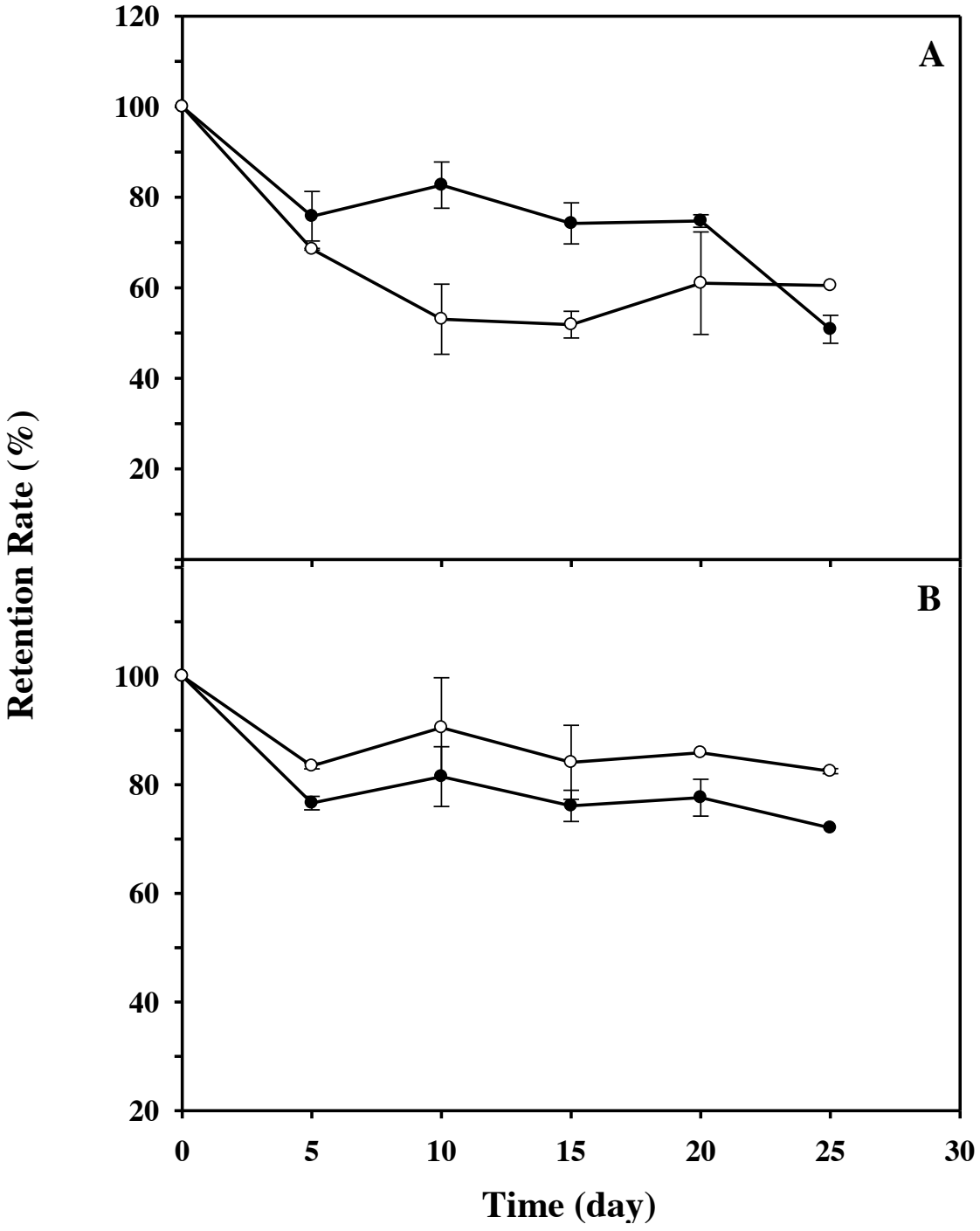

Figure 7-8. Effects of storage temperatures at 25°C (○) and 4°C (●) on the stability of esterified krill oil microcapsules preparing with a pH 6.5 (A) and 8.0 (B) of the gelatin.

7.4.3. Optimum Conditions

Based on the experimental findings reported previously, the microcapsules prepared with a pH of GE of 8.0 were less oxidized and had better storage stability, as compared to those prepared with pH of GE of 6.5, and therefore they were used for further studies. Using the UPL, the optimized conditions for the encapsulation of EKO via complex coacervation were: a pH of GE adjusted to 8.0, a RCW of 1.25:1, a stirring speed of 400 rpm, a concentration of wall materials of 1% and a final pH value of 4.0. Under the optimum conditions, the encapsulation efficiency (EE) of EKO reached 96.18±1.97%, with low amounts of extractable oil from the surface.

7.4.4. Physicochemical Properties of Free and Encapsulated EKO

To investigate whether the microcapsules maintained their integrity after drying, the optimized microcapsules were subjected to lyophilization. Figure 7-9 demonstrates a stereomicroscope view of the EKO microcapsules, prepared under the optimal conditions. Figure 7-9b shows that the capsules maintained their wall integrity after lyophilization, despite the absence of cross-linking agents. These findings are in agreement with those reported in literature (Alvim and Grosso, 2010; Liu *et al*., 2010) for multinucleated microcapsules as well as with those obtained with the KO (Chapter VI).

7.4.5. Oxidative Stability of Lyophilized EKO Capsules

The capsule's ability to inhibit the development of primary (Fig. 7-10A) and secondary (Fig. 7-10B) oxidation products was assessed, directly after encapsulation and at room temperature over a total period of 25 days. The experimental findings showed that the PV and *p*-AnV directly after encapsulation were 0.33±0.02 and 0.44±0.02 as well as 11.42±0.42 and 11.63±0.63 for the non-encapsulated and the encapsulated EKO, respectively. The statistical analyses revealed the difference in the oxidation between that of the non-encapsulated and encapsulated EKO was significant (P <0.05) for the primary oxidation products, but not significant (P >0.05) for the secondary ones.

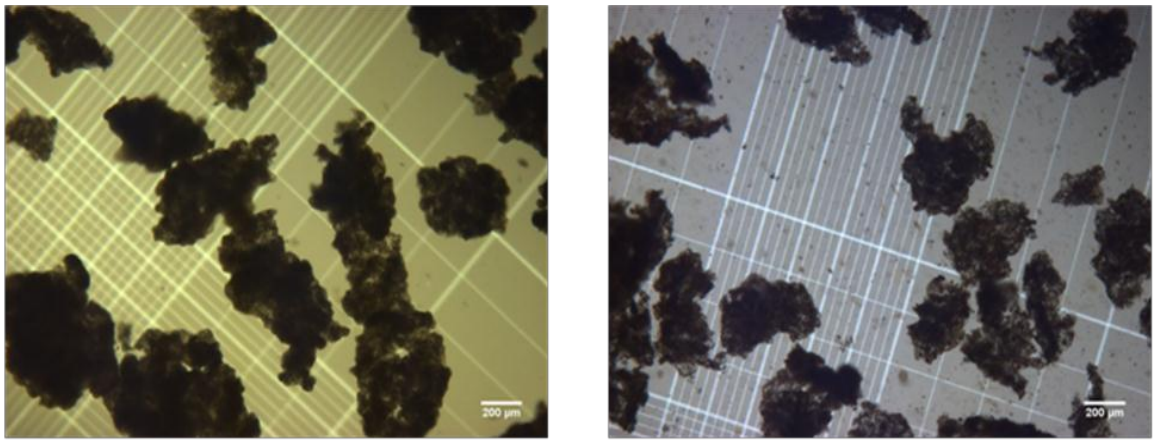

a b

Figure 7-9. Stereomicroscope view of esterified krill oil microcapsules prepared under the optimal conditions obtained: (a) before lyophilization and (b) after lyophilization.

Drusch *et al*. (2006a) indicated that the hydroperoxide concentration showed a 13-fold increase directly after encapsulation for the microencapsulated product as compared to the purified fish oil using spray-drying. On the other hand, Liu *et al*. (2010) reported that the PV and *p*-AnV of the flaxseed oil (FSO), encapsulated via complex coacervation before and immediately after the encapsulation process, were statistically indifferent (P <0.05). Unlike the FSO, the EKO contains long-chain polyunsaturated fatty acids, which are highly susceptible to be prone for oxidation (Massrieh, 2008; Shahidi and Zhong, 2010).

During the storage at room temperature for a total period of 25 days, there was significant increase in PV (P <0.05) after 5 and 15 days for non-encapsulated and encapsulated EKO, respectively. However, there was a significant increase in *p*-AnV (P <0.05) after 10 and 15 days for the non-encapsulated and encapsulated EKO, respectively. After 25 days of storage, the primary and the secondary oxidation products were significantly higher (P <0.05) in the non-encapsulated EKO, as compared to those in the encapsulated one. The results (Fig. 7-10) indicate that the encapsulation of EKO was effective in delaying the development of primary and secondary oxidation products over the period of storage. Liu *et al*. (2010) reported that the PV and *p*-AnV, obtained after a period of storage of 25 days of the encapsulated FSO, suggest that the GE-GA capsule design provided adequate protection against oxidative degradation. On the contrary, Kolanowski *et al*. (2006) indicated that the oxidation changes were much slower in the bulk fish oil as compared to those in the spray-dried fish oil capsules. Rusli *et al*. (2006) reported that the composition of the oil-water interface, the interfacial thickness and strength and the localization of antioxidants in the interface play an important role in stabilizing the emulsified material.

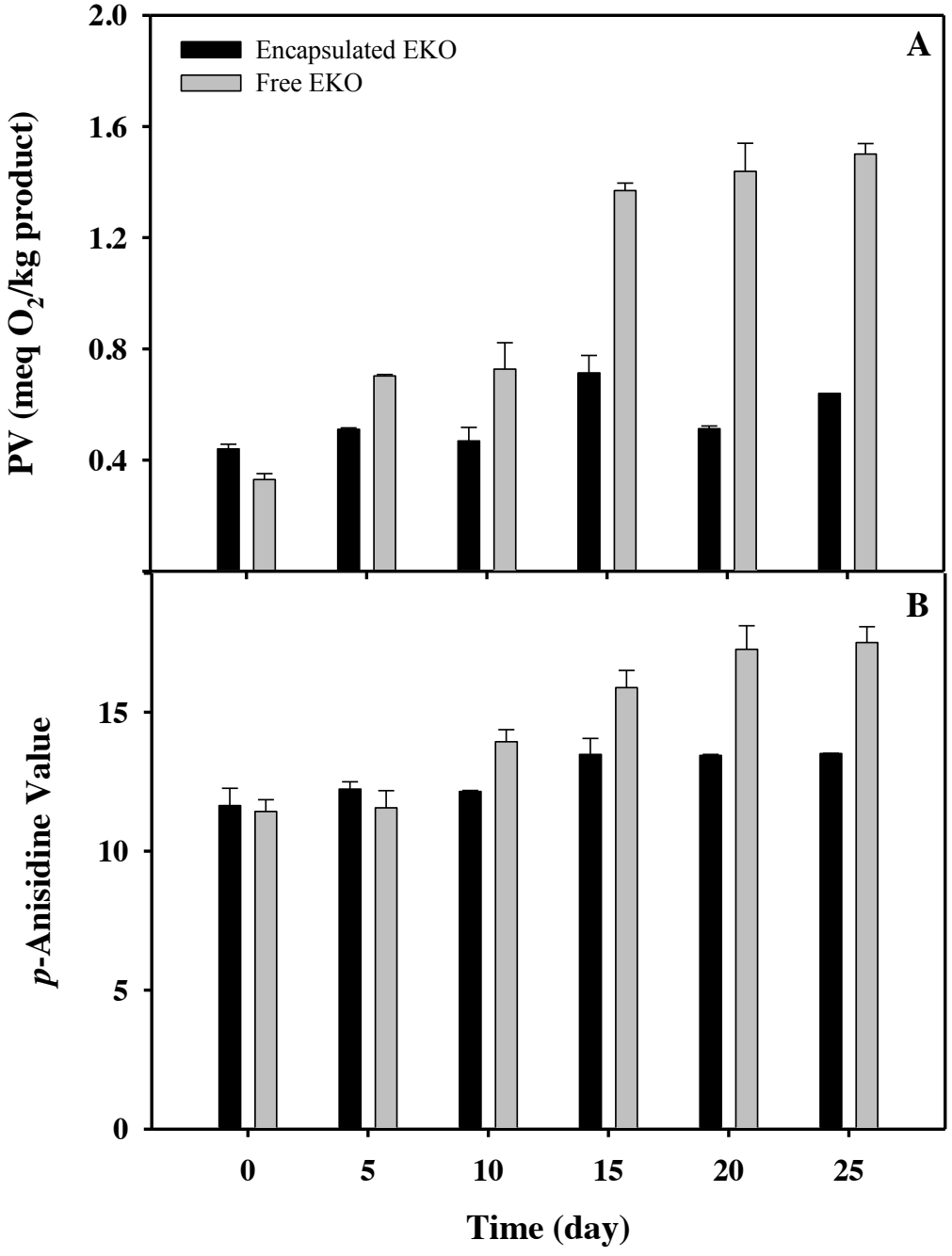

Figure 7-10. Profile of the lipid oxidation products in the encapsulated esterified krill oil (EKO) as compared to the non-encapsulated EKO stored at room temperature in amber vials, over a period of 25 days.

7.5. Conclusion

Using the complex coacervation method, the microencapsulation of EKO resulted in a high encapsulation efficiency (EE). The presence of phenolic acids and phenolic lipids in the esterified oil had an impact on the electrostatic interactions in the system. The pH of GE affected the morphology, EE and storage stability of the capsules by influencing the balance of the molecules charges in the process. The GE-GA capsules design was effective in delaying the oxidative degradation of EKO. This encapsulation design could lay the ground for the use of EKO as nutraceuticals and as antioxidant additive in food products.

GENERAL CONCLUSION

The present study was aimed at the optimization of synthesis of phenolic lipids (PLs), obtained from the lipase-catalyzed transesterification in solvent-free media (SFM) of krill oil (KO) with 3,4-dihydroxyphenylacetic acid (DHPA) and their encapsulation. A chromatographic method (HPLC) for the separation of the complex mixture of triacylglycerols (TAGs) and phospholipids of KO as well as the esterified phenolic lipids (PLs) was developed. As a whole, ELSD was shown to be a more appropriate tool for the quantitative analysis of the components of KO and its esterified PLs as compared to UV. FTIR analysis tentatively confirmed the nature of the separated compounds. In addition, the structural analyses of the synthesized molecules by HPLC-MS-APCI/ESI suggested the formation of two phenolic monoacylglycerols.

Central composite rotatable design (CCRD) was successfully used to optimize the synthesis in SFM of PLs, from KO and DHPA. The presence of phospholipids in KO had a major effect on the dynamics of the transesterification process, in terms of enzyme efficiency and its affinity. In addition, the statistical analyses showed that in order to achieve a higher bioconversion yield (BY), it was essential to maintain the phenolic acid (PA) concentration constant throughout the models. The optimized model could be used to predict the BY of PLs in the investigated range.

The antioxidant capacity and the oxidative stability of the esterified oils containing PLs, obtained by lipase-catalyzed transesterification of PAs with selected edible oils (EOs), including flaxseed (FSO), fish liver (FO) and krill (KO) oils, were determined. The experimental findings indicated that the esterified edible oils containing PLs demonstrated an enhanced chain-breaking antioxidant capacity and a less susceptibility to oxidation after their subjection to relatively high incubation temperatures and in the presence of light and oxygen as compared to those of the unmodified oils. Overall, the phenolic mono- and diacyglycerols, present in the edible oils, have shown to be potential antioxidants in improving the oxidative stability of the oils and enhancing their AOC.

Using complex coacervation, the Box-Behnken design (BBD) was successfully used to optimize a process for yielding gelatin (GE)-gum arabic (GA) multinuclear microcapsules of KO. The encapsulation efficiency (EE) and the stability of the microcapsules were affected by their internal structure, where the multinucleated microcapsules showed better stability as compared to that of their mononucleated counterparts. The experimental findings indicated that the pH had the most significant linear and quadratic effects on the EE of KO and a bilinear one with the ratio of the core material to the wall (RCW), whereas the stirring speed had no effect. The microcapsules, formed by complex coacervation and without any cross-linking agent, were multinucleated, circular in shape and had sufficient stability to maintain their structure.

When the complex coacervation method was used to encapsulate the esterified krill oil (EKO), the experimental findings showed that the presence of PA and PLs, in the esterified oil, affected the electrostatic interactions in the system. As compared to the use of the high-shear homogenizer, the ultrasonic liquid processor was found to be a more appropriate tool for the emulsification of the EKO into GE. An alkaline environment created, by adjusting the pH of GE, resulted in capsules with higher storage and oxidative stability as compared to those prepared at an acidic one. The microencapsulation of the EKO was effective in delaying the development of oxidation products during a period of 25 days of storage at room temperature.

The overall experimental results obtained through the present study could lay the ground for the use of PLs from KO as nutraceuticals and antioxidant additive in food products. The optimized transesterification process could be used to predict the BY of phenolic lipids in SFM, under any given conditions, within the experimental range tested. The developed microencapsulation design could facilitate the incorporation of the KO and its esterified PLs in aqueous food system, so as to contribute to the health and well-being of consumers. Future work should focus on bioavailability studies to better understand the transportation and absorption of these molecules in the human body and to improve their effectiveness.

REFERENCES

Ahmed, T., Atta, S., Sohail, M., Khan, A.R. and Akhtar, S. (2011). Effect of fluorescent light on quality and stability of edible fats and oils. *J. Chem. Soc. Pak.* **33**, 233-237.

Akoh, C.C. and Hee Kim, B. (2008). Structured lipids. In *Food lipids: Chemistry, Nutrition and Biotechnology*, C.C. Akoh and B.M. David (eds.), CRC press, pp. 841-871.

Akoh, C.C. and Yee, L.N. (1998). Lipase-catalyzed transesterification of primary terpene alcohols with vinyl esters in organic media. *J. Mol. Catal. B: Enz.* **4**, 149-153.

Aldercreutz, P. (2008). Fundamentals of biocatalysis in neat organic solvents. In *Organic Synthesis With Enzymes in Non-Aqueous Media*, G. Carrea and S. Riva (eds.), Vch Verlagsgesellschaft Mbh, Weinheim, Germany, pp. 3-24.

Alloue, W., Aguedo, M., Destain, J., Ghalfi, H., Blecker, C., Wathelet, J. and Thonart, P. (2007). Les lipases immobilisées et leurs applications. *Biotechnologie, Agronomie, Société et Environnement* **12**, 55-68.

Almeida, M.C., Ruivo, R., Maia, C., Freire, L., Corrêa de Sampaio, T. and Barreiros, S. (1998). Novozym 435 activity in compressed gases. Water Activity and temperature effects. *Enz. Microbiol. Technol.* **22**, 494-499.

Alvim, I.D. and Grosso, C.R.F. (2010). Microparticles obtained by complex coacervation: Influence of the type of reticulation and the drying process on the release of the core material. *Ciênc. Tecnol. Aliment.* **30**, 1069-1076.

AOAC (1990). Moisture in Animal Feed. Official Methods of Analysis 934.01. 14th Edition. Association of Official Analytical Chemists, Washington, D.C.

AOCS (2009). p-Anisidine Value. Official Method Cd 18-90. American Oil Chemists' Society Press. In *Official Methods and Recommended Practices of the American Oil Chemists' Society*, D. Firerstone (ed.), Champain, IL.

Awang, R., Basri, M., Ahmad, S. and Salleh, A.B. (2004). Lipase-catalyzed esterification of palm-based 9,10-dihydroxystearic acid and 1-octanol in hexane – a kinetic study. *Biotechnol*. *Lett*. **26**, 11-14.

Aybastler, Ö. and Demir, C. (2010). Optimization of immobilization conditions of *Thermomyces lanuginosus* lipase on styrene-divinylbenzene copolymer using response surface methodology. *J*. *Mol*. *Catal*. *B: Enz*. **63**, 170-178.

Aziz, S., Dutilleul, P. and Kermasha, S. (2012a). Lipase-catalyzed transesterification of krill oil and 3,4-dihydroxyphenyl acetic acid in solvent-free medium using response surface methodology. *J*. *Mol*. *Catal*. *B: Enz*. **84**, 189-197.

Aziz, S., St-Louis, R., Yaylayan, V. and Kermasha, S. (2012b). Chromatographic separation of synthesized phenolic lipids from krill oil and dihydroxyphenyl acetic acid. *J*. *Am*. *Oil Chem*. *Soc*. **89**, 597-608.

Balasundram, N., Sundram, K. and Samman, S. (2006). Phenolic compounds in plants and agri-industrial by-products: Antioxidant activity, occurrence, and potential uses. *Food Chem*. **99**, 191-203.

Barrow, C.J., Nolan, C. and Jin, Y. (2007). Stabilization of highly unsaturated fatty acids and delivery into foods. *Lipid Technol*. **19**, 108-111.

Baş, D. and Boyacı, İ.H. (2007). Modeling and optimization I: Usability of response surface methodology. *J*. *Food Engineer*. **78**, 836-845.

Bhatia, A.L., Sharma, A., Patni, S. and Sharma, A.L. (2007). Prophylactic effect of flaxseed oil against radiation-induced hepatotoxicity in mice. *Phytother*. *Res*. **21**, 852-859.

Bisby, R.H., Brooke, R. and Navaratnam, S. (2008). Effect of antioxidant oxidation potential in the oxygen radical absorption capacity (ORAC) assay. *Food Chem*. **108**, 1002-1007.

Blanco, M., Sotelo, C.G., Chapela, M.J. and Pérez-Martín, R.I. (2007). Towards sustainable and efficient use of fishery resources: Present and future trends. *Trends Food Sci. Technol.* **18**, 29-36.

Bunea, R., El Farrah, K. and Deutsch, L. (2004). Evaluation of the effects of Neptune krill oil on the clinical course of hyperlipidemia. *Altern. Med. Rev.* **9**, 420-428.

Burden, D.W. (2008). Guide to the homogenization of biological samples. *Random Primers* **7**, 1-4.

Bustos, R., Romo, L., Yanez, K., Diaz, G. and Romo, C. (2003). Oxidative stability of carotenoid pigments and polyunsaturated fatty acids in microparticulate diets containing krill oil for nutrition of marine fish larvae. *J. Food Engineer.* **56**, 289-293.

Cai, S.-S. and Syage, J.A. (2006). Comparison of atmospheric pressure photoionization, atmospheric pressure chemical ionization, and electrospray ionization mass spectrometry for analysis of lipids. *Anal. Chem.* **78**, 1191-1199.

Cansell, M., Nacka, F. and Combe, N. (2003). Marine lipid-based liposomes increase *in vivo* FA bioavailability. *Lipids* **38**, 551-559.

Carlson, R. and Carlson, J.E. (2005). Canonical analysis of response surfaces: A valuable tool for process development. *Org. Process Res. Develop.* **9**, 321-330.

Carrín, M.E. and Crapiste, G.H. (2008). Enzymatic acidolysis of sunflower oil with a palmitic-stearic acid mixture. *J. Food Engineer.* **84**, 243-249.

Cermak, R., Durazzo, A., Maiani, G., Böhm, V., Kammerer, D.R., Carle, R., Wiczkowski, W., Piskula, M.K. and Galensa, R. (2009). The influence of postharvest processing and storage of foodstuffs on the bioavailability of flavonoids and phenolic acids. *Mol. Nutr. Food Res.* **53**, S184-S193.

Champagne, C.P. and Fustier, P. (2007). Microencapsulation for the improved delivery of bioactive compounds into foods. *Curr. Opin. Biotechnol.* **18**, 184-190.

Chen, S. and Kord, A. (2009). Theoretical and experimental comparison of mobile phase consumption between ultra-high-performance liquid chromatography and high performance liquid chromatography. *J. Chromatogr. A* **1216**, 6204-6209.

Chen, Y., Kele, M., Tuinman, A. and Guiochon, G. (2000). Comparison of the repeatability of quantitative data measured in high-performance liquid chromatography with UV and atmospheric pressure chemical ionization mass spectrometric detection. *J. Chromatogr. A* **873**, 163-173.

Cho, K.H., Hong, J.H. and Lee, K.T. (2010). Monoacylglycerol (MAG)-oleic acid has stronger antioxidant, anti-atherosclerotic, and protein glycation inhibitory activities than MAG-palmitic acid. *J. Med. Food* **13**, 99-107.

Choe, E. and Min, D.B. (2006). Mechanisms and factors for edible oil oxidation. *Compr. Rev. Food Sci. Food Safety* **5**, 169-186.

Choe, E. and Min, D.B. (2009). Mechanisms of antioxidants in the oxidation of foods. *Compr. Rev. Food Sci. Food Safety* **8**, 345-358.

Choo, W.-S., Birch, E. and Stewart, I. (2009). Radical scavenging activity of lipophilized products from transesterification of flaxseed oil with cinnamic acid or ferulic acid. *Lipids* **44**, 807-815.

Crozier, A., Del Rio, D. and Clifford, M.N. (2010). Bioavailability of dietary flavonoids and phenolic compounds. *Mol. Aspects Med.* **31**, 446-467.

Dávalos, A., Gómez-Cordovés, C. and Bartolomé, B. (2003). Extending applicability of the oxygen radical absorbance capacity (ORAC−fluorescein) assay. *J. Agric. Food. Chem.* **52**, 48-54.

Davidson, M.H., Johnson, J., Rooney, M.W., Kyle, M.L. and Kling, D.F. (2012). A novel omega-3 free fatty acid formulation has dramatically improved bioavailability during a low-fat diet compared with omega-3-acid ethyl esters: The ECLIPSE (Epanova® compared to Lovaza® in a pharmacokinetic single-dose evaluation) study. *J. Clin. Lipidol.* **6**, 573-584.

de Pinedo, A.T., Penalver, P., Perez-Victoria, I., Rondon, D. and Morales, J.C. (2007). Synthesis of new phenolic fatty acid esters and their evaluation as lipophilic antioxidants in an oil matrix. *Food Chem*. **105**, 657-665.

Deiana, M., Rosa, A., Cao, C.F., Pirisi, F.M., Bandino, G. and Dessì, M.A. (2002). Novel approach to study oxidative stability of extra virgin olive oils: Importance of α-tocopherol concentration. *J*. *Agric*. *Food*. *Chem*. **50**, 4342-4346.

Deutsch, L. (2007). Evaluation of the effect of Neptune krill oil on chronic inflammation and arthritic symptoms. *J*. *Am*. *Coll*. *Nutr*. **26**, 39-48.

Diks, R.M.M. and Bosley, J.A. (2000). The exploitation of lipase selectivities for the production of acylglycerols. In *Enzymes in Lipid Modification* U.T. Bornscheuer (ed.) Wiley-VCH, Verlag Gmbh, Weinheinm, Germany, pp. 3-22.

Dobarganes, M.C. and Velasco, J. (2002). Analysis of lipid hydroperoxides. *Eur*. *J*. *Lipid Sci*. *Technol*. **104**, 420-428.

Dolan, J., Snyder, L., Djordjevic, N., Hill, D. and Waeghe, T. (1999). Reversed-phase liquid chromatographic separation of complex samples by optimizing temperature and gradient time II. Two-run assay procedures. *J*. *Chromatogr*. *A* **857**, 21-39.

Doleschall, F., Kemény, Z., Recseg, K. and Kővári, K. (2002). A new analytical method to monitor lipid peroxidation during bleaching. *Eur*. *J*. *Lipid Sci*. *Technol*. **104**, 14-18.

Dong, Z., Ma, Y., Hayat, K., Jia, C., Xia, S. and Zhang, X. (2011). Morphology and release profile of microcapsules encapsulating peppermint oil by complex coacervation. *J*. *Food Engineer*. **104**, 455-460.

Dong, Z.J., Touré, A., Jia, C.S., Zhang, X.M. and Xu, S.Y. (2007). Effect of processing parameters on the formation of spherical multinuclear microcapsules encapsulating peppermint oil by coacervation. *J*. *Microencapsul*. **24**, 634-646.

Dossat, V., Combes, D. and Marty, A. (2002). Lipase-catalysed transesterification of high oleic sunflower oil. *Enz*. *Microb*. *Technol*. **30**, 90-94.

Drusch, S., Regier, M. and Bruhn, M. (2012). Recent advances in the microencapsulation of oils high in polyunsaturated fatty acids. In *Novel Technologies in Food Science - Their Impact on Products, Consumer Trends and Environment*, A. McElhatton and P.J.D.A. Sobral eds., Springer, New York, Dordrecht, Heidelberg, London, pp. 159-181.

Drusch, S., Serfert, Y. and Schwarz, K. (2006a). Microencapsulation of fish oil with n-octenylsuccinate-derivatised starch: Flow properties and oxidative stability. *Eur. J. Lipid Sci. Technol.* **108**, 501-512.

Drusch, S., Serfert, Y., Van Den Heuvel, A. and Schwarz, K. (2006b). Physicochemical characterization and oxidative stability of fish oil encapsulated in an amorphous matrix containing trehalose. *Food Res. Intern.* **39**, 807-815.

Elfman-Borjesson, I. and Harrod, M. (1999). Synthesis of monoglycerides by glycerolysis of rapeseed oil using immobilized lipase. *J. Am. Oil Chem. Soc.* **76**, 701-707.

Elizabeth, R.G.N., Annete, H., Francisco, G.L.R., Javier, I.P.F., Graciela, Z.G. and Alberto, G.I.J. (2007). Antioxidant and antimutagenic activity of phenolic compounds in three different colour groups of common bean cultivars (*Phaseolus vulgaris*). *Food Chem.* **103**, 521-527.

Feltes, M., Oliveira, D., Block, J. and Ninow, J. (2013). The production, benefits, and applications of monoacylglycerols and diacylglycerols of nutritional interest. *Food Bioprocess Technol.* **6**, 17-35.

Ferreira, S.L.C., Bruns, R.E., Ferreira, H.S., Matos, G.D., David, J.M., Brandão, G.C., da Silva, E.G.P., Portugal, L.A., dos Reis, P.S., Souza, A.S. and dos Santos, W.N.L. (2007). Box-Behnken design: An alternative for the optimization of analytical methods. *Anal. Chim. Acta* **597**, 179-186.

Gandhi, N.N., Patil, N.S., Sawant, S.B., Joshi, J.B., Wangikar, P.P. and Mukesh, D. (2000). Lipase-catalyzed esterification. *Cat. Rev.-Sci. Eng.* **42**, 439-480.

Gika, H., Macpherson, E., Theodoridis, G. and Wilson, I. (2008). Evaluation of the repeatability of ultra-performance liquid chromatography-TOF-MS for global metabolic profiling of human urine samples. *J. Chromatogr. B* **871**, 299-305.

Gordon, M.H. (2001). Measuring antioxidant activity. In *Antioxidant in Food: Practical Applications*, J. Pokorny, N. Yanishlieva and M. Gordon (eds.), Woodhead Publishing Ltd, Cambridge, U.K., pp. 71-84.

Guillén, M.a.D. and Cabo, N. (2002). Fourier transform infrared spectra data versus peroxide and anisidine values to determine oxidative stability of edible oils. *Food Chem*. **77**, 503-510.

Guillén, M.D. and Cabo, N. (1997). Infrared spectroscopy in the study of edible oils and fats. *J. Sci. Food Agric*. **75**, 1-11.

Guyot, B., Bosquette, B., Pina, M. and Graille, J. (1997). Esterification of phenolic acids from green coffee with an immobilized lipase from Candida antarctica in solvent-free medium. *Biotechnol. Lett*. **19**, 529-532.

Hadzir, N.M., Basri, M., Rahman, M.B.A., Razak, C.N.A., Rahman, R.N.Z.A. and Salleh, A.B. (2001). Enzymatic alcoholysis of triolein to produce wax ester. *J. Chemical Technol. Biotechnol*. **76**, 511-515.

Halling, P.J. (2000). Biocatalysis in low-water media: Understanding effects of reaction conditions. *Curr. Opin. Chem. Biol*. **4**, 74-80.

Heras, A., Schoch, A., Gibis, M. and Fischer, A. (2003). Comparison of methods for determining malondialdehyde in dry sausage by HPLC and the classic TBA test. *Eur. Food Res. Technol* **217**, 180-184.

Horn, A.F., Nielsen, N.S., Andersen, U., Søgaard, L.H., Horsewell, A. and Jacobsen, C. (2011). Oxidative stability of 70% fish oil‐in‐water emulsions: Impact of emulsifiers and pH. *Eur. J. Lipid Sci. Technol*. **113**, 1243-1257.

Hornero-Méndez, D., Pérez-Gálvez, A. and Mínguez-Mosquera, M. (2001). A rapid spectrophotometric method for the determination of peroxide value in food lipids with high carotenoid content. *J. Am. Oil Chem. Soc.* **78**, 1151-1155.

Hu, C., Yuan, Y.V. and Kitts, D.D. (2007). Antioxidant activities of the flaxseed lignan secoisolariciresinol diglucoside, its aglycone secoisolariciresinol and the mammalian lignans enterodiol and enterolactone *in vitro*. *Food Chem. Toxicol.* **45**, 2219-2227.

Huang, D., Ou, B., Hampsch-Woodill, M., Flanagan, J. and Deemer, E. (2002). Development and validation of oxygen radical absorbance capacity assay for lipophilic antioxidants using randomly methylated-cyclodextrin as the solubility enhancer. *J. Agric. Food Chem.* **50**, 1815-1821.

Ierna, M., Kerr, A., Scales, H., Berge, K. and Griinari, M. (2010). Supplementation of diet with krill oil protects against experimental rheumatoid arthritis. *BMC Musculoskelet. Disord.* **11**, 136.

IUPAC (1987). *Standard Methods for the Analysis of Oils Fats and Derivatives*, 2.501. C. Paquot and A. Hautfenne (eds.), Blackwell Scientific Publications, Oxford (UK), pp. 199-200.

Jacobsen, C., Timm, M. and Meyer, A.S. (2001). Oxidation in fish oil enriched mayonnaise: Ascorbic acid and low pH increase oxidative deterioration. *J. Agric. Food. Chem.* **49**, 3947-3956.

Jafari, S.M., Assaidpoor, E., Bhandari, B. and He, Y.H. (2008). Nano-particle encapsulation of fish oil by spray drying. *Food Res. Intern.* **41**, 172-183.

Jeong, G.-T. and Park, D.-H. (2006). Response surface methodological approach for optimization of enzymatic synthesis of sorbitan methacrylate. *Enz. Microb. Technol.* **39**, 381-386.

Kanatt, S., Chander, R., Radhakrishna, P. and Sharma, A. (2005). Potato peel extract - a natural antioxidant for retarding lipid peroxidation in radiation processed lamb meat. *J. Agric. Food Chem.* **53**, 1499-1504.

Karadag, A., Ozcelik, B. and Saner, S. (2009). Review of methods to determine antioxidant capacities. *Food Anal. Methods* **2**, 41-60.

Karam, R., Karboune, S., St-Louis, R. and Kermasha, S. (2009). Lipase-catalyzed acidolysis of fish liver oil with dihydroxyphenylacetic acid in organic solvent media. *Process Biochem.* **44**, 1193-1199.

Karboune, S., Safari, M., Lue, B.M., Yeboah, F.K. and Kermasha, S. (2005). Lipase-catalyzed biosynthesis of cinnamoylated lipids in a selected organic solvent medium. *J. Biotechnol.* **119**, 281-290.

Karboune, S., St-Louis, R. and Kermasha, S. (2008). Enzymatic synthesis of structured phenolic lipids by acidolysis of flaxseed oil with selected phenolic acids. *J. Mol. Catal. B: Enz.* **52-53**, 96-105.

Karim, A.A. and Bhat, R. (2008). Gelatin alternatives for the food industry: Recent developments, challenges and prospects. *Trends Food Sci. Technol.* **19**, 644-656.

Kasote, D. (2013). Flaxseed phenolics as natural antioxidants. *Intern. Food Res. J.* **20**, 27-34.

Kele, M. and Guiochon, G. (1999). Repeatability and reproducibility of retention data and band profiles on reversed-phase liquid chromatography columns I. Experimental protocol. *J. Chromatogr. A* **830**, 41-54.

Kidd, P.M. (2007). Omega-3 DHA and EPA for cognition, behavior, and mood: clinical findings and structural-functional synergies with cell membrane phospholipids. *Altern. Med. Rev.* **12**, 207-227.

Kirkland, K., McCombs, D. and Kirkland, J. (1994). Rapid, high-resolution high-performance liquid chromatographic analysis of antibiotics. *J. Chromatogr. A* **660**, 327-337.

Klaypradit, W. and Huang, Y.-W. (2008). Fish oil encapsulation with chitosan using ultrasonic atomizer. *Food Sci. Technol.* **41**, 1133-1139.

Kling, D.F., Johnson, J., Rooney, M. and Davidson, M. (2011). Omega-3 free fatty acids demonstrate more than 4-fold greater bioavailability for EPA and DHA compared with omega-3-acid ethyl esters in conjunction with a low-fat diet: The ECLIPSE Study. *J. Clin. Lipidol.* **5**, 231.

Kolanowski, W., Ziolkowski, M., Weissbrodt, J., Kunz, B. and Laufenberg, G. (2006). Microencapsulation of fish oil by spray drying-impact on oxidative stability. Part 1. *Eur. Food Res. Technol.* **222**, 336-342.

Kraai, G.N., Winkelman, J.G.M., de Vries, J.G. and Heeres, H.J. (2008). Kinetic studies on the Rhizomucor miehei lipase catalyzed esterification reaction of oleic acid with 1-butanol in a biphasic system. *Biochem. Eng. J.* **41**, 87-94.

Kumari, A., Mahapatra, P., Garlapati, V. and Banerjee, R. (2009). Enzymatic transesterification of Jatropha oil. *Biotechnol. Biofuels* **2**, 1-7.

Laguerre, M., Lecomte, J. and Villeneuve, P. (2007). Evaluation of the ability of antioxidants to counteract lipid oxidation: Existing methods, new trends and challenges. *Prog. Lipid Res.* **46**, 244-282.

Laudani, C., Habulin, M., Primožič, M., Knez, Ž., Della Porta, G. and Reverchon, E. (2006). Optimisation of n-octyl oleate enzymatic synthesis over *Rhizomucor miehei* lipase. *Bioprocess Biosys. Engineer.* **29**, 119-127.

Le Grandois, J., Marchioni, E., Zhao, M., Giuffrida, F., Ennahar, S. and Bindler, F. (2009). Investigation of natural phosphatidylcholine sources: Separation and identification by liquid chromatography-electrospray ionization-tandem mass spectrometry (LC- ESI- MS^2) of molecular species. *J. Agric. Food Chem.* **57**, 6014-6020.

Lee, S.J. and Rosenberg, M. (1999). Preparation and properties of glutaraldehyde cross-linked whey protein-based microcapsules containing theophylline. *J. Controlled Release* **61**, 123-136.

Lemetter, C.Y.G., Meeuse, F.M. and Zuidam, N.J. (2009). Control of the morphology and the size of complex coacervate microcapsules during scale-up. *Am. Inst. Chem. Engineers* **55**, 1487-1496.

Lenihan-Geels, G., Bishop, K. and Ferguson, L. (2013). Alternative sources of omega-3 fats: Can we find a sustainable substitute for fish? *Nutrients* **5**, 1301-1315.

Li, Z., Yang, D., Jiang, L., Ji, J.F., Ji, H.B. and Zeng, X.H. (2007). Lipase-catalyzed esterification of conjugated linoleic acid with L-carnitine in solvent-free system and acetonitrile. *Bioprocess Biosys. Eng.* **30**, 331-336.

Liu, R.H. and Finley, J. (2005). Potential cell culture models for antioxidant research. *J. Agric. Food. Chem.* **53**, 4311-4314.

Liu, S., Low, N. and Nickerson, M. (2010). Entrapment of flaxseed oil within gelatin-gum arabic capsules. *J. Am. Oil Chem. Soc.* **87**, 809-815.

Lue, B.M., Karboune, S., Yeboah, F.K. and Kermasha, S. (2005). Lipase-catalyzed esterification of cinnamic acid and oleyl alcohol in organic solvent media. *J. Chem. Technol. Biotechnol.* **80**, 462-468.

Lule, S.U. and Xia, W.S. (2005). Food phenolics, pros and cons: A review. *Food Rev. Intern.* **21**, 367-388.

Lyberg, A.-M., Fasoli, E. and Adlercreutz, P. (2005). Monitoring the oxidation of docosahexaenoic acid in lipids. *Lipids* **40**, 969-979.

Martin, A. (2007). Le krill antarctique. *Phytothérapie* **5**, 6-13.

Massrieh, W. (2008). Health benefits of omega 3 fatty acids from Neptune krill oil. *Lipid Technol.* **20**, 108-111.

Mitra, S. and Bhowmik, P. (2000). Spectroscopic study of the sorption of isoxaflutole and its diketonitrile metabolite in dissimilar soils. *Bull. Environ. Contam. Toxicol.* **64**, 518-525.

Moniruzzaman, M., Hayashi, Y., Talukder, M.R. and Kawanishi, T. (2007). Lipase-catalyzed esterification of fatty acid in DMSO (dimethyl sulfoxide) modified AOT reverse micellar systems. *Biocatal*. *Biotransform*. **25**, 51-58.

Morton, L.W., Abu-Amsha Caccetta, R., Puddey, I.B. and Croft, K.D. (2000). Chemistry and biological effects of dietary phenolic compounds: Relevance to cardiovascular disease. *Clin*. *Exp*. *Pharmacol*. *Physiol*. **27**, 152-159.

Myers, R.H., Montgomery, D.C. and Anderson-Cook, C.M. (2009). The analysis of second-order response surfaces. In *Response Surface Methodology: Process and Product Optimization Using Designed Experiments*, John Wiley & Sons, Inc., Hoboken, N.J., pp. 219-265.

Naczk, M. and Shahidi, F. (2004). Extraction and analysis of phenolics in food. *J*. *Chromatogr*. *A* **1054**, 95-111.

Neue, U., Alden, B. and Walter, T. (1999). Universal procedure for the assessment of the reproducibility and the classification of silica-based reversed-phase packings II. Classification of reversed-phase packings. *J*. *Chromatogr*. *A* **849**, 101-116.

Nielsen, N., Xu, X., Timm-Heinrich, M. and Jacobsen, C. (2004). Oxidative stability during storage of structured lipids produced from fish oil and caprylic acid. *J*. *Am*. *Oil Chem*. *Soc*. **81**, 375-384.

Nilsson, A., Holmgren, A. and Lindblom, G. (1991). Fourier-transform infrared spectroscopy study of dioleoylphosphatidylcholine and monooleoylglycerol in lamellar and cubic liquid crystals. *Biochem*. **30**, 2126-2133.

Peterson, B.L. and Cummings, B.S. (2006). A review of chromatographic methods for the assessment of phospholipids in biological samples. *Biomed*. *Chromatogr*. **20**, 227-243.

Petersson, A.E.V., Adlercreutz, P. and Mattiasson, B. (2007). A water activity control system for enzymatic reactions in organic media. *Biotechnol*. *Bioeng*. **97**, 235-241.

Platt, D., Pelled, D. and Shulman, A. (2005). *Oils enriched with diacylglycerols and phytosterol esters for use in the reduction of blood cholestrol and triglycerides and oxidative stress*. US Patent Application No 2006/0052351A1.

Prata, A.S., Zanin, M.H.A., Ré, M.I. and Grosso, C.R.F. (2008). Release properties of chemical and enzymatic crosslinked gelatin-gum arabic microparticles containing a fluorescent probe plus vetiver essential oil. *Colloids Surf. B* **67**, 171-178.

Prior, R., Hoang, H., Gu, L., Wu, X., Bacchiocca, M., Howard, L., Hampsch-Woodill, M., Huang, D., Ou, B. and Jacob, R. (2003). Assays for hydrophilic and lipophilic antioxidant capacity (oxygen radical absorbance capacity ($ORAC_{FL}$)) of plasma and other biological and food samples. *J. Agric. Food Chem.* **51**, 3273-3279.

Prior, R.L., Wu, X. and Schaich, K. (2005). Standardized methods for the determination of antioxidant capacity and phenolics in foods and dietary supplements. *J. Agric. Food. Chem.* **53**, 4290-4302.

Qv, X.-Y., Zeng, Z.-P. and Jiang, J.-G. (2011). Preparation of lutein microencapsulation by complex coacervation method and its physicochemical properties and stability. *Food Hydrocoll.* **25**, 1596-1603.

Raatz, S.K., Redmon, J.B., Wimmergren, N., Donadio, J.V. and Bibus, D.M. (2009). Enhanced absorption of n-3 fatty acids from emulsified compared with encapsulated fish oil. *J. Am. Diet. Assoc.* **109**, 1076-1081.

Reis, P., Holmberg, K., Watzke, H., Leser, M.E. and Miller, R. (2009). Lipases at interfaces: A review. *Adv. Colloid Interface Sci.* **147-148**, 237-250.

Reuhs, B.L. and Rounds, M.A. (2010). High-performance liquid chromatography. In *Food Analysis*, S. Nielson (ed.) Springer, USA, West lafayette, IN, pp. 499-512.

Rodrigues, R.C. and Ayub, M.A.Z. (2011). Effects of the combined use of *Thermomyces lanuginosus* and *Rhizomucor miehei* lipases for the transesterification and hydrolysis of soybean oil. *Process Biochem.* **46**, 682-688.

Rusli, J., Sanguansri, L. and Augustin, M. (2006). Stabilization of oils by microencapsulation with heated protein-glucose syrup mixtures. *J. Am. Oil Chem. Soc.* **83**, 965-972.

Saad, B., Wai, W.T., Lim, B.P. and Saleh, M.I. (2006). Flow injection determination of peroxide value in edible oils using triiodide detector. *Anal. Chim. Acta* **565**, 261-270.

Sabally, K., Karboune, S., St-Louis, R. and Kermasha, S. (2006a). Lipase-catalyzed transesterification of dihydrocaffeic acid with flaxseed oil for the synthesis of phenolic lipids. *J. Biotechnol.* **127**, 167-176.

Sabally, K., Karboune, S., St-Louis, R. and Kermasha, S. (2006b). Lipase-catalyzed transesterification of trilinolein or trilinolenin with selected phenolic acids. *J. Am. Oil Chem. Soc.* **83**, 101-107.

Sabally, K., Karboune, S., St-Louis, R. and Kermasha, S. (2007). Lipase-catalyzed synthesis of phenolic lipids from fish liver oil and dihydrocaffeic acid. *Biocatal. Biotransform.* **25**, 211-218.

Sabally, K., Karboune, S., Yebaoh, F.K. and Kermasha, S. (2005a). Enzymatic esterification of dihydrocaffeic acid with linoleyl alcohol in organic solvent media. *Biocatal. Biotransform.* **23**, 37-44.

Sabally, K., Karboune, S., Yeboah, F.K. and Kermasha, S. (2005b). Lipase-catalyzed esterification of selected phenolic acids with linolenyl alcohols in organic solvent media. *Appl. Biochem. Biotechnol.* **127**, 17-27.

Safari, M., Karboune, S., St-Louis, R. and Kermasha, S. (2006). Enzymatic synthesis of structured phenolic lipids by incorporation of selected phenolic acids into triolein. *Biocatal. Biotransform.* **24**, 272-279.

Sampalis, F., Bunea, R., Pelland, M.F., Kowalski, O., Duguet, N. and Dupuis, S. (2003). Evaluation of the effects of Neptune Krill Oil on the management of premenstrual syndrome and dysmenorrhea. *Altern. Med. Rev.* **8**, 171-179.

Sanguansri, P. and Augustin, M.A. (2006). Nanoscale materials development - a food industry perspective. *Trends in Food Sci. Technol.* **17**, 547-556.

Schmitz, G. and Ecker, J. (2008). The opposing effects of n-3 and n-6 fatty acids. *Prog. Lipid Res.* **47**, 147-155.

Schneider, R.d.C.S., Lara, L.R.S., Bitencourt, T.B., Nascimento, M.d.G. and Nunes, M.R.d.S. (2009). Chemo-enzymatic epoxidation of sunflower oil methyl esters. *J. Braz. Chem. Soc.* **20**, 1473-1477.

Schuchardt, J.P. and Hahn, A. (2013). Bioavailability of long-chain omega-3 fatty acids. *Prostag. Leukotr. Ess.* **89**, 1-8.

Schuchardt, J.P., Schneider, I., Meyer, H., Neubronner, J., von Schacky, C. and Hahn, A. (2011). Incorporation of EPA and DHA into plasma phospholipids in response to different omega-3 fatty acid formulations--a comparative bioavailability study of fish oil vs. krill oil. *Lipids Health Dis.* **10**, 145-151.

Shahidi, F. and Zhong, Y. (2005). Lipid Oxidation: Measurement Methods. In *Bailey's Industrial Oil and Fat Products*, 6th Edition, John Wiley & Sons, Inc., NY, pp. 357-374.

Shahidi, F. and Zhong, Y. (2010). Lipid oxidation and improving the oxidative stability. *Chem. Soc. Rev.* **39**, 4067-4079.

Shantha, N.C. and Decker, E.A. (1994). Rapid, sensitive, iron-based spectrophotometric methods for determination of peroxide values of food lipids. *J. Assoc. Off. Anal. Chem. Intern.* **77**, 421-424.

Siriwardhana, N., Lee, K.-W., Kim, S.-H., Ha, J.-H., Park, G.-T. and Jeon, Y.-J. (2004). Lipid peroxidation inhibitory effects of *Hizikia Fusiformis* methanolic extract on fish oil and linoleic acid. *Food Sci. Technol. Int.* **10**, 65-72.

Snyder, L., Dolan, J. and Gant, J. (1979). Gradient elution in high-performance liquid chromatography I. Theoretical basis for reversed-phase systems. *J. Chromatogr. A* **165**, 3-30.

Song, J.H., Inoue, Y. and Miyazawa, T. (1997). Oxidative stability of docosahexaenoic acid-containing oils in the form of phospholipids, triacylglycerols, and ethyl esters. *Biosci. Biotechnol. Biochem.* **61**, 2085-2088.

Song, W., Derito, C.M., Liu, M.K., He, X., Dong, M. and Liu, R.H. (2010). Cellular antioxidant activity of common vegetables. *J. Agric. Food. Chem.* **58**, 6621-6629.

Soobrattee, M.A., Neergheen, V.S., Luximon-Ramma, A., Aruoma, O.I. and Bahorun, T. (2005). Phenolics as potential antioxidant therapeutic agents: Mechanism and actions. *Mutat. Res.* **579**, 200-213.

Soottitantawat, A., Yoshii, H., Furuta, T., Ohkawara, M. and Linko, P. (2003). Microencapsulation by spray drying: Influence of emulsion size on the retention of volatile compounds. *J. Food Sci.* **68**, 2256-2262.

Sorour, N. (2010). In *Lipase-Catalyzed Synthesis of Phenolic lipids in Solvent-Free Medium Using Selected Edible Oils and Phenolic Acids*, Ph.D. Thesis, McGill University, Montreal, Quebec.

Sorour, N., Karboune, S., Saint-Louis, R. and Kermasha, S. (2012a). Enzymatic synthesis of phenolic lipids in solvent-free medium using flaxseed oil and 3,4-dihydroxyphenyl acetic acid. *Process Biochem.* **47**, 1813-1819.

Sorour, N., Karboune, S., Saint-Louis, R. and Kermasha, S. (2012b). Lipase-catalyzed synthesis of structured phenolic lipids in solvent-free system using flaxseed oil and selected phenolic acids as substrates. *J. Biotechnol.* **158**, 128-136.

Sroka, Z. and Cisowski, W. (2003). Hydrogen peroxide scavenging, antioxidant and anti-radical activity of some phenolic acids. *Food Chem. Toxicol.* **41**, 753-758.

Stamatis, H., Sereti, V. and Kolisis, F.N. (1999). Studies on the enzymatic synthesis of lipophilic derivatives of natural antioxidants. *J. Am. Oil Chem. Soc.* **76**, 1505-1510.

Stamatis, H., Sereti, V. and Kolisis, F.N. (2001). Enzymatic synthesis of hydrophilic and hydrophobic derivatives of natural phenolic acids in organic media. *J. Mol. Catal. B: Enz.* **11**, 323-328.

Stasiuk, M. and Kozubek, A. (2010). Biological activity of phenolic lipids. *Cell. Mol. Life Sci.* **67**, 841-860.

Stolyhwo, A., Colin, H. and Guiochon, G. (1985). Analysis of triglycerides in oils and fats by liquid chromatography with the laser light scattering detector. *Anal. Chem.* **57**, 1342-1354.

Strauss, G. and Gibson, S.M. (2004). Plant phenolics as cross-linkers of gelatin gels and gelatin-based coacervates for use as food ingredients. *Food Hydrocoll.* **18**, 81-89.

Sung, H.-W., Huang, R.-N., Huang, L.L.H. and Tsai, C.-C. (1999). *In vitro* evaluation of cytotoxicity of a naturally occurring cross-linking reagent for biological tissue fixation. *J. Biomaterials Sci., Polymer Edition* **10**, 63-78.

Tandy, S., Chung, R., Wat, E., Kamili, A., Berge, K., Griinari, M. and Cohn, J. (2009). Dietary krill oil supplementation reduces hepatic steatosis, glycemia, and hypercholesterolemia in high-fat-fed mice. *J. Agric. Food. Chem.* **57**, 9339-9345.

Tou, J.C., Jaczynski, J. and Chen, Y.C. (2007). Krill for human consumption: Nutritional value and potential health benefits. *Nutr. Rev.* **65**, 63-77.

Tsao, R. and Deng, Z. (2004). Separation procedures for naturally occurring antioxidant phytochemicals. *J. Chromatogr. B, Anal. Technol. Biomed. Life Sci.* **812**, 85-99.

Tsuzuki, W. (2005). Acidolysis between triolein and short-chain fatty acid by lipase in organic solvents. *Biosc. Biotechnol. Biochem.* **69**, 1256-1261.

Valencia, P., Flores, S., Wilson, L. and Illanes, A. (2010). Effect of particle size distribution on the simulation of immobilized enzyme reactor performance. *Biochem. Eng. J.* **49**, 256-263.

Vikbjerg, A., Mu, H. and Xu, X. (2005). Parameters affecting incorporation and by-product formation during the production of structured phospholipids by lipase-catalyzed acidolysis in solvent-free system. *J. Mol. Catal. B: Enz.* **36**, 14-21.

Vikbjerg, A.F., Rusig, J.Y., Jonsson, G., Mu, H.L. and Xu, X.B. (2006). Strategies for-lipase-catalyzed production and the purification of structured phospholipids. *Eur. J. Lipid Sci. Technol.* **108**, 802-811.

Vlachos, N., Skopelitis, Y., Psaroudaki, M., Konstantinidou, V., Chatzilazarou, A. and Tegou, E. (2006). Applications of Fourier transform-infrared spectroscopy to edible oils. *Anal. Chim. Acta* **573–574**, 459-465.

Wang, H., Liu, F., Yang, L., Zu, Y., Wang, H., Qu, S. and Zhang, Y. (2011). Oxidative stability of fish oil supplemented with carnosic acid compared with synthetic antioxidants during long-term storage. *Food Chem.* **128**, 93-99.

Welch, C., Wu, N., Biba, M., Hartman, R., Brkovic, T., Gong, X., Helmy, R., Schafer, W., Cuff, J. and Pirzada, Z. (2010). Greening analytical chromatography. *Trends Anal. Chem.* **29**, 667-680.

Werner, A., Havinga, R., Kuipers, F. and Verkade, H.J. (2004). Treatment of EFA deficiency with dietary triglycerides or phospholipids in a murine model of extrahepatic cholestasis. *Am. J. Physiol. Gastrointest. Liver Physiol.* **286**, G822-G832.

Willis, W.M. and Marangoni, A.G. (2008). Enzymatic interesterification. In *Food Lipids: Chemistry, Nutrition and Biotechnology*, C.C. Akoh and D.B. Min (eds.), CRC Press, pp. 808-834.

Winther, B., Hoem, N., Berge, K. and Reubsaet, L. (2011). Elucidation of phosphatidylcholine composition in krill oil extracted from *Euphausia superba*. *Lipids* **46**, 25-36.

Yadav, G.D. and Devi, K.M. (2004). Immobilized lipase-catalysed esterification and transesterification reactions in non-aqueous media for the synthesis of tetrahydrofurfuryl butyrate: Comparison and kinetic modeling. *Chem. Eng. Sci.* **59**, 373-383.

Yamane, T. (2005). Biocatalysis in microaqueous organic media. In *Handbook of Industrial Biocatalysis*, C. T. Hou (ed.) CRC, pp. 1-10.

Yang, F. and Russell, A.J. (1995). A comparison of lipase-catalyzed ester hydrolysis in reverse micelles, organic solvents, and biphasic systems. *Biotechnol. Bioeng.* **47**, 60-70.

Yang, T.K., Fruekilde, M.B. and Xu, X.B. (2003). Applications of immobilized Thermomyces lanuginosa lipase in interesterification. *J. Am. Oil Chem. Soc.* **80**, 881-887.

Yeo, Y., Bellas, E., Firestone, W., Langer, R. and Kohane, D.S. (2005). Complex coacervates for thermally sensitive controlled release of flavor compounds. *J. Agric. Food. Chem.* **53**, 7518-7525.

Zacharis, E., Halling, P.J. and Rees, D.G. (1999). Volatile buffers can override the "pH memory" of subtilisin catalysis in organic media. *Proc. Nat. Ac. Sci. USA* **96**, 1201-1205.

Zaks, A. and Klibanov, A.M. (1985). Enzyme-catalyzed processes in organic solvents. *Proc. Nat. Ac. Sci. USA* **82**, 3192-3196.

Zhang, J., Chen, S., Yang, R. and Yan, Y. (2010a). Biodiesel production from vegetable oil using heterogenous acid and alkali catalyst. *Fuel* **89**, 2939-2944.

Zhang, X., Do, M.D., Casey, P., Sulistio, A., Qiao, G.G., Lundin, L., Lillford, P. and Kosaraju, S. (2010b). Chemical cross-linking gelatin with natural phenolic compounds as studied by high-resolution NMR spectroscopy. *Biomacromolecules* **11**, 1125-1132.

Zheng, W. and Wang, S.Y. (2002). Oxygen radical absorbing capacity of phenolics in blueberries, cranberries, chokeberries, and lingonberries. *J*. *Agric*. *Food*. *Chem*. **51**, 502-509.

Zheng, Y., Wu, X.-M., Branford-White, C., Quan, J. and Zhu, L.-M. (2009). Dual response surface-optimized process for feruloylated diacylglycerols by selective lipase-catalyzed transesterification in solvent free system. *Bioresour*. *Technol*. **100**, 2896-2901.

Zhu, J.J., Shi, J.H., Qian, W.B., Cai, Z.Z. and Li, D. (2008). Effects of krill oil on serum lipids of hyperlipidemic rats and human SW480 cells. *Lipids Health Dis*. **7**, 1-6.

Zweigenbaum, J., Heinig, K., Steinborner, S., Wachs, T. and Henion, J. (1999). High-throughput bioanalytical LC/MS/MS determination of benzodiazepines in human urine: 1000 samples per 12 hours. *Anal*. *Chem*. **71**, 2294-2300.

LIST OF PUBLICATIONS

REFEREED PUBLICATIONS

Aziz, S., Dutilleul, P. and Kermasha, S. (2012). Lipase-catalyzed transesterification of krill oil and 3,4-dihydroxyphenyl acetic acid in solvent-free medium using response surface methodology. *J. Mol. Catal. B: Enz.* **84**, 189-197.

Aziz, S., St-Louis, R., Yaylayan, V. and Kermasha, S. (2012). Chromatographic separation of synthesized phenolic lipids from krill oil and dihydroxyphenyl acetic acid. *J. Am. Oil Chem. Soc*. **89**, 597-608.

SUBMITTED MANUSCRIPTS

Aziz, **S**. and Kermasha, S. (2013). Assessment of antioxidant capacity and oxidative stability of esterified phenolic lipids in selected edible oils. *J. Food Sci*.

Aziz, **S.**, Gill, J., Dutilleul, P., Neufeld, R. and Kermasha, S. (2013). Microencapsulation of krill oil using complex coacervation. *J. Microencap*.

MANUSCRIPTS TO BE SUBMITTED FOR PUBLICATION

Aziz, **S.**, Gill, J., Neufeld, R. and Kermasha, S. (2013). Microencapsulation of enzymatically esterified krill oil using complex coacervation.